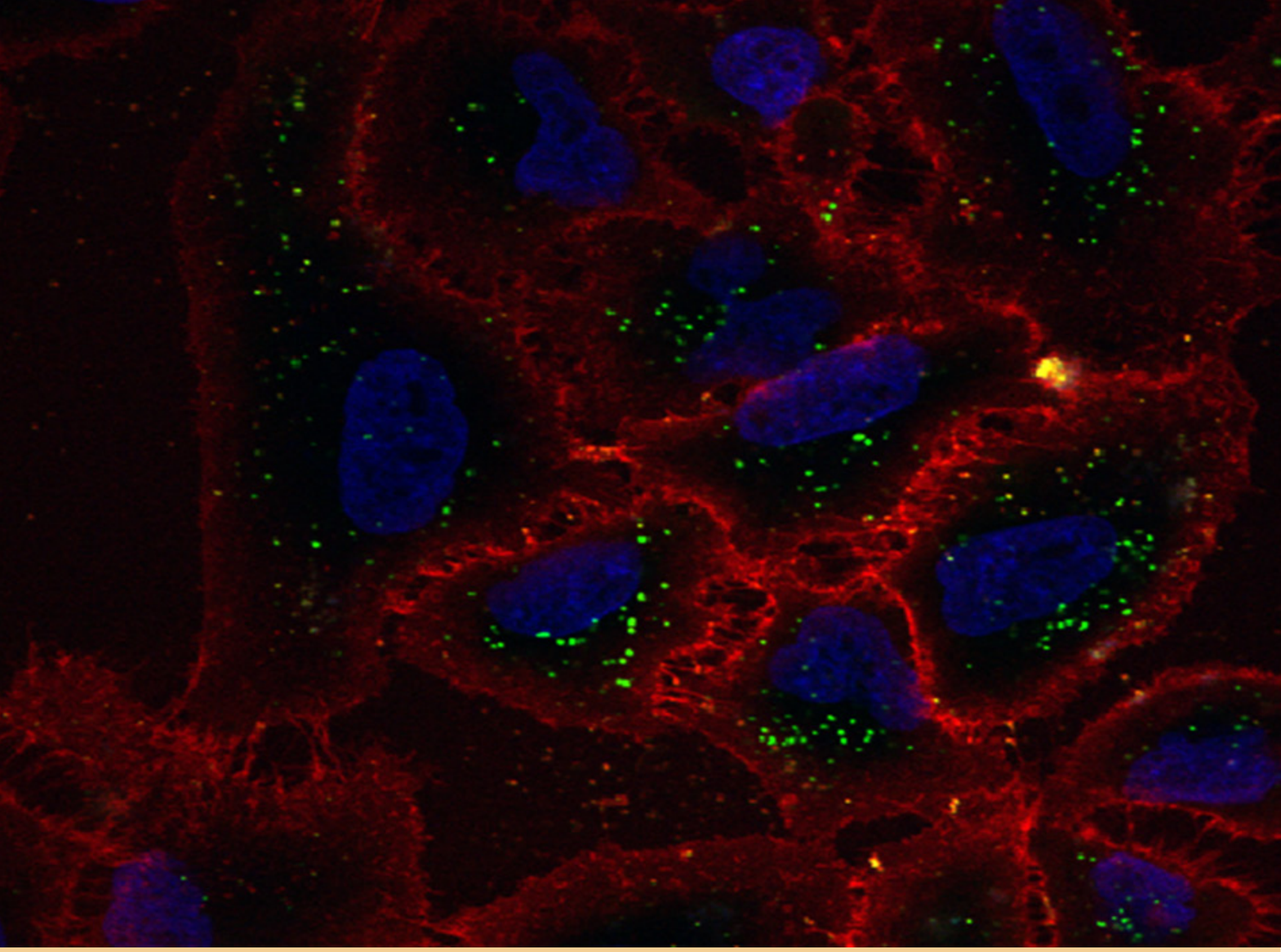

Filipa Raquel Maia Fontes Lebre

Development of chitosan-based nanoparticles for nasal immunization against hepatitis B

Tese de Doutoramento em Ciências Farmacêuticas na área de especialização em Tecnologia Farmacêutica, orientada pela Professora Doutora Olga Maria Fernandes Borges Ribeiro e pela Professora Doutora Maria da Conceição Monteiro Pedroso de Lima e apresentada à Faculdade de Farmácia da Universidade de Coimbra

Abril 2017

· U C ·

Universidade de Coimbra

Front page figure caption: confocal fluorescence microscopy image of protein loaded FITC-labelled chitosan nanoparticles upon internalization by A549 cells. Confocal image shows overlaid images of the fluorescent probes; membrane staining with wheat germ agglutinin Alexa Fluor 594 conjugate (red); FITC-labelled chitosan (green); nuclear staining with Hoechst 33342 (blue).

Development of chitosan-based nanoparticles for nasal immunization against hepatitis B

Filipa Raquel Maia Fontes Lebre

Candidature thesis for doctor degree in Pharmaceutical Sciences, submitted to the Faculty of Pharmacy of the University of Coimbra

Tese de candidatura ao grau de doutor em Ciências Farmacêuticas, apresentada à Faculdade de Farmácia da Universidade de Coimbra

The experimental work presented in this thesis was developed under the scientific supervision of Professor Olga Maria Fernandes Borges Ribeiro from the Pharmaceutical Technology Laboratory of Faculty of Pharmacy, University of Coimbra and Professor Maria da Conceição Monteiro Pedroso Lima of Faculty of Sciences and Technology, University of Coimbra. Financial support was given by FEDER funds through the Operational Program Competitiveness Factors – COMPETE and national funds by FCT – Foundation for Science and Technology under the project PTDC/SAU-FAR/115044/2009, FCT doctoral fellowship SFRH/ BD/ 64046/ 2009 and strategic project POCI-01-0145-FEDER-007440.

O trabalho experimental apresentado no âmbito desta tese foi desenvolvido sob a orientação científica da Professora Olga Maria Fernandes Borges Ribeiro no Laboratório de Tecnologia Farmacêutica da Faculdade de Farmácia da Universidade de Coimbra e da Professora Maria da Conceição Monteiro Pedroso Lima da Faculdade de Ciências e Tecnologia da Universidade de Coimbra. Foi financiado por fundos FEDER através do Programa Operacional Fatores de Competitividade – COMPETE e por Fundos Nacionais através da FCT – Fundação para a Ciência e a Tecnologia no âmbito do projeto PTDC/SAU-FAR/115044/2009, da bolsa de doutoramento SFRH/ BD/ 64046/ 2009, do projeto PTDC/SAU-FAR/115044/2009 e do projeto estratégico POCI-01-0145-FEDER-007440.


FCT
Fundação para a Ciência e a Tecnologia
MINISTÉRIO DA EDUCAÇÃO E CIÊNCIA


QUADRO
DE REFERÊNCIA
ESTRATÉGICO
NACIONAL
PORTUGAL 2007.2013


COMPETE
PROGRAMA OPERACIONAL FACTORES DE COMPETITIVIDADE


UNIÃO EUROPEIA
Fundo Europeu
de Desenvolvimento Regional

Acknowledgments / Agradecimentos

"Aqueles que passam por nós, não vão sós, não nos deixam sós.
Deixam um pouco de si, levam um pouco de nós."
Antoine de Saint-Exupéry

Ao longo do meu doutoramento foram várias as pessoas que me apoiaram quer a nível pessoal, quer a nível profissional, que me incentivaram a nunca desistir e sem as quais não teria conseguido finalizar este grande projeto.

Em primeiro lugar quero expressar o meu profundo agradecimento à Professora Doutora Olga Borges, docente da Faculdade de Farmácia da Universidade de Coimbra, minha orientadora, pela confiança depositada em mim para a concretização deste projeto. Trago sempre presente o meu primeiro dia no laboratório, o qual foi um momento decisivo na minha vida e veio reforçar a certeza que tinha em enveredar pelo Doutoramento. Foi com grande orgulho que me tornei a primeira doutoranda da Professora Olga. O seu acompanhamento, supervisão e apoio foram cruciais para o desenvolvimento do trabalho realizado.

À Professora Doutora Conceição Pedroso de Lima, minha co-orientadora, agradeço pela disponibilidade e generosidade reveladas ao longo destes anos de trabalho, assim como pelas críticas, correções e sugestões relevantes feitas durante a orientação.

Ao Doutor Henrique Faneca, agradeço pelas sugestões e por ter partilhado comigo a sua experiência em diversas técnicas de laboratório. Agradeço a constante disponibilidade e sugestões essenciais para completar o trabalho aqui apresentado.

To Professor Gerrit Borchard from Geneva-Lausanne School of Pharmacy I would like to thank for giving me the opportunity to join his research group. His knowledge and guidance were invaluable to my progress.

To Professor Ed Lavelle, I would like to thank for welcoming me as part of his research laboratory in Trinity College of Dublin, for six months, which was an enriching experience that broadened my scientific knowledge. I am deeply grateful for his scientific support, enormous encouragement and trust shown. From Trinity College of Dublin I would also like to thank all the

members of the Adjuvant Research Group, Liz, Claire, Ewa, Craig, Ciaran, Graham, Cliona and Chris, and more recently Aqel, Aoife, Hannah, Katie, Mimmi, Natalia, Sean and Stephanie for their contribution in many experiments, but above all for their friendship and for helping me to feel at home. And to Barry Moran for the technical support and his valuable help with the flow cytometric studies and analysis.

Agradeço ainda a ajuda prestada no decorrer dos trabalhos realizados pelas técnicas do Centro de Neurociências e Biologia Celular da Universidade de Coimbra, Luísa Cortes, Isabel Nunes e Isabel Dantas.

Agradeço em especial as "meninas do NanoLab", Dulce Bento, Sandra Jesus e Edna Soares, que estiveram ao meu lado em todas as etapas deste projeto e que partilharam de perto os bons e maus momentos. Dulce, longe estava eu de imaginar que o melhor que ia retirar deste Doutoramento seria a tua amizade. Lembro-me dos primeiros tempos em que os silêncios constrangedores eram quebrados por uma ida a máquina do café com conversas banais sobre o tempo e como fiquei em pânico por dividir um quarto minúsculo com cama extra com, na altura, uma perfeita estranha, sem saber que seria um momento decisivo na minha vida. Serás sempre a minha melhor descoberta. Obrigada por todos os conselhos, pelas horas passadas a ver vídeos sobre técnicas experimentais, pelas conversas sérias e parvas, pela rabugice, por lágrimas e risos partilhados. És uma das pessoas que mais admiro pessoal e profissionalmente. Contigo aprendi muito mais do que artigos podem ensinar. Sandra, agradeço-te por não teres desistido do NanoLab, mesmo depois de na cadeira de Iniciação a Investigação teres sido orientada no laboratório por mim. Obrigada por toda a amizade e apoio, pela tua calma e perseverança que me ajudaram a manter a sanidade em momentos cruciais e me incentivaram a nunca desistir. Edna, embora tenhas sido a mais recente aquisição do NanoLab deixaste sem dúvida a tua marca. Obrigada pela revolução que trouxeste ao laboratório, pela tua frontalidade, pelo teu espirito critico e por toda a tua ajuda e incentivo. Sei que vais perpetuar o bom nome do NanoLab. Obrigada por todas as horas partilhadas no laboratório e fora dele as quais recordo sempre com um enorme sorriso.

À Ana Fortuna agradeço a amizade, as conversas matinais acompanhadas por um belo cafezinho e por todos os conselhos que me foi dando ao longo destes anos. Aos meus colegas da Tecnologia e Farmacologia da Faculdade de Farmácia da Universidade de Coimbra: Amélia Vieira, Ana Serralheiro, Carla Varela, Carla Vitorino, Daniela Gonçalves, João Abrantes, Joana Almeida e

Sousa, Joana Bicker, Marisa Gaspar, Raquel Teixeira e Susana Simões, e a D. Gina, por toda a ajuda e todos os bons momentos partilhados dentro e fora da faculdade. Aprendi imenso com a série de seminários do OSGA.

A nível pessoal, agradeço a todos os meus amigos que de um modo ou de outro me acompanharam e me deram força ao longo destes últimos anos. A Gina e a Janice por me aturarem há mais anos do que tenho coragem de admitir. As meninas do LT, Cátia, Melânia e Vânia pela amizade, por estarem presentes desde os meus primeiros tempos em Coimbra e claro pelas belas patuscadas. Vocês sabem que são família para mim. Aos meus amigos da Faculdade, Andreia, Daniela, Miguel, Mónica e Rita e aos maridos/namorados, Dino, Ivo e Luís, que partilharam o meu percurso académico e me moldaram não só em termos profissionais como pessoais. A eles devo muitas gargalhadas no final de semanas stressantes. Todo este esforço teria sido impossível sem vocês.

Ao Pedro, que embora não me tenha acompanhado nesta jornada desde o começo, tem sido fundamental para a terminar. Agradeço do fundo do meu coração todas as horas passadas ao meu lado enquanto escrevia, só para que não me sentisse sozinha, as palavras de incentivo que me disseste para que voltasse a acreditar em mim e nas minhas capacidades, a tua paciência sem fim para me aturares depois de um dia de trabalho em que voltava stressada e rabugenta e tu me acalmavas e fazias um dos teus maravilhosos jantares pois sabias que isso me deixaria de sorriso de orelha a orelha. Tu fazes o impossível parecer fácil!

Por último, um agradecimento muito especial a minha família que sempre apoiou as minhas decisões, e que nunca me fizeram desistir dos meus objetivos. A minha irmã Nocas, pela amizade, por ter sido um exemplo para mim, por me "ter dado na cabeça" sempre que era preciso, sem nunca me deixar ir abaixo e claro por me teres dado a oportunidade de ser a tia babada da Inês e da Maria. Ao Alex por todo o apoio e conselhos e por todos os jantares "a três" que partilhei contigo e com a minha irmã em Coimbra, para que nunca me sentisse sozinha. A tua maneira de ser é contagiante. Aos meus pais Emília e Joaquim, pelo amor e apoio incondicional, em todas as etapas desta jornada. Obrigada por terem sempre acreditado em mim, pelos vossos conselhos sábios, pela vossa paciência e por todos os miminhos que recebia sempre que voltava a casa. Sem vocês não seria a pessoa que sou hoje e não teria concretizado os meus objetivos.

Table of contents

List of abbreviations

ABTS	2,2'-azino-bis(3-ethylbenzothiazoline-6-sulphonic acid
AcB	Sodium acetate buffer
AIM2	Absent in melanoma 2
APC(s)	Antigen presenting cell(s)
AS	Adjuvant systems
ASC	Apoptosis-associated speck-like protein containing a C-terminal caspase recruitment domain
ATCC	American Type Culture Collection
ATP	Adenosine triphosphate
BAL	Bronchoalveolar lavage
BALT	Bronchus-associated lymphoid tissue
BCA	Bicinchoninic acid assay
BCEM	B-cell epitope loaded (PLG) microparticles
BCEP	B-cell epitope peptide
BMDC	Bone-marrow derived dendritic cells
BSA	Bovine serum albumin
CD	Cluster of differentiation
cGAS	Cyclic GMP-AMP synthase
CH NP	Chitosan nanoparticles
CH sol.	Chitosan in solution
CH-Al NP	Chitosan-aluminium nanoparticles
CH-Na NP	Chitosan-sodium nanoparticles
CMR	Cell-mediated response
CNC	Center for Neuroscience and Cell Biology

CpG ODN	Cytosine-phosphate-guanine oligodeoxynucleotides
CT	Cholera toxin
CTB	Cholera toxin subunit B
CTL	Cytotoxic T cells
DAMP	Danger-associated molecular patterns
DC(s)	Dendritic cell(s)
DDC	Dermal dendritic cells
DLS	Dynamic light scattering
DMEM	Dulbecco's Modified Eagle's Medium
DMSO	Dimethyl sulfoxide
DNA	Deoxyribonucleic acid
DOTMA	N-[1-(2,3-dioleyloxy)propyl]-N,N,N-trimethylammonium chloride
DTA	Differential thermal analysis
EDS	Energy-dispersive X-ray spectroscopy
EDTA	Ethylenediaminetetraacetic acid
ELISA	Enzyme-linked immunosorbent assay
ELS	Electrophoretic light scattering
EMA	European Medicines Agency
EPI	Epidermal powder immunization
Ex/Em	Excitation/Emission
FDA	Food and Drug Administration
FITC	Fluorescein isothiocyanate
FTIR	Fourier transform infrared spectroscopy
GALT	Gut-associated lymphoid tissue
GC	Glycol chitosan
GM-CSF	Granulocyte–macrophage colony-stimulating factor
GMT	Geometric mean titer

HA	Hemagglutinin
HA	Influenza hemagglutinin
HBsAg	Hepatitis B surface antigen
HEPES	4-(2-hydroxyethyl)-1-piperazineethanesulfonic acid
HIV	Human immunodeficiency virus
HRP	Horseradish peroxidase
HSA	Human serum albumin
HSA-CH NP/DNA	Human serum albumin-loaded chitosan nanoparticle/DNA complexes
HSA-CH NP/DNA	HSA-loaded chitosan nanoparticle/DNA
HSP	Heat shock proteins
I.M.	Intramuscular
I.N.	Intranasal
I.P.	Intraperitoneal
ICH	International Council for Harmonization
IFNAR	IFN-α/IFN-β receptor
IFN-γ	Interferon-γ
Ig	Immunoglobulin
IL	Interleukin
IP	Isoelectric point
ISCOMs	Immune stimulating complexes
IU/L	International units per liter
LAL	*Limulus Amebocyte* lysate
LBP	LPS-binding protein
LC	Langerhans cells
LC	Loading capacity
LE	Loading efficacy
LM	Lipid microparticles

LMST	Lipid microparticles containing stearylamine
LPS	Lipopolysaccharide
LT	*Escherichia coli* heat-labile enterotoxin
LTA	Lotus tetragonolobus purpureaus
MALT	Mucosal-associated lymphoid tissue
M-Cells	Microfold cells
MD2	Myeloid differentiation protein 2
mDC	Myeloid dendritic cells
MEM	Minimum essential medium
MFI	Mean fluorescence intensity
MHC	Major histocompatibility complex
MPL	Monophosphoryl lipid A
MTT	3-[4, 5-dimethylthiazol-2-yl]-2,5-diphenyl tetrazolium bromide
NALT	Nasal-associated lymphoid tissue
NE	Nanoemulsion
NISV	Nonionic surfactant vesicle
NLR	NOD-like receptors
NLRP3	NOD-like receptor Family Pyrin Domain Containing 3
NOD	Nucleotide-binding oligomerization domain
NP	Nanoparticle
OD	Optical density
OPD	O-phenylenediamine dihydrochloride
OPM	O-palmitoyl mannan
OVA	Ovalbumin
PAMP	Pathogen-associated molecular patterns
PBS	Phosphate buffer saline
pCMVluc	Plasmid DNA encoding luciferase

pDC	Plasmacytoid dendritic cells
pDNA	Plasmid DNA
PEC	Peritoneal exhudate cells
PEG	Poly(ethylene glycol)
PEI	Polyethylenimine
PFA	Paraformaldehyde
PGA	Polyglycolic acid
pH	Potential of hydrogen
pI	Isoelectric points
PI	Polydispersity index
PLA	Polylactic acid
PLGA	Poly(lactic-co-glycolic) acid
PmB	Polymyxin B
PMED	Particle-mediated epidermal delivery
PNA	*Arachis hypogaea*
Poly(dA:dT)	Poly(deoxyadenylic-deoxythymidylic) acid
pRc/CMV-HBs(S)	Reporter Plasmid expressing the hepatitis B surface antigen small protein under the control of the CMV immediate-early promoter
PRR	Pattern recognition systems
PSI	Pound per square inch
QuilA	*Quillaia saponaria*
rCTB	Recombinant cholera toxin B subunit
RLU	Relative light units
ROS	Reactive oxygen species
RPMI	Roswell park memorial institute medium
RT	Room temperature
S.C.	Subcutaneous

SD	Standard deviation
SEM	Scanning electron microscopy
SGF	Simulated gastric fluid
SIF	Simulated intestinal fluid
SLM	Solid lipid microparticles
SMBV	Supramolecular biovector
STING	Stimulator of interferon genes
TBSI	Trinity biomedical sciences institute
TCI	Transcutaneous immunization
TGA	Thermogravimetric analysis
Th	T helper
TI	Topical immunization
TLR	Toll-like receptors
TMC	N-trimethyl chitosan
TNF-α	Tumor necrosis factor-α
TSP	Total soluble protein
UEA-1	*Ulex europaeus* agglutinin 1
UV	Ultraviolet
VLP	Virus-like particles
WHO	World Health Organization

Abstract

Vaccines are one of medicine greatest achievements, reducing the incidence of infectious diseases and eradicating otherwise fatal diseases worldwide. However, hepatitis B virus (HBV) infection is still a major global health concern and the most common cause of chronic liver disease and mortality from hepatocellular carcinoma. New generation vaccines are needed in order to overcome the limitations of the current HBV vaccines in the market. In this regard, mucosal immunization constitutes an attractive alternative to the available parenteral vaccine, especially in developing countries, since it would be best suited for mass immunization and would provide protection at the pathogen entry site.

The main objective of this thesis was to develop the next generation of HBV vaccines exploiting the immunomodulatory and mucoadhesive properties of chitosan-based delivery nanoparticles. This strategy would improve not only mucosal- and cell-mediated immunity, but would also allow the vaccine to be efficiently administered through the nasal mucosa. To achieve this goal, two different approaches were developed and tested. First, a novel prototypic system combining two well-established immunopotentiators, chitosan and aluminium salts, was produced to deliver hepatitis B surface antigen (HBsAg). Adjuvant combination has been considered a promising strategy to boost immunogenicity. The second approach involved the generation of a gene delivery system consisting of complexes of human serum albumin (HSA)-loaded chitosan nanoparticles with DNA (HSA-CH NP/DNA) encoding HBsAg. The two delivery systems were characterized and evaluated, both *in vitro* and *in vivo*.

In order to fulfill the main goal, we established a detailed methodology to easily obtain large quantities of endotoxin-free chitosan without modifying its immunomodulatory properties. Bacterial endotoxins content was assessed according to the recommendations of the International Council for Harmonization (ICH) guideline and validated with *in vitro* data.

Chitosan-aluminium nanoparticles (CH-Al NPs) were prepared using a nanoprecipitation technique; the optimal formulation exhibited a mean diameter of 280 nm and a positive surface charge, showing no cytotoxic effects in two different cell lines and in a primary culture of splenocytes, in the dose used for *in vivo* studies. *In vitro* uptake studies showed that CH-Al NPs were efficiently internalized by epithelial cells, demonstrating potential as a delivery system for a wide range of model antigens. Immunization studies showed that mice subcutaneously immunized with HBsAg adjuvanted with CH NPs displayed enhanced humoral and cellular immune responses.

To understand the underlying mechanisms of adjuvanticity of CH-Al NPs, the ability of CH-Al NPs to promote dendritic cell (DC) activation and their potential to stimulate innate and adaptive immune responses was assessed. Results were correlated to those obtained with chitosan in solution (CH sol.) and conventional chitosan particles (CH-Na NPs). All the formulations were capable of modulating Toll-like receptor (TLR)-9 agonist, CpG, induced cytokine secretion in bone-marrow derived dendritic cells (BMDCs) and induced DC maturation in the absence of cytokine production. After intraperitoneal (I.P.) injection, CH-Al NPs were capable of generating a local immune response comparable to that elicited by the vaccine adjuvant alum, with recruitment of neutrophils and eosinophils and concomitant disappearance of resident macrophages and mast cells. After vaccination with CH-Al NPs in combination with HBsAg, mice developed high antigen-specific immunoglobulin G (IgG) titers in the serum, as well as in nasal and vaginal washes, generating an overall improved immune profile in comparison to the commercially available vaccine Engerix-B.

In the second approach, a DNA vaccine was developed in which a plasmid coding for the HBsAg was adsorbed on the surface of the HSA-loaded CH NPs. The presence of HSA enhanced transfection activity and facilitated DNA release from the complex by weakening the interaction between positively charged nanoparticles and negatively charged plasmid DNA (pDNA). To assess *in vivo* the value of the developed formulation, immunization studies were conducted. Nasal immunization with HSA-CH NP/DNA complexes elicited high levels of serum anti-HBsAg IgG and antigen-specific IgA in nasal and vaginal secretions, while no systemic or mucosal responses were detected after immunization with DNA alone. These results confirm the ability of this novel delivery system to generate a mucosal immune response, making it a valuable adjuvant for nasal vaccination against HBV.

Overall, our findings add to our knowledge of the mechanism of action of chitosan-based formulations and illustrate that proper design is vital in order to generate an effective adjuvant for HBV vaccines, capable of driving mucosal immune responses in addition to potent humoral and cell-mediated immunity.

Keywords: nanoparticles, vaccines, chitosan, hepatitis B antigen, DNA, mucosal vaccination, nasal administration, adjuvant association.

Resumo

As vacinas são uma das maiores conquistas da medicina, reduzindo a incidência de doenças infeciosas e erradicando mundialmente doenças que outrora seriam fatais. Apesar de existir no mercado uma vacina profilática contra a hepatite B, a infeção pelo vírus da hepatite B (VHB) continua a ser um dos principais problemas de saúde pública e a causa mais comum de doença hepática crónica e mortalidade por carcinoma hepatocelular. É por isso necessário uma nova geração de vacinas que ultrapassem as limitações das vacinas contra o VHB atualmente no mercado. Nesse sentido, a imunização pelas mucosas constitui uma alternativa apelativa à vacina parentérica disponível, especialmente nos países em desenvolvimento, uma vez que seria mais adequada para imunização em massa e proporcionaria proteção no local de entrada do patogéneo, nomeadamente no caso de uma doença sexualmente transmitida.

Neste sentido, o principal objetivo desta tese consiste em desenvolver a próxima geração de vacinas contra o VHB explorando as propriedades imunomoduladoras e mucoadesivas de nanopartículas à base de quitosano. Esta nova vacina melhoraria não só a imunidade ao nível das mucosas e a mediada por células, como permitiria que a vacina fosse administrada de forma eficiente através da mucosa nasal. Para atingir este objetivo, duas estratégias diferentes foram desenvolvidas e testadas. Primeiro, foi otimizado um novo sistema protótipico de liberação do antigénio de superfície do vírus da hepatite B (HBsAg), combinando dois imunopotenciadores bem estabelecidos, o quitosano e os sais de alumínio, uma vez que a combinação de adjuvantes tem sido considerada uma estratégia promissora para potenciar a resposta imunológica; segundo, foram também desenvolvidos complexos de nanopartículas de quitosano carregados com albumina de soro humano (HSA) e complexados com ADN (HSA-CH NP/ADN), usados para estimular a resposta imune sistémica e nas mucosas após administração intranasal. Os dois sistemas de libertação de moléculas ativas foram caracterizados e avaliados quer *in vitro*, quer *in vivo*.

Para cumprir o objetivo principal, estabelecemos uma metodologia detalhada de modo a obter facilmente quitosano livre de endotoxinas, sem comprometer as suas propriedades bioquímicas. O conteúdo das endotoxinas bacterianas foi avaliado em conformidade com as recomendações da diretiva do Conselho Internacional de Harmonização (ICH) e validado com dados obtidos em estudos *in vitro*.

As nanopartículas de quitosano alumínio (CH-Al NPs) foram preparadas utilizando uma técnica de nanoprecipitação; a formulação otimizada exibiu um diâmetro médio de 280 nm e uma carga de superfície positiva, não apresentando efeitos citotóxicos em duas linhas celulares

diferentes e numa cultura primária de esplenócitos, para a dose utilizada posteriormente em estudos de imunização. Estudos de internalização *in vitro* demonstraram que as CH-Al NPs foram eficientemente internalizadas por células epiteliais exibindo potencial como sistema de libertação para uma ampla gama de antigénios modelo. Estudos *in vivo* mostraram que murganhos imunizados pela via subcutânea com HBsAg coadjuvado com CH NP apresentaram uma melhor resposta imune humoral e celular quando comparado com o grupo de murganhos vacinados apenas com o antigénio.

Para entender os mecanismos subjacentes de adjuvanticidade das CH-Al NPs, avaliou-se a sua capacidade para promover a ativação de células dendríticas (DC), e o seu potencial para estimular respostas imunes inatas e adaptativas. Os resultados foram correlacionados com os obtidos com quitosano em solução (CH sol.) e partículas de quitosano convencionais (CH-Na NP). Todas as formulações foram capazes de modular a secreção de citoquinas induzida por agonistas dos recetores tipo-Toll (TLR)-9, CpG, em células dendríticas derivadas da medula óssea de murganho (BMDCs) e induziram a maturação de DC na ausência de produção de citoquinas. Após a injeção intraperitoneal (I.P.), as CH-Al NPs foram capazes de gerar uma resposta imunitária local comparável à evocada por sais de alumínio usado com adjuvantes em vacina que se caracterizou por recrutar neutrófilos e eosinófilos e por um desaparecimento de macrófagos e mastócitos. Após a vacinação com CH-Al NP pela via subcutânea em combinação com HBsAg, os murganhos desenvolveram títulos elevados de anticorpos IgG anti-HBsAg no soro, bem como nas lavagens nasais e vaginais, gerando um perfil imunológico melhorado em comparação com a vacina comercialmente disponível, Engerix-B.

Na segunda abordagem foi desenvolvida uma vacina de ADN na qual um plasmídeo que codifica o HBsAg foi adsorvido na superfície das CH-NPs carregadas com HSA. A presença de HSA aumentou a atividade de transfecção e facilitou a libertação de ADN a partir do complexo, por enfraquecer a interação entre nanopartículas positivamente carregadas e o ADN carregado negativamente. Para avaliar o potencial da formulação desenvolvida foram conduzidos estudos *in vivo*. A imunização com complexos HSA-CH NP/ADN originou níveis elevados de anticorpos IgG anti-HBsAg e anticorpos IgA específicos contra o HBsAg nas secreções nasais e vaginais, enquanto não foram detetadas respostas sistémicas ou nas mucosas após imunização com ADN sozinho. Estes resultados demonstram o potencial deste novo sistema de administração em gerar uma resposta imune nas mucosas, tornando-o num adjuvante promissor para a vacinação nasal contra o HBV.

De modo geral, os resultados obtidos melhoram o nosso conhecimento de formulações à base de quitosano e demonstram que o design apropriado é vital para a formular um adjuvante

eficaz para vacinas contra o HBV, capaz de produzir respostas imune ao nível das mucosas além de potenciar imunidade humoral e celular.

Palavras-chave: nanopartículas, vacinas, quitosano, antigénio da hepatite B, ADN, vacina de mucosas, administração nasal, combinação de adjuvantes.

CHAPTER 1

Progress towards a needle-free hepatitis B vaccine

This chapter was adapted from:

Lebre, F., Borchard, G., de Lima, M. C. P., & Borges, O. (2011). Progress towards a needle-free hepatitis B vaccine. *Pharmaceutical research*, *28*(5), 986-1012.

1.1 Introduction

Hepatitis B is one of the most common infectious diseases in the world. It is estimated that 40 % of the world's population has had contact with or are carriers of the hepatitis B virus (HBV). This corresponds to an estimated 350 million HBV carriers [1]. About 780 000 persons die each year due to the acute or chronic consequences of hepatitis B [2]. Despite the availability of effective HBV vaccines, it remains a major global problem. This situation is particularly serious in developing countries, especially since a significant percentage of the population does not have access to the vaccine or do not return for the required booster doses. A number of approaches are being tested in order to minimize this problem and needle-free immunization appears to be the most attractive alternative.

Hepatitis B virus infection has a worldwide distribution, however at different levels of prevalence. According to the World Health Organization (WHO) the prevalence of chronic HBV infection is relatively low in North America, Australia, Northern and Western Europe and New Zealand (less than 1 % of the general population). Areas of high prevalence (5-10 %) include most of Asia (except Japan and India), the Amazon, the southern parts of Eastern and Central Europe and sub-Saharan Africa. The other areas of the globe show an intermediate HBV infection prevalence (Fig. 1.1).

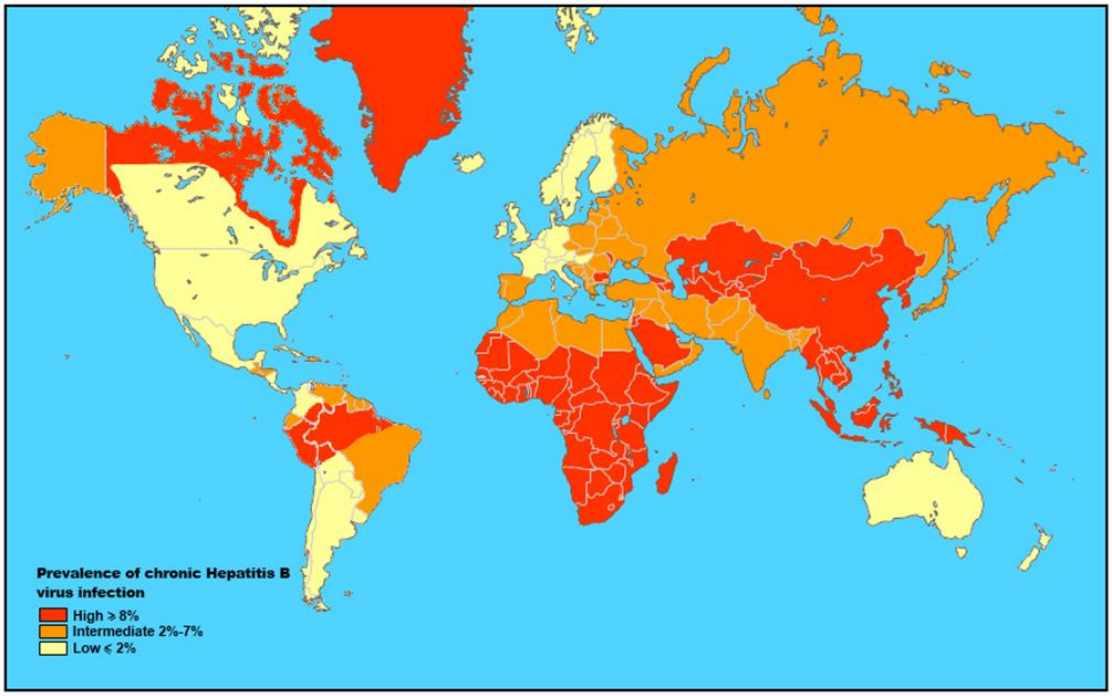

Figure 1.1 - Prevalence of chronic hepatitis B virus infection (Adapted from Center for Disease Control and Prevention Travelers' Health Yellow Book).

Hepatitis B is transmitted among persons by several routes which includes direct contact with the blood or body fluids of an infected person (blood transfusions; reuse of needles and syringes; unprotected sex with an infected person) or from an infected mother to her child at birth. The patterns of transmission vary among different parts of the world. In areas of high endemicity perinatal and person-to-person transmission are the major transmission routes and the greater part of the infections occur at early ages. In low prevalence areas the transmission essentially happens via unprotected sexual intercourse and injected drug use [2, 3]. The incubation period of HBV varies from one to four months after exposure. HBV causes both acute and chronic infections and between one-third and one-quarter of persons infected chronically with HBV are expected to develop long-term consequences such as cirrhosis, liver failure or hepatocellular carcinoma [3, 4].

In 1981 Food and Drug Administration (FDA) approved the first hepatitis B vaccine which was composed by the surface antigen of the hepatitis B virus present in the blood of human carriers of the infection. This plasma derived vaccine successfully immunized millions of individual worldwide until being replaced by a recombinant vaccine due to safety concerns. The currently available vaccine was introduced in the market in 1986 and represents the world's first subunit vaccine, the world´s first licensed vaccine against human cancer and the world's first recombinant expressed vaccine. The gene encoding the hepatitis B surface antigen (HBsAg) is expressed in yeast cells grown in bioreactors. The protein is collected and the HBsAg is induce to refold by chemical treatment to yield virus-like particles subsequently formulated for injection [5].

A great disadvantage of parenteral vaccines is that the immune response produced is mainly systemic and little or no mucosal immunity is elicited. Since mucosal surfaces are the main entry sites for virus and bacteria, mucosal immunization would provide the first line of defense, stimulating the secretion of immunoglobulin A (IgA) that avoids the attachment of the infectious pathogens to the mucosa. Furthermore, although hepatitis B vaccines already in the market are considered safe and effective, in order to maintain their efficiency vaccinees must receive three doses, which reduces patient compliance. In addition, trained medical personal to apply the vaccine and special storage conditions is required, which may pose a problem especially in developing countries. Taking these facts into account needle-free vaccination could have a big impact on the efficacy of immunization against HBV worldwide.

Although no well-established classification of adjuvants concerning needle-free immunization exists, for the sake of clarity in this thesis they will be divided into two major groups: delivery systems and immunopotentiators. Under the delivery system group, a

description will be made for adjuvants designed for mucosal (e.g. oral and nasal routes) immunization and some types of topical immunization.

Mucosal vaccination has been the common generic name attributed to the oral, intranasal, pulmonary, rectal and vaginal routes of vaccine administration. Mucosae, with a combined surface of about 400 m^2, [6] are undoubtedly the major site of entry for most pathogens. Therefore, these vulnerable surfaces are associated with a large and highly specialized mucosal immune system that protects the surface and the body against potential destructive agents and harmful substances from the environment. In a healthy human adult, this local immune system contributes almost 80 % of all immune cells [7]. These immune cells accumulate in a particular mucosa or circulate between various mucosa-associated lymphoid tissues (MALT), which together form the largest mammalian lymphoid organ system [6].

Mucosal vaccines are giving rise to some expectations as they are highly desirable from various perspectives. As noted above, one of the more significant advantages is the increasing evidence that local mucosal immune response is important for protection against disease, primarily for diseases originating on mucosal surfaces, such as HBV. According to some researches mucosal immune responses are in theory more efficiently induced by the administration of vaccines at mucosal surfaces, while injected vaccines are generally poor inducers of mucosal immunity and therefore less effective against infections at mucosal surfaces [8]. Parenteral vaccines generally tend to induce only systemic immune response and the antibodies produced in this kind of response are not capable of conferring adequate protection at the level of the mucosa. Moreover mucosal immunization tends to be considered as an attractive substitute to parenteral immunization as it can stimulate both humoral and cell mediated response and induce mucosal and systemic immunity simultaneously [9]. Cellular and humoral immune responses to HBV antigens are thought to play a crucial role in the elimination of virus by the host. On one hand, humoral immune response leads to defense against infection; on the other hand cellular immune response, associated with the activation of the CD8+ cytotoxic T lymphocytes (CTL), has been reported to be one of the key factors contributing to virus elimination from infected hepatocytes and may play an important role in the pathogenesis and severity of hepatitis and the succeeding development of chronic liver disease [10-13]. CTL can protect the organism against intracellular pathogens because it is able to induce target cells to undergo apoptosis and secret important cytokines (e.g. IFN-γ and TNF-α) [14]. Most non-replicating vaccines administered by intramuscular injection are unable to induce this type of CTL-mediated immune response.

Some types of topical vaccine administration can also be included in the needle-free immunization group. The skin is one of the largest immune organs; it is considered an immunologically attractive target for immunization and a promising vaccination route. The skin is full of antigen presenting cells (APCs) such as Langerhans cells (LCs) in the epidermis and dermal dendritic cells (DDCs) in dermis (Fig. 1.2) [15-17]. Their main function is to capture and process antigen, present it to other cells of the immune system, which then activate a specific T cell mediated response [16, 17]. Antigen presenting cells can stimulate T-lymphocytes and B-lymphocytes, thus making the skin a highly efficient location for the beginning of a cellular and humoral response [18-20]. Unlike the skin, muscle tissue lacks large quantities of APCs and therefore intramuscular (I.M.) injections fail to elicit a good sufficient cell-mediated immune response [15].

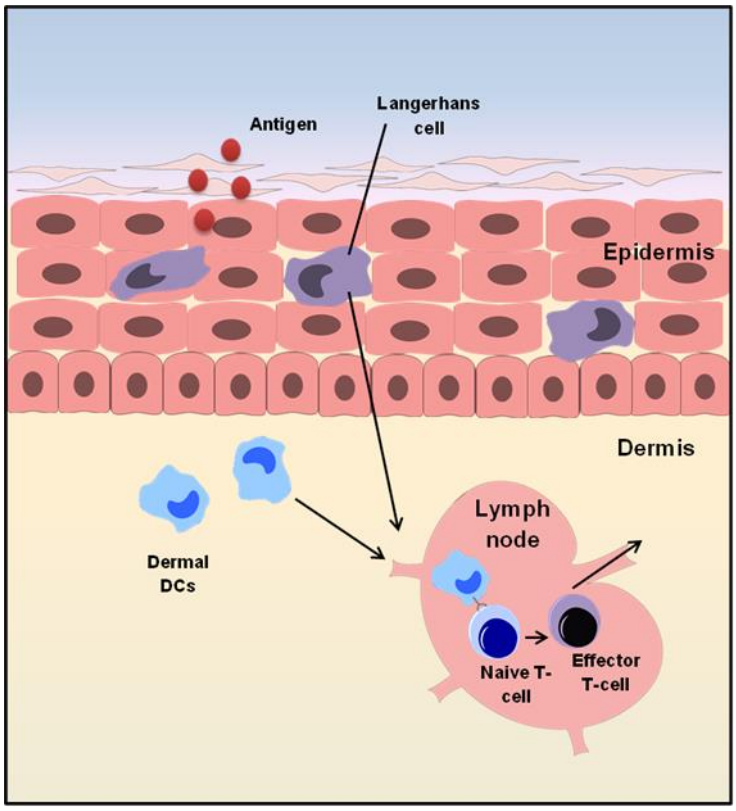

Figure 1.2 - The skin is full of antigen-presenting cells, such as Langerhans cells, in the epidermis and dermal dendritic cells in dermis. Their main function is to capture and process antigen and present it to naïve T cells, which then activate a specific T cell-mediated response.

1.2 Recent advances in the development of a needle-free hepatitis B vaccine

Needle-free immunization is attracting an increased attention by the scientific community because of the advantages associated with it [21, 22]. Although needle-free vaccines pose some

attractive features when compared to parenteral immunization, there are still some inconveniences related to it. Vaccines administered mucosally encounter the same host defense barriers as do microbial pathogens and other foreign macromolecules: they are diluted in mucosal secretions, detained in mucus gels, attacked by acid, proteases and nucleases and barred by epithelial barriers. Therefore, it is estimated that large doses of antigen would be required in order to archive an efficient transport and uptake by MALT where antigens can be processed and presented [23]. In addition it is also necessary to overcome the problem of immunological tolerance. Mucosal surfaces are in a permanent state of alert, but they adapt to the presence of foreign microorganisms. As a consequence, vaccines that produce a strong immune response if injected in sterile tissues such as muscle could be disregarded when administered through mucosal surfaces [8]. This state of unresponsive or so-called immunological tolerance is dependent on the route, frequency of antigen administration and dose [24, 25] and has been recognized as one of the biggest challenges for mucosal vaccine development. Nasal immunization presents some other disadvantages. One of the most important limitations of nasal immunization is the general rapid clearance of the vaccine formulation in the mucosal surface owing to the mucociliary clearance. Also new evidences suggest the existence of antigen transfer to neuronal tissue via olfactory bulb present in the nasal cavity which can lead to potential side effects [26, 27]. In fact, some nasal vaccine systems were linked to serious clinical manifestation such as Bell's palsy syndrome. It was reported that the inactivated I.N influenza vaccine used in Switzerland during 2000–2001 increased the risk of Bell's palsy among vaccinated individuals. In contrast, no significant risk of the adverse event was found to be associated with the parenteral influenza vaccines [26, 27]. Finally, topical immunization has some difficulties to overcome as well as skin forms a protective barrier that is difficult to penetrate.

To circumvent or minimize these problems adjuvants are used. Adjuvants have traditionally been defined as agents added to vaccine formulations to enhance the immunogenicity of antigens *in vivo*. A proposed revision of this definition [28] divides adjuvants into two classes: delivery systems and immunopotentiators, based on their dominant mechanism of action. Both, delivery systems and immunopotentiators are able to augment the antigen-specific immune response *in vivo*, and it is becoming common using them together to develop multi-component adjuvants with the potential to act synergistically. Many adjuvants were tested in order to create an efficient needle-free vaccine against hepatitis B (Tables 1.1-1.4).

Table 1.1 - Delivery systems for mucosal immunization against HBV.

Adjuvant	Type of vaccine	Route	Dose	Immunization schedule	Results	Ref.
Lipid microparticles	Sub-unit vaccine	I.N.	10 μg HBsAg	1,2,3 days; 21st day	Mice developed strong systemic and mucosal immunity.	[29]
Lectinized liposomes	Sub-unit vaccine	Oral	10 μg HBsAg	1,2,3 days; 21st day	Vaccine induced improved systemic, mucosal and cell mediated immunity.	[30]
Chitosan coated liposomes	DNA vaccine	I.N.	100 μg of pDNA	0 weeks; 2 weeks	Vaccine induced good systemic, mucosal and cell mediated immunity.	[31]
Liposome	Sub-unit vaccine	I.N.	10 μg HBsAg	0 day	Increased mucosal responses.	[32]
Bilosomes	Sub-unit vaccine	Oral	3 groups: 10/20/50 μg HBsAg	1,2,3 days; 21st day	Higher dose of vaccine (50 μg) elicited anti-HBsAg titers similar to the ones obtained with commercial vaccine.	[33]
Bilosomes	Sub-unit vaccine	Intra-gastric	20 μg HBsAg	1,2,3 days; 21st day	Increased systemic and mucosal responses.	[34]
ISCOMS	Sub-unit vaccine	I.N.	10 μg HBsAg	0 weeks; 3 weeks; 6 weeks	Vaccine induced a mixed Th1/Th2 response and enhanced specific IgA.	[35]
Mannosylated niosomes	DNA vaccine	Oral	100 μg of pDNA	0 weeks; 3 weeks	The delivery system induced considerable humoral and cellular immune response.	[36]
Nanoemulsion	Sub-unit vaccine	I.N.	20 μg HBsAg	0 weeks; 6 weeks	Vaccine was immunogenic in all species tested. Good Th1-type cytokine production.	[37]
Nanoemulsion	Sub-unit vaccine	I.N.	20 μg HBsAg	0 weeks; 3 weeks; 6 weeks	Delivery system skewed immune response to Th1 and enhanced specific IgA.	[38]
Supramolecular biovector (SMBV™)	Sub-unit vaccine	I.N.	0.2 μg and/or1 μg and/or 3 μg and/or 10 μg according to the assay	0 weeks; 3 weeks 6 weeks (not all groups received it)	Mice immunized with antigen formulated with SMBV™ developed strong systemic, mucosal and cellular immunity.	[39]
Alginate-coated CH NP + CpG	Sub-unit vaccine	Oral	10 μg HBsAg + 10 μg CpG ODN	0 weeks; 3 weeks	Humoral and cellular immune response were better in mice vaccinated with the formulation combining the delivery system and the immunopotentiator.	[40]
Alginate-coated CH NP + CpG	Sub-unit vaccine	I.N.	10 μg HBsAg + 10 μg CpG	0 weeks; 3 weeks 6 weeks	The delivery system in combination with the immunopotentiator in solution gave rise to systemic and mucosal immunity.	[41]
Chitosan nanoparticles	DNA vaccine	I.N.	50 μg of plasmid loaded chitosan nanoparticles	0 weeks; 2 weeks	The delivery system elicited good humoral, mucosal and cellular responses.	[42]
LTA-chitosan nanoparticles	Sub-unit vaccine	Oral	10 μg HBsAg	0 weeks; 2 weeks	Stronger humoral and cell mediated immune response.	[43]
CH/TMC NP	Sub-unit vaccine	I.N.	2/10 μg HBsAg	1 day; 21st day	TMC NP induced enhanced levels of antigen specific antibodies over CH NP.	[44]
CH/TMC NP	Sub-unit vaccine	I.N.	10 μg HBsAg	1 day; 14th day	TMC and CH were equally potent mucosal adjuvants.	[45]
PLGA microparticles	DNA vaccine	Oral	20 μg or 200 μg of plasmid loaded PLGA microparticles	0 weeks;	Mice developed systemic, mucosal and cellular immune responses in a dose-dependent manner.	[46]
Surface modified PLGA microspheres	Sub-unit vaccine	I.N.	10 μg HBsAg	0 weeks; 4 weeks	Vaccine induced good systemic, mucosal and cell mediated immunity. Surface modified formulation elicited significantly higher immune response compared to the non-modified.	[47]
PLG microparticles	Sub-unit vaccine	Oral	100 μg of BCEM	0 weeks;	Vaccine induced good systemic immune response. Mice were I.M. infected with HBsAg which lead	[48]

					to a rapid and vigorous production of antibodies.	
M-cell targeted PLGA nanoparticles	Sub-unit vaccine	Oral	10 µg HBsAg	1,2,3 days; 21st day	The delivery system elicited good humoral, mucosal and cellular responses. M-targeted stabilized formulation elicited significantly higher immune response compared to the non-targeted.	[49]
Triblock copolymer based nanoparticles	Sub-unit vaccine	I.N.	10 µg HBsAg	0 weeks;	Copolymer nanoparticles elicited good systemic and mucosal immunity. The biphasic response of the formulations might have worked as a booster dose.	[50]
Lectin-PLGA particles	Sub-unit vaccine	Oral	10 µg HBsAg	0 weeks; 2 weeks	Delivery system increased IgG class switching and stronger cellular and mucosal responses.	[51]
Coated PLGA particles	Sub-unit vaccine		10 µg HBsAg	1 day; 21st day	Coating promoted antigen uptake on nasal mucosa and an overall better immunological profile.	[52]
Triblock copolymer based nanoparticles	Sub-unit vaccine		20 µg HBsAg	1st day	Copolymer nanoparticles elicited good cellular and mucosal immunity.	[53]
PLGA particles	Sub-unit vaccine		10 µg HBsAg	1 day; 14th day	Particles with positive charge originated significantly better immune response.	[54]
PLGA/PLA particles	Sub-unit vaccine		10 µg HBsAg	1 day; 14th day	Less hydrophilic particles were more internalized which resulted in an improved immune response.	[55]
Salmonella typhimurium	Sub-unit vaccine	I.N.	1 - 1x10^8 CFU of bacterial suspension	0 weeks;	Higher doses induced better systemic and mucosal immune response Nasal administration proved more efficient than oral immunization.	[56]
Salmonella typhimurium	DNA vaccine	Oral	6x 10^9 bacterial cells	0 weeks	Mice developed a strong cellular response but weak humoral immune response. Potential use as therapeutic vaccine.	[57]

1.3 Delivery systems

Delivery systems have two main functions: they help protect the vaccine while inside the body and also help target it to the site of immune function. In recent years several approaches have been designed and tested in order to develop an effective delivery system for mucosal or topical immunization.

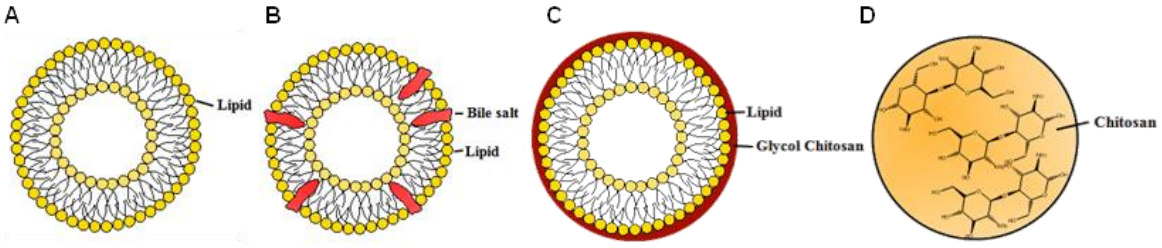

Figure 1.3 - Delivery systems tested for mucosal immunization against hepatitis B. (A) liposome; (B) bilosome; (C) modified liposome; (D) chitosan nanoparticle.

1.3.1 Delivery systems for mucosal immunization

1.3.1.1 Lipid particles

The ability of liposomes to act as adjuvants was first described in 1974 by Allison and Gregoriadis and since then they have been broadly studied. Liposomes are composed of

naturally occurring, biodegradable lipids organized into bilayer membranes surrounding an aqueous core (Fig. 1.3 A) [58]. A great variety of substances can be associated in liposomes, regardless of solubility, charge, size or shape so long as they do not interfere with liposome formation [59]. Although they can promote antigenic responses to various antigens, there are some problems related to their physical and chemical stability. In order to overcome these limitations researchers developed different approaches.

Lipospheres, also known as solid lipid microparticles (SLM), are relatively more stable than liposomes at room temperature and thus more suitable to act as vesicle carriers. These particles consist of a solid fat core based on naturally occurring lipids and stabilized by a layer of surfactant molecules on the surface [60]. SLMs combine the benefits of liposomes and polymeric microparticles, at the same time as avoid various of their drawbacks, such as instability, toxicity, biodegradability problems and production costs [60-62]. Moreover, they are excellent in controlling and sustaining drug release efficiency. Saraf et al. prepared and optimized lipospheres for intranasal delivery of HBsAg [29]. Researchers tested two sets of lipid particles, one containing the cationic polymer stearylamine in the formulation (LMST) and one without it (LM). LMST was shown to be more rapidly taken up by the alveolar macrophages than LM. LMST also revealed considerable stronger mucoadhesion than LM. They suggested that stearylamine imparts cationic charge on to the particle surface, which may lead to a stronger interaction with negatively-charged sialic groups of the mucus. This fact may also explain the localized uptake of LMST. Immunological studies were conducted immunizing mice with different formulations (LM, LMST; Alum-HBsAg; plain HBsAg) by different intranasal (I.N.) or intramuscular routes. In general, LMST formulation proved to be the best. In fact, mice vaccinated with LMST developed strong systemic and mucosal immunity. IgG and IgA levels induced by lipid microparticles without stearylamine were always lower than the ones induced by the particles that contained the cationic polymer. Better mucoadhesive properties displayed by LMST were again pointed out as the reason for these superior results, showing that the use of stearylamine in the lipidic formulation further enhanced the adjuvant capacity of this delivery system.

In order to increase transmucosal uptake in the Peyer's patches, Gupta et al. encapsulated HBsAg into liposomes and conjugated them with the lectin *Ulex europaeus* agglutinin 1 (UEA-1). Lectins are proteins, which specifically and reversibly bind carbohydrates. Lectin receptors are expressed on numerous types of cells; one of those is the specialized epithelial cell, microfold-cell (M-cell), responsible for the uptake and transport of antigens. Lectins allow specific targeting of the particles to these areas of antigen uptake and thus having a greater

chance to inducing stronger immune responses, making it an important target for oral vaccines. *Ex vivo* studies showed that lectinized liposomes specifically targeted carbohydrate receptors of the M-cells, while non-lectinized formulations displayed low level of adhesion. As anticipated, only mice orally immunized with the lectinized formulation containing 10 μg of HBsAg developed comparable serum IgG titers to mice receiving an I.M. injection with alum-adjuvanted vaccine, as well as elevated serum IgA titers and increased production of the Th1-associated cytokines IL-2 and IFN-γ, following antigen restimulation of splenocytes, highlighting the importance of Peyer's patch M-cell targeting in the context of oral immunization [30].

A different strategy to increase mucosal uptake was developed by Tiwari and coworkers. They encapsulated HBsAg within liposomes and decorated their surface with the influenza virus envelope protein hemagglutinin (HA), which is involved in the transport of influenza virus across the mucosa. The adsorption of the HA on the surface of liposomes resulted in an overall better immune response [32].

1.3.1.2 Modified liposomes

A recently published study evaluated the potential of surface modified liposomes for nasal immunization [31]. The group prepared glycol chitosan coated liposomes and loaded them with DNA containing pRc/CMV-HBs(S) (Fig. 1.3 C). Chitosan is known for its mucoadhesive properties [63] and thus the addition of this polymer to the formulation is advantageous for creating an intranasal formulation with prolonged local retention. Uncoated liposomes were found to retain less mucin and have less adherence extent compared to coated ones. To test the immunological response mice were immunized with surface modified glycol chitosan coated liposomes, as well as with "naked" DNA (I.N. and I.M.), uncoated liposomes (I.N.) and conventional alum-based vaccine (I.M.). Immunization with the novel delivery system resulted in lower anti-HBsAg titers compared to intramuscular immunizations with either plain DNA or conventional vaccine. Nevertheless, all mice developed clinically protective levels of antibodies after a couple of weeks. On the other hand, only glycol chitosan treated mice had high levels of sIgA in nasal, salivary and vaginal secretions, while I.M. immunization failed to elicit any significant mucosal immune response. In addition, glycol chitosan coated liposomes induced high levels of IFN-γ and IL-2, indicative of strong cell-mediated response with a Th1-like profile. In all immunological assays coated liposomes tended to produce superior responses than uncoated ones, emphasizing the idea that mucoadhesive properties of chitosan are important for I.N. administration. As expected, recombinant alum-based vaccine

induced a strong humoral response but failed to elicit a good mucosal and cell mediated immune response, important for developing not only a prophylactic vaccine but a therapeutic one, whereas surface modified liposome formulation produced an overall better immunological response.

1.3.1.3 Bilosomes

Lipid vesicles are especially vulnerable to the detergent effect of interstitial bile salts that leads to membrane disruption and vesicle lysis [64]. In order to overcome this problem Conacher and coworkers developed bilosomes [65]. Bilosomes utilize nonionic surfactant vesicle (NISV) technology, which are liposome-like structures of extremely low toxicity that are capable of stimulating humoral and cellular immune response and include bile salts in their formulation, which stabilize the vesicle preparation and prevent premature release of the antigen (Fig. 1.3 B) [65, 66].

Bilosomes showed potential as carrier systems for oral immunization [65, 67, 68] and therefore were tested to develop an oral vaccine for hepatitis B [33]. They prove to be stable in simulated gastric fluid (SGF), as well as in simulated intestinal fluid (SIF) and at different bile salt concentrations. Antibody titers after oral immunization (10, 20 and 50 μg HBsAg/dose) were compared with titers obtained after I.M. immunization (10 μg /dose). Results show that mice receiving the highest orally administrated antigen dose (50 μg) achieved anti-HBsAg titers similar to the ones obtained with the alum-based vaccine. Moreover, all orally administered formulations generated higher sIgA levels, while conventional alum based vaccine failed to elicit a mucosal immune response. The same group later developed an improved formulation, conjugating bilosomes with cholera toxin B subunit (CTB) in order to enhance transmucosal uptake via M-cell. Contrary to non-conjugated bilosomes, with this new strategy the authors were able to efficient target M-cells in the gut-associated lymphoid tissue (GALT), which resulted in enhanced immunogenicity with a lower dose of HBsAg (20 μg instead of 50 μg), proving the potential for targeted oral immunization against hepatitis B [34].

1.3.1.4 Mannosylated niosomes

Niosomes are uni- or multilamellar vesicles formed from synthetic, non-ionic surfactant of alkyl or dialkyl polyglycerol ether class, offering an alternative to liposomes as drug carriers because of their increased chemical stability [69]. The adjuvant capacity of theses nonionic surfactant vesicles have been shown for a long time, [70, 71] but only recently have they been

used to create delivery systems for a HBV oral vaccine. This has to do with the vulnerability of these vesicles to bile salt and enzymatic degradation [36]. In order to overcome this problem, Jain and coworkers improved the plain niosome formulation by coating them with O-palmitoyl mannan (OPM), which confer them protection, and also target the mannose receptors expressed in macrophages and dendritic cells [36]. Plain niosomes and coated niosomes were compared in terms of their stability in both SGF and SIF, demonstrating that the uncoated formulation suffered a significantly higher loss of vesicle and DNA content. Immunological response was assayed after I.M. administration of both HBsAg and DNA and oral immunization with naked DNA, plain niosomes and OPM coated niosomes. Although intramuscular vaccination with HBsAg initially elicited higher IgG levels, those levels started to decline after the fourth week and I.M. vaccination with DNA started to exhibit superior levels. DNA vaccines require more time to elicit higher antibody levels because DNA needs to be transfected and translated before the antigen is expressed. OPM-coated niosomes induced higher anti-HBsAg titers compared to plain niosomes, possibly because of the protection and targeting effect conferred by the OPM coating. In spite of the high dose of pDNA administered (100 μg), when compared with that used in previous studies, mucosally applied formulations induced statistically lower antibody levels compared to I.M. immunization. In contrast, I.M. formulations failed to elicit detectable sIgA levels, while OPM coated and plain niosomes efficiently induced it. Cellular responses (IL-2 and IFN-γ) were only present in mice vaccinated with DNA vaccines.

1.3.1.5 ISCOMs

Immunostimulating complexes or ISCOMs are spherical, cage-like particles that are approximately 40 nm in diameter and can be composed of several different materials. Classical ISCOMs result from a mixture of saponins from *Quillaia saponaria*, (QuilA) cholesterol, phospholipids and amphipathic proteins. Studies have shown that ISCOMs are particularly potent at inducing CD8+ T cell activation in mice [72, 73] and to some extent in humans [74], leading to the development of an adaptive immune response. Pandey and colleagues incorporated HBsAg into ISCOMs originating particles with average size of 44.1 nm and negative zeta potential (−21.7 mV). Mice were I.N. immunized with 10 μg of HBsAg combined with increasing concentrations of ISCOMs at day zero and boosted after 3 and 6 weeks. Results demonstrated that a dose of 5 μg of ISCOMs was sufficient for animals to seroconvert and this response plateaued for doses above 15 μg of ISCOMs. Serum anti-HBsAg IgG titer after three nasal immunizations with ISCOMs originated comparable titers

to alum-HBsAg administered subcutaneously, nevertheless serum IgG subclass showed that intranasal HBsAg.

ISCOM immunization gave rise to a mixed Th1/Th2 response, as well as mucosal immune response illustrated by the presence of IgA in the bronchoalveolar lavage (BAL) [35].

1.3.1.6 Nanoemulsion

A nanoemulsion-based hepatitis B mucosal vaccine was tested for nasal administration [37]. Nanoemulsions (NE) are water-in-oil formulations stabilized by small amounts of surfactant. They proved to have wide biocidal efficacy against bacteria, enveloped viruses, and fungi [75] and their potential as non-toxic mucosal adjuvants for other antigens was previously demonstrated [76-79]. Researchers tested the immune response to the mucosal vaccine composed by a mixture of recombinant hepatitis B surface antigen and nanoemulsion adjuvant (HBsAg-NE). Mice were vaccinated with 20 ug of HBsAg co-administered with either 20 % of NE (I.N.) or aluminium hydroxide (I.M.). Both vaccines produced equivalent protective levels of anti-HBsAg IgG antibodies, but the alum based vaccine produced higher levels of IgG1 subclass antibodies associated with a Th2 response, while HBsAg-NE immunization produced mostly IgG2b (and some IgG2a antibodies) related to a Th1 response. Mucosal and cellular responses were characterized in bronchioalveolar lavage. The nanoemulsion based vaccine induced considerable mucosal immunity as well as high production of Th1-type cytokines (IFN-γ and TNF-α). The immunogenicity of the vaccine was also tested in rats and guinea pigs with both species developing high anti-HBsAg IgG titers. Given the promising results, the same group later evaluated the ability of NE to switch an established Th2 immune responses induced after alum injection to a more balanced Th1/Th2 profile. Mice intranasally immunized with a single dose of HBs-NE at 2 or 6 weeks after two rounds of I.M. HBs-alum sensitization exhibited a notorious increase in IgG2a and IgG2b subclasses, along with an increase in IFN-γ and IL-17 and a decrease in IL-4 and IL-5 levels, compared to mice receiving just 2 rounds of I.M. injections with 20 μg of HBs adsorbed on alum, suggesting that NE adjuvant may be useful to induce antigen-specific Th1 immune responses even in individuals with pre-existing Th2 biased immunity [38]. Overall, HBsAg-NE proved to be safe, stable and an effective mucosal adjuvant.

1.3.1.7 Cationic particles

Researchers tested the ability of supramolecular biovector (SMBV) cationic nanoparticles to work as delivery systems for HBsAg [39]. SMBVs particles were first described in the mid-

90's [80]. They are composed by a hydrophilic internal core surrounded by a lipophilic external layer [81, 82]. This structure allows the entrapment of various substances, such as antigens, facilitating their delivery to APCs. SMBVs were found to be highly muco-resident in nasal mucosa, [83] making them better adjuvants for intranasal administration. In order to test the potential of SMBVs nanoparticles, humoral, mucosal and cellular immune responses were studied following intranasal vaccination of mice with different antigen doses (1, 3, 10 μg) either alone or in association with SMBV nanoparticles. After 3 immunizations all SMBV formulations produced high levels of specific serum IgG antibodies in contrast to free HBsAg formulation that could only elicit small antibody titers and with the maximal dose (10 μg). Similar results were obtained with IgA antibodies and CTL responses. Anti-HBsAg IgG1 and IgG2 isotypes were also determined demonstrating a mixed Th1/Th2 profile.

1.3.1.8 Chitosan nanoparticles

The term chitosan is applied to a family of deacetylated chitins and is the only largely available cationic polysaccharide. It has been considered a non-toxic, biodegradable and biocompatible polymer [84], so a lot of research has been directed towards its use in medical applications such as drug and vaccine delivery [85-88]. One major advantage of this polymer is its ability to easily produce nanoparticles under mild conditions (room temperature) without the application of harmful organic solvents. This has been one of the main reasons for its wide applicability to the encapsulation of different molecules such as DNA and antigens. Chitosan is also known to be mucoadhesive [63]. At physiological pH, sialic acids present in mucus have a negative charge and, as a consequence, positively charged chitosan exerts strong electrostatic interaction with them. Chitosan is widely used and its ability to stimulate cells of the immune system has been shown in numerous studies [89-92]. These unique features make chitosan an attractive polymer to create a novel delivery system for a mucosal vaccine against HBV (Fig. 1.3 D).

Alginate coated chitosan nanoparticles were synthesized and tested for their ability to work as a delivery system for mucosal immunization against HBV [40, 41, 93]. Alginate is a biodegradable and biocompatible natural polysaccharide polymer with negative charge capable of modifying antigen release from chitosan nanoparticles. Moreover, it showed to protect the antigen from enzymatic degradation. The delivery system was composed of a chitosan core, to which the antigen was adsorbed, and was subsequently coated with sodium alginate, all under mild conditions. To further improve the immunological capacities of the delivery system, the Toll-like receptor (TLR)-9 agonist CpG was added to the formulation. Alginate-coated

chitosan nanoparticles have been shown to be non-toxic and their ability to be taken up by M-cells of Peyer's patches was demonstrated in rats [94]. Immunological studies were conducted in different treatment groups. Mice orally immunized with alginate coated nanoparticles loaded with 10 μg of HBsAg, with or without the addition of CpG (10 μg), were able to elicit protective antibody levels after a booster dose. Addition of CpG was proven beneficial as it augmented the number of responder mice, but only when the immunopotentiator was encapsulated inside the nanoparticles. IgG subclass profiling revealed that immunization with HBsAg loaded nanoparticles induced a Th2-like profile, or a mixed Th1/Th2-like response after boost. On the other hand, when CpG motifs were co-administered while inside the nanoparticles, a Th1-like profile was elicited, due to CpG capacity of re-directing Th bias [95, 96]. Mice immunized with plain antigen failed to elicit a mucosal immunological response, even when co-administered with CpG ODN, while in all the other treatment groups detectable sIgA levels were induced. Subsequent studies were carried out by our group using a similar delivery system, this time for nasal administration of HBsAg [41]. Systemic, mucosal and cellular responses were evaluated. Animals were immunized with 15 μl of different formulations. Subcutaneous (S.C.) administration of a current licensed vaccine was used as positive control. Mice parenterally vaccinated elicited the highest anti-HBsAg IgG titers but failed to develop detectable sIgA levels in nasal and vaginal washes, as well as in feces. Upon nasal immunization, only animals vaccinated with formulations containing CpG were able to produce a systemic response suggesting that an immunopotentiator is required for effective immunization by the nasal route with alginate coated nanoparticles. Contrary to the previous report, this time higher IgG titers were detected in groups nasally immunized with formulations where CpG was not associated with the nanoparticles. Evaluation of IgG subclasses demonstrated a predominant Th2-like response in seroconverted mice vaccinated with the commercial vaccine versus a mainly Th1-like response elicited by the other two groups. Regarding mucosal immunization all treatment groups developed quantifiable sIgA levels with the exception of the above mentioned S.C. immunized mice and the unvaccinated ones, once again demonstrating that mucosal immunization was needed in order to elicit a mucosal immune response. Quantification of IFN-γ showed that all nasally vaccinated animals developed higher interferon levels compared to the control group. Overall, the best results were obtained upon nasal administration of chitosan nanoparticles loaded with the antigen plus CpG in solution or with plain HBsAg co-administrated with the immunopotentiator in phosphate buffer saline (PBS).

As mentioned before, an interesting strategy to boost the immune response is the combination of lectins with a delivery system in order to increase mucosal residence time of the formulation and target M-cells to promote transmucosal particle uptake. Conjugation of *Lotus tetragonolobus* (LTA) lectin to CH NPs led to increased M-cell binding in the Peyer patches and resulted in stronger humoral and cell-mediated immune responses [43].

Chitosan has gained attention as a non-viral gene delivery system. Khatri et al. developed chitosan nanoparticles loaded with DNA encoding surface protein of HBV [42] for nasal administration. This group chose the intranasal route bearing in mind chitosan's mucoadhesive properties. To test the potential of the nanoparticles, immunization studies were conducted. Mice were immunized with different formulations and by different routes. Higher anti-HBsAg titers were elicited after I.M. immunization with either recombinant alum-based vaccine or plain DNA in comparison to I.N. immunization with chitosan nanoparticles loaded with DNA or "naked" DNA. Nevertheless, nasal administration of plasmid DNA loaded chitosan nanoparticles was able to elicit seroprotective levels in all mice. In contrast, sIgA levels were induced only upon intranasal immunization, while I.M. formulations failed to elicit them. Statistically higher levels were produced in mice immunized with DNA loaded in chitosan nanoparticles rather than DNA alone. Authors suggested that chitosan-DNA nanoparticles adhere to nasal or gastrointestinal mucosa and are more easily transported to MALT and thus might be taken up by M-cells and induce strong mucosal immune responses. IFN-γ and IL-2 levels revealed a dominant Th1-like profile, which is advantageous for the eradication of HBV. In general, chitosan nanoparticles loaded with DNA showed to elicit good humoral, mucosal and cellular responses, once again demonstrating the potential of this polymer to create an effective delivery system for mucosal immunization against HBV.

Chitosan possesses unique characteristics that make it an attractive candidate for mucosal vaccination; however it is not soluble at physiological pH and several chitosan derivatives, like N-trimethyl-chitosan (TMC), have been synthesized. One group reported that intranasal vaccination with TMC particles resulted in enhanced levels of antigen-specific antibodies compared to chitosan NPs, which authors attributed to a slower clearance rate on the nasal mucosa [44]. However, a separate group observed no differences between both formulations, stating they were equally good mucosal immunoadjuvants against hepatitis B [45].

1.3.1.9 Polymers of lactic and glycolic acids

A number of different polymers have been used to formulate nanoparticulate drug carriers. Among them are the homo- and copolymers of lactic and glycolic acids: poly(lactic acid)

(PLA), poly(glycolic acid) (PGA) and poly(lactide-co-glycolic acid) (PLGA). These polymers have several attractive features such as being non-toxic for humans, tissue compatible, biodegradable and having an adjustable degradation rate [50, 97-99], as well as adjuvant effect in antibody induction [100], but they are not deprived of disadvantages. The synthesis of particles using these polymers requires the use of organic solvents and high shear stress, which affects the antigen integrity. Also the low pH caused by the degradation of the polymer affects the antigen [47, 99, 101, 102]. Notably, PLGA is a FDA-approved biopolymer.

With PLGA microparticles demonstrating good results in eliciting not only systemic but also mucosal immune response after oral delivery, with virus such as HIV [103, 104] and rotavirus [105], He and coworkers decided to develop PLGA microparticles containing DNA encoding HBsAg for oral immunization [46]. Authors proposed that PLGA microparticles act by protecting the antigen from degradation and by promoting a direct delivery to APCs, thus promoting uptake by APC. They compared antibody (IgG and IgA), IFN-γ and CTL levels after I.M. or oral delivery of naked or PLGA-encapsulated DNA (20 or 200 μg per mouse). Orally administered "naked" DNA showed minor immunogenic response, because DNA was exposed to the harsh environment of the stomach and thus was degraded demonstrating the need for protection when given by the oral route. A dose of 20 μg of DNA encapsulated in the PLGA microparticles was able to induce HBsAg-specific antibodies to levels comparable to those induced by I.M. injection of 200 μg of naked DNA. Considerably higher levels were induced when DNA loading of the nanoparticles was increased to 200 μg. Also fecal IgA was detected in mice immunized with PLGA encapsulated DNA contrary to mice immunized I.M., where no IgA response was detected. These two facts proved that this kind of vesicular carriers are able to elicit both systemic and mucosal immune responses. It is accepted that a Th1-like response is important for the elimination of the virus from infected cells and it is associated with CTL activity and IFN-γ production [106]. Induction of IFN-γ responses to the antigen were only achieved when mice were immunized orally with PLGA nanoparticles encapsulating the antigen, whereas the levels achieved with I.M. immunization were almost negligible. Results were similar to the ones obtained with CTL where a much stronger response was reached by oral immunization rather than by I.M. Results show the potential of PLGA microparticles for oral vaccination, as they were able to induce mucosal and systemic cellular and humoral responses.

Another approach using PLGA as a polymer for the development of a novel vaccine carrier system was the development of surface-modified DL–lactide/glycolide copolymer microspheres with chitosan for nasal administration [47]. Researchers improved previous

PLGA formulations by the addition of trehalose, which is a protein stabilizer. As said before, when preparing PLGA nanoparticles the use of organic solvents is necessary. These solvents may affect the antigen integrity. Trehalose acted as a shield preventing protein from getting into contact with the solvent. The addition of chitosan to the surface of the PLGA microspheres also has advantages; it resulted in the shift of the zeta potential from negative to positive, which promoted bioadhesion of the positively charged microspheres to the mucin network in the nasal cavity and thus reduced the nasal clearance rate. Anti-HBsAg levels were determined in the serum, showing that nasal administration of modified PLGA microspheres with or without cholera toxin B, after a booster dose, were similar to the ones obtained with alum-HBsAg vaccine injected subcutaneously. Furthermore, when IgA, IL-2 and IFN-γ levels were measured in different secretions (vaginal, nasal and salivary), they were negligible after S.C. immunization with alum adsorbed HBsAg vaccine. In contrast, modified PLGA microspheres (after booster dose) showed significant levels of those molecules. Authors concluded that modified PLGA microspheres had potential as vesicular carriers for HBsAg as they were able to protect it until uptake, eliciting good mucosal, cellular and humoral responses after intranasal administration and demonstrating a Th1-like cytokine profile important for the treatment of HBV infections. Nevertheless, they required at least two administrations to be effective. Unmodified microspheres were not able to elicit such good results, maybe due to their faster clearance rate. CTB showed to a have no additional benefit.

Rajkannan and co-workers developed a different carrier for hepatitis B oral vaccine using B-cell epitope loaded poly (DL-lactide-co-glycolide (PLG) microparticles (BCEM) [48]. B-cell epitopes are antigenic regions of a protein that are recognized by the binding of immunoglobulin molecules. Authors highlighted PLG microparticles capacity of acting as a depot for the antigen, which allows prolonged and pulsatile release of encapsulated antigens. The release profile of the antigen depends on the degradation rate of PLG microparticles that varies according to the physical characteristics of the polymer. BCEM showed a triphasic release profile that researchers found valuable as it gives primary immunization effects and contributes to the development of a single dose vaccine. BCEM are taken up by M-cells and then transported to Peyer's patches where they are retained and gradually release the antigen. This retention appears to be essential for persistent stimulation of memory B-cells and for maintaining antibody titers over extended periods of time [107]. Immunological tests compared BCEM against B-cell epitope peptide (BCEP) alone. Mice where orally immunized with 100 μg of either BCEM or BCEP. After a single administration both formulations were able to induce IgG anti-HB antibodies in a similar way. At the onset, BCEP elicited higher

IgG titers reaching its maximum around the fourth week. BCEM IgG titers were initially lower reaching their maximum by week 6. After that, these levels remained constantly higher than the ones obtained with BCEP, demonstrating that PLG microencapsulation of BCEP lead to slow release of peptide, which elicited a prolonged immune response ultimately making the need of booster doses unnecessary. After a period of time mice were I.M. injected with HBsAg, which lead to a rapid and vigorous production of antibodies in the group of mice previously immunized with BCEM due to the induction of a secondary immune response. Mice that were immunized with BCEP were only able to elicit a gradual and weaker response.

Another group of researcher proposed a different carrier, also based on PLGA particles [49, 108]. Lectin anchored stabilized biodegradable nanoparticles are PLGA nanoparticles with lectin from *Arachis hypogaea* (PNA) anchored on the surface and present some enhancements relatively to plain PLGA nanoparticles. This vesicular carrier combines two strategies for enhancing immune response. On one hand, PLGA nanoparticles function as a protection to the fragile antigen to the harsh environment, preventing its destruction. On the other hand, lectins target vaccines specifically to M-cells. These PLGA nanoparticles also had the same drawbacks of previously synthesized PLGA based carriers. Keeping that in mind, researchers used trehalose as a protein stabilizer and also added $Mg(OH)_2$ that acted by neutralizing the acidity within the particles, generated by polyester hydrolysis of PLGA, conferring an overall protection to the antigen. Immunological response was assayed in mice after I.M. and oral administration of different formulations [49]. Mice were orally immunized three times and then boosted three weeks later, while I.M. immunized mice received a single dose that was also boosted three weeks later. To prepare an immunological profile, serum anti-HBsAg titers, mucosal IgA levels and IL-2 and IFN-γ levels were determined. Results showed that formulations containing lectin had higher antibody titers, which the authors attributed to its targeting capacity. In addition, the formulations containing trehalose and $Mg(OH)_2$ showed higher immune responses most likely due to the protective capacity of the two agents towards the antigen. Moreover, serum anti-HBsAg titers obtained after oral immunization with the stabilized lectinized nanoparticles were found to be equivalent to the titers obtained after i.m administration of alum-HBsAg. As expected, mucosal IgA levels were negligible after intramuscular administration. The highest levels of IgA were achieved with the stabilized lectinized nanoparticles. Similar results were obtained with IL-2 and IFN-γ levels indicative of a Th1 profile. The same group later investigated the potential of LTA lectin conjugated to PLGA particles to boost the immune responses following oral immunization against hepatitis

B, with similar results [51]. This suggests that the combination of lectins and PLGA particles is an efficient way to enhance mucosal immune response.

PLGA particles show great potential as vaccine adjuvants; however their use for nasal immunization is hindered by their rapid nasal clearance. Thus, the combination with a muchoadhesive polymer to enhance residence time was explored by Pawar and colleagues. Coating PLGA particles with chitosan or glycol chitosan (GC) had no effect on toxicity or antigen release profile of the particles. Interestingly, GC-PLGA particles showed substantially longer nasal retention times when compared to plain and chitosan-coated PLGA NPs; additionally, after nasal administration GC-PLGA NPs exhibited higher antigen distribution into circulation and several tissues, presumably due to increased residence time that promoted antigen uptake in the nasal mucosa. Overall, coating PLGA NPs with glycol chitosan resulted in an improved formulation, increasing the levels of antigen-specific antibodies compared to non-coated or CH-PLGA NPs showing that GC could be a better alternative to create PLGA-based mucosal vaccine against HBsAg [52].

An Indian group described the use of poly-lactic acid (PLA) to synthesize new vesicular carrier to encapsulate HBsAg for mucosal vaccination against hepatitis B [50]. PLA is a well-known polymer, similar to PLGA, with attractive features for the development of vaccine delivery systems [50, 98]. In the study, researchers used different combinations of PLA with another polymer, poly(ethylene glycol) (PEG) to synthesize copolymers blocks. PEG has been shown to confer mucoadhesion and long circulation properties to PLA [50]. Different AB, ABA and BAB (PLA as block-A and PEG as block-B) block-based nanoparticles were prepared and tested to optimize their properties. *In vitro* release profiles of optimized AB, ABA and BAB nanoparticles showed a triphasic release profile, very advantageous for vaccine delivery, as it mimics the three-shot schedule of the conventional vaccine. Immunological studies with the optimized formulations were performed and results were compared with those of plain PLA nanoparticles and alum based vaccine. Mice immunized with the conventional alum-based vaccine presented the highest serum anti-HBsAg titers, but required a booster on day 30. Conversely, AB, ABA and BAB formulations only needed a single administration to present comparative results. This may be due to their triphasic release profile *in vitro*. The initial release acted as a primer and resulted in the generation of memory cells; a subsequent release then had the effect of a booster dose that potentiated the IgG titers in the blood. PLA nanoparticles showed the lowest immunological response, probably because of the degradation of the antigen, which was not as well protected as in the other formulations. IgA levels were significantly higher in mice nasally vaccinated with copolymer nanoparticles,

both at the administration site as well as at distant mucosal surfaces, while I.M. injection of the conventional vaccine did not elicited significant IgA levels. IgG1 and IgG2 levels were also measured. Block copolymers gave a mix Th1/Th2 response, in contrast to alum-based vaccine that failed to generate Th1 immunity. The same group later demonstrated that contrary to traditional PLA particles, copolymeric formulations were able to resist the harsh gastric environment making the suitable candidates for oral immunization. While plain PLA nanoparticles failed to mount an effective immune response following oral administration due to instability in gastric environment, copolymeric nanoparticles efficiently generated humoral, cellular and mucosal immunity. Similarly to intranasal administration, after 3 rounds of oral immunization serum anti-HBsAg IgG responses were comparable to those generated after subcutaneous administration with alum-HBsAg, although with a more mixed Th1/Th2 response. Additionally, copolymeric nanoparticles depict enhanced IgA, IL-2 and IFN-γ levels leading to improved mucosal and cellular immune response. Results showed the potential of copolymer-based nanoparticles as mucosal vaccine delivery system and among them BAB nanoparticles were found to be the most promising, the outcome being superior to other copolymer-based formulations for both intranasal and oral routes [53].

Particle properties such as size, hydrophobicity, structure and surface chemistry are believed to play a role in the type of the generated immune response, because they influence the interactions between the host and the delivery system. In this regard, Thomas and colleagues studied the influence of surface charge after intrapulmonary administration of positively charged PLGA particles using a combination of stearylamine (SA) and polyethylenimine (PEI) in the external aqueous phase. They found that when particles with a positive surface charge were administered by pulmonary route, rats developed significantly higher serum anti-HBsAg IgG levels compared to negatively charged or unmodified PLGA formulations. This difference was also translated into mucosal and cellular immune responses, with cationic formulations eliciting significantly higher sIgA levels in salivary secretion, vaginal wash and BAL fluid, as well as an increased production of IL-2 and IFN-γ by splenocytes [54]. The same group later studied the effects of particle size and hydrophobicity on mucosal and cell-mediated immune responses following pulmonary administration. They developed 3 formulations with PLA, PLGA 85/15 and PLGA 50/50 with a mean size of 940, 774 and 474 nm, respectively, and a negative zeta potential. Larger, less hydrophilic PLA and PLGA 85/15 particles were more efficiently internalized and elicited an overall improved immune response, characterized by higher serum anti-HBsAg IgG levels, a more robust increase in secretory IgA in mucosal fluids and greater IL-2 and IFN-γ levels compared to smaller hydrophilic PLGA

50/50 particles. Hence, the results suggest that is important to evaluate the impact of different physicochemical characteristics on the immune response generated by PLGA particles [55].

1.3.1.10 Salmonella

For many centuries, diseases such as smallpox, cholera and diphtheria killed millions of people. There was no way of preventing infectious diseases until the late 1700s, when Edward Jenner developed the first vaccine with a naturally attenuated virus to protect against smallpox infection. Jenner's technique of inoculating with cowpox to protect against smallpox rapidly spread across Europe, but only more than a century later Louis Pasteur established the basis of modern live attenuated vaccine technology. Although these vaccines prove to be effective there were some safety issues related to the method of preparation and the possibility of it to revert to a virulent form. Over the years many advances have been made towards a safer vaccine and a new generation of rational attenuated vaccines was designed.

Bacterial vectors represent an alternative approach to synthetic (non-living) delivery systems for mammalian cell gene and protein delivery. This technology was first described in the early 1980s [109]. Attenuated strains can induce immune responses against antigens that are only expressed *in vivo* and are not present in an inactivated vaccine preparation. The ability of most attenuated vaccines to replicate in the host results in the elicitation of strong and long-lasting immune responses, which mimic those stimulated by natural infections [110]. There are intrinsic difficulties in this approach. The expression of virulence factors is responsible for the main difficulty associated with the design of live vaccines. The creation of steady immunogenic recombinant strains that express sufficient quantities of antigen *in vivo* and that offer no threat to the vaccinated individual and the environment is the ultimate goal.

One commonly studied live bacterial vector is *Salmonella*. Recombinant *Salmonella* strains are attenuated and became no longer pathogenic, but retained their immunogenicity, making them attractive carriers to deliver antigens for mucosal immunization [111-113]. *Salmonella* invades the host by crossing the intestinal mucosa via M-cells and colonizing GALT [114, 115]. In fact, a benefit of this bacterial vector is that it replicates and expresses the antigen in the intestine, thus delivering it to the mucosal immune system, where local and systemic humoral and cellular responses are strongly stimulated [110, 116, 117].

Schodel and coworkers investigated the use of *Salmonella* as a bacterial carrier to create a mucosal vaccine for hepatitis B [118-127]. The group developed expression systems coding for hybrid HBcAg particles displaying epitopes of the preS1 and preS2 regions in non-virulent *S. typhimurium* (mice) and *S. typhi* (humans) vaccine strains, and was able to prove that, in

animals, recombinant salmonellae induced an immune response against HBV when delivered orally [119, 122-124]. They also tried to establish which route of administration (oral, nasal, rectal and vaginal) was the best to induce the strongest systemic as well as mucosal immunity [125]. Results showed that, although *Salmonella* vaccine was successful at eliciting an immune response after immunization by all routes, the nasal route proved to be the most efficient at inducing both systemic and mucosal immune responses. Nevertheless, oral and rectal route were chosen to continue studies in human volunteers [118, 127]. Results were disappointing when the *S. typhi* based vaccine failed to elicit good antibody responses in both phase I clinical trials, suggesting that much was still to be done.

Further studies were carried out in animals using *Salmonella*-based vaccines to create a hepatitis B mucosal vaccine. Nardelli-Haefliger et al. used attenuated *Salmonella typhimurium* strains expressing the hepatitis B nucleocapsid as a vaccine system [56]. They found that nasal administration of attenuated strains to mice was more efficient in inducing antibody response than oral vaccination but the nasal route gave more adverse effects. Interestingly, on reducing the dose they found that nasal vaccination was still efficient while oral vaccination was ineffective.

Woo et al. and Zheng et al. evaluated the feasibility of *S. typhimurium* delivering plasmid-encoded hepatitis B surface antigen in eliciting effective immune responses in a mouse model [57, 128]. The immunogenicity of the DNA vaccine carried in *S. typhimurium* was compared to recombinant HBsAg vaccines and "naked" DNA vaccines (I.M.). Results showed that live attenuated *S. typhimurium* DNA vaccine was able to elicit a strong CTL response, considerably better than the one induced by the recombinant protein vaccine. This was not unexpected since in DNA vaccines part of the antigen generated is cleaved inside the APCs and presented by the MHC class I pathway, while in recombinant HBsAg vaccine the antigen in generally presented via MHC class II pathway. What was not expected was the weak antibody response elicited by the live attenuated *S. typhimurium* DNA vaccine, especially in comparison with the I.M. DNA vaccine. Authors believe that it may be due to the fact that S. *typhimurium* selectively infects MALT and only little HBsAg is presented through the MHC class II pathway. They concluded that the rather deficient humoral but strong cellular response could make the vaccine a possible candidate for a therapeutic vaccine for chronic HBV carriers as well as for non-responders who do not develop an antibody response to the conventional recombinant protein vaccine.

1.3.2 Edible vaccines

Another interesting approach is the use of transgenic plants as a delivery system for oral vaccines. There are many studies involving the use of plants modified in order to express HBV surface antigen. These expression systems have some advantages when compared to others such as low cost of large scale production, no need for special storage conditions and lack of contamination with animal pathogens [129-131]. Some researchers are using plants not only for the HBsAg production, but also as delivery system for direct human consumption. In addition to the previous advantages, plant-derived vaccines present some benefits over the traditional ones: they are cheaper because there is no need for purification of the antigen which is a very expensive step [130], the bioencapsulation of the antigen can protect it against enzymatic digestion [129, 132] and the administration is easier since it does not require the use of specialized equipment and trained staff. Only few plants have been tested as edible delivery systems for oral immunization against hepatitis B (Table 1.2).

According to Stephen Streatfield, when developing a plant-derived vaccine some aspects should be taken into consideration. First it is necessary to choose the appropriate expression system. Not all plants are good candidates for plant-derived vaccines since they are unpalatable for man [129, 133]. It is also important to choose a resistant plant where the antigen can be stable for long periods of time without requiring cold conservation and which can preferably be dehydrated to avoid rapid protein degradation [129]. Second, the antigen concentration must be high enough to achieve protective doses. Oral vaccines, unlike parenteral ones, are exposed to enzymatic degradation, so the oral dose of antigen required may need to be higher to achieve the same effect [129]. Third, the antigen levels expressed by different plants should be homogeneous so we can be sure that we are giving the same dose to different subjects. Finally, the last aspect is the antigen accumulation location within the plant. Expression levels of the antigen may vary among the different plant parts, and since not all plant parts are edible it is essential that the major accumulation site is fit for human consumption.

HBsAg was the first viral antigen chosen to be produced in transgenic plants, initially in tobacco [134]. Although the antigen could be expressed in this system, the levels of expression were low (≈ 0. 01 % of the soluble leaf protein), and the plant tissue was not adequate for eating.

An edible vaccine for hepatitis only appeared years later with the expression of HBsAg in lettuce as described by Kapusta et al. [135]. The transgenic lettuce leaves were fed to 3 human volunteers twice. Results obtained from sera of the volunteers after the first feeding showed

no relevant levels of HBsAg-specific IgG. However, sera collected after the second feeding revealed HBsAg-specific antibodies and in two volunteers those levels where higher than 10 international units per liter (IU/L), which is indicative of protection in humans. Though this study suggested that humans could be immunized using edible vaccines [135], the expression levels of the antigen in lettuce were very low, and again the plant tissue was not adequate for large scale-vaccines as the leaves needed to be immediately processed. Therefore, other options were considered.

Recombinant hepatitis B surface antigen was also expressed in potato tubers [133, 136, 137]. Potatoes have been frequently used as convenient model system for edible vaccines because transgenic strains are easy to produce [138]. In the first study using potatoes as an oral vaccine for HBsAg, [137] mice were fed with 5 g of transgenic HBsAg potato tubers, expressing 1.1 μg HBsAg/g tuber, plus 10 μg cholera toxin (CT), used as an immunopotentiator. Mice were able to develop an antibody response that reached 73 IU/L three weeks after the last of 3 doses, and then declined. At week 10 an intraperitoneal boost using the commercial vaccine (0.5 μg/mouse) was administered, resulting in a clear immunogenic response, most likely due to immune memory cells formed after oral immunization. Authors highlighted that the value of the results was limited by the low amount HBsAg expressed in potatoes and by the quantity of tubers mice were able to ingest. Although they were able to produce tubers that expressed higher quantities of the antigen, those lines grew badly suggesting that high levels of HBsAg may be toxic to the plant. Researchers found it was necessary to improve those aspects as higher doses of antigen could induce higher antibody levels, but nevertheless, results were promising and opened the way to further studies [136]. Immunogenicity of the edible vaccine was compared to that of an orally delivered yeast-derived HBsAg, usually found in commercial vaccines. No serum HBsAg specific antibodies were found in mice immunized with two doses of 150 μg of yeast derived HBsAg mix with 10 μg CT. An immunogenic response was only elicited when mice were boosted with a subimmunogenic dose of the recombinant vaccine. In contrast, mice fed with 5 g of potatoes (approximately 42 μg HBsAg/dose) and also using 10 μg of CT as an adjuvant were able to elicit a primary antibody response, that peaked up to 103 IU/L, four weeks after the third dose. Also a parenteral boost of a subimmunogenic dose of alum-adsorbed yeast-derived rHBsAg vaccine was able to elicit a memory response, but much stronger than the one obtained with the orally delivered yeast-derived vaccine. Authors believe that these results had to do with the fact that in potatoes HBsAg is retained within vesicular structures that naturally protect the antigen from degradation in the gut and therefore some of the antigen particles

were able to be released near the Peyer's patches and elicit a mucosal immune response. Mice fed with non-transformed potatoes showed no primary or secondary responses. In reverse experiments, mice were first immunized with a single subimmunogenic dose of the recombinant vaccine, which elicited no primary antibody response and then five weeks later fed with transgenic tubers plus CT for 3 weeks that lead to rapid increase of antibody levels. Results might guide towards a new strategy where a single parenteral immunization is combined with additional orally delivered doses of potato edible vaccine. Authors also keep in mind that such promising results were only possible in the presence of CT as an immunopotentiator and results using just the recombinant potato tuber lead to much lower antibody titers, thus suggesting the need for a human appropriated mucosal adjuvant for oral delivery and with uncooked potatoes because boiling the samples before feeding the mice reduced the immunogenicity of the vaccine considerably. This represents a major drawback as most of the people find raw potatoes unpalatable.

Phase I clinical trials were further conducted [133]. Forty-two previously parenterally vaccinated health care workers enrolled in a placebo-controlled, double blind trial. The volunteers were divided into three groups and received 3 portions of placebo potatoes (group one); 3 portions of recombinant potatoes having approximately 8.5 μg of HBsAg/g of potato tuber (group three) or two portions of transgenic tuber intercalated with one of placebo tuber. As expected, none of the individuals ingesting non-transgenic potatoes elicited an immune response during the study. On the other hand, 19 out of 33 subjects (60 %) had their serum anti-HBs titers increased after eating two or three doses of bite-size pieces of raw genetically modified spuds. The authors noted that the study did not use any buffers for stomach pH or additional stimulants, which have been required in past studies of edible vaccines. Incorporating an immunopotentiator could thus award a considerable improvement to both magnitude and rate of response.

Other systems were also tested in order to create an improved edible vaccine. One of those was cherry tomatillo [132]. Tomatillo is an interesting alternative to potato as it is a relatively efficient transformation system that can be eaten raw in contrast to potatoes [138]. The expression levels of the antigen varied within different organs of the plant and were found to be much higher in leaves than in other organs, yet levels of recombinant HBsAg per total soluble protein (rHBsAg/TSP) were superior in the fruit than in the leaf. Mice were immunized orally by feeding them transgenic tissue and I.M. boosted in the fourth week with a subimmunogenic dose (0.5 μg HBsAg) of the commercial vaccine. In none of the mice detectable antibody levels were observed. In contrast, when mice were first immunized with a

single shot of commercial vaccine (2 μg HBsAg) and then weeks later orally immunized with transgenic tomatillo an immediate strong recall immune response was developed. Authors believe that the absence of response in mice primarily immunized with transgenic tomatillo was due to low levels of antigen expression and that many problems still need to be fixed, even though some promising results have been shown.

Table 1.2 - Edible vaccines.

Adjuvant	Dose	Immunization schedule	Results	Ref.
Lettuce	≈ 0.1-0.5 μg HBsAg/100 g fresh tissue	0 months (200 g fresh tissue) 2 months (150 g fresh tissue)	2 out of 3 volunteers developed protective levels against HBV. Expression levels of the antigen in lettuce were very low.	[135]
Potato	5.5 μg HBsAg (1.1 μg HBsAg/g fresh tuber) + 10 μg CT	0 weeks; 1 weeks; 2 weeks. 10 weeks (I.P. boost with 0.5 μg of commercial vaccine)	Mice fed transgenic potato tuber developed a primary immune response greatly boosted by a subimmunogenic dose of commercial vaccine. Low amount HBsAg expressed in potatoes.	[137]
Potato	5 g tuber (8.35 μg HBsAg/g tuber) + 10 μg CT	Experiment 1: 0,1,2 weeks 16 weeks (i.p boost with 0.5 μg of commercial vaccine) Experiment 2: 0 weeks (i.p immunization with 0.5 μg of commercial vaccine) 5,6,7 weeks	Combination of oral immunization with an edible vaccine and parenteral immunization resulted in good antibody response. Oral immunization without CT resulted in much limited antibody response. Cooking the potatoes significantly reduces immunogenicity.	[136]
Potato	100-110 g tuber (≈8.5 μg HBsAg/g tuber)	Group 2: 0 and 28 day (transgenic tuber) 14 day (placebo tuber) Group 3: 0, 14 and 28 day (transgenic tuber)	≈ 60 % of the volunteers had their serum anti-HBs titers increased after eating two or three doses of transgenic potato tuber.	[133]
Cherry tomatillo	20 g transgenic tomatillo (≈ I μg HBsAg)	Experiment 1: Every day for 4 weeks 4 week- parenteral immunization with 0.5 μg of commercial vaccine Experiment 2: 0 week- parenteral immunization with 2 μg of commercial vaccine Boost with transgenic tomatillo when serum antibody levels ↘ to OD<1.0	Only when mice were first immunized with a single shot of commercial vaccine and boosted with transgenic tomatillo later an immune response was elicited. Reverse protocol failed to develop any immune response. Low levels of antigen expression in cherry tomatillo.	[132]

In fact, plant-produced HBV vaccine appeared to be very promising because of the possibility of being an economically viable alternative vaccination strategy for developing countries, however as Edward Rybicki said: "the idealistic vision of a plant-provisioned arsenal of vaccines for poor people may still be far away: it may take commercial exploitation of the lower-hanging fruits to bring in both the production/processing base, and industry and public acceptance of the technology" [139]. Possibly the key event that lead to the decrease of interest in plant-based vaccines was the incident involving ProdiGene Crop. In 2002, regulators found a small amount of "volunteer" corn engineered to express transmissible gastroenteritis virus capsid protein to produce a pig vaccine, growing in soybean and corn fields. The "volunteer" corn had sprouted from seeds left over from a corn field used for the

production of pharmaceuticals that was being grown under contract by ProdiGene. As a result, about 500,000 bushels of soybeans and 155 acres of corn plants had to be destroyed. Although a minuscule amount of volunteer transgenic corn would have posed no real danger to the food supply, the Food and Drug Administration put stronger regulations in place to keep transgenic pharmaceutical crops out of food [139].

It is probable that no edible vaccine for human use will be approved any time soon. Researchers are now focusing their interest in plants on creating novel viral expression systems for new HBV vaccines, and some plants have already been tested: bananas [140]; *Nicotiana benthamiana* leaves [141, 142]; rice seeds [143]; *Nicotiana tabacum and Arabidopsis thaliana* [144]; lettuce [145].

1.3.3 Delivery systems for topical immunization

According to Mahor, topical immunization (TI) or transcutaneous immunization (TCI) is a novel and needle-free strategy involving vaccine delivery through topical application of antigen and adjuvant(s) directly or via a suitable carrier system on intact skin [146]. The skin is a complicated structure, made up of several layers. The superficial region is known as *stratum corneum* and is the primary protective site against percutaneous absorption of compounds. Underlying it is the viable epidermis that is manly composed of keratinocytes. The innermost layer is the dermis and consists of blood vessels, nerves, elastin fibers, collagen, lymphatic channels, hair follicles, oil and sweat glands that serve as a support for the upper skin layers [15]. As told before, the skin is full of antigen presenting cells making it an immunologically active site and an attractive vaccination route (Fig. 1.1).

TI is achieved by physical, chemical or vesicular approaches (Table 1.3). The pursuit for a better HBV vaccine lead researchers to exploit some of the mechanisms within these techniques such as particle-mediated epidermal delivery [147-151] and epidermal powder immunization [152, 153] (physical approaches); niosomes; highly deformable liposomes and ethosomes (vesicular approaches).

1.3.3.1 Physical approaches

1.3.3.1.1 Particle mediated epidermal delivery

One approach to skin immunization is particle-mediated epidermal delivery (PMED). PMED is a needle free technology by which DNA-coated gold microparticles are used to transfect target tissues using a device called gene gun [154]. The gene gun DNA vaccine strategy utilizes a helium jet to accelerate DNA-coated gold particles into to the epidermis,

which is under constant immune surveillance and is the body's first defense against pathogens. This type of transfer method has several advantages: easy and quick procedure of transfection; availability for all species of cells; little volume of DNA required; many target cells hit by a single shot, different from the microinjection method, and higher efficiency of gene transfection rate than attenuated by electroporation or lipofection. However, gene gun immunization also has some disadvantages [155]. First, only small quantities of DNA can be loaded onto the golden beads because they can clump when high amounts are used. This can lead to reduced efficiency of the plasmid delivered and consequently result in the need for multiple shots. Also, gold beads are difficult to handle after coating. Finally, the gene guns themselves are not simple to use.

In the early 90's a gene gun mediated DNA vaccine for HBV was developed by Fuller et al. [156]. Gene guns were originally designed for plant transformation, but were considered to be a promising way to deliver DNA plasmids encoding HBV antigens directly to cells [151]. DNA vaccines are a good alternative to protein vaccines because they are able to induce T cell response. During the research, Fuller and coworkers found that 95 % of the immunized BALB/c mice were able to reach antibody titers higher than 10 IU/L after a boost immunization. Anti-HBsAg antibody titers decreased overtime after some weeks, but remain high enough during the study time (20 months) to be considered protective. In a second study the experimental vaccine was compared to the existent HBV vaccine. Using two different strains of mice, one consisting of high-responders and the other consisting of low or non-responders, they showed the superiority of the gene gun DNA vaccine on eliciting immune response in the low or non-responder mice when compared to vaccination using the protein vaccine. Tests with the epidermal DNA vaccine were also performed in pigs, mainly because of their similarity to humans in terms of skin physiology. The results demonstrated that a dose of 500 ng, administered as two single doses of 250 ng, of the DNA vaccine were able to elicit protective levels of HBsAg-specific antibody similar to the results obtained with the commercial vaccine [151].

As a result of the potential of gene gun mediated DNA vaccines, phase I clinical trials were planned to test the safety, tolerability and immunogenicity of the vaccine in healthy humans [147, 149, 150]. The first trial involved seven healthy adult volunteers that were hepatitis B core antibody negative [150]. They were immunized with the hepatitis B DNA vaccine, given as two shots each consisting of 250 mg gold/0.25 μg of DNA at one of the different forces of delivery (250 psi, 400 psi, or 500 psi). No significant adverse effects were noticed. One of the volunteers developed a strong antibody response after the first

immunization, probably due to pre-exposure to HBV. All the other subjects, including a previous seropositive individual, failed to elicit humoral responses. Researchers believed this fact was due to the low DNA dosage. Four seronegative volunteers later received 3 doses of the commercial vaccine, and developed vigorous antibody responses, suggesting that the hepatitis B DNA vaccine given by a gene delivery system may induce a booster response, but higher doses might be needed to induce primary immune response.

The second trial involved 12 hepatitis-naïve volunteers divided into 3 dosage groups (1, 2 or 4 μg of DNA) [147]. The gold particles coated with DNA were delivered using a PowderJect™ XR1 device to the inner aspect of the upper arm, over a 16 weeks' time period and an immunization interval of 8 weeks between them (except for two volunteers that deviated from the schedule). After the second immunization, 75 % of the volunteers (9 in 12) seroconverted but only 3 showed protective levels of the antibody. By the time of the third immunization all of the 12 volunteers had seroconverted with anti-HBsAg levels varying from 10 up to 5000 IU/L. Results suggested that DNA dose only affects the seroconversion rate rather than the geometric mean titer (GMT). Volunteers with larger time intervals between immunizations develop higher seroprotective levels and faster than other individuals. Although it may not be significant, researchers believe that an extended immunization interval is vital for optimal immune induction as some studies suggest [157]. Some volunteers (the ones whose antibody titers were below 100 IU/L after 3 months of the last immunization) received a single boost with the commercial vaccine, all successively developing a strong immune response. Cellular response was also evaluated showing that the DNA vaccine elicited, in some cases, a mixed Th1/Th2-like immune response, but mainly Th1-like response. In terms of safety and tolerability the adverse effects reported were mild to moderate local inflammation that disappeared within days or weeks.

A clinical trial in subjects of low to non-responsiveness to commercial hepatitis B protein vaccines was conducted to determine if particle-mediated DNA vaccines could be similarly used to overcome vaccine non-responsiveness in humans [148]. It is well know that conventional vaccines fail to elicit protective antibody responses in a percentage of vaccine recipients. Using a DNA vaccine against hepatitis B administered by PMED, researchers were able to elicit antibody responses in 12 of the 16 subjects that had previously failed to acceptably respond to 3–9 doses the commercial vaccine. Although 12 volunteers demonstrated a response to the DNA vaccine, by the end of the study (280 or 392 days, depending on the group the subjects were in) only 7 still had protective levels. It is important to highlight that the subjects of the study were pre-selected as being low to non-responders to

the conventional vaccine, which could have had an impact on the overall result. This study also showed that a single DNA vaccine dose was sufficient to boost a pre-existing hepatitis B antibody response as subsequent clinical trial support [149]. The latest study served mainly to test the safety and efficacy of a commercial prototype device (ND5.5) for PMED versus the previous clinical research device (XR-1) [149]. The two devices were shown to be safe and well tolerated with no difference in magnitude of antibody responses, cell mediated response (CMR) or proportion of responders between them.

The results obtained illustrate the potential of particle-mediated epidermal delivery in eliciting good cellular and humoral immune responses and suggest that it may be an attractive alternative approach for prophylactic vaccination against hepatitis B.

1.3.3.1.2 Epidermal powder immunization

Topical immunization demonstrated good results not only with DNA vaccines but with conventional sub-unit vaccines, as well [152, 153]. Epidermal powder immunization (EPI) is very similar to PMED. It is a needle-free technology for delivery of the antigen to the top layers of the skin using helium gas released gene-guns to propel the vaccine powder into the epidermis [158].

Chen and coworkers used EPI in the development of a new hepatitis B vaccine [153]. The group demonstrated that EPI was able to target not only the epidermis, but in particular the Langerhans cells, that later migrate to draining lymph nodes. BALB/c mice were immunized with 2 μg of HBsAg to study the humoral and cellular immune response; mice I.M. injected with 2 μg of HBsAg were used as control. EPI was able to elicit primary and secondary antibody responses with IgG titers similar to the ones obtained after I.M. injection. However, EPI induced CTL responses the control group failed to elicit. Further studies compared EPI (2 μg HBsAg) with PMED (2 μg DNA) immunization. Both methods were able to induce a primary and secondary response as well as CTL responses in a similar way. Achieving a CTL response usually requires endogenously produced proteins. Nevertheless, EPI was able to elicit a CTL response. Authors believe this to be correlated to the intracellular delivery of the antigen to LCs that may lead to a MHC class-I restricted antigen presentation, and to a cross-priming effect by antigens delivered to the keratinocytes [159, 160]. Results present EPI as a viable alternative to create not only a prophylactic, but also a therapeutic vaccine.

Some researcher from the previous group tried to further improve the vaccine by adding synthetic CpG oligonucleotides [152]. CpG has many effects that contribute to its adjuvant activity [161-165].

The obtained results suggest that EPI is a better method to deliver HBsAg when compared to unadjuvanted HBsAg and as good as the alum-adjuvanted commercial vaccine and therefore it could overcome the need for an adjuvant. Nevertheless, the use of CpG can further induce the immune response. Antibody titers obtained using EPI and CpG (0.1 μg HBsAg/ 10 μg CpG) in the same formulation, were statistically higher than those induced by the same dose of alum-adjuvanted HBsAg, and comparable to those induce by I.M. injection of 20 μg HBsAg/50 μg $Al(OH)_3$. Increasing doses of CpG resulted in increasing antibody titers in EPI delivery but not in I.M. injection. The use of CpG affected the cytokine profile, as well. For EPI the IgG1/IgG2a ratio correlated inversely to the quantity of CpG present in the vaccine formulation. CpG adjuvanted formulation helped stimulate the production of TNF-α, IFN-γ, IL-6 and IL-12 demonstrating a Th1-like profile in contrast to the one revealed by alum-adjuvanted recombinant vaccine. The addition of the immunopotentiator CpG was shown to further enhance EPI capacities.

1.3.3.2 Vesicular approaches

Topical immunization via vesicular systems is a subject of rising interest for a growing number of researchers. Vesicular carriers have the advantage of providing controlled delivery to the target tissue via different pathways such as keratinolytic, transfollicular or pilosebaceous routes.

In late 90's, Fan et al. described the use of naked plasmid vector of hepatitis B surface antigen for topical immunization via hair follicles [166]. They showed that an aqueous solution of "naked" DNA applied topically to the skin was able to induce IgG class antibodies at a titer 34.4 % of that of intramuscular polypeptide vaccination. Even though it is possible to induce an immune response using "naked" DNA, it has been proven that its uptake by APC is minimal. Also "naked" DNA is vulnerable to hydrolysis by enzymes present in the interstitial space and therefore needs to be protected, thus making vesicular carriers an even more appealing approach [146].

1.3.3.2.1 Niosomes

Niosomes are nonionic surfactant vesicles that can be used as topical carriers for immunoagents for transdermal delivery [20]. They are considered a better alternative to liposomes because they are cheap, highly pure, uniform in content, very stable and easy to store [20, 146].

The potential of niosomes as efficient vesicular carriers for the delivery of plasmid DNA encoding HBsAg through topical route was studied [20]. Serum antibody titers and interleukin-2 and interferon-γ levels of topical immunized mice with niosomes was compared to those of I.M. (recombinant and DNA vaccines) and topically (with naked DNA and with liposomes) immunized mice. Results showed that niosomes were capable of inducing strong cellular and humoral responses. When compared to I.M. immunization of naked DNA, niosomes showed a lower response. Encapsulation of the plasmid within the niosomes resulted in improved immunological responses in comparison to topically applied naked DNA, probably due to the enhanced transport and protection of plasmid DNA across the skin that leads to better APC presentation. Niosomes demonstrated to be slightly better than liposomes; authors believed that this finding might be explained by the composition of the niosomes. Surfactants in their formulation serve as penetration enhancers by raising the fluidity and reducing the barrier property of *stratum corneum*. Niosomes have also been shown to efficient delivery HBsAg for transcutaneous immunization [167]. Niosomes mixed with the immunopotentiators cholera toxin B induced systemic immune responses higher than subcutaneous vaccine adjuvanted with alum. Moreover, higher IgG2a titers in serum were observed in the mice vaccinated with the particle vaccine formulated together with CTB. Overall, the results support the potential of niosomes as topical vaccine delivery systems.

1.3.3.2.2 Highly deformable liposomes

Deformable vesicles like elastic liposomes or transfersomes have been found to be more effective in enhancing drug transport compared to rigid vesicles like conventional liposomes [168]. Elastic liposomes are composed of a mixture of lipids and biocompatible membrane softeners [168]; the elasticity of the vesicle depends on the combination of these two components [168, 169]. The advantage of this system is due not only to its ultradeformability but also to the sensitivity to water gradient throughout the skin [170, 171]. The potential of elastic liposomes as vesicle carriers for HBsAg was first described by Mishra et al. [169]. They prepared and characterized the system and performed *ex vivo* and *in vivo* studies. Mice were immunized topically using HBsAg-loaded elastic liposomes and I.M. by HBsAg injection. IgG levels of both kinds of immunization were very similar. In contrast, IgA levels in serum were much higher in mice topically immunized, suggesting the potential of this formulation in enhancing mucosal immunity in addition to systemic response. Elastic liposomes were presented as having good topical carrier characteristics (higher entrapment efficiency; enhanced penetration and effective immuno-adjuvant properties) [169], thus further studies

were carried out. Murine dendritic cells were studied for their *in vivo* uptake of HBsAg-loaded elastic liposomes and capacity of generating a T cell-dependent immune response [16]. Elastic liposomes were quickly internalized by DC and were shown to be non-toxic. A robust Th1-like immune response was generated, with a marked increase of IL-2, IFN-γ and TNF-α levels as compared to control. Th2 cytokines levels also recorded a slight, but not significant, increase.

Another group also worked with elastic vesicles, referring to them as cationic transfersomes [172]. These vesicular carriers are prepared using two main components: a cationic lipid (DOTMA) and sodium deoxycholate that confer transfersomes their ultra-deformable characteristic, which enables them to efficaciously transfer molecules across the *stratum corneum*. Transfersomes were optimized and loaded with DNA encoding HBsAg. Immune response after different routes of administration (I.M. HBsAg; I.M. DNA; topical "naked" DNA; topical optimized transfersome formulation) was studied. As expected, mice I.M. immunized with HBsAg elicited initial higher levels of anti-HBsAg that started to decline after the fourth week. On the other hand, mice that received an I.M. injection of DNA encoding HBsAg elicited the highest and well-sustained antibody titers after an initial period of time required for transfection and translation of the antigen. Topically vaccinated mice with the optimized transfersome formulation elicited lower, but clinical protective, levels of antibody. Also DNA formulations were able to induce a stronger cellular response important to eliminate the virus from the host, with comparable values between the topical and I.M. immunized groups. In all cases the transfersome formulation proved to be better than "naked" DNA for topical immunization.

1.3.3.2.3 Ethosomes

Ethosomes are novel and attractive vesicular carriers for topical immunization that were first developed by Touitou et al. [173]. Essentially, they are lipid vesicles with a high content of ethanol [146], which is a well-known permeation enhancer, since it fluidizes both lipid and bilayer of the *stratum corneum* allowing a more effective delivery of active substances through the skin than conventional liposomes [146, 174, 175].

The potential of ethosomes as a delivery system for topical immunization against hepatitis B was assayed by Mishra et al. [176]. Researchers prepared and characterized antigen loaded ethosomes. Ethosomes exhibited the best permeation profile when compared to conventional liposomes and plain antigen and showed to be efficiently internalized by DCs. Pulsed DCs elicited a predominant Th1-like immune response with two to five-fold increases in IL-2,

IFN-γ and TNF-α levels. No significant increase in Th2-like cytokines levels was reported. Mice immunized with the ethosomes formulation induced better and stronger humoral and mucosal immune responses.

Overall, topical immunization presents itself as an attractive alternative for achieving a needle-free vaccine against hepatitis B.

Table 1.3 - Delivery systems for topical immunization.

Adjuvant	Type of vaccine	Dose	Immunization schedule	Results	Ref.
PMED	DNA vaccine	0.25 μg DNA 0.5 μg DNA 1.5 μg DNA	0 week 8 weeks 16 weeks	Pigs Immunized with higher doses (2nd and 3rd groups) developed comparable humoral response to commercial vaccine.	[151]
PMED	DNA vaccine	0.25 μg pDNA	0 day 56 day	Only 1 out of 7 volunteers developed protective antibody levels.	[150]
PMED	DNA vaccine	1 μg DNA 2 μg DNA 4 μg DNA	0 week 8 weeks 16 weeks	All volunteers developed protective antibody responses as well as detectable cell-mediated immune response.	[147]
PMED	DNA vaccine	4 μg DNA	0 week 8 weeks 16 weeks	Vaccine was able to elicit antibody responses in 12 of the 16 subjects that had previously failed to acceptably respond to 3–9 doses the commercial vaccine.	[148]
EPI	Sub-unit vaccine	2 μg of HBsAg	0 day 28 day	EPI was able to elicit humoral as well as cell mediated immunity.	[153]
EPI	Sub-unit vaccine	Varying doses (0.05 – 2 μg HBsAg + 0.1-20 μg CpG DNA)	0 day 28 day (some studies)	The delivery system induced considerable humoral and cellular immune response especially with the addition of the immunopotentiator that further enhanced EPI capacities.	[152]
Niosomes	DNA vaccine	100 μg pDNA	1 day 14 day	Niosomes were capable of inducing cellular and humoral responses but with lower results compared to i.m immunization of naked DNA.	[20]
Niosomes	Sub-unit vaccine	10 μg HBsAg	1,3 day 14 day	Niosomes induced higher systemic and increased IgG2a in combination with CTB.	[167]
Elastic liposomes	Sub-unit vaccine	10 μg HBsAg	1 day 14 day	Mice developed strong systemic and mucosal immunity.	[169]
Cationic transfersomes	DNA vaccine	100 μg pDNA	1 day 14 day	Vaccine formulation elicited clinical protective antibody levels and strong cellular response in mice.	[172]
Ethosomes	Sub-unit vaccine	10 μg HBsAg	1 day 14 day	Good systemic and mucosal humoral immune response was observed. Ethosomes elicited a predominant Th1-like immune.	[176]

1.4 Immunopotentiators

1.4.1 Cholera toxin, heat-labile enterotoxin and derivatives

Two of the most potent immunopotentiators available are the bacterial toxins secreted from *Escherichia coli* and *Vibrio cholerae*, which are called heat-labile enterotoxin (LT) and cholera toxin. They are commonly used in animal models [177-179] and are considered too toxic for human use because these molecules are respectively responsible for traveler's

diarrhea and cholera. To overcome this problem two solutions have been found: the use of the non-toxic B subunit that lack enzymatic activity, which lead to some diverse results [178, 180-183], or the use of detoxified mutants that have little or no enzymatic activity with significantly less toxicity but some adjuvanticity [184-190].

In the year 2001, a Japanese group published an article where they tested the use of recombinant cholera toxin B subunit (rCTB) as an adjuvant for an intranasal hepatitis B vaccine [191] (Table 1.4). Recombinant CTB proved to be an effective mucosal adjuvant for HBsAg. Intranasal administration of 3 doses of HBsAg combined with rCTB showed statistically higher IgG levels when compared to HBsAg alone. Recombinant CTB elevated not only the systemic response but also mucosal immune response in all sites examined (nasal cavity; lungs; saliva; small intestines; large intestines; vagina). Co-administration of rCTB an HBsAg resulted in a mixed Th1 and Th2-like response.

1.4.2 CpG motifs

The need to find an alternative to cholera toxin and *Escherichia coli* heat-labile enterotoxin also led to the development of a new class of immunopotentiators, the CpG motifs.

According to the definition of Krieg [192], CpG motifs are DNA oligodeoxynucleotides sequences that include an unmethylated cytosine-guanosine sequence and certain flanking nucleotides, which have been found to induce innate immune responses through interaction with TLR9. There are three major classes of CpG, A, B and C-class, that are structurally and phenotypically distinct. B-class CpG has been frequently used in animal studies due to the strong B cell activation and capacity to induce potent Th1-type immune response. The same B-class CpG have also been shown to be a safe and efficacious vaccine adjuvant in humans [193, 194]. Although most cell types have the capacity to internalize CpG via endocytosis [161], only those cells that express the TLR9 are activated. In humans, only B cells and plasmacytoid dendritic cells (pDCs) are able to express the TLR9, whereas in mice, TLR9 is also found on myeloid dendritic cells (mDCs), macrophages and monocytes [195]. Within minutes after exposure to CpG, these cells take it up into endosomal compartments where the interaction with the TLR9 occurs [196]. This leads to the activation of cell signaling pathways comprehensively described by McCluskie [195].

CpG has been shown to be an effective mucosal adjuvant after the administration to different mucosal surfaces such as respiratory tract [96, 197, 198], the genitourinary tract [199] and the gastrointestinal tract [200, 201] in combination with different antigens including the hepatitis B antigen [96, 202]. Co-administration of CpG with other immunopotentiators or

delivery systems has been considered to be useful especially because it is a strong Th1 profile inducer which has been shown to be able to dominate the Th2 bias associated with other adjuvants [95, 96].

McCluskie et al. were the first to describe the use of CpG as a mucosal adjuvant against HBsAg [96]. They measured the anti-HBs titers of mice immunized by intranasal inhalation of HBsAg (1 or 10 μg) alone or in combination with CT and/or CpG. Immunization with of HBsAg alone resulted in no or low anti-HBs IgG and IgA titers in most mice. On the other hand, mice immunized with HBsAg in combination with CpG induced high anti-HBs IgG titers in all mice, with results comparable to those elicited when CT was used. CpG and CT demonstrated to have a synergistic effect, since the immune response generated was 5 to 10 times higher than with each adjuvant alone. No IgA was detected in mice that received the lower dose of HBsAg, even when CpG or CT were mixed; low IgA titers were detected with CpG/CT that increased after boost. With the higher Ag dose, IgA was detected in the presence of CT and CpG, either alone or in combination. A synergistic effect was also noted; authors suggested that this synergy may be due to the fact that both CpG and CT activate B cells, but by different mechanisms [203, 204]. This effect offers the possibility of using lower doses of CT in addition to CpG to elicit stronger immune responses. CpG and CT induce different IgG isotypes, with CpG having a more Th1-like response and CT a Th2-like response. The same group further investigated the potential of CpG as a mucosal adjuvant [205]. As found before, both systemic (humoral and cellular) and mucosal immune responses were induced following mucosal delivery of HBsAg with CpG and/or CT, but not with the antigen alone; the synergistic effect between CT and CpG was once again reported. In addition, new data showed that higher doses or boosting additionally enhanced the immune response.

Based on the promising results with the CpG when HBsAg was delivered by intranasal immunization [96, 205-207], McCluskie and coworkers investigated their potential to be used as an adjuvant for oral immunization [201]. The group demonstrated that CpG was an effective oral adjuvant as it was able to enhance both systemic and mucosal immune responses. Mice were immunized by oral administration of 100 μg HBsAg alone or in combination with different doses of CpG (50, 100, 500 μg) or CT (10 μg). Immunization with the antigen alone failed to elicit detectable levels of anti-HBs IgG, but induced high antibody levels in combination with CpG. Ten μg of CT could only induced same (50, 500 μg/CpG) or worse immune responses (100 μg/CpG). Similar results were obtained for IgA levels, with no apparent dose-response effect. CpG also enhanced T cell proliferation, as well as CTL activity.

CpG proved to induce better immune responses when co-administered with CT, since they acted synergistically. Even though the combination of CpG with CT allows the use of lower doses of the toxin, these concentrations might still be too toxic for human use. Concerned with this fact McCluskie et al. tested the immune responses elicited by the use of CT or LT and by their non-toxic version (B subunit of CT and LTK63, respectively) [208], as well as CpG, alone or combined, using small (20 µl) or large volumes (150 µl). CpG, CT and LT were shown to induce same or higher antibody titers when compared to CTB or LTK63. Also, CpG exhibited a synergistic effect with CT and LT but not with their non-toxic versions suggesting, according to the authors, that some enzymatic activity is still needed for this synergic effect. Apart from the adjuvant the use of larger volumes yielded better results than small ones. With small volumes higher doses of adjuvant needed to be used in order to obtain similar results, as well as more administrations.

Table 1.4 - Immunopotentiators.

Adjuvant	Type of vaccine	Route	Dose	Immunization schedule	Results	Ref.
rCholera Toxin B	Sub-unit vaccine	IN	1 or 5 µg HBsAg + 10 µg rCTB	1 day 14 day 21 day 28 day	Addition of rCTB elevated systemic and mucosal immune response.	[191]
CpG	Sub-unit vaccine	IN	1 or 10 µg HBsAg + 1 or 10 µg CpG and/or 1 or 10 µg CT	0 weeks 8 weeks (some mice)	Immunization with formulations containing CpG induced high systemic response in all mice and strong mucosal immune response (w/higher CpG dose). CpG and CT act synergistically.	[96, 205]
	Sub-unit vaccine	Oral	100 µg HBsAg + 50 or 100 or 500 ug CpG	0 day 7 day 14 day	Combination of the antigen with the immunopotentiator resulted in high systemic, mucosal and cell mediated immune response in contrast to antigen alone.	[201]

To test the possibility that some enzymatic activity is needed to obtain a synergistic effect with CpG, McCluskie et al. used a different genetically detoxified mutants of LT that have varying levels of residual enzymatic activity [209]. Mice were intranasally or orally immunized with 10 µg of HBsAg alone or by co-administrated with 1 or 10 µg of CpG and/or LT or its mutants. Although all adjuvants were able to increase Ag-specific immune response, they varied in terms of adjuvant activity. LT, LTR192G and LTA69G elicited strong immune responses (IgG, IgA and CTL). Weaker responses were obtained with the other LT-derivates (LTB, LTE112K and LTS61F). Overall, adjuvants with higher enzymatic activities had the best adjuvant effect in contrast to those with less or no enzymatic activity. An interesting finding was that no synergistic effect was seen when CpG was combined with any of the LT-derivatives, only a shift in antibody isotype was observed. When administered alone CpG gave

predominantly Th1-like response and LT as well as its derivatives a Th2-like response, while co-administrated they produced a mix response.

CpG motifs are considered to be a promising tool in the development of better and more potent needle-free HBV vaccines.

1.5 Aim and outline of the thesis

The development of novel vaccine adjuvants and/or antigen optimized delivery platforms is as important as the generation of the novel vaccine itself. Presently, most of the vaccines are given by intramuscular injection, which requires the use of needles that are painful and potentially dangerous, and involve expensive trained medical personnel, making them unsuitable for mass vaccination campaigns, especially in developing countries. Moreover, with few exceptions, parenteral immunization fails to induce appropriate mucosal and cell-mediated immune responses also important for protection against some pathogens. Recently, many researchers have focused their interest on needle-free technologies. Although several strategies have been proposed, there is not an approved needle-free vaccine against HBV.

The aim of this project was to develop a chitosan-based delivery system in association with aluminium salts as a novel adjuvant for different vaccination strategies against hepatitis B virus (HBV) infection and explore the mechanism of action behind the adjuvant effect of chitosan-based formulations. We hypothesized that the mucoadhesive chitosan nanoparticles would extend the residence time of the antigen on the nasal cavity increasing mucosal immunity. Simultaneously, aluminium salts would further potentiate the development of an efficient immune response. Additionally, the generation of a DNA vaccine would contribute to the improvement of cell-mediated immunity. Therefore, with this aim in mind, two different delivery systems were prepared and evaluated in parallel, a novel prototypic system combining chitosan and aluminium salts to deliver hepatitis B surface antigen and the gene delivery system consisting of complexes of HSA-loaded chitosan nanoparticles with DNA encoding HBsAg.

Chapter 1 reviews several adjuvants tested over the years for their adjuvant potential to create a needle-free vaccine against HBV.

Chapter 2 describes the design, characterization and preliminary *in vitro* and *in vivo* evaluation of chitosan-aluminium nanoparticles.

Chapter 3 describes the optimization of a methodology to obtain large quantities of endotoxin-free chitosan without modifying its biochemical properties.

Chapter 4 describes the mechanisms underlying the adjuvanticity of CH-Al NPs and the evaluation of their potential to modulate innate and adaptive immune responses.

Chapter 5 describes the design, characterization and the evaluation of the potential of HSA-CH NP/DNA complexes to act as an adjuvant for nasal vaccination against hepatitis B virus.

Chapter 6 presents the concluding remarks of the thesis and future perspectives.

References

1. Mauss, S., et al., *Hepatology: A clinical textbook*2009, Duesseldorf: Flying Publisher.
2. WHO, *http://www.who.int/mediacentre/factsheets/fs204/en/*. p. accessed: 28-05-2009.
3. Flying PublisherMauss, S., et al., *Hepatology: A clinical textbook*2009, Duesseldorf: Flying Publisher.
4. Yuen, M. and C. Lai, *Treatment of chronic hepatitis B.* Lancet Infect Dis, 2001. **1**(4): p. 232 - 24.
5. Sitrin, R. and D. Wampler, *Hepatitis B Vaccines in Clinical Practice*, ed. R. Ellis1992, New York: Dekker, M. . 418.
6. Goldsby, A., et al., *Cells and organs of the immune system*, in *Immunology*2002, W H Freeman & Co. p. 50.
7. Holmgren, J. and C. Czerkinsky, *Mucosal immunity and vaccines.* Nat Med, 2005. **11**(4 Suppl): p. S45-53.
8. Neutra, M.R. and P.A. Kozlowski, *Mucosal vaccines: the promise and the challenge.* Nat Rev Immunol, 2006. **6**(2): p. 148-58.
9. Vajdy, M. and D.T. O'Hagan, *Microparticles for intranasal immunization.* Adv Drug Deliv Rev, 2001. **51**(1-3): p. 127-41.
10. Kagi, D. and H. Hengartner, *Different roles for cytotoxic T cells in the control of infections with cytopathic versus noncytopathic viruses.* Curr Opin Immunol, 1996. **8**(4): p. 472-7.
11. Kurts, C., B.W. Robinson, and P.A. Knolle, *Cross-priming in health and disease.* Nat Rev Immunol. **10**(6): p. 403-14.
12. Wieland, S.F. and F.V. Chisari, *Stealth and cunning: hepatitis B and hepatitis C viruses.* J Virol, 2005. **79**(15): p. 9369-80.
13. Baumert, T.F., R. Thimme, and F. von Weizsacker, *Pathogenesis of hepatitis B virus infection.* World J Gastroenterol, 2007. **13**(1): p. 82-90.
14. Cullen, S.P. and S.J. Martin, *Mechanisms of granule-dependent killing.* Cell Death Differ, 2008. **15**(2): p. 251-62.
15. Combadiere, B. and B. Mahe, *Particle-based vaccines for transcutaneous vaccination.* Comp Immunol Microbiol Infect Dis, 2008. **31**(2-3): p. 293-315.
16. Mishra, D., et al., *Evaluation of uptake and generation of immune response by murine dendritic cells pulsed with hepatitis B surface antigen-loaded elastic liposomes.* Vaccine, 2007. **25**(39-40): p. 6939-44.
17. Toebak, M.J., et al., *Dendritic cells: biology of the skin.* Contact Dermatitis, 2009. **60**(1): p. 2-20.
18. Warger, T., H. Schild, and G. Rechtsteiner, *Initiation of adaptive immune responses by transcutaneous immunization.* Immunol Lett, 2007. **109**(1): p. 13-20.
19. Banchereau, J. and R.M. Steinman, *Dendritic cells and the control of immunity.* Nature, 1998. **392**(6673): p. 245-52.

20. Vyas, S.P., et al., *Non-ionic surfactant based vesicles (niosomes) for non-invasive topical genetic immunization against hepatitis B.* Int J Pharm, 2005. **296**(1-2): p. 80-6.
21. Mitragotri, S., *Immunization without needles.* Nat Rev Immunol, 2005. **5**(12): p. 905-16.
22. Giudice, E.L. and J.D. Campbell, *Needle-free vaccine delivery.* Adv Drug Deliv Rev, 2006. **58**(1): p. 68-89.
23. Borges, O., et al., *Mucosal vaccines: recent progress in understanding the natural barriers.* Pharm Res. **27**(2): p. 211-23.
24. Dubois, B., et al., *Oral tolerance and regulation of mucosal immunity.* Cell Mol Life Sci, 2005. **62**(12): p. 1322-32.
25. Tsuji, N.M. and A. Kosaka, *Oral tolerance: intestinal homeostasis and antigen-specific regulatory T cells.* Trends Immunol, 2008. **29**(11): p. 532-40.
26. Kiyono, H. and S. Fukuyama, *NALT- versus Peyer's-patch-mediated mucosal immunity.* Nat Rev Immunol, 2004. **4**(9): p. 699-710.
27. Csaba, N., M. Garcia-Fuentes, and M.J. Alonso, *Nanoparticles for nasal vaccination.* Adv Drug Deliv Rev, 2009. **61**(2): p. 140-57.
28. O'Hagan, D.T. and R. Rappuoli, *Novel approaches to vaccine delivery.* Pharm Res, 2004. **21**(9): p. 1519-30.
29. Saraf, S., et al., *Lipid microparticles for mucosal immunization against hepatitis B.* Vaccine, 2006. **24**(1): p. 45-56.
30. Gupta, P.N. and S.P. Vyas, *Investigation of lectinized liposomes as M-cell targeted carrier-adjuvant for mucosal immunization.* Colloids Surf B Biointerfaces, 2011. **82**(1): p. 118-25.
31. Khatri, K., et al., *Surface modified liposomes for nasal delivery of DNA vaccine.* Vaccine, 2008. **26**(18): p. 2225-33.
32. Tiwari, S., et al., *Viral protein complexed liposomes for intranasal delivery of hepatitis B surface antigen.* Int J Pharm, 2011. **413**(1-2): p. 211-9.
33. Shukla, A., et al., *Oral immunization against hepatitis B using bile salt stabilized vesicles (bilosomes).* J Pharm Pharm Sci, 2008. **11**(1): p. 59-66.
34. Shukla, A., et al., *M-cell targeted delivery of recombinant hepatitis B surface antigen using cholera toxin B subunit conjugated bilosomes.* Int J Pharm, 2010. **385**(1-2): p. 47-52.
35. Pandey, R.S. and V.K. Dixit, *Evaluation of ISCOM vaccines for mucosal immunization against hepatitis B.* J Drug Target, 2010. **18**(4): p. 282-91.
36. Jain, S., et al., *Mannosylated niosomes as adjuvant-carrier system for oral genetic immunization against hepatitis B.* Immunol Lett, 2005. **101**(1): p. 41-9.
37. Makidon, P.E., et al., *Pre-clinical evaluation of a novel nanoemulsion-based hepatitis B mucosal vaccine.* PLoS One, 2008. **3**(8): p. e2954.
38. Bielinska, A.U., et al., *Immunomodulation of TH2 biased immunity with mucosal administration of nanoemulsion adjuvant.* Vaccine, 2016. **34**(34): p. 4017-24.
39. Debin, A., et al., *Intranasal immunization with recombinant antigens associated with new cationic particles induces strong mucosal as well as systemic antibody and CTL responses.* Vaccine, 2002. **20**(21-22): p. 2752-63.
40. Borges, O., et al., *Evaluation of the immune response following a short oral vaccination schedule with hepatitis B antigen encapsulated into alginate-coated chitosan nanoparticles.* Eur J Pharm Sci, 2007. **32**(4-5): p. 278-90.
41. Borges, O., et al., *Immune response by nasal delivery of hepatitis B surface antigen and codelivery of a CpG ODN in alginate coated chitosan nanoparticles.* Eur J Pharm Biopharm, 2008. **69**(2): p. 405-16.
42. Khatri, K., et al., *Plasmid DNA loaded chitosan nanoparticles for nasal mucosal immunization against hepatitis B.* Int J Pharm, 2008. **354**(1-2): p. 235-41.
43. Mishra, N., et al., *Development and characterization of LTA-appended chitosan nanoparticles for mucosal immunization against hepatitis B.* Artif Cells Nanomed Biotechnol, 2014. **42**(4): p. 245-55.

44. Mangal, S., et al., *Pharmaceutical and immunological evaluation of mucoadhesive nanoparticles based delivery system(s) administered intranasally.* Vaccine, 2011. **29**(31): p. 4953-62.
45. Tafaghodi, M., et al., *Hepatitis B surface antigen nanoparticles coated with chitosan and trimethyl chitosan: Impact of formulation on physicochemical and immunological characteristics.* Vaccine, 2012. **30**(36): p. 5341-8.
46. He, X.W., et al., *Induction of mucosal and systemic immune response by single-dose oral immunization with biodegradable microparticles containing DNA encoding HBsAg.* J Gen Virol, 2005. **86**(Pt 3): p. 601-10.
47. Jaganathan, K.S. and S.P. Vyas, *Strong systemic and mucosal immune responses to surface-modified PLGA microspheres containing recombinant hepatitis B antigen administered intranasally.* Vaccine, 2006. **24**(19): p. 4201-11.
48. Rajkannan, R., et al., *Development of hepatitis B oral vaccine using B-cell epitope loaded PLG microparticles.* Vaccine, 2006. **24**(24): p. 5149-57.
49. Gupta, P., et al., *M-cell targeted biodegradable PLGA nanoparticles for oral immunization against hepatitis B.* J Drug Target, 2007. **15**(10): p. 701-713.
50. Jain, A.K., et al., *Synthesis, characterization and evaluation of novel triblock copolymer based nanoparticles for vaccine delivery against hepatitis B.* J Control Release, 2009. **136**(2): p. 161-9.
51. Mishra, N., et al., *Lectin anchored PLGA nanoparticles for oral mucosal immunization against hepatitis B.* J Drug Target, 2011. **19**(1): p. 67-78.
52. Pawar, D., et al., *Development and characterization of surface modified PLGA nanoparticles for nasal vaccine delivery: effect of mucoadhesive coating on antigen uptake and immune adjuvant activity.* Eur J Pharm Biopharm, 2013. **85**(3 Pt A): p. 550-9.
53. Jain, A.K., et al., *PEG-PLA-PEG block copolymeric nanoparticles for oral immunization against hepatitis B.* Int J Pharm, 2010. **387**(1-2): p. 253-62.
54. Thomas, C., V. Gupta, and F. Ahsan, *Influence of surface charge of PLGA particles of recombinant hepatitis B surface antigen in enhancing systemic and mucosal immune responses.* Int J Pharm, 2009. **379**(1): p. 41-50.
55. Thomas, C., et al., *Aerosolized PLA and PLGA nanoparticles enhance humoral, mucosal and cytokine responses to hepatitis B vaccine.* Mol Pharm, 2011. **8**(2): p. 405-15.
56. Nardelli-Haefliger, D., et al., *Nasal vaccination with attenuated Salmonella typhimurium strains expressing the Hepatitis B nucleocapsid: dose response analysis.* Vaccine, 2001. **19**(20-22): p. 2854-61.
57. Woo, P.C., et al., *Unique immunogenicity of hepatitis B virus DNA vaccine presented by live-attenuated Salmonella typhimurium.* Vaccine, 2001. **19**(20-22): p. 2945-54.
58. Smyth Templeton, N., *Liposomal delivery of nucleic acids in vivo.* DNA Cell Biol, 2002. **21**(12): p. 857-67.
59. Gregoriadis, G., et al., *Liposomes as immunological adjuvants and vaccine carriers.* Journal of Controlled Release, 1996(41): p. 49-56.
60. Jaspart, S., et al., *Solid lipid microparticles: formulation, preparation, characterization, drug release and applications.* Expert Opin Drug Deliv, 2005. **2**(1): p. 75-87.
61. S. Scalia, R.T., N. Sala and V. Iannuccelli, *Encapsulation in lipospheres of the complex between butyl methoxydibenzoylmethane and hydroxypropyl-β-cyclodextrin.* Int. J. Pharm., 2006. **320**: p. 79–85.
62. Trotta, M., et al., *Solid lipid micro-particles carrying insulin formed by solvent-in-water emulsion-diffusion technique.* Int J Pharm, 2005. **288**(2): p. 281-8.
63. Deacon, M.P., et al., *Atomic force microscopy of gastric mucin and chitosan mucoadhesive systems.* Biochem J, 2000. **348 Pt 3**: p. 557-63.
64. Schubert, R., et al., *Studies on the mechanism of bile salt-induced liposomal membrane damage.* Digestion, 1983. **28**(3): p. 181-90.

65. Conacher, M., J. Alexander, and J.M. Brewer, *Oral immunisation with peptide and protein antigens by formulation in lipid vesicles incorporating bile salts (bilosomes).* Vaccine, 2001. **19**(20-22): p. 2965-74.
66. Senior, K., *Bilosomes: the answer to oral vaccine delivery?* Drug Discov Today, 2001. **6**(20): p. 1031-1032.
67. Mann, J.F., et al., *Oral delivery of tetanus toxoid using vesicles containing bile salts (bilosomes) induces significant systemic and mucosal immunity.* Methods, 2006. **38**(2): p. 90-5.
68. Singh, P., et al., *Cholera toxin B subunit conjugated bile salt stabilized vesicles (bilosomes) for oral immunization.* Int J Pharm, 2004. **278**(2): p. 379-90.
69. Conacher M., J. Alexander, and J.M. Brewer, *Niosomes as Immunological Adjuvants. In "Synthetic Surfactant Vesicles"*, ed. I.F. Uchegbu2000, Singapore: International Publishers Distributors Ltd. 185-205.
70. Brewer, J.M. and J. Alexander, *The adjuvant activity of non-ionic surfactant vesicles (niosomes) on the BALB/c humoral response to bovine serum albumin.* Immunology, 1992. **75**(4): p. 570-5.
71. Brewer, J.M., et al., *Lipid vesicle size determines the Th1 or Th2 response to entrapped antigen.* J Immunol, 1998. **161**(8): p. 4000-7.
72. Duewell, P., et al., *ISCOMATRIX adjuvant combines immune activation with antigen delivery to dendritic cells in vivo leading to effective cross-priming of CD8+ T cells.* J Immunol, 2011. **187**(1): p. 55-63.
73. Wilson, N.S., et al., *ISCOMATRIX vaccines mediate CD8+ T-cell cross-priming by a MyD88-dependent signaling pathway.* Immunol Cell Biol, 2012. **90**(5): p. 540-52.
74. Frazer, I.H., et al., *Phase 1 study of HPV16-specific immunotherapy with E6E7 fusion protein and ISCOMATRIX adjuvant in women with cervical intraepithelial neoplasia.* Vaccine, 2004. **23**(2): p. 172-81.
75. Hamouda, T., et al., *A novel surfactant nanoemulsion with a unique non-irritant topical antimicrobial activity against bacteria, enveloped viruses and fungi.* Microbiol Res, 2001. **156**(1): p. 1-7.
76. Bielinska, A.U., et al., *Nasal immunization with a recombinant HIV gp120 and nanoemulsion adjuvant produces Th1 polarized responses and neutralizing antibodies to primary HIV type 1 isolates.* AIDS Res Hum Retroviruses, 2008. **24**(2): p. 271-81.
77. Donovan, B.W., et al., *Prevention of murine influenza A virus pneumonitis by surfactant nano-emulsions.* Antivir Chem Chemother, 2000. **11**(1): p. 41-9.
78. Myc, A., et al., *Development of immune response that protects mice from viral pneumonitis after a single intranasal immunization with influenza A virus and nanoemulsion.* Vaccine, 2003. **21**(25-26): p. 3801-14.
79. Bielinska, A.U., et al., *Mucosal immunization with a novel nanoemulsion-based recombinant anthrax protective antigen vaccine protects against Bacillus anthracis spore challenge.* Infect Immun, 2007. **75**(8): p. 4020-9.
80. PEYROT, M., et al., *Supramolecular biovectors (SMBV): a new family of nanoparticulate drug delivery systems. Synthesis and structural characterization.* Int J Pharm, 1994. **102**(1-3): p. 25-33.
81. De Miguel, I., et al., *Synthesis and characterization of supramolecular biovector (SMBV) specifically designed for the entrapment of ionic molecules.* Biochim Biophys Acta, 1995. **1237**(1): p. 49-58.
82. von Hoegen, P., *Synthetic biomimetic supra molecular Biovector (SMBV) particles for nasal vaccine delivery.* Adv Drug Deliv Rev, 2001. **51**(1-3): p. 113-25.
83. Kravtzoff R, F.A., De Miguel I, Perkins A, Major M, Betbeder D, et al., *Nasal residence time evaluation of cationic biovector in human volunteers.* Proceedings of the International Symposium on Controlled Release of Bioactive Materials, 1998. **25**: p. 818–19.

84. van der Lubben, I.M., et al., *Chitosan for mucosal vaccination.* Adv Drug Deliv Rev, 2001. **52**(2): p. 139-44.
85. Baldrick, P., *The safety of chitosan as a pharmaceutical excipient.* Regul Toxicol Pharmacol. **56**(3): p. 290-9.
86. Panos, I., N. Acosta, and A. Heras, *New drug delivery systems based on chitosan.* Curr Drug Discov Technol, 2008. **5**(4): p. 333-41.
87. Shaji, J., V. Jain, and S. Lodha, *Chitosan: A Novel Pharmaceutical Excipient.* International Journal of Pharmaceutical and Applied Sciences, 2010. **1**(1): p. 11-28.
88. Kang, M.L., C.S. Cho, and H.S. Yoo, *Application of chitosan microspheres for nasal delivery of vaccines.* Biotechnol Adv, 2009. **27**(6): p. 857-65.
89. Shibata, Y., et al., *Alveolar macrophage priming by intravenous administration of chitin particles, polymers of N-acetyl-D-glucosamine, in mice.* Infect Immun, 1997. **65**(5): p. 1734-41.
90. Babensee, J.E. and A. Paranjpe, *Differential levels of dendritic cell maturation on different biomaterials used in combination products.* J Biomed Mater Res A, 2005. **74**(4): p. 503-10.
91. Borges, O., et al., *Induction of lymphocytes activated marker CD69 following exposure to chitosan and alginate biopolymers.* Int J Pharm, 2007. **337**(1-2): p. 254-64.
92. Zaharoff, D.A., et al., *Chitosan solution enhances both humoral and cell-mediated immune responses to subcutaneous vaccination.* Vaccine, 2007. **25**(11): p. 2085-94.
93. Borges, O., et al., *Preparation of coated nanoparticles for a new mucosal vaccine delivery system.* Int J Pharm, 2005. **299**(1-2): p. 155-66.
94. Borges, O., et al., *Uptake studies in rat Peyer's patches, cytotoxicity and release studies of alginate coated chitosan nanoparticles for mucosal vaccination.* J Control Release, 2006. **114**(3): p. 348-58.
95. Weeratna, R., et al., *CpG ODN can re-direct the Th bias of established Th2 immune responses in adult and young mice.* FEMS Immunol Med Microbiol, 2001. **32**(1): p. 65-71.
96. McCluskie, M.J. and H.L. Davis, *CpG DNA is a potent enhancer of systemic and mucosal immune responses against hepatitis B surface antigen with intranasal administration to mice.* J Immunol, 1998. **161**(9): p. 4463-6.
97. Giteau, A., et al., *How to achieve sustained and complete protein release from PLGA-based microparticles?* Int J Pharm, 2008. **350**(1-2): p. 14-26.
98. Avgoustakis, K., *Pegylated poly(lactide) and poly(lactide-co-glycolide) nanoparticles: preparation, properties and possible applications in drug delivery.* Curr Drug Deliv, 2004. **1**(4): p. 321-33.
99. Mundargi, R.C., et al., *Nano/micro technologies for delivering macromolecular therapeutics using poly(D,L-lactide-co-glycolide) and its derivatives.* J Control Release, 2008. **125**(3): p. 193-209.
100. Gupta, R.K., M. Singh, and D.T. O'Hagan, *Poly(lactide-co-glycolide) microparticles for the development of single-dose controlled-release vaccines.* Adv Drug Deliv Rev, 1998. **32**(3): p. 225-246.
101. Ravi Kumar, M.N., U. Bakowsky, and C.M. Lehr, *Preparation and characterization of cationic PLGA nanospheres as DNA carriers.* Biomaterials, 2004. **25**(10): p. 1771-7.
102. Shenderova, A., T.G. Burke, and S.P. Schwendeman, *The acidic microclimate in poly(lactide-co-glycolide) microspheres stabilizes camptothecins.* Pharm Res, 1999. **16**(2): p. 241-8.
103. Kaneko, H., et al., *Oral DNA vaccination promotes mucosal and systemic immune responses to HIV envelope glycoprotein.* Virology, 2000. **267**(1): p. 8-16.
104. Sharpe, S., et al., *Mucosal immunization with PLGA-microencapsulated DNA primes a SIV-specific CTL response revealed by boosting with cognate recombinant modified vaccinia virus Ankara.* Virology, 2003. **313**(1): p. 13-21.

105. Herrmann, J.E., et al., *Immune responses and protection obtained by oral immunization with rotavirus VP4 and VP7 DNA vaccines encapsulated in microparticles.* Virology, 1999. **259**(1): p. 148-53.
106. Rico, M.A., et al., *Hepatitis B virus-specific T-cell proliferation and cytokine secretion in chronic hepatitis B e antibody-positive patients treated with ribavirin and interferon alpha.* Hepatology, 2001. **33**(1): p. 295-300.
107. Coombes, A.G., E.C. Lavelle, and S.S. Davis, *Biodegradable lamellar particles of poly(lactide) induce sustained immune responses to a single dose of adsorbed protein.* Vaccine, 1999. **17**(19): p. 2410-22.
108. Gupta, P.N., et al., *Lectin anchored stabilized biodegradable nanoparticles for oral immunization 1. Development and in vitro evaluation.* Int J Pharm, 2006. **318**(1-2): p. 163-73.
109. Formal, S.B., et al., *Construction of a potential bivalent vaccine strain: introduction of Shigella sonnei form I antigen genes into the galE Salmonella typhi Ty21a typhoid vaccine strain.* Infect Immun, 1981. **34**(3): p. 746-50.
110. Shata, M.T., et al., *Recent advances with recombinant bacterial vaccine vectors.* Mol Med Today, 2000. **6**(2): p. 66-71.
111. Curtiss, R., 3rd, K. Nakayama, and S.M. Kelly, *Recombinant avirulent Salmonella vaccine strains with stable maintenance and high level expression of cloned genes in vivo.* Immunol Invest, 1989. **18**(1-4): p. 583-96.
112. Fairweather, N.F., et al., *Use of live attenuated bacteria to stimulate immunity.* Res Microbiol, 1990. **141**(7-8): p. 769-73.
113. Darji, A., et al., *Oral somatic transgene vaccination using attenuated S. typhimurium.* Cell, 1997. **91**(6): p. 765-75.
114. Jones, B.D., N. Ghori, and S. Falkow, *Salmonella typhimurium initiates murine infection by penetrating and destroying the specialized epithelial M cells of the Peyer's patches.* J Exp Med, 1994. **180**(1): p. 15-23.
115. Clark, M.A., et al., *Preferential interaction of Salmonella typhimurium with mouse Peyer's patch M cells.* Res Microbiol, 1994. **145**(7): p. 543-52.
116. Kraehenbuhl, J.P. and M.R. Neutra, *Molecular and cellular basis of immune protection of mucosal surfaces.* Physiol Rev, 1992. **72**(4): p. 853-79.
117. McDermott, M.R. and J. Bienenstock, *Evidence for a common mucosal immunologic system. I. Migration of B immunoblasts into intestinal, respiratory, and genital tissues.* J Immunol, 1979. **122**(5): p. 1892-8.
118. Nardelli-Haefliger, D., et al., *Oral and rectal immunization of adult female volunteers with a recombinant attenuated Salmonella typhi vaccine strain.* Infect Immun, 1996. **64**(12): p. 5219-24.
119. Schodel, F., et al., *Development of recombinant Salmonellae expressing hybrid hepatitis B virus core particles as candidate oral vaccines.* Dev Biol Stand, 1994. **82**: p. 151-8.
120. Schodel, F. and H. Will, *Expression of hepatitis B virus antigens in attenuated Salmonellae for oral immunization.* Res Microbiol, 1990. **141**(7-8): p. 831-7.
121. Schodel, F., et al., *Recognition of a hepatitis B virus nucleocapsid T-cell epitope expressed as a fusion protein with the subunit B of Escherichia coli heat labile enterotoxin in attenuated salmonellae.* Vaccine, 1990. **8**(6): p. 569-72.
122. Schodel, F., D.R. Milich, and H. Will, *Hepatitis B virus nucleocapsid/pre-S2 fusion proteins expressed in attenuated Salmonella for oral vaccination.* J Immunol, 1990. **145**(12): p. 4317-21.
123. Schodel, F., et al., *A virulent Salmonella expressing hybrid hepatitis B virus core/pre-S genes for oral vaccination.* Vaccine, 1993. **11**(2): p. 143-8.

124. Schodel, F., et al., *Hybrid hepatitis B virus core-pre-S proteins synthesized in avirulent Salmonella typhimurium and Salmonella typhi for oral vaccination.* Infect Immun, 1994. **62**(5): p. 1669-76.
125. Hopkins, S., et al., *A recombinant Salmonella typhimurium vaccine induces local immunity by four different routes of immunization.* Infect Immun, 1995. **63**(9): p. 3279-86.
126. Schodel, F., et al., *Hybrid hepatitis B virus core antigen as a vaccine carrier moiety. II. Expression in avirulent Salmonella spp. for mucosal immunization.* Adv Exp Med Biol, 1996. **397**: p. 15-21.
127. Tacket, C.O., et al., *Safety and immunogenicity in humans of an attenuated Salmonella typhi vaccine vector strain expressing plasmid-encoded hepatitis B antigens stabilized by the Asd-balanced lethal vector system.* Infect Immun, 1997. **65**(8): p. 3381-5.
128. Zheng, B., et al., *A crucial role of macrophages in the immune responses to oral DNA vaccination against hepatitis B virus in a murine model.* Vaccine, 2001. **20**(1-2): p. 140-7.
129. Streatfield, S.J., *Oral hepatitis B vaccine candidates produced and delivered in plant material.* Immunol Cell Biol, 2005. **83**(3): p. 257-62.
130. Shchelkunov, S.N., et al., *Immunogenicity of a novel, bivalent, plant-based oral vaccine against hepatitis B and human immunodeficiency viruses.* Biotechnol Lett, 2006. **28**(13): p. 959-67.
131. Thanavala, Y. and A.A. Lugade, *Oral transgenic plant-based vaccine for hepatitis B.* Immunol Res. **46**(1-3): p. 4-11.
132. Gao, Y., et al., *Oral immunization of animals with transgenic cherry tomatillo expressing HBsAg.* World J Gastroenterol, 2003. **9**(5): p. 996-1002.
133. Thanavala, Y., et al., *Immunogenicity in humans of an edible vaccine for hepatitis B.* Proc Natl Acad Sci U S A, 2005. **102**(9): p. 3378-82.
134. Mason, H.S., D.M. Lam, and C.J. Arntzen, *Expression of hepatitis B surface antigen in transgenic plants.* Proc Natl Acad Sci U S A, 1992. **89**(24): p. 11745-9.
135. Kapusta, J., et al., *A plant-derived edible vaccine against hepatitis B virus.* Faseb J, 1999. **13**(13): p. 1796-9.
136. Kong, Q., et al., *Oral immunization with hepatitis B surface antigen expressed in transgenic plants.* Proc Natl Acad Sci U S A, 2001. **98**(20): p. 11539-44.
137. Richter, L.J., et al., *Production of hepatitis B surface antigen in transgenic plants for oral immunization.* Nat Biotechnol, 2000. **18**(11): p. 1167-71.
138. Mason, H.S., et al., *Edible plant vaccines: applications for prophylactic and therapeutic molecular medicine.* Trends Mol Med, 2002. **8**(7): p. 324-9.
139. Rybicki, E.P., *Plant-produced vaccines: promise and reality.* Drug Discov Today, 2009. **14**(1-2): p. 16-24.
140. G.B. Sunil Kumar, T.R.G., C.J. Revathi, L. Srinivas, V.A. Bapat,, *Expression of Hepatitis B Surface Antigen in Transgenic Banana Plants and NT- I Cell Line of Tobacco.* Planta, 2005. **222**: p. 484–493.
141. Huang, Z., et al., *Virus-like particle expression and assembly in plants: hepatitis B and Norwalk viruses.* Vaccine, 2005. **23**(15): p. 1851-8.
142. Huang, Z., et al., *Rapid, high-level production of hepatitis B core antigen in plant leaf and its immunogenicity in mice.* Vaccine, 2006. **24**(14): p. 2506-13.
143. Qian, B., et al., *Immunogenicity of recombinant hepatitis B virus surface antigen fused with preS1 epitopes expressed in rice seeds.* Transgenic Res, 2008. **17**(4): p. 621-31.
144. Greco, R., et al., *Production of recombinant HIV-1/HBV virus-like particles in Nicotiana tabacum and Arabidopsis thaliana plants for a bivalent plant-based vaccine.* Vaccine, 2007. **25**(49): p. 8228-40.
145. Marcondes, J. and E. Hansen, *Transgenic lettuce seedlings carrying hepatitis B virus antigen HBsAg.* Braz J Infect Dis, 2008. **12**(6): p. 469-71.

146. Mahor, S., et al., *A needle-free approach for topical immunization: antigen delivery via vesicular carrier system(s).* Curr Med Chem, 2007. **14**(27): p. 2898-910.
147. Roy, M.J., et al., *Induction of antigen-specific CD8+ T cells, T helper cells, and protective levels of antibody in humans by particle-mediated administration of a hepatitis B virus DNA vaccine.* Vaccine, 2000. **19**(7-8): p. 764-78.
148. Rottinghaus, S.T., et al., *Hepatitis B DNA vaccine induces protective antibody responses in human non-responders to conventional vaccination.* Vaccine, 2003. **21**(31): p. 4604-8.
149. Roberts, L.K., et al., *Clinical safety and efficacy of a powdered Hepatitis B nucleic acid vaccine delivered to the epidermis by a commercial prototype device.* Vaccine, 2005. **23**(40): p. 4867-78.
150. Tacket, C.O., et al., *Phase 1 safety and immune response studies of a DNA vaccine encoding hepatitis B surface antigen delivered by a gene delivery device.* Vaccine, 1999. **17**(22): p. 2826-9.
151. Fuller, J.T., et al., *Gene-gun-mediated DNA immunization with HBsAg: Efficacy in Small and large animals*, in *Vaccines 97: Molecular approaches to the control of infectious diseases*, F. Brown, D. Burton, and E. Norrby, Editors. 1997, Cold Spring Harbor Laboratory Press. p. 157-161.
152. Osorio, J.E., et al., *Immune responses to hepatitis B surface antigen following epidermal powder immunization.* Immunol Cell Biol, 2003. **81**(1): p. 52-8.
153. Chen, D., et al., *Epidermal Powder Immunization Induces both Cytotoxic T-Lymphocyte and Antibody Responses to Protein Antigens of Influenza and Hepatitis B Viruses* Journal of Virology, 2001. **75**(23): p. 11630-11640.
154. Fuller, D.H., P. Loudon, and C. Schmaljohn, *Preclinical and clinical progress of particle-mediated DNA vaccines for infectious diseases.* Methods, 2006. **40**(1): p. 86-97.
155. Babiuk, L.A., S.L. Babiuk, and M. Baca-Estrada, *Novel vaccines strategies*, in *Advances in Virus Research*2002, Academic Press. p. 55.
156. Fuller, J.T., et al., *Gene-gun-mediated DNA immunization with HBV antigens: Immune responses in mice, monkeys and pigs.*, in *Vaccines 96 : Molecular Approaches to the Control of Infectious Diseases*, F. Brown, Editor 1996, Cold Spring Harbor Laboratory Press. p. 87.
157. WW Leitner, M.S., WR Ballou, JP Seitz, AM Schultz, MJ Sheehy and JA Lyon *Immune responses induced by intramuscular or gene gun injection of protective deoxyribonucleic acid vaccines that express the circumsporozoite protein from Plasmodium berghei malaria parasites.* Journal of Immunology, 1997. **159**.
158. Maa, Y.F., et al., *Hepatitis-B surface antigen (HBsAg) powder formulation: process and stability assessment.* Curr Drug Deliv, 2007. **4**(1): p. 57-67.
159. Fu, T.M., et al., *Priming of cytotoxic T lymphocytes by DNA vaccines: requirement for professional antigen presenting cells and evidence for antigen transfer from myocytes.* Mol Med, 1997. **3**(6): p. 362-71.
160. Ulmer, J.B., et al., *Generation of MHC class I-restricted cytotoxic T lymphocytes by expression of a viral protein in muscle cells: antigen presentation by non-muscle cells.* Immunology, 1996. **89**(1): p. 59-67.
161. Krieg, A.M., et al., *CpG motifs in bacterial DNA trigger direct B-cell activation.* Nature, 1995. **374**(6522): p. 546-9.
162. Yi, A.K., et al., *Rapid immune activation by CpG motifs in bacterial DNA. Systemic induction of IL-6 transcription through an antioxidant-sensitive pathway.* J Immunol, 1996. **157**(12): p. 5394-402.
163. Klinman, D.M., et al., *CpG motifs present in bacteria DNA rapidly induce lymphocytes to secrete interleukin 6, interleukin 12, and interferon gamma.* Proc Natl Acad Sci U S A, 1996. **93**(7): p. 2879-83.

164. Sparwasser, T., et al., *Bacterial DNA and immunostimulatory CpG oligonucleotides trigger maturation and activation of murine dendritic cells.* Eur J Immunol, 1998. **28**(6): p. 2045-54.
165. Davis, H.L., et al., *CpG DNA is a potent enhancer of specific immunity in mice immunized with recombinant hepatitis B surface antigen.* J Immunol, 1998. **160**(2): p. 870-6.
166. Fan, H., et al., *Immunization via hair follicles by topical application of naked DNA to normal skin.* Nat Biotechnol, 1999. **17**(9): p. 870-2.
167. Maheshwari, C., et al., *Non-ionic surfactant vesicles mediated transcutaneous immunization against hepatitis B.* Int Immunopharmacol, 2011. **11**(10): p. 1516-22.
168. Mishra, D., et al., *Elastic liposomes mediated transdermal delivery of an anti-hypertensive agent: propranolol hydrochloride.* J Pharm Sci, 2007. **96**(1): p. 145-55.
169. Mishra, D., et al., *Elastic liposomes mediated transcutaneous immunization against Hepatitis B.* Vaccine, 2006. **24**(22): p. 4847-55.
170. Gompper, G. and D.M. Kroll, *Driven transport of fluid vesicles through narrow pores.* Phys Rev E Stat Phys Plasmas Fluids Relat Interdiscip Topics, 1995. **52**(4): p. 4198-4208.
171. Cevc, G. and G. Blume, *Lipid vesicles penetrate into intact skin owing to the transdermal osmotic gradients and hydration force.* Biochim Biophys Acta, 1992. **1104**(1): p. 226-32.
172. Mahor, S., et al., *Cationic transfersomes based topical genetic vaccine against hepatitis B.* Int J Pharm, 2007. **340**(1-2): p. 13-9.
173. Touitou, E., M. Alkabes, and N. Dayan, *Ethosomes: novel vesicular carriers for enhanced skin delivery.* Pharm. Res., 1997. **14**: p. S305-S306.
174. Williams, A., *Transdermal and Topical Drug Delivery*2005: Pharmaceutical Press. 256.
175. Dubey, V., et al., *Vesicles as tools for the modulation of skin permeability.* Expert Opin Drug Deliv, 2007. **4**(6): p. 579-93.
176. Mishra, D., et al., *Systemic and mucosal immune response induced by transcutaneous immunization using Hepatitis B surface antigen-loaded modified liposomes.* Eur J Pharm Sci, 2008. **33**(4-5): p. 424-33.
177. Lycke, N., T. Tsuji, and J. Holmgren, *The adjuvant effect of Vibrio cholerae and Escherichia coli heat-labile enterotoxins is linked to their ADP-ribosyltransferase activity.* Eur J Immunol, 1992. **22**(9): p. 2277-81.
178. Holmgren, J., N. Lycke, and C. Czerkinsky, *Cholera toxin and cholera B subunit as oral-mucosal adjuvant and antigen vector systems.* Vaccine, 1993. **11**(12): p. 1179-84.
179. Spangler, B.D., *Structure and function of cholera toxin and the related Escherichia coli heat-labile enterotoxin.* Microbiol Rev, 1992. **56**(4): p. 622-47.
180. Yamamoto, S., et al., *Mutants in the ADP-ribosyltransferase cleft of cholera toxin lack diarrheagenicity but retain adjuvanticity.* J Exp Med, 1997. **185**(7): p. 1203-10.
181. Verweija, R., et al., *Musosal immunoadjuvant activity of recombinant Escherichia coli heatlabile enterotoxin and its B subunit: Induction of systemic IgG and secretory IgA responses in mice by intranasal immunization with influenza virus surface antigen* Vaccine, 1998. **16**(20): p. 2069-2076
182. Yamamoto, S., et al., *A nontoxic mutant of cholera toxin elicits Th2-type responses for enhanced mucosal immunity.* Proc Natl Acad Sci U S A, 1997. **94**(10): p. 5267-72.
183. Tochikubo, K., et al., *Recombinant cholera toxin B subunit acts as an adjuvant for the mucosal and systemic responses of mice to mucosally co-administered bovine serum albumin.* Vaccine, 1998. **16**(2-3): p. 150-5.
184. Komase, K., et al., *Mutants of Escherichia coli heat-labile enterotoxin as an adjuvant for nasal influenza vaccine.* Vaccine, 1998. **16**(2-3): p. 248-54.
185. Douce, G., et al., *Mucosal immunogenicity of genetically detoxified derivatives of heat labile toxin from Escherichia coli.* Vaccine, 1998. **16**(11-12): p. 1065-73.
186. Chong, C., M. Friberg, and J.D. Clements, *LT(R192G), a non-toxic mutant of the heat-labile enterotoxin of Escherichia coli, elicits enhanced humoral and cellular immune responses*

associated with protection against lethal oral challenge with Salmonella spp. Vaccine, 1998. **16**(7): p. 732-40.
187. Rappuoli, R., et al., *Genetic detoxification of bacterial toxins: a new approach to vaccine development.* Int Arch Allergy Immunol, 1995. **108**(4): p. 327-33.
188. Fontana, M.R., et al., *Construction of nontoxic derivatives of cholera toxin and characterization of the immunological response against the A subunit.* Infect Immun, 1995. **63**(6): p. 2356-60.
189. Di Tommaso, A., et al., *Induction of antigen-specific antibodies in vaginal secretions by using a nontoxic mutant of heat-labile enterotoxin as a mucosal adjuvant.* Infect Immun, 1996. **64**(3): p. 974-9.
190. Giuliani, M.M., et al., *Mucosal adjuvanticity and immunogenicity of LTR72, a novel mutant of Escherichia coli heat-labile enterotoxin with partial knockout of ADP-ribosyltransferase activity.* J Exp Med, 1998. **187**(7): p. 1123-32.
191. Isaka, M., et al., *Mucosal immunization against hepatitis B virus by intranasal co-administration of recombinant hepatitis B surface antigen and recombinant cholera toxin B subunit as an adjuvant.* Vaccine, 2001. **19**(11-12): p. 1460-6.
192. Krieg, A.M., *Therapeutic potential of Toll-like receptor 9 activation.* Nat Rev Drug Discov, 2006. **5**(6): p. 471-84.
193. Cooper, C.L., et al., *CPG 7909 adjuvant improves hepatitis B virus vaccine seroprotection in antiretroviral-treated HIV-infected adults.* Aids, 2005. **19**(14): p. 1473-9.
194. Cooper, C., et al., *CPG 7909, an Immunostimulatory TLR9 Agonist Oligodeoxynucleotide, as Adjuvant to Engerix-B® HBV Vaccine in Healthy Adults: A Double-Blind Phase I/II Study* Journal of Clinical Immunology, 2004. **24**(6): p. 693-701.
195. McCluskie, M.J. and R. Weeratna, *Cpg oligodeoxynucletides as vaccine adjuvants in "Immunopotentiators in Modern Vaccines "*, ed. V. Schijns and D. O'Hagan2006: Academic Press. 73-92.
196. Ahmad-Nejad, P., et al., *Bacterial CpG-DNA and lipopolysaccharides activate Toll-like receptors at distinct cellular compartments.* Eur J Immunol, 2002. **32**(7): p. 1958-68.
197. Gallichan, W.S., et al., *Intranasal immunization with CpG oligodeoxynucleotides as an adjuvant dramatically increases IgA and protection against herpes simplex virus-2 in the genital tract.* J Immunol, 2001. **166**(5): p. 3451-7.
198. McCluskie, M.J. and H.L. Davis, *Oral, intrarectal and intranasal immunizations using CpG and non-CpG oligodeoxynucleotides as adjuvants.* Vaccine, 2000. **19**(4-5): p. 413-22.
199. Kwant, A. and K.L. Rosenthal, *Intravaginal immunization with viral subunit protein plus CpG oligodeoxynucleotides induces protective immunity against HSV-2.* Vaccine, 2004. **22**(23-24): p. 3098-104.
200. Eastcott, J.W., et al., *Oligonucleotide containing CpG motifs enhances immune response to mucosally or systemically administered tetanus toxoid.* Vaccine, 2001. **19**(13-14): p. 1636-42.
201. McCluskie, M.J., et al., *CpG DNA is an effective oral adjuvant to protein antigens in mice.* Vaccine, 2000. **19**(7-8): p. 950-7.
202. McCluskie, M.J., et al., *Parenteral and mucosal prime-boost immunization strategies in mice with hepatitis B surface antigen and CpG DNA.* FEMS Immunol Med Microbiol, 2002. **32**(3): p. 179-85.
203. Munoz, E., et al., *Cholera toxin discriminates between T helper 1 and 2 cells in T cell receptor-mediated activation: role of cAMP in T cell proliferation.* Journal of Experimental Medicine, 1990. **172**: p. 95-103.
204. Klinman, D., et al., *CpG motifs expressed by bacterial DNA rapidly induce lymphocytes to secrete IL-6, IL-12 and IFN-γ.* Proc. Natl. Acad. Sci. U.S.A., 1996. **93**: p. 2879.
205. McCluskie, M.J. and H.L. Davis, *CpG DNA as mucosal adjuvant.* Vaccine, 1999. **18**(3-4): p. 231-7.

206. Moldoveanu, Z., et al., *CpG DNA, a novel immune enhancer for systemic and mucosal immunization with influenza virus.* Vaccine, 1998. **16**(11-12): p. 1216-24.
207. Horner, A.A., et al., *Immunostimulatory DNA is a potent mucosal adjuvant.* Cell Immunol, 1998. **190**(1): p. 77-82.
208. McCluskie, M.J., R.D. Weeratna, and H.L. Davis, *Intranasal immunization of mice with CpG DNA induces strong systemic and mucosal responses that are influenced by other mucosal adjuvants and antigen distribution.* Mol Med, 2000. **6**(10): p. 867-77.
209. McCluskie, M.J., et al., *Mucosal immunization of mice using CpG DNA and/or mutants of the heat-labile enterotoxin of Escherichia coli as adjuvants.* Vaccine, 2001. **19**(27): p. 3759-68.

CHAPTER 2

Association of chitosan and aluminium as a new adjuvant strategy for improved vaccination

Abstract

The use of particulate adjuvants offers an interesting possibility to enhance and modulate the immune responses elicited by vaccines. Aluminium salts have been extensively used as vaccine adjuvants, but they lack the capacity to induce a strong cellular and mucosal immune response. Taking this into consideration, in this study we designed a new antigen delivery system combining aluminium salts with chitosan. Chitosan-aluminium nanoparticles (CH-Al NPs) exhibited a mean diameter of 280 nm and a positive surface charge. The newly developed CH-Al NPs are more stable at physiological environment than classical CH NPs, showing no cytotoxic effects and revealing potential as a delivery system for a wide range of model antigens. *In vivo* studies showed that mice immunized with hepatitis B surface antigen (HBsAg)-containing CH NPs display high anti-HBsAg IgG titers in the serum, as well as the highest antigen-specific IgG on vaginal washes. Furthermore, in contrast to mice receiving antigen alone, mice immunized with the particulate adjuvant were able to elicit IgG2c antibody titers and exhibited higher antigen-specific IFN-γ levels in splenocytes. In conclusion, we established that CH-Al NPs, combining two immunostimulants to enhance both humoral and cellular immune responses, are a safe and promising system for antigen delivery. Our findings point towards their potential in future vaccination approaches.

2.1 Introduction

The use of vaccine adjuvants provides an interesting approach to modulate the type and magnitude of immune responses. Aluminium salts, often designated as alum, have been widely used as adjuvants in licensed vaccine due to their immunomodulatory properties [1-3]. Even though they were first introduced to the market in the 1930s, the mechanism of adjuvanticity of aluminium salts is still unclear. Originally it was suggested that alum would allow a sustained released of the antigen, resulting in a prolonged and effective stimulation of the immune system. However, this so-called "depot-effect" [4] was later challenged [5, 6]. Indeed, Hutchison et al. reported that, 2 h after immunization, excision of the depot site did not alter the humoral response elicited by alum, thus suggesting that this was dispensable for adjuvanticity. In addition to the depot theory, several other mechanisms of alum action have been proposed, namely the controversial requirement of the NLRP3 inflammasome activation and the downstream effects elicited on the adjuvant effect of alum *in vitro* and *in vivo* [7-10]. More recently, aluminium salts have been shown to induce cell death at the injection site leading to the release of host DNA, which would act as a danger associated molecular pattern (DAMP), boosting the immune response [11]. Aluminium-containing adjuvants are known to induce a strong humoral response, mainly characterized by the secretion of antigen-specific antibodies; however they lack the capability to induce a Th1-type response, which is important for protection against diseases that require strong cell-mediated immune response (e.g. HIV, tuberculosis, malaria) [1, 2]. Therefore, an attractive approach to solve this issue would be to combine aluminium salts with a Th1-biased immunostimulant. Previous studies have demonstrated that chitosan has the ability to induce dendritic cell (DC) maturation, antigen-specific Th1 responses and, in contrast to other adjuvants, it does not promote inhibition of the Th1 cell-polarizing cytokine IL-12 [12, 13]. This makes chitosan an ideal candidate to combine with aluminium salts towards the generation of effective parenteral as well as mucosal vaccines.

Chitosan is a natural cationic polymer of β-(1-4)-linked glucosamine and N-acetyl-glucosamine obtained after the alkaline deacetylation of chitin, which is naturally present in the exoskeletons of crustacean and fungal cell walls. Chitosan is a very versatile molecule and, depending on the deacetylation process, the resulting polymer varies in molecular weight and degree of deacetylation, which has a strong impact on its physicochemical and biological properties [14-16]. In addition to its common use as a drug and gene delivery system, chitosan has a number of other promising applications in the biomedical field, in particular, as a vaccine adjuvant [17-19], due to its safety profile, biodegradability, mucoadhesive properties

and immunostimulatory potential [13, 20-22]. Moreover, by making use of simple and mild processes (e.g. ionotropic gelation, precipitation/coacervation), it is possible to produce particles with controlled physicochemical characteristics.

The use of particles as vaccine adjuvants offers several advantages, including enhanced uptake by antigen presenting cells (APCs), protection of antigen from enzymatic degradation, promotion of a depot effect with gradual release of the antigen and the ability to facilitate antigen cross-presentation and co-delivery of antigens and immunomodulators to the same cell population [23, 24]. When developing a new particulate adjuvant, physicochemical characteristics such as size, surface charge/chemistry and shape are known to play an important role in the way the body interacts and responds to it [25-27]. For example, Lunov et al. showed that amino-functionalized, but not carboxy or non-functionalized polystyrene particles with a comparable mean diameter of 110 nm, activate the NLRP3 inflammasome in macrophages through the lysosomal rupture model [28]. Moreover, while there is still a great deal of debate on whether small or large particles are more effective in inducing specific immune response, particles with a size within the viral range (< 500 nm) are known to be more extensively internalized by APCs, drain better through the lymphatics and activate the inflammasome, which can be beneficial for the induction of cell mediated immunity [26]. Kobiasi et al. addressed the relationship between chitosan particle size and dispersity in *in vivo* cell trafficking and uptake and found that 150 nm chitosan nanoparticles drained approximately 50 times faster to the lymph nodes after 24 h than their 1.3 μm microparticle counterparts [29].

The main aim of this study was first to develop a particulate adjuvant that combines chitosan and aluminium in the same particle and second to investigate whether the combination of the recognized immunostimulatory properties of aluminium salts and chitosan would result in enhanced adjuvant effects, enabling a mixed Th1/Th2-type of immune response, while additionally facilitating the antigen draining to local lymph nodes. For this purpose, we optimized the production of chitosan nanoparticles using aluminium sulfate in place of the conventionally used sodium sulfate as a cross-linking agent for chitosan. Remarkably, chitosan particles prepared with aluminium salts demonstrated to be much more stable than traditional particles, which is critical for formulation development. We then evaluated the cytotoxicity of chitosan-aluminium nanoparticles in 3 distinct cell cultures and investigated their capacity to be internalized and to act as a delivery system for 6 different model antigens. Finally, we tested the ability of CH-Al NPs to modulate the immune response following subcutaneous immunization using the recombinant hepatitis B surface antigen

(HBsAg). Collectively, our data show that CH-Al NPs can be used as adjuvant towards effective vaccination, combining their stability and ability to mediate delivery of various model antigens with the immunomodulatory properties of aluminium salts and chitosan.

2.2 Experimental section

2.2.1 Chitosan nanoparticle optimization and characterization

Chitosan (CH) (ChitoClear, 95 % degree of deacetylation; Primex Bio-Chemicals AS) was purified using a previously described method, with some modifications [19, 30]. To optimize the preparation method of the CH-Al NPs, nine CH/Al ratios were tested. Therefore, chitosan-aluminium nanoparticles (CH-Al NPs) were prepared by adding equal volumes of 0.05-0.15 % CH (in 25 mM sodium acetate buffer (AcB)) solution and 0.25-1.50 % aluminium sulfate (Al) aqueous solution, under high-speed vortexing for 20 s, followed by incubation at room temperature for 1 h. For the preparation of chitosan nanoparticles (CH-Na NPs), equal volumes of a chitosan solution (0.1 % in 25 mM AcB, pH 5.0) and a sodium sulfate solution (0.625 %) were mixed under high-speed vortexing for 20 s. The resulting nanoparticle suspensions were centrifuged for 30 min at 4500 *g*, the supernatants were discarded and the pellet resuspended in 25 mM AcB, pH 5.5.

Size and zeta potential of CH NPs were measured by dynamic light scattering (DLS) and electrophoretic light scattering (ELS), respectively, in a Delsa Nano C (Beckman Coulter, USA). The analysis was performed at 25 °C, in 25 mM AcB, pH 5.5.

The presence of aluminium in the particles was evaluated by energy-dispersive X-ray spectroscopy (EDS) analysis using a high resolution FEI Quanta 400 FEG E Scanning Electron Microscope coupled to an EDAX Genesis X4M X-Ray Energy Dispersive Electron Spectrometer (EDAX Inc., USA). Aluminium quantification was performed indirectly, by determining the amount that remained free in the particle supernatants, using the eriochrome cyanine R method, after minor modifications [31]. Briefly, the volumes described on the protocol were reduced allowing the reaction to be performed with 90 % less sample.

Particle morphology was evaluated by scanning electron microscopy (SEM) (JSM-700 1FA, JEOL, Japan). Prior to image acquisition, one drop of nanoparticle suspension was placed over a copper surface and let to dry overnight. Afterward, samples were mounted on microscope stub, coated with gold, and then observed under the microscope.

2.2.2 Stability studies

To assess the physical integrity of the NPs, 2 mL of nanoparticle suspensions were centrifuged for 30 min at 4500 g, the supernatants were discarded and the pellet resuspended in 1 mL of either PBS, pH 7.4; 200 mM phosphate buffer (PB), pH 7.4; 10 mM HEPES, pH 7.4 or 25 mM AcB, pH 5.5, at 20 °C or 37 °C. Transmittance (500 nm) of the resulting suspension was measured straight after, in a spectrophotometer (UV-1601, Shimadzu Corporation, Japan).

The thermal degradation process and the stability of the nanoparticles were investigated. The CH-Al NPs and CH-Na NPs curves were obtained followed by thermogravimetric analysis (TGA) and differential thermal analysis (DTA) (DTA/TGA – Scientific Rheometrics 1500, UK). Approximately 3 mg to 6 mg of the freeze-dried samples were weighed into ceramic pans, which were heated from 30 °C to 800 °C at a heating rate of 10 °C/min per cycle. Inert atmosphere was maintained by purging argon at the flow rate of 100 mL/min.

2.2.3 Protein adsorption studies

Nanoparticle suspensions were mixed with different proteins (α-casein, bovine serum albumin (BSA), ovalbumin (OVA), lactalbumin, lysozyme, myoglobin (Sigma-Aldrich) and HBsAg (Aldevron)) at various ratios, followed by incubation at 20 ºC in 25 mM PB, pH 7.1. At appropriate intervals (5, 10, 30 or 180 min), 1.0 mL aliquots were collected for indirect quantification of protein adsorption using the bicinchoninic acid (BCA) method (Pierce, USA), and replaced by 1.0 mL of fresh PB buffer. Collected aliquots were centrifuged at 13000 *g* for 15 min and the supernatant was tested for non-bound protein quantification, according to manufacturer's protocol. Loading efficacy (LE) and loading capacity (LC) were determined using equations 1 and 2, respectively.

$$LE\ (\%) = \frac{(total\ amount\ of\ protein - unbound\ protein)}{total\ amount\ of\ protein} \times 100 \qquad (1)$$

$$LC\ (\%) = \frac{(total\ amount\ of\ protein - unbound\ protein)}{weight\ of\ the\ particles\ (mg)} \times 100 \qquad (2)$$

2.2.4 Cell viability studies

Cell viability was assessed by the MTT assay in 2 human lung epithelial cell lines, A549 (ATCC, CCL-185) and Calu-3 (ATCC, HTB-55), and in a primary culture of splenocytes obtained according with a protocol described elsewhere [32].

A549 and Calu-3 cells were cultured in F12 Ham nutrient mixture (Sigma-Aldrich) and Dulbecco's modified Eagle medium (DMEM) (Sigma-Aldrich), respectively, supplemented with 10 % heat-inactivated foetal bovine serum (FBS) (Gibco), 50 $U \cdot mL^{-1}$ penicillin (Gibco) and 50 $\mu g \cdot mL^{-1}$ streptomycin (Gibco), at 37 °C and 5 % CO_2. Cells were seeded in a 96-well plate at a density of 1×10^6 $cells \cdot mL^{-1}$ and incubated overnight. For splenocytes, cell suspensions were adjusted to a final concentration of 1×10^7 $cells \cdot mL^{-1}$ in RPMI 1640 medium (Sigma-Aldrich) supplemented with 10 % heat-inactivated foetal bovine serum, 2 mM L-glutamine (Gibco), 50 $U \cdot mL^{-1}$ penicillin, 50 $\mu g \cdot mL^{-1}$ streptomycin and 2 % (v/v) 1 M HEPES buffer (Sigma-Aldrich). For cell viability studies, serial dilutions of the CH-Al NPs were performed in the same culture media, and the NPs were then added to 200 µl of cells. After 2 h (A549, Calu-3) or 24 h (splenocytes) of incubation, 20 µL of MTT (5 $mg \cdot mL^{-1}$ in PBS, pH 7.4) were added to each well following 2 h (A549, Calu-3) or 4 h (splenocytes) of additional incubation at 37 °C. The formazan crystals were solubilized with 200 µL of dimethyl sulfoxide (DMSO), added to each well, and optical density (OD) of plate solutions was read at 540 nm with 630 nm as reference wavelength (Multiskan EX; Thermo Scientific). The viability of non-treated cells (control) was defined as 100 % and the relative viability (%) of the treated cells was calculated using equation 3.

$$Cell\ viability\ (\%) = \frac{OD\ sample\ (540nm) - OD\ sample\ (630nm)}{OD\ control\ (540nm) - OD\ control\ (630nm)} \times 100 \qquad (3)$$

2.2.5 Cellular uptake studies

The synthesis of fluorescein-isothiocyanate (FITC) (Santa Cruz, USA)-labelled chitosan was performed using a previously described protocol [19], based on the reaction between the isothiocyanate groups of FITC (Ex/Em: 490/525) and the primary amino groups of chitosan.

For confocal microscopy, A549 cells were seeded on glass coverslips in 12-well plates at a density of 1.5 x 10^5 cells per well and cultured overnight. On the second day, the growth medium was replaced with fresh medium with FITC-labelled CH-Al NPs. After 4 h, the medium containing the CH-Al NPs was removed and the cells were washed three times with PBS, pH 7.4, and fixed with 4 % paraformaldehyde (PFA) in PBS for 15 min at 37 °C. Plasma membrane and cell nucleus of the pre-fixed cells were then labelled using Alexa Fluor 594 wheat germ agglutinin (Ex/Em: 591/618 nm) and Hoechst 33342 dye (Ex/Em: 350/461 nm), respectively, according to manufacturer's instructions. After labelling, cells were washed twice with PBS and the coverslips mounted in microscope slides with DAKO mounting medium,

and examined under an inverted laser scanning confocal microscope (Zeiss LSM 510 META, Carl Zeiss, Germany) equipped with a imaging software (LSM 510 software, Carl Zeiss).

2.2.6 Immunization studies

Seven-week-old C57BL/6 female mice were obtained from Charles River Laboratories (France), acclimated for 1 week prior to the initiation of experiments and maintained in the Center for Neuroscience and Cell Biology (CNC) animal facility, and provided food and water *ad libitum*. All experiments were approved (ORBEA_50_2013/27092013) and carried out in accordance with institutional ethical guidelines and with National (Dec. No. 113/2013) and International (normative 2010/63 from EU) legislation. Mice (5 per group), were subcutaneously immunized with 100 μL of a suspension containing 5 μg HBsAg, either alone or adsorbed onto CH-Al NPs or CH-Na NPs, on days 0 and 14, and culled on day 88.

2.2.7 Biological sample collection

Blood was collected by submandibular lancet method into centrifuge tubes on days 28, 58 and 88, followed by centrifugation at 1000 g for 15 min and the serum fraction collected. Vaginal washes were collected on day 87, as previously described [19], and spleens were collected on day 88. Collected and processed samples were stored at −20 °C until further analysis.

2.2.8 Immunoglobulin determination

Quantification of IgG, IgG1 and IgG2c was performed using a protocol previously described by our group [33]. Ninety-six well plates were coated with 100 μL of 1 $\mu g \cdot mL^{-1}$ HBsAg solution (50 mM sodium carbonate/bicarbonate, pH 9.6) and left overnight at 4 °C. To reduce non-specific binding, the wells were blocked by adding 2 % (w/v) BSA in PBS-Tween, followed by 1 h incubation at 37 °C. After washing, serial dilutions of serum were applied, whereas vaginal washes were added undiluted. After incubation for 2 h at 37 °C and extensive washing, immunoglobulins were detected upon incubation with horseradish peroxidase (HRP) conjugated goat anti-mouse IgG, IgG1 or IgG2c for 30 min at 37 °C, followed by a further incubation with OPD substrate solution (5 mg OPD in 10 mL citrate buffer and 10 μl H_2O_2) for 10 min at room temperature. The reaction was stopped by adding 1 M H_2SO_4 and the optical density was determined at 492 nm using a microplate reader. The end-point titers displayed in the results section represent the antilog of the last log 2 dilution,

for which the OD values were at least two-fold higher than that of the naive mice serum, equally diluted. The log 2 end-point titers were used for statistical analysis.

2.2.9 Spleen cell restimulation

Spleens were harvested on day 88 after immunization and a single cell suspension was then prepared using a 40 μm cell strainer. Cells were centrifuged for 5 min at 400 g and resuspended in T cell media (RPMI 1640, 10 % FBS, 1 % HEPES, 50 $U \cdot mL^{-1}$ penicillin, 50 $\mu g \cdot mL^{-1}$ streptomycin, 0.1 % 2-mercaptoethanol, 1% of 1 M NaOH solution, 1 % sodium pyruvate, 1 % MEM non-essential amino acids, 2 % MEM amino acids). For the restimulation assay, 500 μL of the cell suspension were plated at a density of 2.5 x 10^6 $cells \cdot mL^{-1}$ in 48-well plate and 500 μL of T cell media, either alone or containing 5 $\mu g \cdot mL^{-1}$ of HBsAg (final concentration of 2.5 $\mu g \cdot mL^{-1}$), were added to the cells. The plates were incubated at 37 ºC for 98 h to induce cytokine production by antigen-specific T cells and the supernatants were collected into 96-well plates and stored at −80 ºC until further analysis.

2.2.10 Cytokine quantification

The concentration of the cytokines IL-4 and IFN-γ (PeproTech) was determined by the enzyme-linked immunosorbent assay (ELISA), according to the manufacturer's instructions. Briefly, 96-well high binding ELISA plates (Greiner Bio-one) were coated with capture antibody and incubated overnight at 4 °C. The plates were washed in wash buffer (0.05 % PBS-Tween) and blocked with 1 % BSA in PBS solution at room temperature for 1 h. After washing, samples and standards were added to the plates and incubated for 2 h at room temperature. Following this incubation step, biotinylated goat anti-mouse detection antibody was added to the plates which were incubated for 2 h, before washing and incubating with the avidin-HRP conjugate for an additional 30 min. Finally, plates were washed and ABTS substrate solution was added to the plate. After 15 min incubation in the dark, the OD values were measured at 405 nm with wavelength correction set at 650 nm using a Multiskan EX 96-well plate reader. A standard curve was generated and this was then used to determine the cytokine concentration of the unknown replicates.

2.2.11 Statistical analysis

Results are expressed as mean values ± standard deviation (SD) and were analysed by ANOVA, followed by Tukey´s post-test with $P \leq 0.05$ considered as a statistically significant difference, using GraphPad Prism v 5.03, (GraphPad Software Inc.).

2.3 Results and discussion

2.3.1 Characterization of chitosan-aluminium nanoparticles

The coacervation/precipitation method used to prepare CH-Al NPs is an easy and safe technique that does not require expensive equipment, harmful organic solvents or high temperatures, thus making it ideal to generate protein delivery systems. The ability of chitosan to react with aluminium sulfate relies on the interactions between polyelectrolytes of opposite charges, the cationic amino groups in chitosan and the anionic groups in sulfate, and the particle characteristics, such as size and zeta potential, are known to be dependent upon the ratio of chitosan to the cross-linking agent [32, 34]. In order to evaluate the potential of associating two immunopotentiators, chitosan and aluminium, towards the design of an effective adjuvant, initial experiments were conducted to optimize the preparation method of the CH-Al NPs. Therefore, several ratios of CH:Al sulfate were tested and the mean size of the CH-Al NPs was found to range between 280 nm and 1110 nm (Fig. 2.1 A, B). As observed (Fig. 2.1 A), when $Al_2(SO_4)_3$ concentration was kept at 0.50 % (w/v), CH concentrations outside the 0.100 % to 0.125 % (w/v) range produced larger particles, whereas within that range, particles were smaller than 500 nm and more monodisperse (Fig. 2.1 C). For CH concentrations higher than 0.075 %, our findings are similar to those observed by Koppolu et al., showing that high amounts of unreacted CH increase the chance of the polymer to interact and form larger particles [35].

Likewise, figure 2.1 B shows that, at a fixed CH concentration of 0.10 % (w/v), the concentration of 0.50 % (w/v) aluminium sulfate was found to be optimal for obtaining particles smaller than 500 nm and the Al^{3+} loading efficacy of the CH-Al NPs ranged from 76.0 % to 89.6 % over the tested CH:Al sulfate ratios (Fig. 2.1 A, B).

The zeta potential of all the formulations tested was positive and generally increased with the increase of chitosan concentration owing to the cationic nature of this polymer (Fig. 2.1 A, B). [20]. Particles produced with higher amounts of chitosan and lower concentrations of aluminium sulfate were smaller and gave rise to more stable formulations, which correlates well with the notion that a zeta potential above +30 mV or below –30 mV is required for colloidal dispersion stability, whereas particles carrying a net charge close to neutrality experience lower repulsion, thus being more prone to form large aggregates that may flocculate [32].

The generation of chitosan formulations with adequate properties for *in vivo* application is critical, as particle intrinsic characteristics, such as size and zeta potential, are known to be key parameters when developing effective vaccine delivery systems [25-27]. For instance, even

though DCs can efficiently internalize particles of up to 10 μm, they are primarily involved in taking up smaller particles, in the nanometer range, which are believed to evoke a stronger immune responses [25, 27]. This immunostimulatory effect may be partially explained by the size effect of the particles on their half-life time *in vivo,* with smaller particles having longer circulation times and trafficking to the draining lymph nodes faster than their larger counterparts [26].

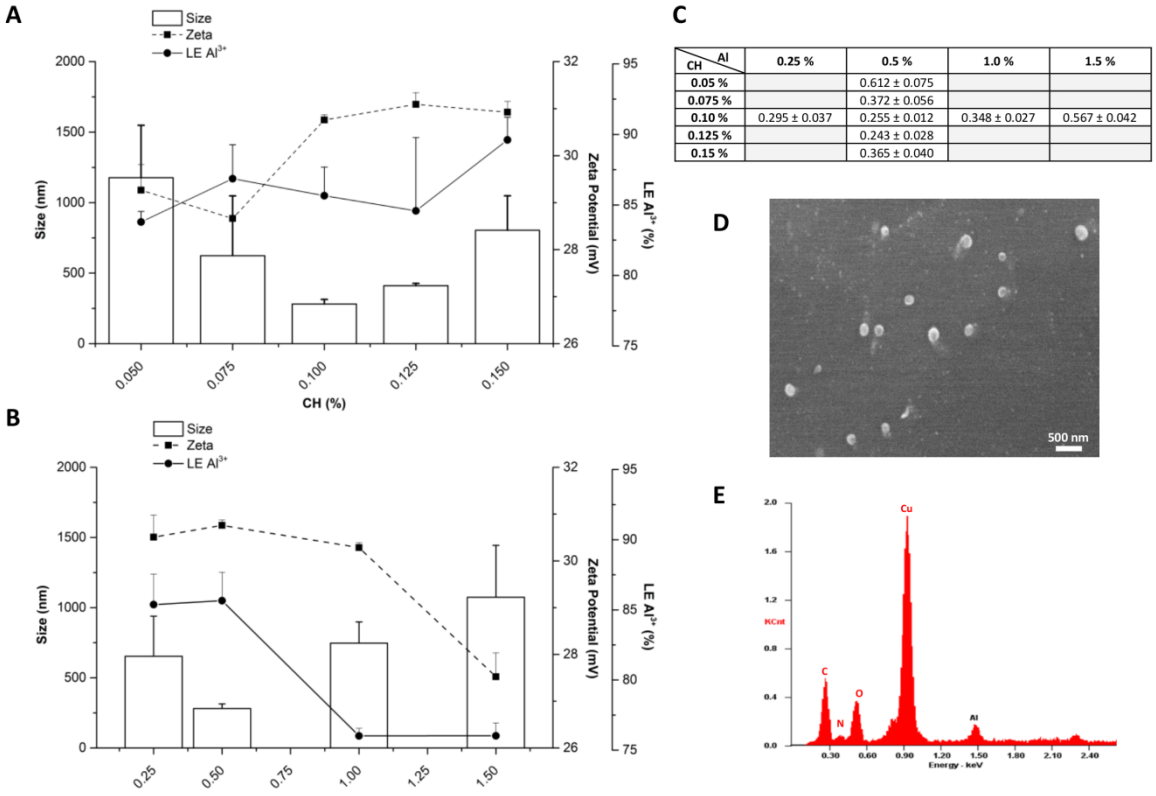

Figure 2.1 - Effect of chitosan concentration (A) and aluminium sulfate concentration (B) on size, zeta potential and aluminium loading efficacy of chitosan-aluminium nanoparticles. Chitosan-aluminium nanoparticles were prepared by adding equal volumes of a chitosan solution, with concentrations ranging from 0.050 % up to 0.015 % (w/v), to an 0.50 % (w/v) aluminium sulfate solution (A), or by adding equal volumes of a chitosan solution (0.10 %) to an aluminium sulfate solution with concentrations between 0.25 % and 1.50 % (w/v) (B), under high speed vortexing. Particle size was measured by dynamic light scattering and zeta potential was determined by electrophoretic light scattering. The analysis was performed at 25 °C, in 25 mM acetate buffer, pH 5.5; polydispersity index of the formulations (C); Aluminium loading efficacy was determined based on the eriochrome cyanine R method. Data (mean ± SD, obtained from triplicates) are representative of at least three independent experiments; cryo-scanning electron micrographs of CH-Al NPs (CH 0.1 %, Al 0.5 %) (D); energy-dispersive X-ray spectroscopy confirms the presence of aluminium in CH-Al NPs. (E)

The association of chitosan at 0.10 % (w/v) with aluminium sulfate at 0.50 % (w/v) gave rise to the smallest nanoparticles, with a mean size of 280.9 ± 32.7 nm, and a positive zeta potential of +30.1 ± 1.9 mV. The nanoparticle size observed in cryo-SEM images was in accordance with that obtained for DLS measurements (Fig. 2.1 D), showing round-shaped particles with a smooth surface. The presence of aluminium in this nanoparticle formulation, which was used in all the subsequent studies, was confirmed by energy-dispersive x-ray spectroscopy (EDS) (Fig. 2.1 E).

2.3.1.1 Chitosan-aluminium nanoparticles are more stable than chitosan-sodium nanoparticles

Changes in the surrounding environment can affect the colloidal stability of nanoparticles, and therefore, it is important to ascertain their potential degradation under different experimental conditions aiming at their application as delivery systems. In order to investigate the stability of CH-Al NPs, we performed transmittance measurements in 3 different buffers (10 mM PBS, pH 7.4; 200 mM PB, pH 7.4; 10 mM HEPES, pH 7.4), either at room temperature (RT) or 37 °C, and acetate buffer (25 mM AcB, pH 5.5) was used as a control. Results presented in figure 2.2 A clearly show that CH-Na NPs were completely degraded after being resuspended in all the 3 buffers, both at RT and 37 °C. Notably, this was not the case when they were resuspended in AcB. On the other hand, when CH-Al NPs were resuspended in the same conditions, only a fraction of the particles was degraded, even at 37 °C. This suggests that aluminium sulfate establishes stronger interactions with chitosan than sodium sulfate; hence CH-Al NPs can tolerate environmental changes better than traditional CH-Na NPs and will be better suited for mucosal or parenteral administration.

As demonstrated by several researchers and confirmed by our group [34], chitosan TGA curves normally exhibit, at least, two important degradation stages; the first, in the temperature range 60 ºC to 120 ºC has been attributed to the loss of absorbed water and the second, at around 270 ºC, corresponds to chemical degradation of the polymer. In order to investigate the influence of the sulfate salt on thermal stability of the chitosan particles, the two CH NPs formulations were analysed by DTA (Fig. 2.2 B) and TGA (Fig. 2.2 C). Comparing DTA curves obtained for chitosan nanoparticles, it is possible to observe, that both formulations present an initial endothermic peak at temperatures below 100 ºC (CH-Na NPs) and 200 ºC (CH-Al NPs) that corresponds to the weight loss (TGA curve) of 15 % and 25 %, respectively. This first stage degradation corresponds to the dehydration process, due to the highly hygroscopic character of the freeze-dried formulations. However, in the case of the

CH-Al NPs, a greater influence of the aluminium sulfate-18 hydrate, used to prepare the particles, was observed on DTA/TGA curves. In fact, the large endothermic peak (about 131 ºC) corresponds to dehydration of the aluminium sulfate, entrapped into the particles in which the water tightly bound to hydrophilic groups does not freeze therefore requiring considerable amounts of activation energy to evaporate [36].

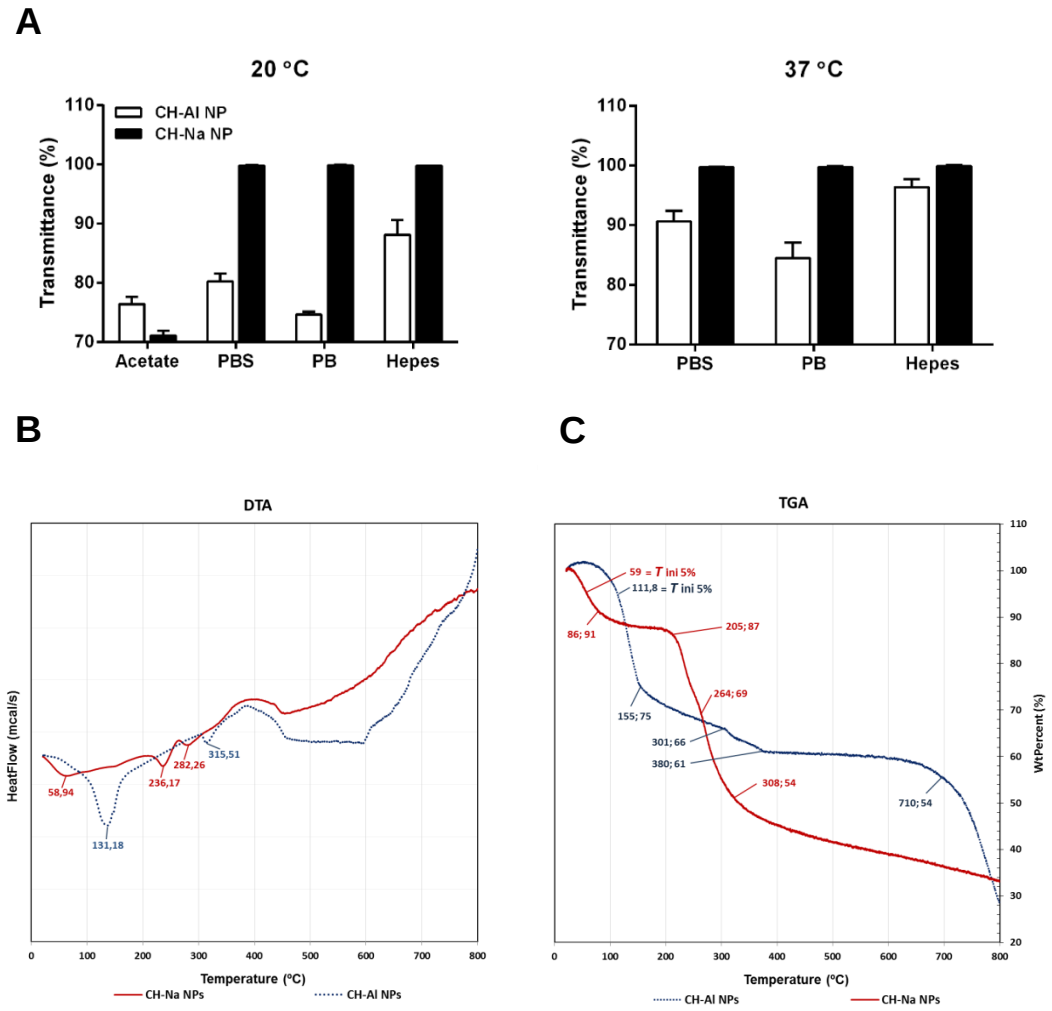

Figure 2.2 - Influence of aluminium sulfate as a cross-linking agent on the stability of CH NPs. (A) CH-Al NPs and CH-Na NPs were resuspended in either 10 mM PBS, pH 7.4; 200 mM PB, pH 7.4; 10 mM HEPES, pH 7.4 or 25 mM AcB, pH 5.5, at 20 °C or 37 °C, and transmittance was measured at 500 nm. DTA (B) and TGA (C) curves of CH-Na NPs (red) and CH-Al NPs (blue).

In line with previous DSC results from our group [34], DTA analysis of CH-Na NPs revealed 2 additional endothermic peaks, 236 ºC (weight loss (TGA curve) of 18 %) and 282 °C (weight loss (TGA curve) of 15 %), attributed to the disruption of unspecific electrostatic interactions, and the cleavage of the electrostatic interactions between chitosan and the sulfate ions, respectively. CH-Al NPs showed only one small peak, corresponding to 5 % weight loss

(Fig. 2.2 C), attributed to the disruption of the interactions between the polymer and cross-linker, which was shifted to a higher temperature (around 315 °C), suggesting a stronger interaction between chitosan and aluminium sulfate. However, a secondary stage (weight loss of 9 %) between 155 ºC and 301 ºC can be observed (Fig. 2.2 C), which does not have a correspondence with a clear peak on DTA curve (Fig. 2.2 B) or might be fused with the large peak. This secondary stage can be attributed to the disruption of unspecific electrostatic interactions in the particles or to the last molecules of water that leaves the aluminium sulfate hydrate [36]. Collectively, our data show that a weight loss about 54 % was observed around 300 ºC for CH-Na NPs, whereas to observe the same extent of weight loss for CH-Al NPs it was necessary to reach the temperature of 710 ºC. Therefore, our findings clearly show that CH-Al NPs are more thermostable than the traditional CH-Na NPs.

2.3.1.2 Incorporation of aluminium sulfate into chitosan particles does not affect cell viability

When developing a new formulation for *in vivo* application, it is important to assess its safety profile in cultured cells prior conducting animal experiments. In this context, the cytotoxicity of CH-Al NPs was evaluated in two different human epithelial cell lines (A549 and Calu-3) as a model for short-term mucosal exposure, and in a primary culture of murine spleen cells (splenocytes), following incubation with increasing particle concentrations, using the MTT assay to evaluate cell viability. The results in figure 2.3 A show that, for both cell lines, no significant effect on cell metabolic activity was observed after 2 h of incubation with the particles over the range of concentrations examined (up to 1500 $\mu g \cdot mL^{-1}$). This demonstrates that the particles were non-toxic at concentrations up to 4 times higher than the one used in *in vivo* experiments (400 $\mu g \cdot mL^{-1}$). The spleen plays an important role in innate and adaptive immune response [37], being, therefore, a relevant organ to evaluate the cytotoxicity of vaccine adjuvants. In splenocytes, a dose-dependent toxicity was observed, which became apparent only at CH-Al NP concentrations above 500 $\mu g \cdot mL^{-1}$ (Fig. 2.3 B).

Collectively, these findings provide evidence that CH-Al NPs exhibit good biocompatibility over a relevant concentration range and, therefore, can be safely applied in *in vivo* studies.

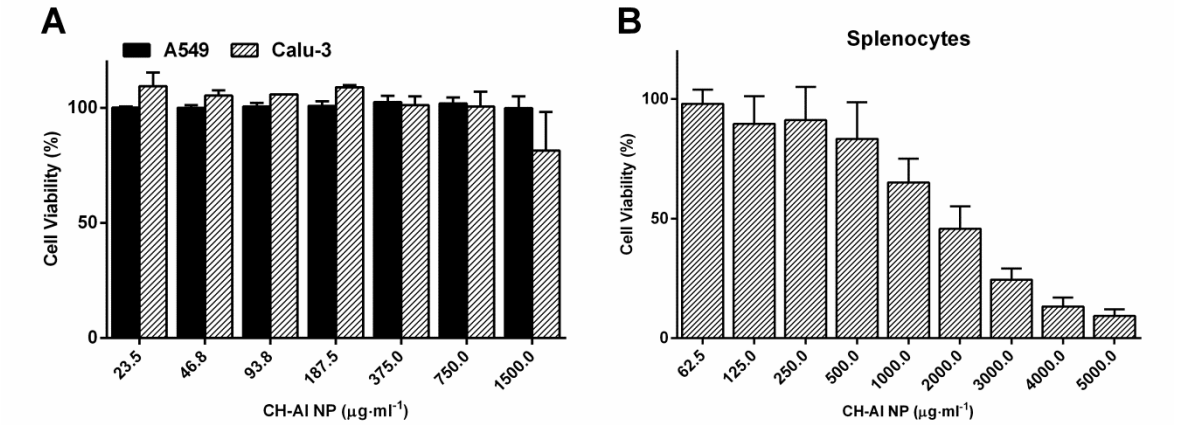

Figure 2.3 - Effect of chitosan-aluminium nanoparticles on cell viability. Increasing concentrations of CH-Al NPs were incubated with (A) A549 or Calu-3 cells for 2 h or (B) murine spleen cells (splenocytes) for 24 h. Cellular viability was assessed by the MTT assay, as described in Materials and Methods. Results are expressed as the mean percentage of the untreated control cells (± SD) from triplicates and are representative of at least two independent experiments.

2.3.1.3 Chitosan-aluminium nanoparticles preferentially adsorb antigens with low isoelectric point

The development of effective mucosal vaccine formulations usually requires the use of a large amount of antigens, generally adsorbed onto the surface of a delivery system. In this regard, understanding how the antigen characteristics affect adsorption onto particulate adjuvants will be instrumental in order to predict antigen loading efficacy, thus enabling to decrease the amount of antigen. In this study, six different model protein antigens, α-casein, bovine serum albumin, ovalbumin, lactalbumin, lysozyme and myoglobin, and the clinically relevant HBsAg were tested for their adsorption efficacy onto CH-Al NPs. Such proteins were selected in order to cover a wide range of protein molecular weights (MWs), isoelectric points (pI) and structures, as shown in the inset of figure 2.4 A.

Adsorption studies were performed at 20 ºC in phosphate buffer at neutral pH in order to avoid protein degradation. The time-course of protein adsorption was assayed by incubation of CH-Al NPs with the proteins (ratio 1.33:1) and aliquots were taken at defined time points (5, 10, 30 and 180 min) to determine the amount of unbound protein. Protein adsorption onto the particles occurred almost instantaneously and remained almost unchanged overtime (Fig. 2.4 A). As observed, negatively charged proteins, such as OVA, BSA, lactalbumin and casein, at neutral pH have high loading efficacy; on the other hand, low LE was observed for proteins displaying high isoelectric points (lysozyme and myoglobin). Considering that CH-Al NPs are positively charged in phosphate buffer at pH 7.1, the results obtained for the LE were

consistent with the predominance of electrostatic interactions between chitosan and the proteins. Even though electrostatic interaction was, most likely, the driving force for protein adsorption, thus making pI a key feature for predicting the adsorption behavior, other factors, such as conformational characteristics and amino acid composition and distribution [38] might influence protein adsorption, thus determining their LE. In this regard, it is possible that these factors have been responsible for the adsorption extent (although small) observed for myoglobin and lysozyme, despite the hypothetical predominant electrostatic repulsion between these proteins and the CH-Al NPs. Remarkably, for α-casein, the adsorption efficacy was found to be 100 %. This result could be attributed to, but not limited to, the dynamic nature of the protein, whose conformation adapts to the external environment [39]. This theory explains why this protein, with a pI between 4.2 and 4.7, exhibited a much higher adsorption efficacy as compared with the other proteins of similar pI.

Next, we examined the effect of the concentration of CH-Al NPs on protein loading efficacy and NPs loading capacity. With that purpose, the protein/antigen concentration was fixed and added to different NPs concentrations. The results displayed (Fig. 2.4 B) showed that for BSA and HBsAg, with a pI of 4.7 and 4.5, respectively, the amount of adsorbed protein increased linearly with increasing particle concentration, resulting in higher LE and lower LC. On the contrary, incubation of the NPs with myoglobin and lysozyme led to slightly lower LE and LC when two fold NPs concentration was tested, which remained unaltered for the others NPs concentration tested. Although the adsorption efficiency observed for α-casein was essentially 100 % over the NP concentration range tested, LC decreased, as expected, with increasing NP concentrations. It was interesting to note that the HBsAg adsorption profile was identical to that of BSA, further reinforcing the notion that it might be possible to predict the antigen loading behavior using less expensive model antigens with similar intrinsic properties, like the pI.

Taken together, our findings indicate that CH-Al NPs appear to have a great potential as a delivery system for a wide range of antigens and that it is possible to predict the adsorption profile of antigens with known physicochemical characteristics, a key factor at early stages in the design of new vaccine formulations.

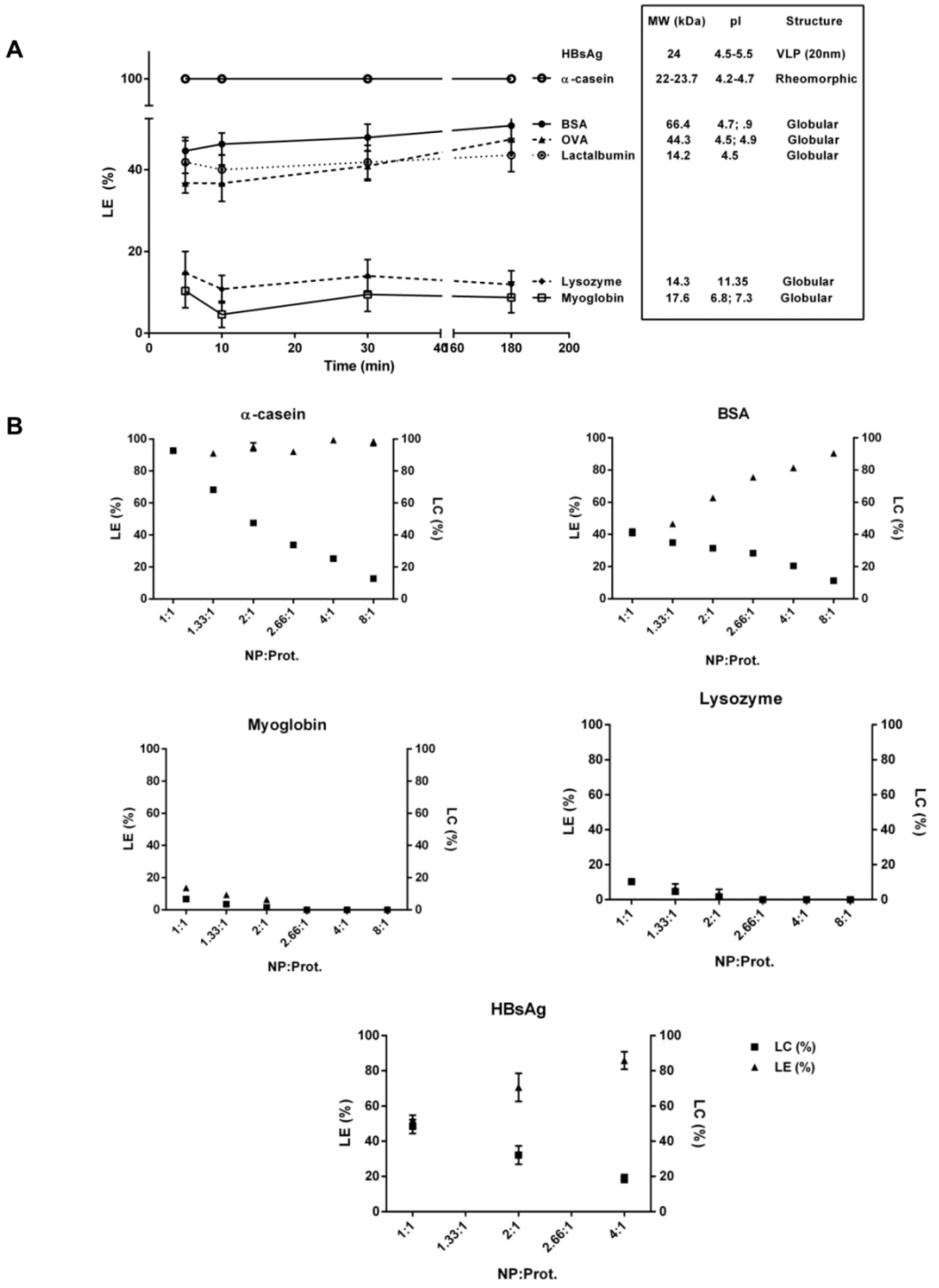

Figure 2.4 - Effect of incubation time of the proteins with CH-Al NP (A) and CH-Al NP:protein ratio (B) on loading efficiency (LE▲) and loading capacity (LC■). Protein adsorption studies were performed at 20 ºC in phosphate buffer, pH 7.1. (A) CH-Al NPs were incubated with the proteins, at the 1.33:1 ratio, and aliquots were taken at the indicated time points (5, 10, 30 and 180 min) to determine the amount of unbound protein. (B) CH-Al NPs, prepared at different concentrations, were added to the antigen at a fixed concentration (CH-Al NP:protein ratios of 1:1-8:1) and aliquots were taken after 30 min incubation to determine the amount of unbound protein. Results are expressed as the mean ± SD from triplicates and are representative of at least two independent experiments.

2.3.1.4 Chitosan-aluminium nanoparticles are efficiently internalized by cells

In order for an antigen to induce an immune response, it has first to be taken up and processed by the antigen-presenting cells (APCs). APCs are predominantly located in the submucosal region of the respiratory mucosa. Therefore, the translocation of the nanoparticles across the respiratory epithelium is a condition that should be observed to guarantee particles to reach nasal-associated lymphoid tissue (NALT) APCs. Hence, it was important to ascertain if the protein-loaded CH-Al NPs were efficiently internalized by the epithelial cells. For this purpose, a technically simple and broadly used approach was chosen [40] employing A549 cells, an adenocarcinomic human alveolar basal epithelial cell line. The cells were incubated with FITC-labelled CH-Al NPs loaded with BSA for 4 h and the uptake efficiency was assessed by confocal microscopy. To confirm that the presence of the model antigen would not affect cell internalization of the NPs, plain particles were used as a control. As shown in figure 2.5, both plain and antigen-loaded NPs were extensively internalized by A459 cells, as concluded from the presence of numerous and intensely green fluorescent speckles throughout the cytoplasm of the treated cells, which suggests that CH-Al NPs might constitute a suitable delivery system for proteins of interest.

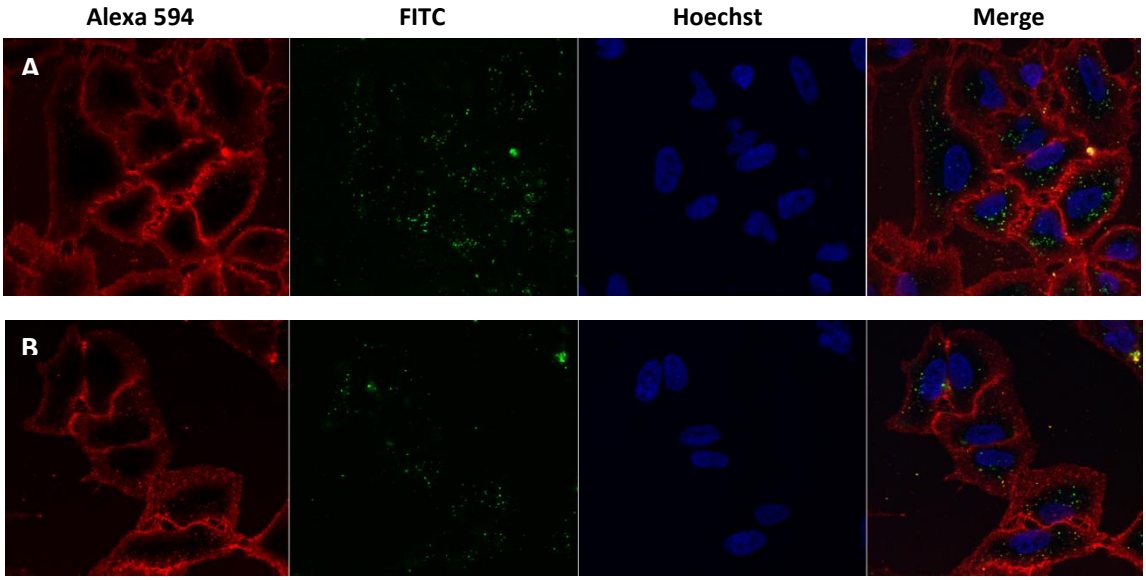

Figure 2.5 - Cellular internalization of CH-Al NPs. Representative confocal fluorescence images of intracellular distribution of (A) protein loaded FITC-CH-Al NPs and (B) plain FITC-CH-Al NPs after 4 h incubation with A549 cells. Confocal images show single and overlaid images of membrane staining with wheat germ agglutinin Alexa Fluor 594 conjugate (red); FITC-labelled chitosan (green); nuclear staining with Hoechst 33342 (blue).

Evidence has been provided that particulate antigens are more actively internalized by DCs than soluble antigens and can effectively undergo cross-presentation onto MHC class I molecules [41, 42], the particle size being a key factor limiting the efficiency of this process [43]. Therefore, our results suggest that using CH-Al NPs would be a good strategy to transform soluble antigens into particulate antigens.

2.3.1.5 Chitosan-aluminium nanoparticles are an effective adjuvant for the hepatitis B antigen

To assess the adjuvant potential of CH-Al NPs to induce a strong antigen-specific immune response, a study using the HBsAg adsorbed onto CH-Al NPs was performed in a prime-boost immunization regimen. The classical chitosan particles (produced with sodium sulfate; CH-Na NPs) were also tested in parallel experiments. Mice were subcutaneously immunized on day 0 and boosted on day 14 with a suspension containing 5 μg HBsAg or in combination with either CH-Al NPs or CH-Na NPs. The levels of serum anti-HBsAg IgG in these animals were analysed at 3 different time points (days 28, 58 and 88), and compared with those in mice that had received the same amount of antigen alone. On day 28, mice vaccinated with the antigen adsorbed on the CH-Al NPs or CH-Na NPs showed significantly higher anti-HBsAg IgG titer, as compared to the antigen alone group (Fig. 2.6 A). This may be attributed to the ability of the NPs to enhance the antigen uptake and activate APCs. Indeed, Koppolu et al. reported that chitosan particles enhance antigen internalization by macrophages and bone-marrow derived dendritic cells (BMDCs) and induce upregulation of co-stimulatory molecules and activation of markers on the surface of DCs [44]. As expected, serum titers declined over time, but were still detectable after 88 days.

To understand the impact of the different NP formulations on the type of the generated immune response, anti-HBsAg IgG1 and IgG2c titers were determined at day 88 (Fig. 2.6 B). Based on the IgG subclass elicited, we can gain some insight into which type of T cell response is predominately mounted. IgG1 is predictive of a Th2 response, while IgG2c indicates a more Th1-like response. In line with the total IgG titers, all NP formulations induced comparable levels of IgG1. Nevertheless, unlike free HBsAg administration, both HBsAg-loaded NP formulations (CH-Al and CH-Na NPs) were able to induce detectable IgG2c levels after 88 days. It has been reported that loading of an antigen into biodegradable poly(lactic-co-glycolic acid) (PLGA) particles enhanced cross-presentation by DCs in comparison to the soluble protein [41], which is in line with our observations regarding the

ability of HBsAg-loaded NPs, as opposed to free HBsAg, to induce a more balanced Th1/Th2 immune response.

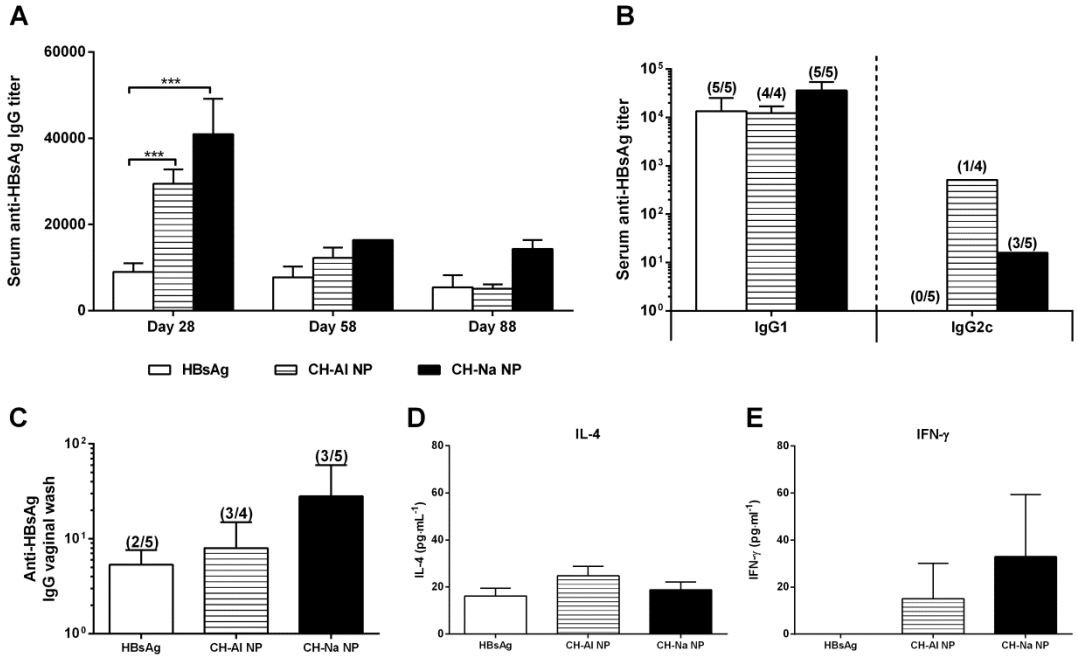

Figure 2.6 - Immune profile after mouse immunization with HBsAg, either alone or loaded into chitosan nanoparticles. Serum anti-HBsAg IgG (A), IgG1 and IgG2c (B) and mucosal IgG (C) titers of mice subcutaneously immunized with chitosan nanoparticles (CH-Al and CH-Na NPs) containing 5 μg HBsAg, or with 5 μg of free HBsAg. Blood was collected on days 28, 58 and 88 and vaginal secretions and spleens were collected on day 88. Antibody levels were determined by ELISA, as described in 'Materials and methods'. The end-point titers presented in the figure represent the antilog of the last log 2 dilution for which the OD values were at least two-fold higher than that of the naive serum sample equally diluted. The log 2 endpoint titers were used for statistical analysis. Numbers above bars represent the number of mice in which antibody levels were detected; at day 88, splenocytes were cultured at a density of 2.5 x 10^6 cells·mL^{-1} in T cell culture medium, in the presence or absence of 2.5 μg·$mL^{-1}$of HBsAg. Supernatants were collected after 98 h restimulation and levels of IL-4 (D) and IFN-γ (E) were measured by ELISA. Data (mean ± SD) correspond to groups of 5 mice each (HBsAg vs CH NP ***$p \leq 0.001$).

Notably, association of HBsAg with the NPs also resulted in an increase of antigen-specific IgG on vaginal washes and higher seroconversion rate, when compared with free antigen (Fig. 2.6 C), which reflects the antibody transudation phenomena.

To further characterize the immune response elicited by CH NPs loaded with HBsAg and the antigen alone, T cell activity was analysed upon *ex vivo* stimulation of splenocytes with HBsAg, either *per se* or formulated into the CH NPs, and quantifying the production of interferon-γ, a key Th1 cytokine, and interleukin-4, a key Th2 cytokine, by ELISA. Concerning

the cellular response, no important differences among mice groups were observed for antigen–specific secretion of the Th2 type cytokine IL-4 (Fig. 2.6 D); on the other hand, only the mice immunized with HBsAg-loaded CH NPs were able to induce antigen-specific IFN-γ, capable of driving cellular immune response against the hepatitis B virus (Fig. 2.6 E). Taken together, mice immunized with the antigen alone presented a higher IL-4/IFN-γ ratio, which further helps to explain why HBsAg-loaded CH NPs were able to elicit both IgG subclasses, while HBsAg alone was able to elicit only a strong IgG1 serum antibody.

Overall, our findings highlight the importance of associating HBsAg to chitosan nanoparticles to increase antibody titers and skew the Th2 profile for a balanced Th1/Th2 immune response. The HBsAg is not a soluble antigen, in fact already being a particulate antigen. The hepatitis surface antigen produced in yeast, is known to self-assemble into virus-like particles (VLPs) of 22 nm [45], which might explain the high serum IgG titers found in mice immunized with the antigen alone. Hence, using other model antigens would prove useful to obtain greater differences between antigen alone and antigen associated with NPs and further assess the synergistic adjuvant potential of combining two different immunopotentiators, chitosan and aluminium in the same nanoparticle formulation. Nevertheless, we showed the adjuvanticity of both chitosan nanoparticles formulations when associated with the HBsAg. For the classical chitosan nanoparticles, this result was expected since we observed similar effects in a previous study with BALB/c mice. For the new NPs, containing aluminium the present study shows that, apparently a similar adjuvant effect was induced. To gain more knowledge on the potential of these new CH-Al NPs, it will be necessary to make a more detailed evaluation of the immune response generated, to determine if the inclusion of the aluminium in the nanoparticles could stimulate other cells of the immune system. The exact mechanism of adjuvanticity of aluminium salts *in vivo* remains unclear [1, 10]. Further studies should be addressed to determine the detailed mechanisms by which CH-Al NPs activate the immune system, which might help improve their adjuvant features towards effective vaccination.

2.4 Conclusion

The present work represents an important step on the way to introduce chitosan nanoparticles in the vaccine adjuvant market. It was proven that, in addition to the sodium sulfate often used to prepare chitosan particles, aluminium sulfate can advantageously be used. The nanoparticles formed with the latter compound show to be physically more stable at physiological temperature and pH and constitute versatile delivery systems for antigens with

low isoelectric point, making them ideal as vaccine adjuvants. The physical stability of the particles is a tremendous improvement when particle preparation enters the adjuvant or vaccine industry. Moreover, these new nanoparticles with aluminium incorporated did not cause significant *in vitro* cytotoxicity, which constitutes an important hope towards future applications in animals, for which toxicity studies are required by regulatory agencies. Finally, the development of adjuvants that combine multiple immunostimulants has been considered a promising strategy to boost immunogenicity. In this work, we developed and optimized the preparation of a particulate adjuvant associating the immunomodulatory properties of aluminium salts and chitosan. Future and more dedicate immunopharmacological studies would bring to the state of art, the effect of the aluminium, associated to the chitosan particles, on the innate immune system as well the adjuvant mechanism, both studies required by regulatory authorities.

References

1. Oleszycka, E. and E.C. Lavelle, *Immunomodulatory properties of the vaccine adjuvant alum.* Curr Opin Immunol, 2014. **28**: p. 1-5.
2. Marrack, P., A.S. McKee, and M.W. Munks, *Towards an understanding of the adjuvant action of aluminium.* Nat Rev Immunol, 2009. **9**(4): p. 287-93.
3. Kool, M., K. Fierens, and B.N. Lambrecht, *Alum adjuvant: some of the tricks of the oldest adjuvant.* J Med Microbiol, 2012. **61**(Pt 7): p. 927-34.
4. Glenny, A.T., et al., *Immunological notes. XVII–XXIV.* The Journal of Pathology and Bacteriology, 1926. **29**(1): p. 31-40.
5. Holt, L.B., *Developments in diphtheria prophylaxis*. Heinemann-Medical books Ltd1950: Heinemann-Medical books Ltd.
6. Hutchison, S., et al., *Antigen depot is not required for alum adjuvanticity.* FASEB J, 2012. **26**(3): p. 1272-9.
7. Li, H., et al., *Cutting edge: inflammasome activation by alum and alum's adjuvant effect are mediated by NLRP3.* J Immunol, 2008. **181**(1): p. 17-21.
8. Eisenbarth, S.C., et al., *Crucial role for the Nalp3 inflammasome in the immunostimulatory properties of aluminium adjuvants.* Nature, 2008. **453**(7198): p. 1122-6.
9. Franchi, L. and G. Nunez, *The Nlrp3 inflammasome is critical for aluminium hydroxide-mediated IL-1beta secretion but dispensable for adjuvant activity.* Eur J Immunol, 2008. **38**(8): p. 2085-9.
10. Oleszycka, E., et al., *IL-1alpha and inflammasome-independent IL-1beta promote neutrophil infiltration following alum vaccination.* FEBS J, 2016. **283**(1): p. 9-24.
11. Marichal, T., et al., *DNA released from dying host cells mediates aluminum adjuvant activity.* Nat Med, 2011. **17**(8): p. 996-1002.
12. Mori, A., et al., *The vaccine adjuvant alum inhibits IL-12 by promoting PI3 kinase signaling while chitosan does not inhibit IL-12 and enhances Th1 and Th17 responses.* Eur J Immunol, 2012. **42**(10): p. 2709-19.

13. Carroll, E.C., et al., *The Vaccine Adjuvant Chitosan Promotes Cellular Immunity via DNA Sensor cGAS-STING-Dependent Induction of Type I Interferons.* Immunity, 2016. **44**(3): p. 597-608.
14. Zhou, H.Y., et al., *Effect of molecular weight and degree of chitosan deacetylation on the preparation and characteristics of chitosan thermosensitive hydrogel as a delivery system.* Carbohydrate polymers, 2008. **73**(2): p. 265-273.
15. Kiang, T., et al., *The effect of the degree of chitosan deacetylation on the efficiency of gene transfection.* Biomaterials, 2004. **25**(22): p. 5293-301.
16. Huang, M., et al., *Transfection efficiency of chitosan vectors: effect of polymer molecular weight and degree of deacetylation.* J Control Release, 2005. **106**(3): p. 391-406.
17. Arca, H.C., M. Gunbeyaz, and S. Senel, *Chitosan-based systems for the delivery of vaccine antigens.* Expert Rev Vaccines, 2009. **8**(7): p. 937-53.
18. Hu, L., Y. Sun, and Y. Wu, *Advances in chitosan-based drug delivery vehicles.* Nanoscale, 2013. **5**(8): p. 3103-11.
19. Lebre, F., et al., *Intranasal Administration of Novel Chitosan Nanoparticle/DNA Complexes Induces Antibody Response to Hepatitis B Surface Antigen in Mice.* Mol Pharm, 2016. **13**(2): p. 472-82.
20. Illum, L., *Chitosan and its use as a pharmaceutical excipient.* Pharm Res, 1998. **15**(9): p. 1326-31.
21. Baldrick, P., *The safety of chitosan as a pharmaceutical excipient.* Regul Toxicol Pharmacol, 2010. **56**(3): p. 290-9.
22. Borges, O., et al., *Induction of lymphocytes activated marker CD69 following exposure to chitosan and alginate biopolymers.* Int J Pharm, 2007. **337**(1-2): p. 254-64.
23. Schijns, V.E. and E.C. Lavelle, *Trends in vaccine adjuvants.* Expert Rev Vaccines, 2011. **10**(4): p. 539-50.
24. Smith, D.M., J.K. Simon, and J.R. Baker, Jr., *Applications of nanotechnology for immunology.* Nat Rev Immunol, 2013. **13**(8): p. 592-605.
25. Lebre, F., C.H. Hearnden, and E.C. Lavelle, *Modulation of Immune Responses by Particulate Materials.* Adv Mater, 2016. **28**(27): p. 5525-41.
26. Hotaling, N.A., et al., *Biomaterial Strategies for Immunomodulation.* Annu Rev Biomed Eng, 2015. **17**: p. 317-49.
27. Oyewumi, M.O., A. Kumar, and Z. Cui, *Nano-microparticles as immune adjuvants: correlating particle sizes and the resultant immune responses.* Expert Rev Vaccines, 2010. **9**(9): p. 1095-107.
28. Lunov, O., et al., *Amino-functionalized polystyrene nanoparticles activate the NLRP3 inflammasome in human macrophages.* ACS Nano, 2011. **5**(12): p. 9648-57.
29. Al Kobiasi, M., et al., *Control of size dispersity of chitosan biopolymer microparticles and nanoparticles to influence vaccine trafficking and cell uptake.* J Biomed Mater Res A, 2012. **100**(7): p. 1859-67.
30. Gan, Q. and T. Wang, *Chitosan nanoparticle as protein delivery carrier--systematic examination of fabrication conditions for efficient loading and release.* Colloids Surf B Biointerfaces, 2007. **59**(1): p. 24-34.
31. Clesceri, L., A. Greenberg, and A. Eaton, *Standard Methods for Examination of Water and Wastewater* 20 ed, ed. A.P.H. Association1998.
32. Lebre, F., et al., *Chitosan-based nanoparticles as a hepatitis B antigen delivery system.* Methods Enzymol, 2012. **509**: p. 127-42.
33. Borges, O., et al., *Immune response by nasal delivery of hepatitis B surface antigen and codelivery of a CpG ODN in alginate coated chitosan nanoparticles.* Eur J Pharm Biopharm, 2008. **69**(2): p. 405-16.
34. Borges, O., et al., *Preparation of coated nanoparticles for a new mucosal vaccine delivery system.* Int J Pharm, 2005. **299**(1-2): p. 155-66.

35. Koppolu, B.P., et al., *Controlling chitosan-based encapsulation for protein and vaccine delivery.* Biomaterials, 2014. **35**(14): p. 4382-9.
36. Çılgı, G.K. and H. Cetişli, *Thermal decomposition kinetics of aluminum sulfate hydrate.* Journal of thermal analysis and calorimetry, 2009. **98**(3): p. 855.
37. Bronte, V. and M.J. Pittet, *The spleen in local and systemic regulation of immunity.* Immunity, 2013. **39**(5): p. 806-18.
38. Song, K.B. and S. Damodaran, *Structure-function relationship of proteins: adsorption of structural intermediates of bovine serum albumin at the air-water interface.* Journal of agricultural and food chemistry, 1987. **35**(2): p. 236-241.
39. Horne, D.S., *Casein structure, self-assembly and gelation.* Current opinion in colloid & interface science, 2002. **7**(5): p. 456-461.
40. Braakhuis, H.M., et al., *Progress and future of in vitro models to study translocation of nanoparticles.* Arch Toxicol, 2015. **89**(9): p. 1469-95.
41. Waeckerle-Men, Y., et al., *Encapsulation of proteins and peptides into biodegradable poly(D,L-lactide-co-glycolide) microspheres prolongs and enhances antigen presentation by human dendritic cells.* Vaccine, 2006. **24**(11): p. 1847-57.
42. Shen, Z., et al., *Cloned dendritic cells can present exogenous antigens on both MHC class I and class II molecules.* J Immunol, 1997. **158**(6): p. 2723-30.
43. Tran, K.K. and H. Shen, *The role of phagosomal pH on the size-dependent efficiency of cross-presentation by dendritic cells.* Biomaterials, 2009. **30**(7): p. 1356-62.
44. Koppolu, B. and D.A. Zaharoff, *The effect of antigen encapsulation in chitosan particles on uptake, activation and presentation by antigen presenting cells.* Biomaterials, 2013. **34**(9): p. 2359-69.
45. Roldao, A., et al., *Virus-like particles in vaccine development.* Expert Rev Vaccines, 2010. **9**(10): p. 1149-76.

CHAPTER 3

Easy and effective method to generate endotoxin-free chitosan particles for immunotoxicology and immunopharmacology studies

Abstract

The cationic biopolymer chitosan (CH) has emerged as a promising candidate adjuvant due to its safety profile and immunostimulatory properties. The presence of endotoxin contamination in biomaterials is generally underappreciated and can generate misleading results. It is important to establish a convenient methodology to obtain large amounts of high quality chitosan nanoparticles for biomedical applications. Here, we developed an effective method to generate endotoxin-free chitosan and assessed its purity. Purified chitosan-based formulations alone failed to induce production of the proinflammatory cytokines tumor necrosis factor alpha (TNF-α) and interleukin (IL)-6 in bone marrow derived dendritic cells (BMDCs) generated from C57BL/6 mice, while maintaining its ability to promote IL-1β secretion in combination with the Toll-like receptor (TLR)-9 agonist, CpG. Moreover, BMDCs from C3H/HeN and TLR4-defective mice, C3H/HeJ were stimulated with endotoxin-free chitosan based formulations and no differences were observed in IL-6 and IL-1β secretion, excluding the involvement of TLR-4 signaling pathway in the immunomodulatory effects of chitosan.

3.1 Introduction

The discovery of pattern recognition receptors (PRRs) and specific PRR ligands provides the opportunity to design new and improved vaccines and therapeutics. However, it is essential to be aware that materials can potentially be contaminated with bacterial lipopolysaccharides (LPS). LPS, also known as endotoxins, are heat-stable molecules that constitute the major structural components of the outer cell wall of gram-negative bacteria. Cells of the immune system (e.g. macrophages and dendritic cells) can recognize LPS as a pathogen-associated microbial pattern (PAMP), in a mechanism that involves TLR4, LPS-binding protein (LBP), cluster of differentiation 14 (CD14) and myeloid differentiation protein 2 (MD2) [1], and drive the secretion of proinflammatory cytokines including IL-6 and TNF-α [2], activating the immune system. Remarkably, given its unique potency, endotoxin contamination in preparations of reported putative endogenous ligands of TLRs and NLRs is not always reported, which may cast doubt over published studies. For instance, heat shock proteins (HSPs) are molecular chaperones that were initially shown to have immunostimulatory effects, inducing the secretion of inflammatory cytokines as IL-6, TNF-α and IL-12 by dendritic cells and macrophages, as well as inducing the upregulation of costimulatory molecules on the surface of BMDCs including CD40, CD80, CD86, and upregulating the expression of MHCcII [3-5]. Nevertheless, since the early 2000s, some reports suggested that most of the immunomodulatory effects previously attributed to HSPs were probably the result of the direct response to molecules other than HSPs, which were bound or present as contaminants in the formulations used [6]. Gao et al, in a series of simple experiments using 2 recombinant human HSP70 formulations with the same protein content but markedly different endotoxin content (577 ± 74.2 EU·mg^{-1} vs 4.1 ± 0.2 EU·mg^{-1}), showed that the highly purified HSP70 preparation failed to induce the release of TNF-α by a murine macrophage cell line [7]. Moreover, when the preparation containing higher levels of LPS was purified using a polymyxin B column, no cytokine production was detected, demonstrating that the HSP70 immunostimulatory effects previously reported were in fact a result of contaminating bacterial products. Low levels of LPS can be difficult to detect by conventional approaches, and can therefore be a major problem in interpreting results. It is vital for researchers to evaluate whether LPS or other contaminants could be wholly or partially responsible for observed effects of putative danger-associated molecular patterns (DAMPs). In the particular case of chitosan this practice becomes more relevant since the cationic nature of the polymer favors the interactions with the negatively charged phosphate groups in LPS [8].

Chitosan is a cationic polysaccharide obtained by the chemical deacetylation of chitin found mainly in crustacean shells and the cell wall of fungi [9]. It has attracted significant interest in many biomedical fields owing to its safety profile [10, 11] and ability to stimulate cells of the immune system [12-14]. Recently, chitosan was reported to be capable of activate the NOD-like receptor family, pyrin domain containing 3 (NLRP3) inflammasome, leading to the release of the proinflammatory cytokines IL-1β, from antigen presenting cells (APCs) [12, 14], and induce the upregulation of maturation markers in BMDCs via type I interferons (IFNs) [12], thus extensive research has been directed toward its use as a vaccine adjuvant.

The aim of this study was to develop a convenient and effective method to prepare endotoxin-free chitosan particles for biomedical use. We established a robust methodology to obtain endotoxin-free chitosan as a starting material without affecting its chemical properties. *In vitro* results confirm that the methodology developed was suitable to produce endotoxin-free chitosan-based formulations, since particles alone failed to promote the secretion of the proinflammatory cytokines IL-6, TNF-α and IL-1β by BMDCs, routinely reported when the polymer is contaminated, while retaining its immunomodulatory activity, in combination with a TLR-ligand.

3.2 Experimental section

3.2.1 Reagents

Cytidine-phosphate-guanosine (CpG) oligonucleotide 1826 was supplied by Oligos etc. Lipopolysaccharide from E. coli, Serotype R515, Toll-like receptor grade was purchased from Enzo Life Sciences. Aluminium hydroxide gel, referred to as 'alum', was supplied by Brenntag Biosector. Pyrogen-free water was purchased from Baxter Healthcare. Polymyxin B was purchased from Sigma.

3.2.2 Chitosan purification

In order to obtain endotoxin-free chitosan all the steps described below used decontaminated labware and pyrogen-free water and reagents; all the procedures were conducted in a strict endotoxin-free environment, under the laminar flow hood. Labware was decontaminated by soaking in strong base (0.5 M NaOH) for 2 h and rinsed thoroughly with pyrogen-free water.

For chitosan (ChitoClear, 95 % degree of deacetylation; Primex Bio-Chemicals AS) purification, 1 g of the polymer was suspended in 10 mL of a 1 M NaOH solution, and stirred

for 3 h at 50 °C. The suspension was then filtered using a Buchner funnel with a 0.45 μm membrane (Millipore) and the resultant pellet washed with 20 mL of pyrogen-free water. The recovered chitosan was washed with 200 mL of 1 % acetic acid solution and stirred for 1 h to solubilize the chitosan. The solution was filtered (0.45 μm membrane) and 1 M NaOH solution was used to adjust the pH of the filtrate to 8.0, resulting in insoluble purified chitosan that was centrifuged for 30 min, at 4500 g and the supernatant discarded. The resultant pellet was thoroughly washed with pyrogen-free water and the centrifugation-washing step repeated 2 more times. Chitosan was freeze-dried (FreezeZone 6, Labconco), and the dry powder keep in a desiccator until further use.

3.2.3 Chitosan nanoparticle preparation

In order to obtain endotoxin-free chitosan nanoparticles, all preparation steps were carried out using decontaminated labware and pyrogen-free water and reagents; all the procedures were conducted in a strict endotoxin-free environment, under the laminar flow hood to avoid endotoxin contamination, meeting the same requirements used for the purification step.

Chitosan nanoparticles (CH NPs) were prepared by a coacervation/precipitation technique using sulfate ions as a cross-linking agent as described [15]. Briefly, CH NPs were obtained by adding equal volumes of a 0.1 % chitosan solution (25 mM sodium acetate buffer (AcB), pH 5.0) and an aqueous 0.5 % aluminium sulfate solution, under high speed vortexing for 20 s, followed by incubation at room temperature for 1 h. In order to remove unreacted compounds, the resulting nanoparticle suspensions were centrifuged for 30 min at 4500 g. The supernatant was discarded and the pellet resuspended in 25 mM AcB, pH 5.5.

3.2.4 Characterization of purified chitosan by Fourier transform infrared spectroscopy

The Fourier transform infrared spectroscopy (FTIR) spectra of purified and non-purified chitosan were recorded on a Bruker IFS 66 V FTIR spectrometer (Germany). The instrument operated with a resolution of 2 cm^{-1} and 30 scans were collected for each sample. The IR absorbency scans were analysed between 650 and 4000 cm^{-1} for changes in the intensity of the sample peaks.

3.2.5 Limulus Amebocyte lysate assay

PYROGEN Gel Clot *Limulus Amebocyte* lysate (LAL) assay (Lonza) was used as a qualitative test for endotoxin contamination and was carried out according to the manufacturer's protocol. Briefly, samples were dispersed in phosphate buffer (PB), pH 6, prepared with pyrogen-free water. PB prepared with pyrogen-free water was used as a negative control and LPS from *Escherichia coli*, Serotype R515 as a positive control. *Limulus amebocyte* lysate was added to each test tube containing experimental samples and immediately mixed thoroughly and the tube placed in a 37 °C non-circulating hot water bath. After 1 h, tubes were carefully removed and inverted to test for clot formation. Clot formation is a positive response, indicating endotoxin levels greater than 0.125 $EU \cdot mL^{-1}$.

3.2.6 Mice

Eight to 16-week-old Female C57BL/6 mice were obtained from Harlan Olac (Bicester, UK) and 8-16 week old female TLR4-defective C3H/HeJ or TLR4 wild-type C3H/HeN mice were bred in the Trinity Biomedical Sciences Institute (TBSI) Bioresources Unit. Animals were maintained according to the regulations of the European Union and the Irish Department of Health (Reference Number 091210). All animal studies were approved by the Trinity College Dublin Animal Research Ethics Committee.

3.2.7 Measurement of Dendritic Cell Activation

Murine bone marrow-derived dendritic cells (BMDCs) were generated as described previously [16]. Briefly, bone marrow cells were isolated from tibiae and femora of mice. Cells were grown in RPMI 1640 medium (Biosera) supplemented with 8 % ultra-low endotoxin heat-inactivated foetal bovine serum (FBS) (Biosera), 2 mM L-glutamine (Gibco), 50 $U \cdot mL^{-1}$ penicillin (Gibco), 50 $\mu g \cdot mL^{-1}$ streptomycin (Gibco) and 20 $ng \cdot mL^{-1}$ of granulocyte–macrophage colony-stimulating factor (GM-CSF) derived from the J588 myeloma cell line. On day 10, the loosely adherent cells were harvested and plated in 96-well plate at a density of 0.625×10^6 $cells \cdot mL^{-1}$ and incubated overnight. On day 11, cells were incubated with the appropriate stimuli as indicated in figure legends. Supernatants were collected and analysed for cytokine secretion.

3.2.8 Cytokine ELISA

The concentration of the cytokine IL-6 was measured by ELISA using antibodies obtained from Biolegend. IL-1β and TNF-α concentrations were also determined by ELISA according to the manufacturer's instructions (R&D Systems). Briefly, 96-well high binding ELISA plates (Greiner Bio-one) were coated with capture antibody and incubated overnight at 4 °C. The plates were washed in wash buffer (0.05 % PBS-tween) and blocked with 1 % BSA in PBS solution at room temperature for 1 h. After washing, samples and standards were added to the plates and incubated for 2 h at room temperature. Following this incubation step, biotinylated goat anti-mouse detection antibody was added to the plates which were incubated for 2 h, before washing and incubation with the avidin-HRP conjugate for an additional 30 min. Finally, plates were washed and OPD substrate solution was added to the plate. After 15 min incubation in the dark, the OD values were measured at 492 nm using a Multiskan EX 96-well plate reader. A standard curve was generated and this was then used to determine the cytokine concentration of the unknown replicates.

3.2.9 Statistical analysis

Results are expressed as mean values ± standard deviation (SD) and were analysed by ANOVA followed by Tukey´s post-test with $p \leq 0.05$ considered as a statistically significant difference. (GraphPad Prism v6, GraphPad Software Inc., USA).

3.3 Results and discussion

3.3.1 Characterization of purified chitosan

Efficient endotoxin removal in pharmaceutical preparations is challenging, hence it is important to address this issue early during formulation development. Depending on the material that needs to be depyrogenated, an array of methods for endotoxin removal or destruction are available. Most depyrogenation methodologies involve the use of high temperatures (250 °C for 2 h) or highly acidic (e.g., 0.1 M hydrochloric acid) or basic (e.g., 0.5 M NaOH) solutions that may compromise the integrity and composition of a drug or delivery system, making it essential to purify the starting material prior to any formulation development. Therefore, to prepare endotoxin-free chitosan nano- and microparticles, the best strategy is to start with endotoxin-free chitosan and buffers. In this process, chitosan was first suspended in NaOH at 50 °C for 3 h to remove possible protein contamination. Remarkably, the liquid phase turned yellow, indicating that some contaminants separate from

chitosan onto solution. The resultant suspension was then filtered and the pellet washed with pyrogen-free water prior to being solubilized in acetic acid solution. Ultimately, chitosan was precipitated by adding the NaOH solution dropwise. These series of precipitation/dissolution steps under strong acidic/basic conditions were crucial to destroy any endotoxin contaminant. To access whether the purification method affected the resulting chitosan, both purified and non-purified formulations were characterized using FTIR spectroscopy. FTIR spectrum analysis revealed no shift in the 3 characteristic peaks of purified chitosan when compared with the polymer before the purification process (Fig. 3.1). They exhibited a broad band at 3360 cm^{-1} due to O-H and N-H stretching, one band at 2863 cm^{-1} assigned to C-H stretching and a doublet at 1650 and 1584 cm^{-1} attributed to the two types of H-bonds in which the C=O groups are involved [17]. These observations indicate that no structural change occurred following the purification steps, validating this methodology.

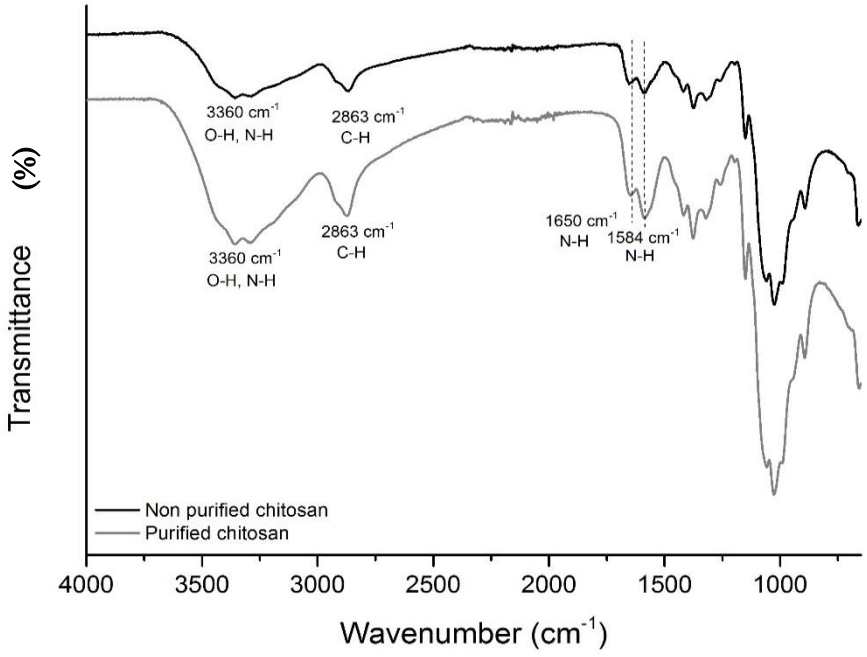

Figure 3.1 - FTIR spectra of chitosan before and after the purification process.

3.3.2 Chitosan purification efficiently eliminates endotoxin contamination

During preclinical development of a new formulation it is important to determine the levels of endotoxin contaminants considering they are responsible for misleading results as well as serious toxic reactions in humans [18]. Bacterial endotoxin content was assessed according to the recommendations of International Council for Harmonization (ICH) guideline Q4B, using

the gel-clot LAL assay with a detection limit of 0.125 EU·mL^{-1} [19]. One hundred microliters of non-purified chitosan (0.1 %), purified chitosan (0.1 %), cross-link solution (0.5 %), AcB, pH 5.5 and LPS (1 EU·mL^{-1}) were mixed with the same volume of the reconstituted lysate. After 1 h, LPS and non-purified CH solution formed a firm gel-clot, indicative of a positive reaction while all the other formulations failed to do so, suggesting that chitosan purification was effective and that the endotoxin content of purified chitosan was below 0.125 EU·mL^{-1}, therefore not detectable by LAL test. Currently, the LAL assay is the test of choice for the evaluation of endotoxin in biological products and medical devices, however it has its limitations; for instance, certain molecules, like LPS-binding proteins are known to adhere to LPS molecules, inhibiting the ability of endotoxin to catalyze the activation of a proenzyme to coagulase thus interfering with the function of the LAL assay [20]. Furthermore, since the LAL assay is based on the interaction of endotoxins with enzymes, characteristics including the optimal pH or use of denaturing agents might interfere with the test, leading to false results. Hence, the use of a complementary method that provides better sensitivity for endotoxin testing might prove advantageous. Dendritic cells are very sensitive to low levels of endotoxin contamination. Tynan and colleagues investigated the minimum LPS concentration required to induce DC cytokine secretion and maturation, and observed that concentrations as low as 10 pg·ml^{-1} and 20 pg·ml^{-1} triggered secretion of IL-6 and TNF-α, respectively [21]; thus measuring dendritic cell activation in the presence of the molecule of interest is a useful and simple method to assess if residual endotoxin contamination might be responsible for the observed immunomodulatory effects.

Polymyxin B (PmB) is an antibiotic capable of binding to, and to some degree neutralizing LPS [21], while having no effect on other PAMPs. In order to confirm that the purification process was effective and did not affect the capacity of chitosan to form particles, we prepared nanoparticles using the purified chitosan and aluminium sulfate as a cross-linker, and pre-incubated them alone or in the presence of 100 μg·ml^{-1} of PmB for 2 h at 37 ºC. Additionally, we also pre-incubated LPS under the same conditions as a control and stimulated BMDCs with each of the formulations. As shown in figure 3.2, stimulation with any of the formulations alone was inefficient at inducing TNF-α production, irrespective of whether they were pre-incubated with PmB or not. On the other hand, LPS-induced TNF-α secretion was completely abrogated after PmB treatment.

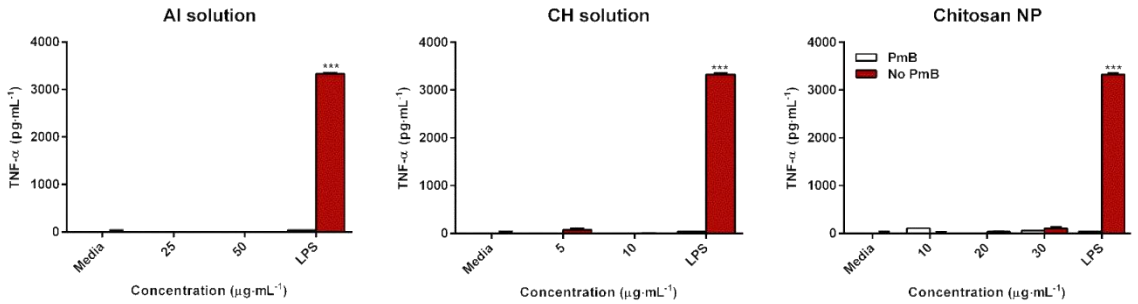

Figure 3.2 - Polymyxin B treatment has no effect on TNF-α secretion by BMDCs in response to purified chitosan formulations alone. BMDCs (0.625 x 10^6 cells·mL^{-1}) from C57BL/6 mice were stimulated with cross-link (Al) solution, CH solution and CH NP suspension, which were pre-incubated alone or in the presence of PmB (100 μg·mL^{-1}) for 2 h at 37 °C. Supernatants were collected 24 h later and tested for TNF-α by ELISA. Results are mean cytokine concentrations (±SD) for triplicate samples. (vs PmB treated *** $p < 0.001$), and are representative of two independent experiments.

Overall these results show that pre-treatment with PmB had no effect on chitosan-stimulated cytokine secretion but hindered LPS induced dendritic cell activation, suggesting that any immunomodulatory effects observed for chitosan are not due to endotoxin contamination.

3.3.3 Purified chitosan formulations modulate TLR-induced secretion of IL-1β but do not affect IL-6 or TNF-α secretion by BMDCs

The next question we addressed was whether purified chitosan-based formulations had an intrinsic ability to activate dendritic cells or could modulate cytokine secretion of DCs primed with a TLR-agonist, since there are divergent reports in the literature. While Park et al. showed that clinical grade chitosan was able to promote the secretion of TNF-α and IL-6 in dendritic cells [22], Ma and colleges observed that chitosan oligosaccharides were capable of inhibiting LPS-induced expression of TNF-α and IL-6 in macrophages [23]. To assess the immunomodulatory abilities of chitosan, BMDCs were incubated with a range of concentrations of the cross-link solution (6.25 to 50 μg·mL^{-1}), CH solution (2.5 to 10 μg·mL^{-1}) or CH NP (10 to 40 μg·mL^{-1}), either alone or in combination with the TLR-9 ligand CpG and supernatants were collected after 24 h and analysed to determine concentrations of the proinflammatory cytokines, TNF-α, IL-6 and IL-1β. Treatment of DCs with increasing concentrations of all formulations alone failed to induce any detectable levels of the proinflammatory cytokines (Fig. 3.3). Our results corroborate observations by Bueter and

coworkers, where chitosan alone was unable to promote proinflammatory cytokine secretion in bone marrow-derived macrophages (BMDM) [14].

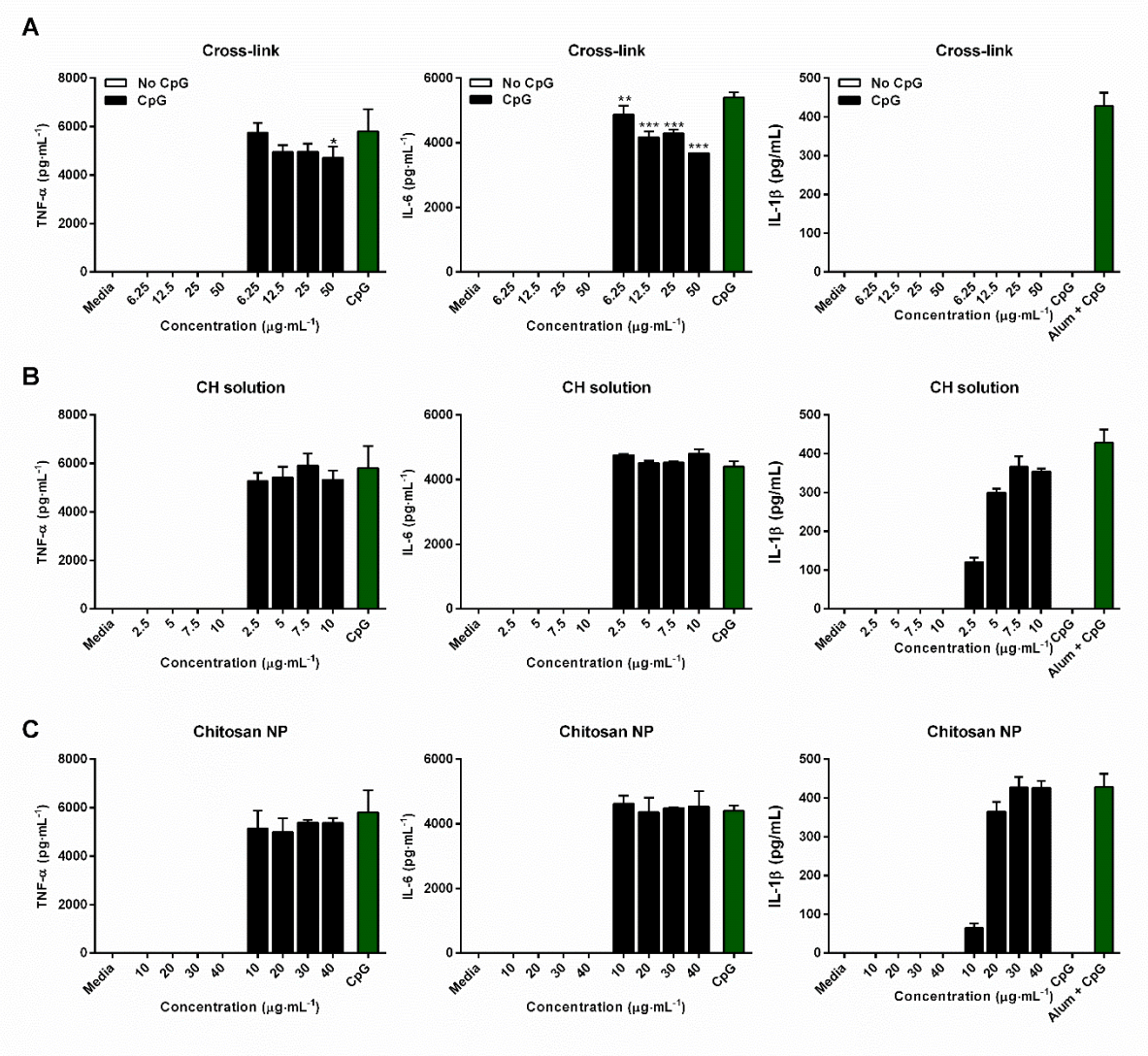

Figure 3.3 - Purified CH solution and NP enhance TLR-induced IL-1β secretion but do not directly induce IL-6 or TNF-α secretion by BMDCs. BMDCs (0.625 x 10^6 cells·ml^{-1}) from C57/BL6 mice were stimulated with (A) cross-link solution, (B) CH solution, (C) CH NP suspension and alum (500 μg·mL^{-1}) alone or after priming with CpG (4 μg·mL^{-1}) for 3 h. Supernatants were collected 24 h later and tested for TNF-α, IL-6 and IL-1β secretion by ELISA. Results are mean cytokine concentrations (±SD) for triplicate samples. (vs CpG alone * $p < 0.05$, ** $p < 0.01$ and *** $p < 0.001$), and are representative of three independent experiments.

Furthermore, to assess how each formulation modulated TLR ligand-induced cytokine production by dendritic cells, the BMDCs were primed with CpG 3 h prior to stimulation with chitosan, to trigger the NF-κB-dependent transcription of pro-IL-1β. Contrary to the report from Ma et al., we found that neither of the chitosan formulations altered CpG-

induced secretion of TNF-α and IL-6 in the range of concentrations tested (Fig. 3.3 B and Fig. 3.3 C). Interestingly the aluminium sulfate solution exerted a significantly suppressive effect on the production of these cytokines, similar to the observation made by Mori et al. when using alum to stimulate BMDCs [24] (Fig. 3.3 A). When combined with the TLR9 agonist CpG, CH and CH NP promoted a dose-dependent increase in secretion of the proinflammatory cytokine IL-1β by BMDCs, while the cross-link solution did not enhance IL-1β secretion. Moreover, at the highest concentrations tested, chitosan-based formulations enhanced CpG-mediated IL-1β secretion to a comparable extent to the vaccine adjuvant alum, used as a control (Fig. 3.3 B and Fig. 3.3 C).

Overall our results support the suitability of purified chitosan for use in biomedical applications.

3.3.4 Modulation of IL-6 and IL-1β secretion in response to chitosan-based formulations is independent of TLR-4

Finally we examined cytokine responses to chitosan in wild-type C3H/HeN and TLR4-defective C3H/HeJ BMDCs, as a means to establish whether endotoxin contamination might be involved in biological activity observed. The C3H/HeJ substrain of mice has a spontaneous mutation in the TLR-4 gene making them hyporesponsive to LPS [25]. In a similar way as before, BMDCs from C3H/HeJ mice and the closely-related TLR4-sufficient substrain, C3H/HeN, were incubated with CH solution or CH NP, as well as alum as a control. IL-6 and IL-1β concentrations in supernatants were subsequently determined in response to these stimuli. BMDCs generated from C3H/HeJ mice but not from C3H/HeN mice, failed to secrete IL-6 in response to LPS, while the TLR-9 agonist CpG induced similar levels of IL-6 secretion in cells from both substrains (Fig. 3.4 A). As expected, incubation of cells with the chitosan-based formulations alone had no effect on IL-6 secretion. Furthermore, there was no significant difference in the extent of IL-1β secretion by BMDCs from C3H/HeJ and C3H/HeN mice stimulated with a combination of the TLR-9 agonist CpG and both chitosan-based formulations (Fig. 3.4 B). As an experimental control, BMDCs from both mice substrains were stimulated with alum following 3 h priming with 5 $ng \cdot mL^{-1}$ of LPS. As anticipated, C3H/HeN DCs secreted IL-1β in response to alum after LPS priming. In contrast, C3H/HeJ DCs did not secrete detectable concentrations of IL-1β in response to the same stimulus. Altogether these data suggest that purified chitosan contains no endotoxins and its ability to promote IL-1β secretion is TLR-4 independent.

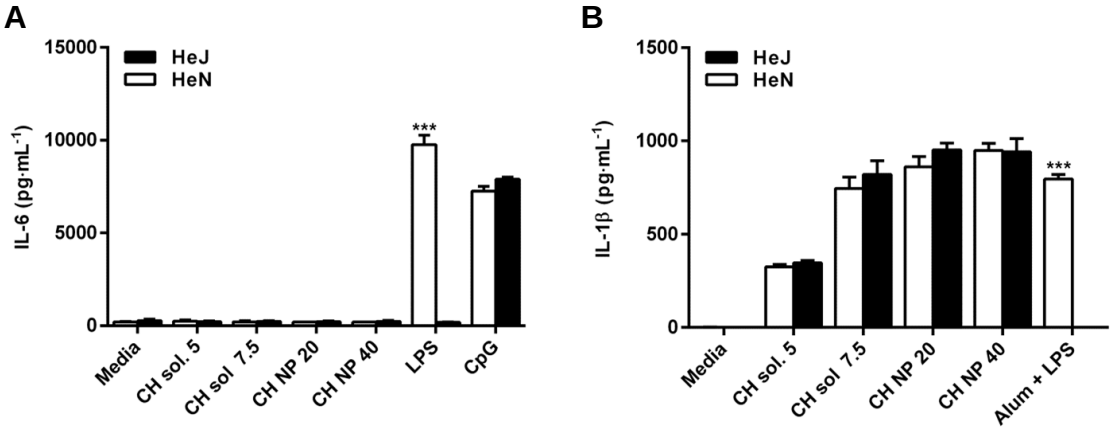

Figure 3.4 - Chitosan-based formulation retained their capacity to promote IL-1β secretion in TLR4-defective C3H/HeJ mice. BMDCs (0.625 x 10^6 cells·mL^{-1}) from C3H/HeN and C3H/HeJ mice were stimulated with CH solution and CH NP suspension (A) alone or (B) after priming with CpG (4 μg·mL^{-1}) for 3 h. LPS (5 ng·mL^{-1}) and alum (500 μg·mL^{-1}) were used as controls. Supernatants were collected 24 h later and tested for (A) IL-6 and (B) IL-1β secretion by ELISA. Results are mean cytokine concentrations (±SD) for triplicate samples. (vs HeJ *** $p < 0.001$), and are representative of two independent experiments.

3.4 Conclusion

The presence of residual amounts of endotoxin contaminants can alter the bioactivity of biological molecules generating misleading results. With the developed purification method we can produce endotoxin-free chitosan without affecting its structure and capacity to enhance IL-1β secretion by dendritic cells. We have shown that in the absence of contaminating endotoxin, chitosan-based formulations alone do not promote the secretion of IL-6 by BMDCs, while retaining its ability to synergize with a TLR-agonist to promote IL-1β secretion, thus making it suitable for biological and medical applications.

References

1. Tan, Y. and J.C. Kagan, *A cross-disciplinary perspective on the innate immune responses to bacterial lipopolysaccharide.* Mol Cell, 2014. **54**(2): p. 212-23.
2. Zweigner, J., et al., *High concentrations of lipopolysaccharide-binding protein in serum of patients with severe sepsis or septic shock inhibit the lipopolysaccharide response in human monocytes.* Blood, 2001. **98**(13): p. 3800-8.
3. Basu, S., et al., *Necrotic but not apoptotic cell death releases heat shock proteins, which deliver a partial maturation signal to dendritic cells and activate the NF-kappa B pathway.* Int Immunol, 2000. **12**(11): p. 1539-46.
4. Somersan, S., et al., *Primary tumor tissue lysates are enriched in heat shock proteins and induce the maturation of human dendritic cells.* J Immunol, 2001. **167**(9): p. 4844-52.

5. Flohe, S.B., et al., *Human heat shock protein 60 induces maturation of dendritic cells versus a Th1-promoting phenotype.* J Immunol, 2003. **170**(5): p. 2340-8.
6. Tsan, M.F. and B. Gao, *Heat shock proteins and immune system.* J Leukoc Biol, 2009. **85**(6): p. 905-10.
7. Gao, B. and M.F. Tsan, *Endotoxin contamination in recombinant human heat shock protein 70 (Hsp70) preparation is responsible for the induction of tumor necrosis factor alpha release by murine macrophages.* J Biol Chem, 2003. **278**(1): p. 174-9.
8. Lieder, R., et al., *Endotoxins affect bioactivity of chitosan derivatives in cultures of bone marrow-derived human mesenchymal stem cells.* Acta Biomater, 2013. **9**(1): p. 4771-8.
9. Illum, L., *Chitosan and its use as a pharmaceutical excipient.* Pharm Res, 1998. **15**(9): p. 1326-31.
10. Kean, T. and M. Thanou, *Biodegradation, biodistribution and toxicity of chitosan.* Adv Drug Deliv Rev, 2010. **62**(1): p. 3-11.
11. Baldrick, P., *The safety of chitosan as a pharmaceutical excipient.* Regul Toxicol Pharmacol, 2010. **56**(3): p. 290-9.
12. Carroll, E.C., et al., *The Vaccine Adjuvant Chitosan Promotes Cellular Immunity via DNA Sensor cGAS-STING-Dependent Induction of Type I Interferons.* Immunity, 2016. **44**(3): p. 597-608.
13. Borges, O., et al., *Induction of lymphocytes activated marker CD69 following exposure to chitosan and alginate biopolymers.* Int J Pharm, 2007. **337**(1-2): p. 254-64.
14. Bueter, C.L., et al., *Spectrum and mechanisms of inflammasome activation by chitosan.* J Immunol, 2014. **192**(12): p. 5943-51.
15. Lebre, F., et al., *Intranasal Administration of Novel Chitosan Nanoparticle/DNA Complexes Induces Antibody Response to Hepatitis B Surface Antigen in Mice.* Mol Pharm, 2016. **13**(2): p. 472-82.
16. Lutz, M.B., et al., *An advanced culture method for generating large quantities of highly pure dendritic cells from mouse bone marrow.* J Immunol Methods, 1999. **223**(1): p. 77-92.
17. Duarte, M.L., et al., *An optimised method to determine the degree of acetylation of chitin and chitosan by FTIR spectroscopy.* Int J Biol Macromol, 2002. **31**(1-3): p. 1-8.
18. Burrell, R., *Human responses to bacterial endotoxin.* Circ Shock, 1994. **43**(3): p. 137-53.
19. use, C.f.m.p.f.h., *ICH guideline Q4B, Annex 14 to Note for Evaluation and Recommendation of Pharmacopoeial Texts for Use in the ICH Regions on Bacterial Endotoxins Tests.* 2010.
20. Majerle, A., J. Kidrič, and R. Jerala, *Enhancement of antibacterial and lipopolysaccharide binding activities of a human lactoferrin peptide fragment by the addition of acyl chain.* Journal of Antimicrobial Chemotherapy, 2003. **51**(5): p. 1159-1165.
21. Tynan, G.A., et al., *Polymyxin B inadequately quenches the effects of contaminating lipopolysaccharide on murine dendritic cells.* PLoS One, 2012. **7**(5): p. e37261.
22. Park, J. and J.E. Babensee, *Differential functional effects of biomaterials on dendritic cell maturation.* Acta Biomater, 2012. **8**(10): p. 3606-17.
23. Ma, P., et al., *Chitosan oligosaccharides inhibit LPS-induced over-expression of IL-6 and TNF-α in RAW264. 7 macrophage cells through blockade of mitogen-activated protein kinase (MAPK) and PI3K/Akt signaling pathways.* Carbohydrate polymers, 2011. **84**(4): p. 1391-1398.
24. Mori, A., et al., *The vaccine adjuvant alum inhibits IL-12 by promoting PI3 kinase signaling while chitosan does not inhibit IL-12 and enhances Th1 and Th17 responses.* Eur J Immunol, 2012. **42**(10): p. 2709-19.
25. Hoshino, K., et al., *Cutting edge: Toll-like receptor 4 (TLR4)-deficient mice are hyporesponsive to lipopolysaccharide: evidence for TLR4 as the Lps gene product.* J Immunol, 1999. **162**(7): p. 3749-52.

CHAPTER 4

Exploring the adjuvant effect of chitosan-aluminium nanoparticles

Abstract

The use of tailored particle-based adjuvants constitutes a promising way to enhance antigen-specific humoral and cellular immune responses. However, a thorough understanding of the mechanisms underlying their adjuvanticity is of crucial importance to generate more effective vaccines. The objective of this study was to address the ability of chitosan-aluminium nanoparticles (CH-Al NPs), which combine the immunostimulatory effects of chitosan and aluminium salts, to promote dendritic cell (DC) activation, assess their impact on innate and adaptive immune responses and compare the results to those reported for conventional chitosan particles (CH-Na NPs). All the tested CH-Al NP formulations were capable of modulating cytokine secretion by murine bone-marrow derived dendritic cells (BMDCs). CH-Al NPs promoted NLRP3 inflammasome activation, enhancing the release of IL-1β without significantly inhibiting the T helper 1 (Th1) and Th17 cell- polarizing cytokines, IL12p70 or IL-23, and induced DC maturation, but did not promote pro-inflammatory cytokine production alone.

In vivo results showed that subcutaneous (S.C.) injection of mice with CH-Al NPs generated a local inflammatory response comparable to that elicited by alum, characterized by an increase in the recruitment of neutrophils and eosinophils. Importantly, after subcutaneous immunization with CH-Al NPs combined with the hepatitis B surface antigen (HBsAg), mice developed high antigen-specific IgG titers in serum, nasal and vaginal washes. Overall, our results established that CH-Al NPs are a promising adjuvant to enhance both innate and adaptive immune responses.

4.1 Introduction

Vaccines are one of medicine's greatest achievements, helping to reduce the incidence and even eradicate otherwise potentially fatal diseases worldwide. Current prophylactic vaccines mainly generate humoral immune responses and many are assessed on the basis of promoting neutralizing antibodies. However, successful vaccines have yet to be introduced for diseases that require cellular immune response, including tuberculosis, malaria and AIDS, or to be used as therapeutic vaccines to control chronic infections (e.g. hepatitis B virus).

Particulate adjuvants can provide an effective means to increase the immunogenicity of a purified antigen. They act as antigen delivery systems to protect antigens from degradation or, prolong antigen residence in target tissues. They also promote antigen internalization by antigen presenting cells (APCs) and antigen cross-presentation [1-3]. Aluminium salts (alum) have been used as a vaccine adjuvant for more than 80 years, being very efficient at inducing antigen-specific antibodies. Despite this, pre-clinical and clinical studies have shown that alum is a poor inducer of cellular immune response and particularly of protective Th1 associated immune responses [4, 5], pointing to a clear need for the development of improved adjuvants.

To achieve successful vaccination, the recipient needs to generate a protective immune response, which involves cross-talk between the innate and the adaptive immune systems. Dendritic cells (DCs) are central in coordinating both systems, as they are professional antigen-presenting cells and capable of stimulating naïve T cells [6, 7], and their unique characteristics make them ideal targets for new adjuvants. In order to design improved adjuvants, it will be crucial to fully understand their mechanism of action and how they interact with the immune system. Recently, the NLRP3 inflammasome has been linked to the immunostimulatory properties of alum [8, 9]. NLRP3 inflammasome assembly leads to the formation of an active caspase-1, which catalyses the cleavage of the pro-cytokines IL-1β and IL-18, generating their biologically active forms [10]. The release of these cytokines has been shown to boost cellular immunity, in particular IL-1β can enhance the priming of naïve T cells, as well as the expansion of Th1, Th2 and Th17 cells [11]. Additionally, IL-1β has shown to synergize with IL-23 to stimulate Th17 cells [12] and induce IL-17 secretion by γδ and CD4+ T cells [13]. All of these cell types play crucial roles in immune responses. Of note, the induction of pyroptosis, a caspase-1 dependent type of cell death, by particulate material can promote the release of damage-associated molecular patterns (DAMPs), potentially augmenting the inflammatory response [14].

Chitosan is a cationic polymer consisting of β-(1-4)-linked D-glucosamine and N-acetyl-D-glucosamine monomers, obtained by deacetylation of chitin [15]. It has been considered a

safe, biodegradable and biocompatible polymer [16], and, therefore, extensive research has been directed toward its use in medical applications, namely as a drug and vaccine delivery system [17-19]. One major advantage of this polymer is its ability to be formulated into nanoparticles under mild conditions without the need of employing harmful organic solvents, which constitutes one of the main reasons for its widespread application in delivering different molecules such as therapeutic proteins, DNA, and vaccine antigens. Notably, the ability of chitosan to stimulate cells of the innate immune system has been shown in many studies [20-22]. Chitosan has been recently identified as an immunomodulatory agent that promotes strong NLRP3 inflammasome activation [23-25] and, unlike alum, without inhibiting crucial Th1 and Th17 polarizing cytokines [20]. Furthermore, chitosan was shown to engage the cGAS-STING pathway to induce type I interferons (IFNs), that in turn mediates DC activation and enhancement of antigen-specific Th1 responses [22]. While chitosan nanoparticles have been widely studied as antigen delivery systems, their ability to act as immunopotentiators and the mechanisms behind this are still not clear. Bueter et al. showed that chitosan in solution is capable of activating the NLRP3 inflammasome to induce IL-1β secretion, while Neumann and colleagues demonstrated that conventional chitosan nanoparticles exhibit the same ability, both *in vitro* and *in vivo* [25]. We have recently developed an improved chitosan-based delivery system, combining the immunomodulatory properties of aluminium salts and chitosan, for nasal vaccination against hepatitis B virus. In this study we aimed to assess the adjuvant potential of chitosan-aluminium nanoparticles (CH-Al NPs) in the induction of innate and adaptive immune responses and explore the mechanism behind their adjuvanticity. For that, we investigated the immunomodulatory effect of the particulate system on DCs regarding inflammasome activation, cytokine production and DC maturation, comparing it with chitosan in solution and conventional chitosan nanoparticles. We then determined the ability of these particles to induce cell recruitment at the injection site, characterizing the nature of infiltrating immune cells and how CH-Al NPs modulate the ability of peritoneal exudate cells to secrete cytokines in response to CpG. Finally, we assessed the ability of CH-Al NPs in combination with HBsAg to induce an adaptive immune response following subcutaneous immunization. Collectively, our data suggest that CH-Al NPs can be used as an improved vaccine adjuvant.

4.2 Materials and methods

4.2.1 Reagents

Cytidine-phosphate-guanosine (CpG) oligonucleotide 1826 was supplied by Oligosetc. Lipopolysaccharide from E. coli, Serotype R515, Toll-like receptor grade was purchased from Enzo Life Sciences. Aluminium hydroxide gel, referred to as 'alum', was supplied by BrenntagBiosector. Pyrogen-free water was purchased from Baxter Healthcare. Poly(deoxyadenylic-deoxythymidylic) acid (poly(dA:dT)), cytochalasin B, bafilomycin A, CA-074-Me and KCl were obtained from Sigma. Lipofectamine 2000 was supplied by Thermo Fisher Scientific. Recombinant hepatitis B surface antigen (HBsAg) was acquired from Aldevron (Fargo, USA). Engerix-B was obtained from GlaxoSmithKline Biologicals (Rixensart, BE). All other reagents were analytical grade.

4.2.2 Mice

Female C57BL/6 mice were obtained from Charles River (UK) and used at 8-16 weeks of age. Eight to 16 week old female NLRP3$^{-/-}$ and ASC$^{-/-}$ mice were bred in the Trinity Biomedical Sciences Institute (TBSI) Bioresources Unit and maintained according to the regulations of the European Union and the Irish Department of Health (Reference Number 091210). All *in vitro* and *ex vivo* studies involving murine primary cells were approved by the Trinity College Dublin Animal Research Ethics Committee.

For subcutaneous immunizations studies, 6-8 week old female C57BL/6 mice were purchased from Charles River (France), housed in the Center for Neuroscience and Cell Biology (CNC) animal facility, and provided with food and water *ad libitum*. Animal protocols were approved by CNC (ORBEA) and national ethics Committees in accordance with national (Dec. No. 1005/92 23rd October) and International (normative 2010/63 from EU) legislation.

4.2.3 Preparation and characterization of chitosan nanoparticles

A low molecular weight chitosan (ChitoClear, 95 % degree of deacetylation; Primex Bio-Chemicals AS) was purified according to a method previously described [26]. Chitosan nanoparticles (CH NPs) were prepared by a coacervation/precipitation technique described by Lebre et al. [26]. Briefly, CH NPs were obtained by adding equal volumes of a chitosan solution (0.1 % in 25 mM sodium acetate buffer (AcB), pH 5.0) and an aqueous aluminium sulfate solution (0.5 %), for CH-Al NP, or a sodium sulfate solution (0.625 %) for CH-Na

NP, under high speed vortexing for 20 s, followed by incubation at room temperature for 1 h. In order to remove unreacted compounds, the resulting nanoparticle suspensions were centrifuged for 30 min at 4500 g. Supernatants were discarded and the pellets resuspended in 25 mM AcB, pH 5.5.

Size and zeta potential of CH NPs were measured by dynamic light scattering (DLS) and electrophoretic light scattering (ELS), respectively, in a Delsa Nano C (Beckman Coulter). Both analyses were performed at 25 °C, in 25 mM AcB, pH 5.5.

For the immunization studies, HBsAg was loaded onto particle surface by physical adsorption. After centrifugation, the pellet was resuspended at 400 $\mu g.mL^{-1}$ and 325 μL of nanoparticle suspension was incubated with a similar volume of an HBsAg solution (100 $\mu g.mL^{-1}$) for 30 min.

4.2.4 Measurement of dendritic cell activation

Murine bone marrow-derived dendritic cells (BMDCs) were generated, as described previously [27]. Briefly, BMDCs were isolated from tibiae and femora of mice. Cells were grown in RPMI 1640 medium (Biosera) supplemented with 8 % ultra-low endotoxin heat-inactivated foetal bovine serum (FBS) (Biosera), 2 mM L-glutamine (Gibco), 50 $U \cdot mL^{-1}$ penicillin (Gibco), 50 $\mu g \cdot mL^{-1}$ streptomycin (Gibco) and 20 $ng \cdot mL^{-1}$ of granulocyte–macrophage colony-stimulating factor (GM-CSF) derived from the J588 myeloma cell line. On day 10, the loosely adherent cells were harvested and plated in 96-well plates at a density of 0.625×10^6 $cells \cdot mL^{-1}$ and incubated overnight, being further incubated with the appropriate stimuli on the next day. Supernatants were collected and analysed for cytokine secretion and cells were harvested for flow cytometry analysis.

4.2.5 Evaluation of cell surface marker expression

For analysis of the expression of DC maturation markers, BMDCs were harvested using a PBS-EDTA (5 mM) solution and transferred to flow cytometry tubes. Cells were incubated with Aqua dead cell dye (Invitrogen) for 30 min at 4 ºC. After washing with PBS, cells were stained with anti-mouse antibodies CD11c-PerCP-Cy5.5, CD80-PE, CD86-FITC, I-A/I-E-e450 and CD40-APC (eBiosciences, Biolegend or BD Pharmingen) for an additional 30 min at 4 ºC, washed with PBS and resuspended in flow cytometry buffer. Samples were acquired on a BD Canto II (BD Biosciences) flow cytometer and the data analysed using FlowJo software (Tree Star Inc).

4.2.6 Innate immune responses

Mice were injected intraperitoneally (I.P.) with either 200 μL of AcB, pH 5.5 or 200 μL of CH-Al NP (1 mg/mouse), CH-Na NP (1 mg/mouse) or alum (1 mg/mouse). After 24 h, peritoneal exudate cells (PECs) were collected by washing the peritoneal cavity of mice with 5 mL of PBS. Cells were pelleted by centrifugation (400 g, 5 min, 4 °C) and resuspended in complete RPMI 1640 medium.

The peritoneal lavage cells were stained with Aqua dead cell dye for 30 min at 4 ºC. After washing with PBS, cells were subsequently stained with the following fluorescently labelled antibodies: CD11b-PE-Cy7, Gr1-APC, F4/80-PerCP-Cy5.5, Siglec F-PE, cKit-FITC (eBiosciences, Biolegend or BD Pharmingen). A Fortessa (BD Biosciences) flow cytometer was used, and data were analysed using FlowJo software. Results were expressed as percentage of single/live cells.

For *ex vivo* analysis of cytokine production, PECs were plated in 96-well-plates at 1.0 x 10^6 cell·mL^{-1} in RPMI 1640 medium. Cells were supplemented with the culture medium or stimulated with CpG (5 μg·mL^{-1}), and supernatants were collected 24 h later and stored at −20 ºC until further analysis.

4.2.7 Cellular uptake studies

The synthesis of fluorescein-isothiocyanate (FITC) (Santa Cruz, USA)-labelled chitosan was performed according to a previously described protocol [26], based on the reaction between the isothiocyanate groups of FITC (Ex/Em: 490/525) and the primary amino groups of chitosan. The nanoparticles were prepared with FITC-labelled chitosan, as described above.

For confocal microscopy analysis, PECs from mice intraperitoneally injected with 1 mg FITC-labelled CH-Al NPs were collected 4 h after injection and seeded on glass coverslips in 12-well plates at a density of 1.0 x 10^6 cell·$mL^{-1}$and cultured overnight. On the second day after seeding, the growth medium was removed, cells were washed three times with PBS, pH 7.4, and incubated with fresh medium containing 300 nM Lysotracker® Red DND 99 (Ex/Em: 577/590 nm) (Life Technologies Corporation) for 30 min. Cells were then washed three times with PBS, pH 7.4, and fixed with 4 % paraformaldehyde (PFA) in PBS for 15 min at 37 °C. Cell nucleus of the pre-fixed cells were then labelled using Hoechst 33342 dye (Ex/Em: 350/461 nm), according to manufacturer's instructions. After labelling, cells were washed twice with PBS and the coverslips mounted on microscope slides with DAKO mounting medium, and examined under an inverted laser scanning confocal microscope

(Zeiss LSM 510 META, Carl Zeiss, Germany) equipped with imaging software (LSM 510 software, Carl Zeiss).

4.2.8 Immunization studies

Mice (5 per group) were subcutaneously immunized into the interscapular area, on days 0 and 14, with 100 μL of vaccine formulation, under slight isoflurane anaesthesia and were culled on day 42. All mice received 5 μg of HBsAg alone or loaded on CH-Al NPs or CH-Na NPs. A volume of 250 μL of a commercial formulation (Engerix 20 $\mu g \cdot mL^{-1}$) containing 5 μg of HBsAg was injected into mice in the positive control group.

4.2.9 Biological sample collection

Blood was collected using the submandibular lancet method into centrifuge tubes on day 14 and by cardiac puncture on day 42 and centrifuged at 1000 g for 15 min. Vaginal washes were collected on day 41, and nasal washes on day 42, as previously described by our group [26, 28]. Briefly, vaginal washes were collected by instilling 100 μL of PBS into the vaginal cavity and flushing the lavage fluid in−out a few times before collection. Samples were centrifuged at 11500 g for 10 min, and supernatants were stored. Nasal lavage samples were collected from euthanized mice. The lower jaw of the mice was cut away and the nasal lavage collected by instilling 200 μL of sterile PBS posteriorly into the nasal cavity. Fluid exiting the nostrils was collected and spun at 11500 g at 4 °C for 20 min. Collected and processed samples were stored at −20 °C until further analysis.

4.2.10 Determination of specific IgG, IgG1 and IgG2c

Quantification of IgG, IgG1 and IgG2c was performed using a protocol previously described by our group [29]. Ninety-six well plates were coated with 100 μL of a 1 $\mu g \cdot mL^{-1}$ HBsAg solution (50 mM sodium carbonate/bicarbonate, pH 9.6) and left overnight at 4 °C. To reduce non-specific binding, wells were blocked by adding 2 % (w/v) BSA in PBS-tween, followed by 1 h incubation at 37 °C. After washing, serial dilutions of serum were applied, whereas vaginal washes were added undiluted. After incubation for 2 h at 37 °C and extensive washing, immunoglobulins were detected upon incubation with horseradish peroxidase (HRP) conjugated goat anti-mouse IgG, IgG1 or, IgG2c for 30 minutes at 37 °C, followed by a further incubation with o-phenylenediamine dihydrochloride (OPD) solution (5 mg OPD to 10 ml citrate buffer and 10 μl H_2O_2) for 10 min at room temperature. The reaction was

stopped by adding 1M H_2SO_4 and the absorbance was determined at 492 nm using a microplate reader. The end-point titers presented in the results represent the antilog of the last log2 dilution, for which the OD values were at least two-fold higher than that of the naive sample, equally diluted. The log 2 end-point titers were used for statistical analysis.

4.2.11 Determination of cytokine levels

The concentration of the cytokine IL-10 was measured by the enzyme-linked immunosorbent assay (ELISA), using antibodies obtained from Biolegend. IL-1β, IL-12p70, IL-23, IFN-γ and TNF-α concentrations were determined by ELISA (R&D Systems) according to the manufacturer's instructions. Briefly, 96-well high binding ELISA plates (Greiner Bio-one) were coated with capture antibody and incubated overnight at 4 °C. The plates were washed in wash buffer (0.05 % PBS-tween) and blocked with 1 % BSA in PBS solution at room temperature for 1 h. After washing, samples and standards were added to the plates and incubated for 2 h at room temperature. Following this incubation step, biotinylated goat anti-mouse detection antibody was added to the plates, which were incubated for 2 h before washing and incubation with the avidin-HRP conjugate for an additional 30 min. Finally, plates were washed and OPD substrate solution was added to the plate. After 15 min incubation in the dark, the OD values were measured at 405 nm with wavelength correction set at 650 nm using a Multiskan EX 96-well plate reader. A standard curve was generated and used to determine the cytokine concentration of the unknown replicates.

4.2.12 Statistical analysis

Statistical analysis was performed with the GraphPad Prism v6 software (GraphPad Software Inc.). ANOVA followed by Tukey's post-test was used for multiple comparisons. Statistical analysis of cytokine secretion was performed using a Kruskal–Wallis non-parametric test followed by Dunn's post-test. In all cases, p-values ≤ 0.05 were considered statistically significant ($* p < 0.05$, $** p < 0.01$ and $*** p < 0.001$).

4.3 Results and discussion

4.3.1 Chitosan nanoparticle-mediated modulation of IL-1β secretion by dendritic cells is NLRP3- and ASC-dependent

Chitosan nanoparticles exhibit great potential as vaccine adjuvants; however, the mechanism underlying their adjuvanticity has not been fully clarified. In this study, we compared the adjuvant activity of an improved chitosan-based delivery system (CH-Al NP) developed in our laboratory [26], which combines the well-established immunopotentiator effect of aluminium salts and the recently described immunostimulatory effect of chitosan [22], with the conventional chitosan nanoparticles (CH-Na NP), extensively described in the literature. Particle size, surface charge and morphology play an important role in cellular uptake and biodistribution, and consequently, in nanoparticle biological activity [30, 31]. In order to allow a proper comparison between the two chitosan nanoparticle formulations, CH-Na NPs were prepared with the same amount of chitosan as CH-Al NPs. Results from formulation characterization showed that CH-Na NPs exhibit a mean diameter of 754.2 ± 114.4 nm with a polydispersity index (PI) of 0.382 ± 0.049 and a zeta potential of + 28.3 ± 2.5 mV, while CH-Al NPs display a size of 280.9 ± 32.7 with a PI of 0.255 ± 0.012 and a zeta potential of +30.1 ± 1.9 mV. The morphology of the formulations was studied by scanning electron microscopy and revealed the presence of smaller particles in both formulations (data not shown). It is believed that zeta potentials above +30 mV or below –30 mV are required for colloidal dispersion stability, hence particles with a surface charge close to neutrality tend to interact, thus generating larger aggregates [32].

Dendritic cell activation is essential for the generation of an effective immunological response as they are the bridge between innate and adaptive immune response [33]. Hence, assessment of BMDC activation, through quantification of costimulatory molecule expression and cytokine secretion, is a well-established procedure to evaluate the immunostimulatory potential of a novel adjuvant. When studying the immunomodulatory effects of a biomaterial, it is important to address the question of possible residual bacterial endotoxin contamination that might contribute to documented stimulatory effects [34]. Endotoxins are potent stimulatory molecules and small amounts (10 $pg \cdot mL^{-1}$) are enough to induce proinflammatory cytokine secretion by BMDCs [35]. To exclude the possibility that endotoxin contamination is responsible for the results generated, prior to any study, chitosan-based formulations and aluminium salts were incubated with BMDCs and tested for the secretion of the inflammatory cytokine IL-6, a highly sensitive readout for the presence of LPS contamination. The results

obtained showed that none of the chitosan formulations tested induced detectable IL-6 secretion by DCs (data not shown).

The next question we addressed regarded the ability of CH-Al NPs to modulate cytokine production by BMDC. Responses were compared with those induced by chitosan solution and CH-Na NPs. BMDCs were stimulated with CH-Al NPs (2.5 $\mu g \cdot mL^{-1}$ to 20 $\mu g \cdot mL^{-1}$), CH-Na NPs (2.5 $\mu g \cdot mL^{-1}$ to 20 $\mu g \cdot mL^{-1}$), CH solutions (0.25 $\mu g \cdot mL^{-1}$ to 2 $\mu g \cdot mL^{-1}$) or aluminium salt solutions (6.25 $\mu g \cdot mL^{-1}$ to 50 $\mu g \cdot mL^{-1}$), alone or in combination with the Toll-like receptor (TLR)-9 agonist, CpG (4 $\mu g \cdot mL^{-1}$). Low concentrations of chitosan in solution were employed, since at higher concentrations a significant increase in cell death was induced (data not shown). Alum (500 $\mu g \cdot mL^{-1}$) was used as a positive control. As expected, treatment of DCs with the formulations alone failed to induce appreciable IL-1β secretion (data not shown). On the other hand, as portrayed in figure 4.1, a concentration-dependent enhancement of IL-1β secretion in cells treated with CH-Al NPs in combination with CpG was observed, these results being similar to those obtained with CH-Na NPs and CH solution. For CH NPs, this effect plateaued at concentrations higher than 20 $\mu g \cdot mL^{-1}$ (data not shown). Interestingly, contrary to alum, the aluminium salts solution did not enhance IL-1β secretion, at least at the concentrations tested.

Since alum has been shown to activate the NLRP3 [8], studies have been conducted to investigate whether inflammasomes could be a target for the design of effective adjuvants. Some particulate adjuvants, such as poly(lactide-co-glycolide) (PLG) particles, Quil A and ISCOMATRIX have previously been shown to promote IL-1β and IL-18 secretion as a result of inflammasome activation [8, 36, 37]. Having established that CH-Al NPs can modulate TLR-induced IL-1β secretion, the next set of experiments was conducted to assess the involvement of NLRP3 and the apoptosis speck-like protein (ASC) in this immunomodulatory effect. For this purpose, BMDCs from $NLRP3^{-/-}$ and $ASC^{-/-}$ mice were stimulated with increasing concentrations of CH-Al NPs, CH-Na NPs, CH solution and aluminium sulfate solution. As observed (Fig. 4.1), an enhancement of IL-1β secretion by CH-Al NPs was found to be dependent upon the NLRP3 inflammasome and ASC, as particle-induced cytokine secretion was ablated in BMDCs from $NLRP3^{-/-}$ and $ASC^{-/-}$ mice, for all the concentrations tested. Similarly, IL-1β was severely reduced in supernatants of CH-Na NP- and CH solution-stimulated DCs from $NLRP3^{-/-}$ and $ASC^{-/-}$ mice. As expected, IL-1β release from $NLRP3^{-/-}$ DCs was not detected in response to alum, which activates the NLRP3 inflammasome, but remained intact in response to the double stranded-DNA analogue poly(dA:dT), which activates the AIM2 inflammasome. In ASC KO mice, all stimuli failed to

induce cytokine production, since ASC plays an important role in caspase-1 activation by both NLRP3 and AIM2 inflammasomes.

IL-1β is a potent proinflammatory cytokine that needs to be tightly regulated, thus 2 signals are required for its release in the active form [38]. Similarly to what happens with other particulates [25, 36], CH-Al NPs were able to act as a second stimulus leading to inflammasome activation. This, in combination with CpG, which triggers production of pro-IL-1β, culminates in the secretion of bioactive IL-1β. Overall, our results clearly demonstrate the enhancing effect of all chitosan-based formulations tested, including CH-Al NPs, on the secretion of IL-1β by DC via a NLRP3 and ASC dependent process.

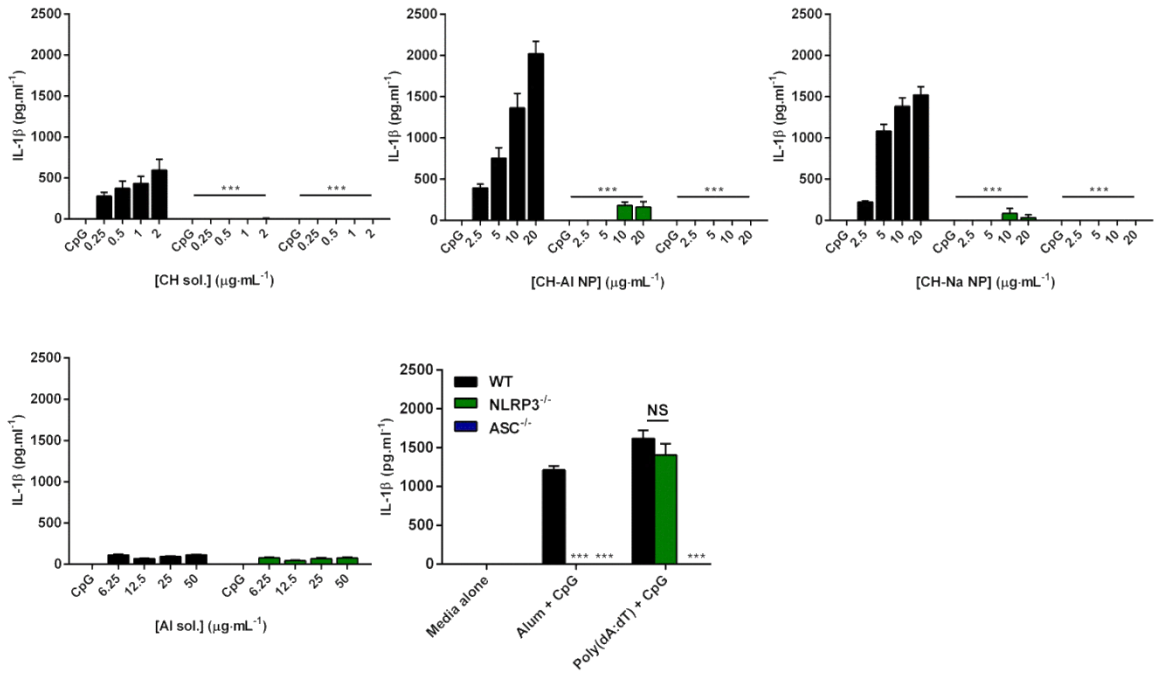

Figure 4.1 - Chitosan-based formulations promote ASC and NLRP3 inflammasome-dependent secretion of IL-1β by dendritic cells. BMDCs (0.625 x 10^6 cells·mL^{-1}) from C57BL/6 WT (black), $NLRP3^{-/-}$ (green) and $ASC^{-/-}$ (blue) mice were stimulated with increasing concentrations of chitosan solution (CH sol.); chitosan-aluminium nanoparticle suspension (CH-Al NP); chitosan-sodium nanoparticle suspension (CH-Na NP) or aluminium sulfate solution (Al sol.) after priming with CpG (4 μg·mL^{-1}) for 3 h. Alum (500 μg·mL^{-1}) and poly(dA:dT) combined with lipofectamine as a transfection agent were used as positive controls. Supernatants were collected 24 h later and tested for IL-1β secretion by ELISA. Results are mean cytokine concentrations (± SD) for triplicate samples. (*** $p < 0.001$ WT versus KO mice), and are representative of at least two independent experiments.

4.3.2 Particle uptake and lysosomal destabilization are necessary to activate the NLRP3 inflammasome *in vitro*

Although the events following NLRP3 inflammasome formation are well described, the exact mechanism by which structurally diverse stimuli trigger its activation is unclear. Three main mechanisms have been reported to be involved in NLRP3 inflammasome activation: reactive oxygen species (ROS) formation; potassium (K^+) efflux and lysosomal destabilization with cathepsin B release [10, 30]. It is possible that these distinct pathways are not mutually exclusive, contributing to a universal trigger that leads to inflammasome assembly. To determine the mechanism underlying CH-Al NP mediated activation of the NLRP3 inflammasome, BMDCs were pre-incubated with 4 distinct chemical inhibitors: bafilomycin A (250 nM), an inhibitor of lysosomal acidification; the cathepsin B inhibitor, CA-074-Me (10 μM); cytochalasin D (5 μM), an actin destabilizing drug that inhibits phagocytosis, and KCl (50 mM), to prevent K^+ efflux. As expected, in the absence of any inhibitor (NT), BMDCs primed with CpG (4 μg·mL^{-1}) and stimulated with 8 μg·mL^{-1} of CH solution or 20 μg·mL^{-1} of either CH NP formulation secreted high concentrations of IL-1β (Fig. 4.2).

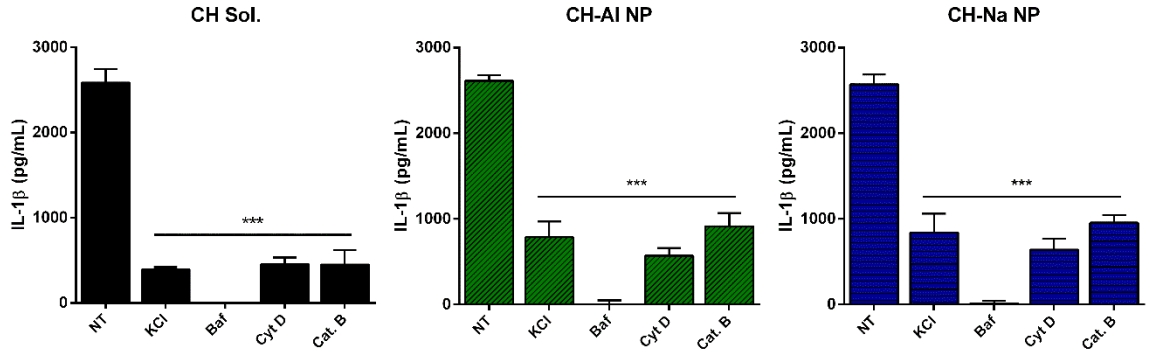

Figure 4.2 - Inhibitors of NLRP3 inflammasome activation significantly decrease chitosan-CpG- induced enhancement of IL-1β secretion. BMDCs (0.625 x 10^6 cells·mL^{-1}) generated from C57BL/6 mice were incubated in the presence or absence (non-treated - NT) of NLRP3 inflammasome inhibitors: KCl (50 mM); bafilomycin A (250 nM); cytochalasin D (5 μM) and the cathepsin B inhibitor CA-074-Me (10 μM) for 1 h prior to the addition of CH sol. (8 μg·mL^{-1})-CpG (4 μg·ml^{-1}); CH-Al NP (20 μg·ml^{-1})-CpG (4 μg·ml^{-1}) and CH-Na NP (20 μg·ml^{-1})-CpG (4 μg·ml^{-1}). Supernatants were collected 24 h later and tested for Il-1β by ELISA. Results are mean cytokine concentrations (± SD) for triplicate samples. (*** $p < 0.001$ treated versus NT BMDCs), and are representative of three independent experiments.

On the other hand, BMDC pre-treatment with any of the inhibitors resulted in a statistically significant decrease in IL-1β secretion. This was especially evident after treatment with the inhibitor of lysosomal acidification, bafilomycin A, which abrogated cytokine secretion. BMDC treatment with this inhibitor did not affect the capacity of CpG to induce a robust

secretion of IL-6 (data not shown). Interestingly, both chitosan particle formulations showed a similar profile to that of chitosan solution, suggesting that both chitosan-based formulations share a common activation mechanism. Studies by Neumann and colleagues [25] reported the involvement of lysosomal destabilization in the mechanism of inflammasome assembly by CH-Na NPs. Here, we show that inflammasome activation by chitosan-based formulations relies on a combination of distinct pathways, these being partially dependent on particle phagocytosis, cathepsin B activity and K^+ efflux and, to a greater extent, on lysosomal destabilization. This is also in line with previous findings reporting that particulates, like silica and alum, activate the NLRP3 inflammasome by a mechanism requiring low intracellular K^+ concentrations [39], cathepsin B activity and lysosomal acidification and rupture [40]. Overall, the obtained data help to shed light on the mechanism behind the CH NP/CpG-induced enhancement of IL-1β production by DCs.

4.3.3 Chitosan particles enhance expression of the co-stimulatory molecules CD80, CD86 and CD40 on DCs

After demonstrating that chitosan nanoparticles enhance NLRP3-dependent IL-1β secretion, experiments were undertaken to elucidate if the CH-Al NPs could induce DC maturation. Dendritic cells are present in the body in an immature state and after interacting with exogenous microbes or endogenous danger molecules undergo a maturation process, characterized by several physiological changes, including the upregulation of the surface markers CD80, CD86, CD40 and MHCcII molecules [41]. Dendritic cell maturation promotes their migration to draining lymph nodes, and enhances the ability of the DCs to interact with antigen-specific T cells [6, 7]. To determine the capacity of chitosan particles to promote DC maturation, BMDCs were incubated with CH-Al NPs (5 $\mu g \cdot mL^{-1}$ to 40 $\mu g \cdot ml^{-1}$), CH solution (1.25 $\mu g \cdot mL^{-1}$ to 5 $\mu g \cdot mL^{-1}$) and cross-linker solution (12.5 $\mu g \cdot mL^{-1}$ to 50 $\mu g \cdot mL^{-1}$) for 24 h. CpG (4 $\mu g \cdot mL^{-1}$) was used as a control. As illustrated in figure 4.3, BMDCs treated with CpG showed a marked enhancement of CD80, CD86 and CD40 expression; stimulation of DCs with CH-Al NPs also upregulated the expression of all markers, in a concentration-dependent manner, although not to the same extent as CpG. In line with findings by Carroll et al. [22], the CH solution also induced a concentration-dependent enhancement in the expression of co-stimulatory molecules, while aluminium sulfate had a negligible effect on DC maturation. Although the mechanism behind this effect is unclear, as referred to above, chitosan-based formulations seem to share a common inflammasome activation mechanism, making it plausible that the same mechanism holds true for DC maturation and that this is dependent

upon IFN-α/IFN-β receptor (IFNAR) signaling [22]. However, further studies will be essential to confirm this hypothesis.

Collectively, our data suggest that CH-Al NPs alone have the capacity to induce DC maturation, resulting in the upregulation of DC surface expression of co-stimulatory molecules, thus contributing to their adjuvanticity.

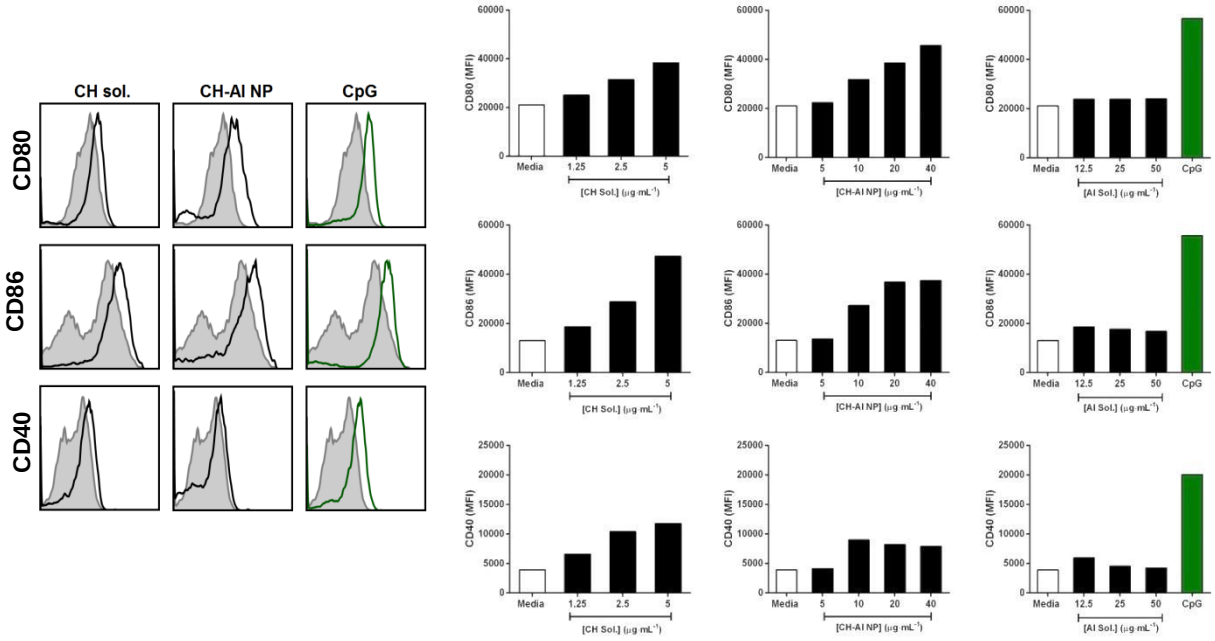

Figure 4.3 - Chitosan particles enhance the expression of co-stimulatory molecules on DCs. BMDCs (0.625 x 10^6 cells·mL^{-1}) generated from C57BL/6 mice were stimulated with medium or increasing concentrations of CH solution, CH-Al NP or Al solution. CpG (4 µg·mL^{-1}) was used as a control. Cells were collected 24 h later and stained for expression of CD80, CD86 and CD40 and analysed by flow cytometry. Representative histograms are shown for cells treated with medium (shaded histogram) or 5 µg·mL^{-1} CH sol, 40 µg·mL^{-1} CH-Al NP and 4 µg·mL^{-1} CpG (solid line). Data are represented as MFI values of a pool of triplicates and are representative of at least two independent experiments.

4.3.4 Chitosan nanoparticles do not inhibit the secretion of IL-12p70 and IL-23

The vaccine adjuvant alum has previously been shown to inhibit the secretion of the Th1 cell polarizing cytokine IL-12p70, which could help to explain why alum is inefficient at inducing Th1 responses [20]. On the other hand, figure 4.4 A shows that in contrast to alum (500 µg. mL^{-1}), which significantly decreased CpG-induced IL-12p70 secretion by BMDCs, CH solution did not prevent cytokine secretion at concentrations ranging from 2 µg. mL^{-1} to 8 µg. mL^{-1} (Fig. 4.4 A).To investigate whether CH-Al NP stimulation would hinder the secretion

of IL-12 family members, we assessed the effect of a broad range of particle concentrations on IL-12p70 and IL-23 secretion by BMDCs. In the absence of CpG, CH-Al NPs alone did not elicit significant secretion of IL-12p70 (Fig. 4.4 A) or IL-23 (Fig. 4.4 B). IL-12 is an important polarizing cytokine that contributes to the differentiation of Th1 cells, which secrete interferon (IFN)-γ that plays a pivotal role in cellular immunity [42]. IL-23 is implicated in the Th17 cell commitment and maintenance, which is important for protection against fungal pathogens and extracellular bacteria [42]. Therefore, the development of adjuvants that are effective in activating both Th1/17 mediated immune response is urgently needed.

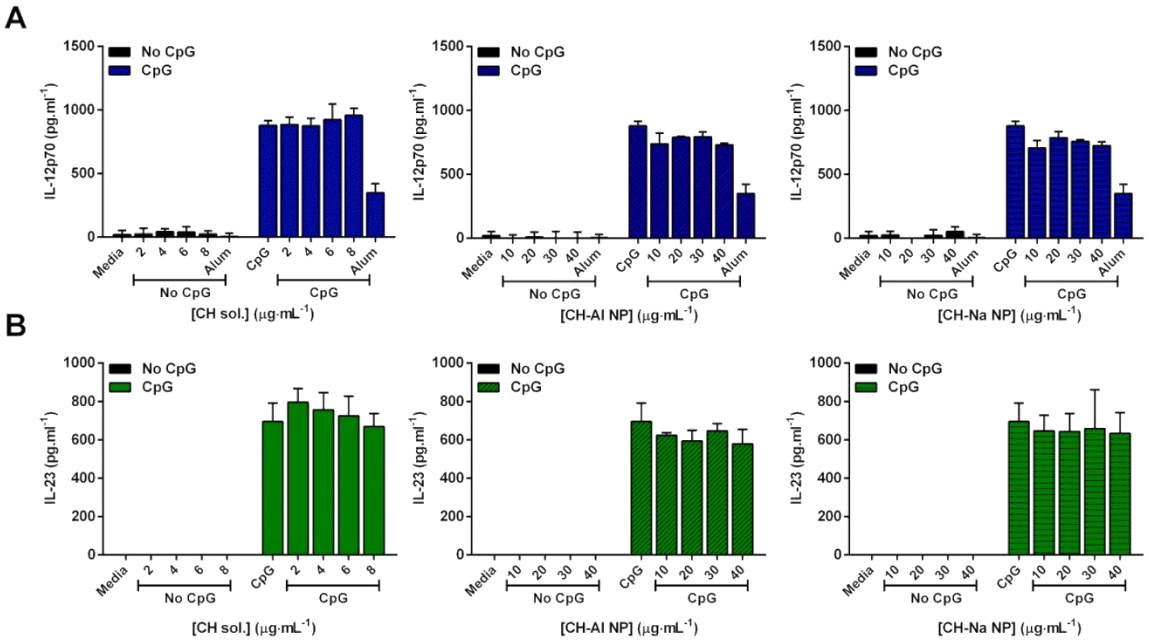

Figure 4.4 - Chitosan nanoparticles do not suppress CpG-mediated production of IL-12p70 and IL-23 by BMDCs. BMDCs (0.625 x 10^6 cells·mL^1) isolated from C57BL/6 mice were stimulated with CH solution (2 μg.$mL^{-1}$to 8 μg.mL^{-1}) or CH NPs (10 μg.$mL^{-1}$to 40 μg.mL^{-1}), either alone or after priming with CpG (4 μg·mL^{-1}). Alum (500 μg·mL^{-1}) was used as control. Supernatants were collected 24 h later and tested for IL-12p70 (A) or IL-23 (B) by ELISA. Results are mean cytokine concentrations (± SD) for triplicate samples and are representative of three independent experiments.

Taken together, our data suggest that, similarly to chitosan in solution, chitosan nanoparticles can activate DCs by modulating cytokine secretion and expression of co-stimulatory molecules. Combining the immunostimulatory properties of CH NPs with their capacity to act as a delivery system makes them a promising adjuvant in the development of more immunogenic vaccines.

4.3.5 Chitosan nanoparticles and alum drive comparable inflammatory response at the injection site

Aiming at the future clinical application of CH-Al NPs, we assessed their immunostimulatory effect *ex vivo* after intraperitoneal injection, as the peritoneal cavity encompasses a complex composition of innate immune cells [43, 44]. The innate immune system provides the first line of host defense against foreign material and plays a pivotal role in the initiation of adaptive immune responses [45]. To investigate how CH NPs influence the innate immune response, mice were injected with 200 µL of AcB alone or with 1 mg of each type of CH NPs (CH-Al or CH-Na) suspended in the buffer. Alum-immunized mice (1 mg/mouse) were used as a control. Twenty-four hours later, mice were sacrificed and PECs were collected to characterize the nature of infiltrating immune cells by flow cytometry.

Under steady-state conditions, the peritoneal cavity is composed of a mixture of immune cell subsets, mainly B cells, as well as DCs, T cells, NK cells, mast cells and resident macrophages that account for 30 % of total cells [43, 44]. As shown in figure 4.5 A, mice injected with vehicle solution displayed a high percentage of peritoneal resident macrophages ($CD11b^{hi}$ $F4/80^{hi}$), moderate percentage of mast cells ($SiglecF^{-}$ $cKit^{+}$), low percentage of eosinophils ($CD11b^{+}SiglecF^{+}$ $Gr1^{-}SSC^{hi}$) and an almost complete absence of neutrophils ($CD11b^{+}SiglecF^{-}$ $F4/80^{-}$ $Gr1^{hi}$). As expected, injection of CH-Al NPs and CH-Na NPs drove a significant increase in cell numbers with a clear recruitment of neutrophils and eosinophils. In contrast to enhanced inflammatory cell recruitment, macrophage and mast cell disappearance was observed (Fig. 4.5 A). When a foreign substance enters the peritoneal cavity, it is sensed by innate cells, including tissue resident macrophages capable of secreting cytokines and chemokines that drive the recruitment of neutrophils and monocytes [30]. Additionally, it is known that the number of resident macrophages declines during the acute inflammatory stage [46].The basis for this macrophage depletion is still debatable, but has been attributed to cell death, increased adherence to the peritoneal cavity and migration to the draining lymph nodes [47]. In agreement with previous reports [48, 49], a single injection of alum resulted in significant immune cell infiltration, characterized by the recruitment of granulocytes to a greater extent compared to CH NPs, and a depletion of resident macrophages and mast cells. As shown in figure 4.5 B, CH-Al NPs were internalized by peritoneal cells, and found to co-localize with lysosomes. In addition to a shared ability to activate the NLRP3 inflammasome, these similar changes at the injection site between alum- and CH NP-injected mice suggest they might share common aspects of the mechanism by which they exert adjuvant activity. Kool and colleagues showed that I.P. injection of alum

promotes recruitment of inflammatory monocytes capable of internalizing antigen and migrating to the lymph nodes, where they become inflammatory DCs and induce adaptive immunity [49]. It is conceivable that CH NPs can elicit an immune response similar to the vaccine adjuvant alum. Nevertheless, it is still necessary to further investigate the mechanism underlying the inflammatory effects of CH NPs in the peritonitis model.

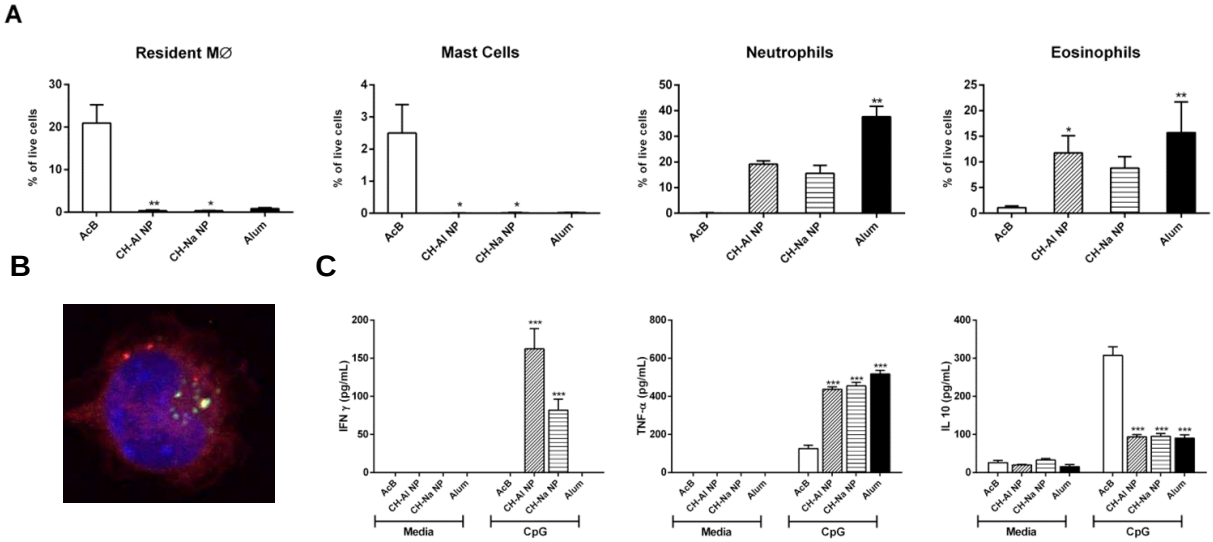

Figure 4.5 - CH NPs are potent inducers of innate immune cell recruitment into the peritoneum, modulating cytokine production from restimulated PECs. Female C57BL/6 mice (n = 4), aged 6-8 weeks, were injected intraperitoneally with AcB vehicle, CH-Al NPs (1 mg/mouse), CH-Na NPs (1 mg/mouse), or alum (1 mg/mouse). After 24 h, peritoneal lavage cells were collected and (A) stained for cell recruitment and analysed by flow cytometry or (C) plated for restimulation. (A) To characterize the nature of infiltrating immune cells, PECs were stained using a combination of markers for peritoneal resident macrophages ($CD11b^{hi}$ $F4/80^{hi}$), mast cells ($SiglecF^{-}cKit^{+}$), neutrophils ($CD11b^{+}SiglecF^{-}$ $F4/80^{-}$ $Gr1^{hi}$) and eosinophils ($CD11b^{+}SiglecF^{+}$ $Gr1^{-}$ SSC^{hi}). Results are representative of two independent experiments and are expressed as percentage of single/live cells (* $p< 0.05$, ** $p < 0.01$, *** $p < 0.001$). (B) Confocal microscopy image of PEC uptake, 4 h post-injection; LysoTracker (red); FITC-labelled CH-Al NPs (green); nuclear staining with Hoechst 33342 (blue); colocalization of CH-Al NPs with lysosomes (yellow); (C) PECs were plated at 1.0 x 10^6 cell·$mL^{-1}$and restimulated with complete RPMI medium or CpG (5 μg·mL^{-1}) for 24 h. Supernatants were collected and the levels of secreted IFN-γ, TNF-α and IL-10 were determined by ELISA. Results are mean cytokine concentrations (± SEM) for triplicate samples (***$p < 0.001$ versus AcB) and are representative of 2 independent experiments.

Since the nature of infiltrating immune cells changed after particle injection, we investigated whether injection of the nanoparticles affected the capacity of cells to secrete different cytokines. Therefore, cells collected from the peritoneal cavity of mice injected with AcB, CH NPs or alum were re-stimulated *ex vivo* with complete medium or CpG (5 μg·mL^{-1}) for 24 h

and assessed for the secretion of IFN-γ, TNF-α and IL-10 by ELISA. As displayed in figure 4.5 C, PECs re-stimulated with medium alone showed marginal cytokine production. On the other hand, following re-stimulation with CpG, PECs from mice injected with CH NPs and alum secreted significantly higher concentrations of the pro-inflammatory cytokine TNF-α when compared with PECs recovered from mice injected with AcB. This is in line with the increased recruitment of immune cells in these animal groups. Interestingly, PECs from mice injected with alum failed secrete IFN-γ following CpG restimulation, in sharp contrast with those injected with CH NPs. In fact, PECs from mice injected with CH-Al NPs secreted the highest concentrations of IFN-γ, which correlates with the *in vitro* data. Bioactive IL-12 secretion is inhibited in cells treated with alum, but not in cells treated with CH-Al NPs. IL-12 secretion from antigen-presenting (APCs) is capable of polarizing naive T cells into Th1 cells, which leads to a positive feedback loop, where IFN–γ secretion by T cells upregulates IL-12 production, inhibiting the differentiation of other T cell subsets [42]. Furthermore, all particulate formulations showed a significantly diminished capacity to enhance secretion of the immunoregulatory cytokine IL-10, compared to AcB-injected mice. Overall, our results reinforce the potential of CH-Al NPs to act as a promising vaccine adjuvant.

4.3.6 Chitosan nanoparticles induce superior systemic and mucosal immune response than the commercial formulation

Considering the promising results on the modulation of innate immune responses by CH NPs, we investigated the potential of CH-Al NPs and CH-Na NPs to induce an adaptive immune response following subcutaneous vaccination with HBsAg. For that, mice were vaccinated on day zero with 5 μg of HBsAg alone or in combination with CH-Al NPs or CH-Na NPs and boosted on day 14. To assess if co-administration of CH NPs and HBsAg would enhance antigen-specific systemic immune responses, serum IgG anti-HBsAg titers in mice immunized with CH NPs were analysed prior to boosting (day 14) and on day 42 (end-point) and compared with those in mice that had received the antigen alone. The commercially available vaccine against hepatitis B, Engerix-B, was used as a positive control. Before boost, mice vaccinated with the antigen adsorbed on the particles exhibited statistically higher anti-HBsAg IgG titers compared to the HBsAg alone group (Fig. 4.6 A). On day 42, antigen-specific IgG titers were still significantly increased when HBsAg was combined with either CH-NP formulation. HBsAg is a very immunogenic antigen, which may be attributed to its capacity to spontaneously assemble into virus-like particles [50]. Moreover, CH NPs were able to synergize with the antigen, thus inducing a more robust humoral response. Remarkably, CH

NPs were capable of originating an overall better immune response profile that Engerix-B, which was comparable for CH-Al NPs and CH-Na NPs.

To understand how IgG subclasses are affected by the different formulations, anti-HBsAg IgG1 and IgG2c titers were determined on day 42 (Fig. 4.6 B). Consistent with total IgG titers, subcutaneous immunization with all the formulations induced the production of antigen-specific IgG1, the titers being higher for CH NPs. Similarly, mice immunized with antigen alone were capable of inducing antigen-specific IgG2c antibody responses. However, CH NPs induced the production of the highest antigen-specific total IgG2c antibody titers. Analysis of antibody isotypes revealed that CH NPs allowed a more balanced Th1/Th2 response, as IgG1 is predictive of a Th2 response while IgG2c indicates a more Th1 like-response.

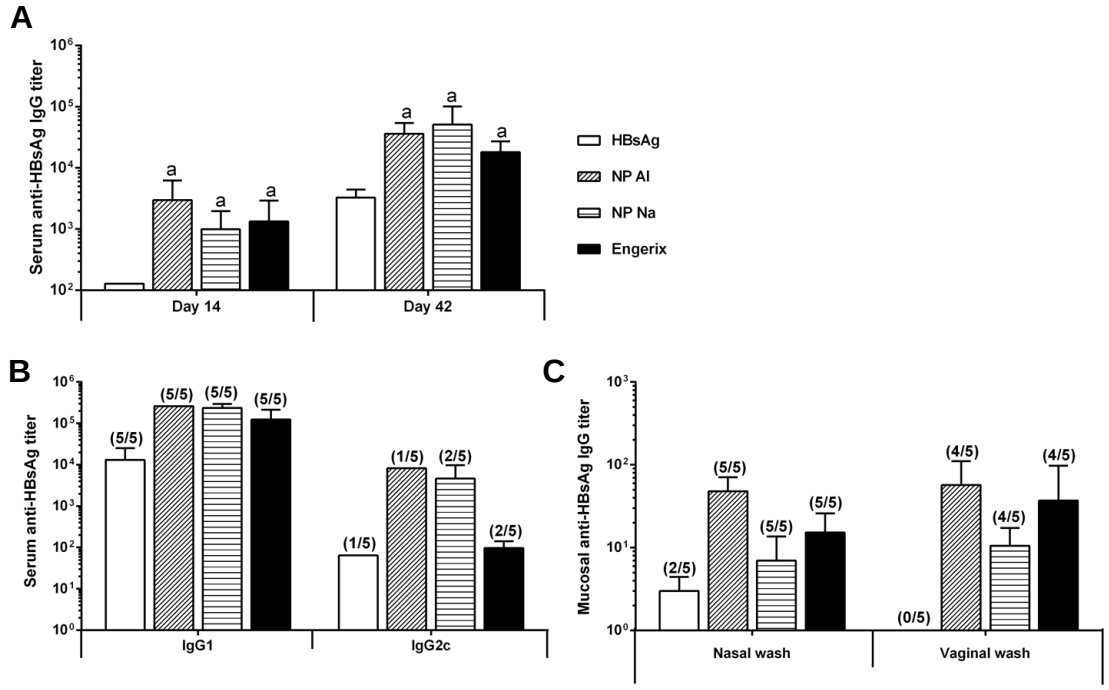

Figure 4.6 - Immune response profiles. Serum anti-HBsAg IgG (A); IgG1 and IgG2c (B); nasal and vaginal IgG (C) titers in mice subcutaneously immunized with CH-Al NPs and CH-Na NPs loaded with 1.5 μg of HBsAg, on days 0 and 14. Control corresponds to free HBsAg and Engerix-B was loaded with the same amount of antigen as the CH NP formulations. Blood was collected on days 14 and 42; vaginal secretions were collected on day 42. Antibody levels were determined by ELISA, as described in 'Materials and methods'. The end-point titer presented in the results represents the antilog of the last log 2 dilution for which the OD values were at least two-fold higher than that of the naive sample equally diluted. The log 2 endpoint titers were used for statistical analysis. The number of mice in which antibody levels were detected is indicated above the bars. Data (mean ± SD) correspond to groups of 5 mice each. a indicates values that differ significantly from HBsAg alone ($p < 0.01$).

Notably, co-administration of HBsAg and CH-NPs also resulted in an increase of antigen-specific IgG in nasal and vaginal washes and a higher seroconversion percentage compared with antigen alone (Fig. 4.6 C), revealing that plasma IgG was able to reach mucosal locations. It is important to highlight that immunization with CH-Al NPs elicited the highest antigen specific antibody titers in mucosal washes. Even though IgG levels in the serum are frequently used as readout for vaccine efficacy, it has been previously shown that IgG transudation from serum to mucosal surfaces could mediate mucosal protection against rotavirus infection [51]. Additionally, Wang and co-workers demonstrated that mucosal IgG was capable to bind to herpes simplex virus serotype 1 surface. The IgG present in this Ag-pathogen complex could in turn interact with the mucus layer efficiently entrapping the pathogen [52]. Thus, the induction of protective antibodies in mucosal surfaces, especially in the vaginal tract, would be a great advantage for the prevention of sexually transmitted HBV.

Altogether, these results demonstrate the benefits of using chitosan nanoparticles, particularly CH-Al NPs, as a strategy to induce strong systemic and mucosal immune responses.

4.4 Conclusion

In conclusion, we were able to demonstrate that CH-Al NPs modulate IL-1β secretion by dendritic cells in a NLRP3- and ASC-dependent manner. Moreover, in contrast to alum, CH NPs did not inhibit secretion of IL-12p70 and IL-23, key cytokines to mount cellular immune responses. We further found that following subcutaneous immunization, CH-Al NPs were internalized by mouse peritoneal cells and elicited an inflammatory profile similar to the vaccine adjuvant alum. Importantly, in comparison with the HBV vaccine Engerix, CH-Al NPs induced higher antigen-specific IgG titers in serum and mucosal sites with the additional benefit of eliciting higher IgG2c levels.

References

1. Schijns, V.E. and E.C. Lavelle, *Trends in vaccine adjuvants.* Expert Rev Vaccines, 2011. **10**(4): p. 539-50.
2. Smith, D.M., J.K. Simon, and J.R. Baker, Jr., *Applications of nanotechnology for immunology.* Nat Rev Immunol, 2013. **13**(8): p. 592-605.
3. Rice-Ficht, A.C., et al., *Polymeric particles in vaccine delivery.* Curr Opin Microbiol, 2010. **13**(1): p. 106-12.
4. Oleszycka, E. and E.C. Lavelle, *Immunomodulatory properties of the vaccine adjuvant alum.* Curr Opin Immunol, 2014. **28**: p. 1-5.
5. Marrack, P., A.S. McKee, and M.W. Munks, *Towards an understanding of the adjuvant action of aluminium.* Nat Rev Immunol, 2009. **9**(4): p. 287-93.

6. Steinman, R.M., *Lasker Basic Medical Research Award. Dendritic cells: versatile controllers of the immune system.* Nat Med, 2007. **13**(10): p. 1155-9.
7. Lanzavecchia, A. and F. Sallusto, *Regulation of T cell immunity by dendritic cells.* Cell, 2001. **106**(3): p. 263-6.
8. Li, H., et al., *Cutting edge: inflammasome activation by alum and alum's adjuvant effect are mediated by NLRP3.* J Immunol, 2008. **181**(1): p. 17-21.
9. Eisenbarth, S.C., et al., *Crucial role for the Nalp3 inflammasome in the immunostimulatory properties of aluminium adjuvants.* Nature, 2008. **453**(7198): p. 1122-6.
10. Latz, E., T.S. Xiao, and A. Stutz, *Activation and regulation of the inflammasomes.* Nat Rev Immunol, 2013. **13**(6): p. 397-411.
11. Ben-Sasson, S.Z., et al., *IL-1 acts directly on CD4 T cells to enhance their antigen-driven expansion and differentiation.* Proc Natl Acad Sci U S A, 2009. **106**(17): p. 7119-24.
12. Zielinski, C.E., et al., *Pathogen-induced human TH17 cells produce IFN-gamma or IL-10 and are regulated by IL-1beta.* Nature, 2012. **484**(7395): p. 514-8.
13. Lalor, S.J., et al., *Caspase-1-processed cytokines IL-1beta and IL-18 promote IL-17 production by gammadelta and CD4 T cells that mediate autoimmunity.* J Immunol, 2011. **186**(10): p. 5738-48.
14. Miao, E.A., J.V. Rajan, and A. Aderem, *Caspase-1-induced pyroptotic cell death.* Immunol Rev, 2011. **243**(1): p. 206-14.
15. Illum, L., *Chitosan and its use as a pharmaceutical excipient.* Pharm Res, 1998. **15**(9): p. 1326-31.
16. Baldrick, P., *The safety of chitosan as a pharmaceutical excipient.* Regul Toxicol Pharmacol, 2010. **56**(3): p. 290-9.
17. Lebre, F., et al., *Progress towards a needle-free hepatitis B vaccine.* Pharm Res, 2011. **28**(5): p. 986-1012.
18. Panos, I., N. Acosta, and A. Heras, *New drug delivery systems based on chitosan.* Curr Drug Discov Technol, 2008. **5**(4): p. 333-41.
19. van der Lubben, I.M., et al., *Chitosan for mucosal vaccination.* Adv Drug Deliv Rev, 2001. **52**(2): p. 139-44.
20. Mori, A., et al., *The vaccine adjuvant alum inhibits IL-12 by promoting PI3 kinase signaling while chitosan does not inhibit IL-12 and enhances Th1 and Th17 responses.* Eur J Immunol, 2012. **42**(10): p. 2709-19.
21. Borges, O., et al., *Induction of lymphocytes activated marker CD69 following exposure to chitosan and alginate biopolymers.* Int J Pharm, 2007. **337**(1-2): p. 254-64.
22. Carroll, E.C., et al., *The Vaccine Adjuvant Chitosan Promotes Cellular Immunity via DNA Sensor cGAS-STING-Dependent Induction of Type I Interferons.* Immunity, 2016. **44**(3): p. 597-608.
23. Bueter, C.L., et al., *Chitosan but not chitin activates the inflammasome by a mechanism dependent upon phagocytosis.* J Biol Chem, 2011. **286**(41): p. 35447-55.
24. Bueter, C.L., et al., *Spectrum and mechanisms of inflammasome activation by chitosan.* J Immunol, 2014. **192**(12): p. 5943-51.
25. Neumann, S., et al., *Activation of the NLRP3 inflammasome is not a feature of all particulate vaccine adjuvants.* Immunol Cell Biol, 2014. **92**(6): p. 535-42.
26. Lebre, F., et al., *Intranasal Administration of Novel Chitosan Nanoparticle/DNA Complexes Induces Antibody Response to Hepatitis B Surface Antigen in Mice.* Mol Pharm, 2016. **13**(2): p. 472-82.
27. Lutz, M.B., et al., *An advanced culture method for generating large quantities of highly pure dendritic cells from mouse bone marrow.* J Immunol Methods, 1999. **223**(1): p. 77-92.
28. Jesus, S., E. Soares, and O. Borges, *Poly-epsilon-caprolactone/Chitosan and Chitosan Particles: Two Recombinant Antigen Delivery Systems for Intranasal Vaccination.* Methods Mol Biol, 2016. **1404**: p. 697-713.

29. Borges, O., et al., *Immune response by nasal delivery of hepatitis B surface antigen and codelivery of a CpG ODN in alginate coated chitosan nanoparticles.* Eur J Pharm Biopharm, 2008. **69**(2): p. 405-16.
30. Lebre, F., C.H. Hearnden, and E.C. Lavelle, *Modulation of Immune Responses by Particulate Materials.* Adv Mater, 2016. **28**(27): p. 5525-41.
31. Hotaling, N.A., et al., *Biomaterial Strategies for Immunomodulation.* Annu Rev Biomed Eng, 2015. **17**: p. 317-49.
32. Lebre, F., et al., *Chitosan-based nanoparticles as a hepatitis B antigen delivery system.* Methods Enzymol, 2012. **509**: p. 127-42.
33. Pulendran, B. and R. Ahmed, *Translating innate immunity into immunological memory: implications for vaccine development.* Cell, 2006. **124**(4): p. 849-63.
34. Wakelin, S.J., et al., *"Dirty little secrets"--endotoxin contamination of recombinant proteins.* Immunol Lett, 2006. **106**(1): p. 1-7.
35. Tynan, G.A., et al., *Polymyxin B inadequately quenches the effects of contaminating lipopolysaccharide on murine dendritic cells.* PLoS One, 2012. **7**(5): p. e37261.
36. Sharp, F.A., et al., *Uptake of particulate vaccine adjuvants by dendritic cells activates the NALP3 inflammasome.* Proc Natl Acad Sci U S A, 2009. **106**(3): p. 870-5.
37. Wilson, N.S., et al., *Inflammasome-dependent and -independent IL-18 production mediates immunity to the ISCOMATRIX adjuvant.* J Immunol, 2014. **192**(7): p. 3259-68.
38. Eder, C., *Mechanisms of interleukin-1beta release.* Immunobiology, 2009. **214**(7): p. 543-53.
39. Petrilli, V., et al., *Activation of the NALP3 inflammasome is triggered by low intracellular potassium concentration.* Cell Death Differ, 2007. **14**(9): p. 1583-9.
40. Hornung, V., et al., *Silica crystals and aluminum salts activate the NALP3 inflammasome through phagosomal destabilization.* Nat Immunol, 2008. **9**(8): p. 847-56.
41. Palucka, K., J. Banchereau, and I. Mellman, *Designing vaccines based on biology of human dendritic cell subsets.* Immunity, 2010. **33**(4): p. 464-78.
42. Vignali, D.A. and V.K. Kuchroo, *IL-12 family cytokines: immunological playmakers.* Nat Immunol, 2012. **13**(8): p. 722-8.
43. Ghosn, E.E., et al., *Two physically, functionally, and developmentally distinct peritoneal macrophage subsets.* Proc Natl Acad Sci U S A, 2010. **107**(6): p. 2568-73.
44. Cassado Ados, A., et al., *Cellular renewal and improvement of local cell effector activity in peritoneal cavity in response to infectious stimuli.* PLoS One, 2011. **6**(7): p. e22141.
45. Iwasaki, A. and R. Medzhitov, *Control of adaptive immunity by the innate immune system.* Nat Immunol, 2015. **16**(4): p. 343-53.
46. Davies, L.C., et al., *A quantifiable proliferative burst of tissue macrophages restores homeostatic macrophage populations after acute inflammation.* Eur J Immunol, 2011. **41**(8): p. 2155-64.
47. Davies, L.C., et al., *Tissue-resident macrophages.* Nat Immunol, 2013. **14**(10): p. 986-95.
48. Oleszycka, E., et al., *IL-1alpha and inflammasome-independent IL-1beta promote neutrophil infiltration following alum vaccination.* FEBS J, 2016. **283**(1): p. 9-24.
49. Kool, M., et al., *Alum adjuvant boosts adaptive immunity by inducing uric acid and activating inflammatory dendritic cells.* J Exp Med, 2008. **205**(4): p. 869-82.
50. Roldao, A., et al., *Virus-like particles in vaccine development.* Expert Rev Vaccines, 2010. **9**(10): p. 1149-76.
51. Westerman, L.E., et al., *Serum IgG mediates mucosal immunity against rotavirus infection.* Proc Natl Acad Sci U S A, 2005. **102**(20): p. 7268-73.
52. Wang, Y.Y., et al., *IgG in cervicovaginal mucus traps HSV and prevents vaginal herpes infections.* Mucosal Immunol, 2014. **7**(5): p. 1036-44.

CHAPTER 5

Intranasal administration of novel chitosan nanoparticles/DNA complexes induces antibody response to hepatitis B surface antigen in mice

This chapter was adapted from:

Lebre, F., Borchard, G., Faneca, H., Pedroso de Lima, M. C., & Borges, O. (2016). Intranasal administration of novel chitosan nanoparticle/DNA complexes induces antibody response to hepatitis B surface antigen in mice. *Molecular pharmaceutics*, 13(2), 472-482.

Abstract

The generation of strong pathogen-specific immune responses at mucosal surfaces where hepatitis B virus (HBV) transmission can occur is still a major challenge. Therefore, new vaccines are urgently needed in order to overcome the limitations of existing parenteral ones. Recent studies show that this may be achieved by intranasal immunization. Chitosan has gained attention as a nonviral gene delivery system; however, its use *in vivo* is limited due to low transfection efficiency mostly related to strong interaction between the negatively charged DNA and the positively charged chitosan. We hypothesize that the adsorption of negatively charged human serum albumin (HSA) onto the surface of the chitosan particles would facilitate the intracellular release of DNA, enhancing transfection activity. Here, we demonstrate that a robust systemic immune response was induced after vaccination using HSA-loaded chitosan nanoparticle/DNA (HSA-CH NP/DNA) complexes. Furthermore, intranasal immunization with HSA-CH NP/DNA complexes induced HBV specific IgA in nasal and vaginal secretions; no systemic or mucosal responses were detected after immunization with DNA alone. Overall, our results show that chitosan-based DNA complexes elicited both humoral and mucosal immune response, making them an interesting and valuable gene delivery system for nasal vaccination against HBV.

5.1 Introduction

Hepatitis B disease is an important worldwide health problem. According to the latest WHO data [1], millions of people are infected with hepatitis B virus, with more than 240 million chronically infected. Hepatitis B mortality is estimated at 780 000 deaths annually. Despite the availability of a safe and effective parenteral HBV vaccine, there are drawbacks associated with this route of administration. Among these are the requirement of trained medical personnel and the risk of the reuse of needles. In addition, parenteral HBV vaccination requires an intensive dose regimen (3 doses in 6 months), which is especially challenging in developing countries where the cold chain often is hardly sustained. Another challenge is the fact that a high percentage of the population does not have access to the vaccine or does not return for the required booster doses. Furthermore, approximately 5 % to 10 % of vaccine recipients do not generate antibodies against hepatitis B surface antigen (HBsAg) at a protective level (≥10 mIU/mL) [2]. In this regard, clinicians have followed several strategies, not always successfully, like doubling the dose of the vaccine or using the intradermal route.

Mucosal vaccines constitute an attractive alternative to available parenteral vaccines, especially in developing countries where they would be best suited for mass immunization, due to the lack of a sufficiently developed infrastructure. Among the mucosal routes, the nasal administration of vaccines holds great promise. The nasal mucosa offers a fairly large surface area allowing effective absorption, with relatively low enzymatic activity. In addition, the nasal epithelium layer contains specialized antigen sampling microfold-cells (M-cells) overlaying the nasal associated lymphoid tissue (NALT). NALT serves as a portal for antigen uptake and subsequent systemic and mucosal immune induction [3-5], even at distant mucosal tissue such as salivary glands, upper and lower respiratory tracts and male and female genital tracts [6, 7]. Since mucosal surfaces are among the entry sites for hepatitis B virus, mucosal immunization would provide the first line of defense against infection, stimulating the secretion of IgA that prevents the attachment of the infectious pathogens to the mucosa [8-10].

DNA vaccines are recognized as an encouraging technology due to their ease of production, safety profile, stability, non-requirement for cold chain and potential to induce humoral and cell mediated immunity [11, 12]. To induce an effective immune response by DNA vaccination, the plasmid must enter the cell and be delivered to the nucleus for transcription and sub subsequent protein translation to occur [11, 13]. As "naked" plasmid DNA (pDNA) is ineffective in overcoming extracellular barriers and vulnerable to degradation (e.g., by serum nucleases), thus being rapidly cleared from systemic circulation

[14], the use of appropriate delivery systems is needed to overcome limitations in cellular uptake, protection and bioavailability. Although attenuated pathogen- and live vector-based vaccines are highly effective, there are some safety concerns related to their application. Non-viral delivery systems have been proposed as a safer alternative to viral vectors because of their potential to be administered repeatedly with minimal side effects, stability, low cost and high susceptibility to physical/chemical modifications. Among non-viral systems, chitosan-based carriers have become attractive for the delivery of gene materials. Chitosan is a cationic polymer that can be obtained by deacetylation of chitin [15]. It has been shown to be nontoxic, biodegradable, and biocompatible [16]. Therefore, its use in medical applications such as drug and vaccine delivery has been extensively examined [17-19]. One major advantage of this polymer is its ability to easily form positively charged particles under mild conditions, avoiding the use of harmful organic solvent, which facilitates the encapsulation or adsorption of therapeutic proteins and antigens, or the formation of polyplexes with negatively charged nucleotides by electrostatic interaction. Chitosan has also been explored as an adjuvant for mucosal vaccination, especially for intranasal immunization, due to its mucoadhesive properties [20], and its ability to stimulate cells of the immune system [21, 22]. The main drawback of chitosan-DNA particles is their low transfection efficiency compared to viral vectors. This low transfection observed by non-viral gene delivery systems has been attributed to the weak attachment of DNA-containing particles to the cell surface, impaired cellular uptake of the particles, inability to escape the lysosomal degradation and poor release of DNA from the particles [23-25]. Current knowledge suggests that a balanced and moderate interaction between the carrier and pDNA is one of the key factors to successful transfection and that the incorporation of a negatively charged component could be beneficial for transfection efficiency [26-28]. Kimberly et al. demonstrated that the incorporation of alginate reduced the strength of interaction between chitosan and DNA, contributing to improved transfection. Likewise, poly(g-glutamic acid) was found to have a similar effect [27, 28].

In this study we developed human serum albumin (HSA)-loaded chitosan nanoparticle/DNA (HSA CH NP/DNA) complexes. We hypothesized that the adsorption of negatively charged HSA onto the surface of the chitosan particles would facilitate the DNA release by weakening the interaction between positively charged nanoparticles and negatively charged pDNA. Moreover, we have previously shown that association of HSA to cationic liposomes enhances transgene expression in different cell types [29]. The mechanism was not entirely clarified but is hypothesized that HSA is able to undergo a low pH-induced conformational change under acidic conditions, thereby acquiring fusogenic properties which

facilitates endosomal membrane destabilization and DNA release from the endosomes. To our knowledge, this is the first study involving the preparation of these systems and evaluation of their potential to mediate the delivery of pDNA encoding the surface protein of hepatitis B virus, as well as their ability to stimulate systemic and mucosal immune response after intranasal administration.

5.2 Materials and Methods

5.2.1 Reagents

Plasmid DNA (pCMVluc) encoding luciferase and plasmid DNA (encoding HBsAg) from Aldevron (Fargo, USA) were amplified in *E. coli* bacteria and purified using QIAGEN Plasmid Giga Kit (QIAGEN, Germany). The purified pDNA was dissolved in MilliQ water and concentration/purity was determined by UV spectrophotometry by measuring the absorbance at 260/280 nm. Recombinant hepatitis B surface antigen (HBsAg) was acquired from Aldevron (Fargo, USA).

5.2.2 Methods

5.2.2.1 Nanoparticle/DNA complexes: preparation and characterization

Chitosan (CH) (ChitoClear, 95 % degree of deacetylation; Primex Bio-Chemicals AS) was purified as previously described with some modifications [30]. Chitosan nanoparticles (CH NP) were prepared by a coacervation/precipitation technique using sulfate ions as a cross-linking agent. Briefly, nanoparticles were prepared by adding equal volumes of a chitosan solution (0.1 % in 25 mM sodium acetate buffer (AcB), pH 5.0) and an aqueous aluminium sulfate solution (0.5 %), under high speed vortexing for 20 s, followed by incubation at room temperature for 1 h. In order to remove unreacted compounds, the resulting nanoparticle suspension was centrifuged for 30 min at 4500 g. The supernatant was discarded and the pellet resuspended in either 100 mM phosphate buffer (PB), pH 5.7, or 25 mM AcB, pH 5.5. In order to obtain HSA-loaded CH NP, equal volumes of HSA (Sigma) (500 $\mu g \cdot mL^{-1}$) and chitosan nanoparticle suspension (500 $\mu g \cdot mL^{-1}$) were mixed and incubated for 30 min in a rotating mixer. Particles were then centrifuged for 30 min at 4500 g. Chitosan nanoparticle/DNA (CH NP/DNA) complexes were prepared by incubation of CH NP with pDNA aqueous solution (100 $\mu g \cdot mL^{-1}$) for 30 min at room temperature, in the presence or absence of HSA, at different NP:DNA ratios.

Size and zeta potential of CH NP and their complexes with DNA were measured by dynamic light scattering (DLS) and electrophoretic light scattering (ELS), respectively, in a Delsa™ Nano C (Beckman Coulter, California, United States). The analysis was performed at 25 °C, in 25 mM AcB, pH 5.0, 100 mM PB, pH 5.7 or in supplemented F12 Ham nutrient mixture (cF12 Ham - Sigma).

The loading efficacy (LE) of HSA onto CH NP was assessed by determining the amount of the unbound protein. After incubation of HSA with CH NP, as described above, particle suspension was centrifuged at 13000 g for 15 min and the supernatant was collected and analysed for protein quantification by using the Bicinchoninic acid (BCA) protein assay (Pierce Chemical Company, USA), according to the supplier protocol. Loading efficacy was determined using the following equation (1):

$$\text{LE}\ (\%) = \frac{(\text{total amount of protein} - \text{unbound protein})}{\text{total amount of protein}} \times 100 \quad (1)$$

5.2.2.2 Gel retardation assay

The stability of CH NP/DNA complexes was evaluated by agarose gel electrophoresis. Complexes prepared at different NP:DNA ratios were pre-incubated in AcB or PB at room temperature for 1 h, or in supplemented F12 Ham medium for 4 h, at 37 °C. Aliquots corresponding to 200 ng of DNA per lane were separated on a 1 % agarose gel containing 0.5 $\mu g \cdot mL^{-1}$ of ethidium bromide at a constant voltage of 100 V for 45 min. DNA bands were visualized using a UV-transilluminator.

5.2.2.3 DNase I assay

Resistance of the carried DNA to DNase I degradation was evaluated by electrophoresis as previously reported [29]. Briefly, DNase I (Sigma) was maintained in a 50 mM Tris-HCl buffer solution (pH 7.5, 50 $\mu g \cdot mL^{-1}$ BSA (Sigma), 10 mM $MnCl_2$). CH NP/DNA complexes were submitted to DNase I digestion (1U DNase I/μg of DNA), at 37 °C for 15 min, followed by inactivation of the enzyme upon incubation with 0.5 M EDTA (1 μL/unit of DNase I). Analogous experiments were performed by incubating samples under the same experimental conditions, except that DNase I was inactivated prior to the incubation with CH NP/DNA complexes. Samples were separated in a 1 % agarose gel containing 0.5 $\mu g \cdot mL^{-1}$ of ethidium bromide at a constant voltage of 100 V, for 45 min. DNA bands were visualized using a UV-transilluminator.

5.2.2.4 Cell Culture

A549, human alveolar basal epithelial cells (ATCC, CCL-185) were maintained under 5 % CO_2, at 37 °C, in F12 Ham nutrient mixture supplemented with 10 % FBS (Life Technologies Corporation), penicillin (100 units·mL^{-1}) and streptomycin (100 μg·mL^{-1}).

5.2.2.5 Transfection studies

The protocol for was adapted from methods previously described by our group [29]. A549 cells were seeded in 48-well plates at a density of 5 x 10^4 cells/well in complete medium. After 32 h of incubation, the medium was aspirated and replenished with serum-free transfection medium, and cells were incubated with CH NP/DNA complexes corresponding to 1 μg of pDNA (encoding luciferase) per well for 4 h. Free pDNA was used as a control. Cells were washed to remove the complexes and complete medium was added to the cells, followed by incubation for an additional 48 h. To determine luciferase activity, cells were washed with PBS and 100 μL of lysis buffer (1 mM DTT, 1 mM EDTA, 25 mM Tris-phosphate, pH 7.8, 8 mM $MgCl_2$, 15 % glycerol, 1 % (v/v) Triton X-100) were added to each well. The level of gene expression in the lysates was evaluated by measuring light production (relative light units - RLU) by luciferase in a luminometer (LMax II 384, Molecular Devices), according to standard protocols and normalized against total protein content, measured by BCA protein assay kit.

5.2.2.6 Cell viability studies

Cells were seeded in 48-well plates at a density of 5 x 10^4 cells/well in complete medium. After 32 h, cell culture medium was discarded and replaced by FBS-free medium and the different CH NP/DNA complex formulations were added to the cells. After 4 h of incubation, medium was replaced with fresh F12 Ham nutrient mixture supplemented with 10 % FBS. The cells were further incubated for 48 h and their viability was evaluated by measuring the reduction of soluble 3-[4,5-dimethylthiazol-2-yl]-2,5-diphenyl tetrazolium bromide (MTT - Sigma) (yellow) to insoluble formazan crystals (purple). Fifty μL of MTT solution (5 mg·mL^{-1} in PBS, pH 7.4) were added to each well, followed by 1.5 h of additional incubation at 37 °C. To ensure solubilization of the formazan crystals, 200 μL of DMSO were added to each well and the optical density (OD) was measured at 570 nm using a microplate reader (Multiskan EX; Thermo Scientific, MA, USA). The viability of non-treated control cells was arbitrarily defined as 100 % and cell viability (%) was calculated by equation (2):

$$\text{Cell viability (\%)} = \left(\frac{\text{OD treated cells}}{\text{OD control cells}}\right) \times 100 \qquad (2)$$

5.2.2.7 Cellular uptake studies

Chitosan was labelled with fluorescein isothiocyanate (FITC - Santa Cruz Biotechnology) using a procedure based on the reaction between the isothiocyanate group of FITC (Ex/Em: 490/525) and the primary amino group of chitosan. Briefly, 35 mL of dehydrated methanol containing 25 mg of FITC were mixed with 25 mL of a 1 % w/v chitosan in 0.1 M of acetic acid solution. After 3 h of reaction in the dark at room temperature, the FITC-labelled chitosan was precipitated with 0.2 M NaOH up to pH 10 followed by centrifugation for 30 min at 4500 g. The resulting pellet was washed twice with a mixture of methanol:water (70:30, v/v). FITC-labelled chitosan was resuspended in 15 mL of 0.1 M acetic acid solution and stirred overnight. The polymer solution was dialyzed 3 days under darkness against 2.5 L of distilled water before freeze-drying (FreezeZone 6, Labconco, Kansas City, USA).

For cellular uptake studies, cells were seeded in 48-well plates at a density of 5 x 10^4 cells/well in complete medium. After 32 h, cell culture medium was discarded and replaced with FBS-free medium and different FITC-CH NP/DNA complexes formulations were added followed by 4 h of incubation. Cells were washed three times with PBS at 37 °C and then lysed with 1 mL of 0.5 % Triton X-100 in 0.2 N NaOH. Internalized chitosan was quantified by analyzing the cell lysate in a fluorescence plate reader (Synergy HT, Bio-Tek, Winooski, USA). For the calibration curve, FITC-CH NP/DNA suspensions were diluted to final concentrations ranging from 100 $\mu g \cdot mL^{-1}$ to 2 $\mu g \cdot mL^{-1}$. Uptake was expressed as the ratio of FITC-CH NP/DNA (μg) per cellular protein mass (mg). The protein content of the cell lysate was measured using BCA protein assay kit.

For confocal microscopy, FITC-labelled CH NPs were complexed with Cy5-pDNA. Plasmid DNA was fluorescently labelled with Cy5 (Ex/Em: 649/670 nm) according to the manufacturer's instructions (Label IT®Tracker™ Intracellular Nucleic Acid Localization Kit, Mirus Bio LLC). A549 cells were seeded on glass coverslips in 12-well plates at a density of 1.5 x 10^5 cells/well and cultured at 37 °C in an atmosphere containing 5 % CO_2. After 24 h, the growth medium was replaced with serum-free medium and cells were incubated with FITC-labelled CH NP/Cy5-pDNA complexes, for specified time periods ranging from 4 h to 18 h. Following cell uptake, the medium containing the complexes was removed and cells were washed three times with PB, pH 7.4 and fixed with 4 % paraformaldehyde (PFA) in PBS for 15 min at 37 °C. Plasma membrane and nucleus of the pre-fixed cells were then labelled using Alexa Fluor® 594 wheat germ agglutinin (Ex/Em: 591/618 nm) and Hoechst 33342 dye (Ex/Em: 350/461 nm), respectively, according to the manufacturer's instructions (Image-iT™ LIVE Plasma Membrane and Nuclear Labeling Kit, Life Technologies). Labeling of the cell

membrane with the fluorescent conjugate allowed a better visualization of the nanoparticles inside the cells. After labeling, cells were washed twice with PBS and the coverslips mounted on microscope slides with DAKO mounting medium, and examined under an inverted confocal laser scanning microscope (Zeiss LSM 510 META, Carl Zeiss, Oberkochen, Germany) equipped with an imaging software (LSM 510 software, Carl Zeiss).

5.3 Immunogenicity study

5.3.1 Nasal vaccination

Female C57BL/6 mice of 6-8 weeks of age were purchased from Charles River (France) and housed in the Center for Neuroscience and Cell Biology (CNC) animal facility, Coimbra, and provided food and water ad libitum. Female mice were used in our experiments, since mucosal samples are easily accessed, mainly those associated with genital tract. All experiments were carried out in accordance with institutional ethical guidelines and with national (Dec. nº 1005/92 23rd October) and international (normative 2010/63 from EU) legislation. Mice (5 per group), were intranasally immunized on days 0, 7 and 21 with 15 μL of vaccine formulation (7.5 μL per nostril), under slight isoflurane anesthesia. All mice, except naïve group, received 50 μg of DNA encoding HBsAg alone or complexed with HSA-loaded CH NP (CH NP:DNA ratio of 7.5:1) or the previous formulation plus 10 μg of HBsAg either in PB, pH 5.7 or AcB, pH 5.7. Blood was collected by submandibular lancet method on days 21 and 42 and allowed to coagulate for 30 min prior centrifugation at 1000 g for 10 min. Spleens, nasal washes, and vaginal washes were collected on day 42. Vaginal washes were collected by instilling 100 μL of PBS into the vaginal cavity and flush the lavage fluid in - out a few times before collection. Samples were centrifuged at 11500 g for 10 min and supernatants were stored. Nasal lavage samples were collected from euthanized mice. The lower jaw of the mice was cut way and the nasal lavage collected by instilling 200 μL of sterile PBS posteriorly into the nasal cavity. Fluid exiting the nostrils was collected and spun at 11500 g at 4 °C for 20 min. Collected and processed samples were stored at −80 °C and −20 ºC (serum) until further analysis.

5.3.1.1 Determination of serum IgG, IgG1, IgG2c and secretory IgA

Quantification of immunoglobulins was performed using a protocol described by Slutter et al. [31]. High-binding 96-well plates (Nunc immunoplate Maxisorb) were coated with 100 μL of a 1 $\mu g \cdot mL^{-1}$ HBsAg in 50 mM sodium carbonate/bicarbonate solution, pH 9.6, overnight at

4 °C. Plates were washed 5 times with PBS-Tween (PBS-T) and blocked with 2 % (w/v) BSA in PBS-T for 1 h at 37 °C. After washing, serial dilutions of serum starting at 1:128 were applied, whereas nasal and vaginal washes were added undiluted. After incubation for 2 h at 37 °C and extensive washing, specific antibodies were detected using horseradish peroxidase (HRP) conjugated goat anti-mouse IgG (Bethyl Laboratories), IgG1 (Rockland), IgG2c (GenTex) or IgA (Bethyl Laboratories), for 30 min at 37 °C followed by an incubation with o-phenylenediamine (OPD - Sigma) solution (5 mg OPD to 10 mL citrate buffer and 10 µl H_2O_2) for 10 min at room temperature. The reaction was stopped by adding 50 µL of 1 M H_2SO_4 and absorbance was determined at 492 nm in a microplate reader. The end-point titer presented in the results represents the antilog of the last log2 dilution for which the OD values were at least two-fold higher than the value of the naive sample equally diluted. The log 2 endpoint titers were used for statistical analysis.

5.3.1.2 Statistical Analyses

Results were expressed as mean± standard deviation (SD). Data were analysed for significance by ANOVA, followed by Bonferroni post-test with $P \leq 0.05$ considered as a statistically significant difference (GraphPad Prism v 5.03, GraphPad Software Inc., La Jolla, CA, USA).

5.4 Results and discussion

5.4.1 Chitosan nanoparticles complexed DNA to form stable complexes

In the present study chitosan nanoparticles were prepared by coacervation/precipitation technique, a simple and mild method that does not require the use of organic solvents. Particle size, surface charge and morphology are known to have an impact on nanoparticle biological activity. In this regard, physicochemical properties of the formulations were studied in two different buffers in order to optimize the conditions for complex formation, and also in cell culture media to study their behavior during in vitro tests. Particle size and zeta potential were shown to depend on the solvent used in their preparation (Fig. 5.1 A). Chitosan particles prepared in AcB exhibited an average hydrodynamic diameter of 290 nm and a zeta potential of +30 mV. Particle size increased to 600 nm by increasing salt concentration (25 mM in AcB to 100 mM in PB) and zeta potential was close to neutral (+4.3 mV). Similar results were obtained by Nimesh et al. [32], where an increased salt concentration was proposed to induce

particle aggregation by reduced electrostatic repulsion in agreement with the DLVO theory of colloid stability.

A

	AcB, pH 5.5			PB, pH 5.7			cF12 Ham		
	Size (nm)	PI[1]	ZP[2] (mV)	Size (nm)	PI[1]	ZP[2] (mV)	Size (nm)	PI[1]	ZP[2] (mV)
CH NP	280.9 ± 32.7	0.255 ± 0.012	+30.1 ± 1.9	605.6 ± 18.6	0.276 ± 0.321	+4.3 ± 1.7	927.7 ± 192.7	0.323 ± 0.070	-7.6 ± 0.27
HSA-CH NP	301.5 ± 93.0	0.235 ± 0.020	+29.9 ± 0.2	368.8 ± 62.1	0.254 ± 0.087	+5.9 ± 0.8	367.4 ± 98.6	0.348 ± 0.043	-13.2 ± 1.42
CP[3] 10:1	341.0 ± 57.7	0.202 ± 0.047	+31.2 ± 0.2	1945.8 ± 282.3	0.604 ± 0.039	+1.2 ± 0.5	184.8 ± 81.0	0.191 ± 0.095	-18.8 ± 3.2
CP[3] 7.5:1	258.3 ± 21.5	0.216 ± 0.033	+29.7 ± 0.6	1011.0 ± 177.2	0.353 ± 0.021	+1.6 ± 1.5	186.0 ± 53.7	0.299 ± 0.067	-18.3 ± 1.2
CP[3] 5:1	209.0 ± 12.7	0.239 ± 0.014	+29.7 ± 1.7	692 ± 46.4	0.356 ± 0.019	+1.2 ± 1.8	212.1 ± 43.4	0.265 ± 0.023	-16.0 ± 3.0

[1]Polydispersity index, [2]Zeta Potential, [3]HSA-loaded CH NP/DNA complexes (ratio)

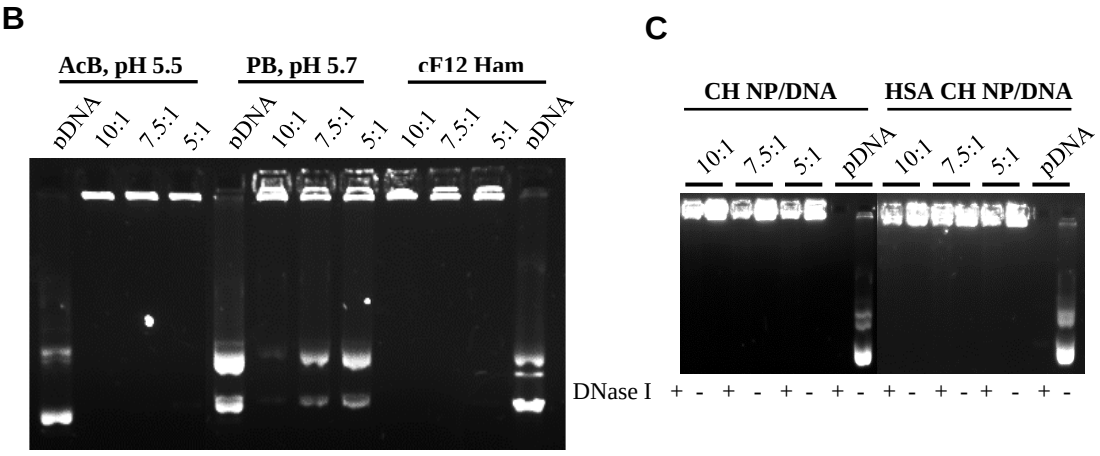

Figure 5.1 - Chitosan nanoparticles complexed DNA to form stable complexes. Size and zeta potential of CH NP, HSA-loaded CH NP and their complexes with DNA were measured by dynamic light scattering and electrophoretic light scattering, respectively (A).The analysis was performed as described in 'Materials and methods'. Stability of the complexes was analysed by gel electrophoresis assay (B). HSA-loaded CH NP/DNA complexes were pre-incubated either in the preparation buffer at room temperature or in supplemented F12 Ham medium (cF12 Ham) for 4 h, at 37 °C, using different NP:DNA ratios, as described in 'Materials and methods'. Electrophoresis was performed in 1 % agarose gel containing 0.5 $\mu g \cdot mL^{-1}$ of ethidium bromide. To evaluate DNA resistance to DNase I (C), complexes resuspended in AcB were incubated with active DNase I or with inactive DNase I, the incubation being performed at 37 ºC, for 15 min, using 1U DNase I per µg of DNA. Electrophoresis was performed in 1 % agarose gel containing 0.5 $\mu g \cdot mL^{-1}$ of ethidium bromide. Results (mean ± SD, obtained from triplicates) are representative of at least three independent experiments.

This explanation is furthermore reinforced by the significant reduction in NP zeta potential observed on switching from AcB to PB. The mean hydrodynamic diameter was further increased to 930 nm in culture medium supplemented with FBS, probably due to the

interaction between negatively charged serum proteins and the positively charged particles. Even though the solvent had a major impact on CH NP size, the association of HSA to particles led to similar sizes in the different media (around 360 nm). This overall increase in stability may be explained by abnormal colloidal stability of protein coated particles at high ionic strength [33].

Plasmid DNA encoding luciferase (pCMVluc), used as a reporter gene for these studies, spontaneously formed polyplexes with CH NPs due to electrostatic interactions between opposite charged molecules. Results summarized in figure 5.1 A show that complexes resuspended in AcB presented small hydrodynamic diameter that slightly decreased with decreasing CH NP:DNA ratios. The resuspension of complexes in PB greatly increased their size, probably due to the same effect described for plain nanoparticles. Interestingly, complexes resuspended in cF12 Ham exhibited the smallest average hydrodynamic diameter.

It was reported that the strength of electrostatic interactions between chitosan and DNA precludes their dissociation inside the cell, thus impeding transcription of DNA [34]. Fine balance between the stability of the complexes and the intracellular release of DNA from these polyplexes is required to ensure DNA protection and to achieve high levels of gene expression. Stability of the complexes was assessed in their respective preparation buffer at room temperature and in supplemented F12 Ham medium during 4 h of incubation at 37 °C. DNA released from the complexes was visualized on agarose gel electrophoresis. As shown in figure 5.1 B, gel retardation assay revealed different complexation strengths for the different CH NP:DNA ratios in the various media. CH NPs were capable of fully complex all DNA at all ratios, either in AcB or cF12 Ham. In PB, CH NPs were able to complex a substantial amount of pDNA, although bands corresponding to unbound pDNA were still visible, particularly for lower NP:DNA ratios.

To study the degree of DNA protection against nuclease degradation conferred by CH NPs or HSA-loaded CH NPs, all formulations were subjected to DNase I digestion (1U DNase I/μg DNA). Undigested pDNA was recovered and visualized by agarose gel electrophoresis. The integrity of pDNA was assessed immediately before transfection studies and was compared to naked pDNA (as a control). As shown in figure 5.1 C, free DNA was completely degraded under the experimental conditions. In contrast to naked pDNA, pDNA complexed with CH NP remained intact after DNase I treatment. The degree of protection was independent of the presence of HSA and the NP:DNA ratio. Our results suggest that CH NP/DNA complexes are stable in the presence of cell endonucleases, being able to deliver pDNA in an active form with structural integrity.

5.4.2 Association of albumin to complexes improves transfection activity

Chitosan was first proposed as a gene delivery vector by Mumper et al. [35]. Since then, transfection efficacy of DNA associated with chitosan-based delivery systems has been extensively studied and shown to be affected by many factors, including intrinsic properties of the polymer, such as molecular weight, degree of deacetylation and chemical composition, or conditions of the assay, such as the presence of serum and pH of the transfection medium [36, 37], even though the reported results were not consistent.

In the present study, DNA was used as a crosslinking agent to form chitosan nanoparticles, and thus the genetic material was entrapped into the polymer matrix and the release rate was dependent on chitosan biodegradation. Although chitosan was found to successfully transfect cells *in vitro*, the transfection efficiency showed to be lower than that observed with other cationic polymers or liposome formulations [34, 38, 39]. A possible explanation for this observation is that the strength of the interaction between the positively charged amino groups in chitosan and the negatively charged phosphate groups in DNA originates very stable particles, thereby precluding dissociation inside the cell and eventually impeding translation of the DNA, hence causing low transfection.

Considering the inadequate efficiency of chitosan nanoparticles to mediate transfection and in an effort to overcome this limitation, we assessed whether the association of HSA to chitosan nanoparticles would improve gene transfer by modulating the interactions of the DNA with the nanoparticles and with the cell. Indeed, previous studies performed in our laboratory have shown that association of albumin to cationic liposomes enhances transgene expression in different cell types [29]. We found that DNA was not entrapped into the CH NPs, but was adsorbed after particle preparation, therefore DNA release would not be entirely dependent on particle biodegradation. To evaluate the influence of the complex suspension buffer and NP:DNA ratio on transfection efficiency, a preliminary set of experiments was performed in A549 cells. Figure 5.2 A illustrates the influence of the buffer and NP:DNA ratio on the transfection activity of the complexes. As expected, naked pDNA did not induce any biological activity. However, in contrast to our expectations, stable complexes prepared in AcB also did not show any biological activity for any of the NP:DNA ratios studied. On the other hand, the biological activity of complexes prepared in PB showed to be dependent on the NP:DNA ratio, complexes prepared at a ratio of 7.5:1 being the most active. It has been reported that transfection efficiency of CH/DNA polyplexes is pH-dependent, generating better responses under acidic conditions. Indeed, chitosan is more protonated at acidic pH

and, therefore, binding to negatively charged cell surfaces and cell uptake are enhanced [32, 40]. We suggest that the reason for the different observed behavior might be due to differences in the ionic strength of the buffer systems, which affects particle stability, as high ionic strength weakens the electrostatic repulsion and contributes to increased particle aggregation [32].

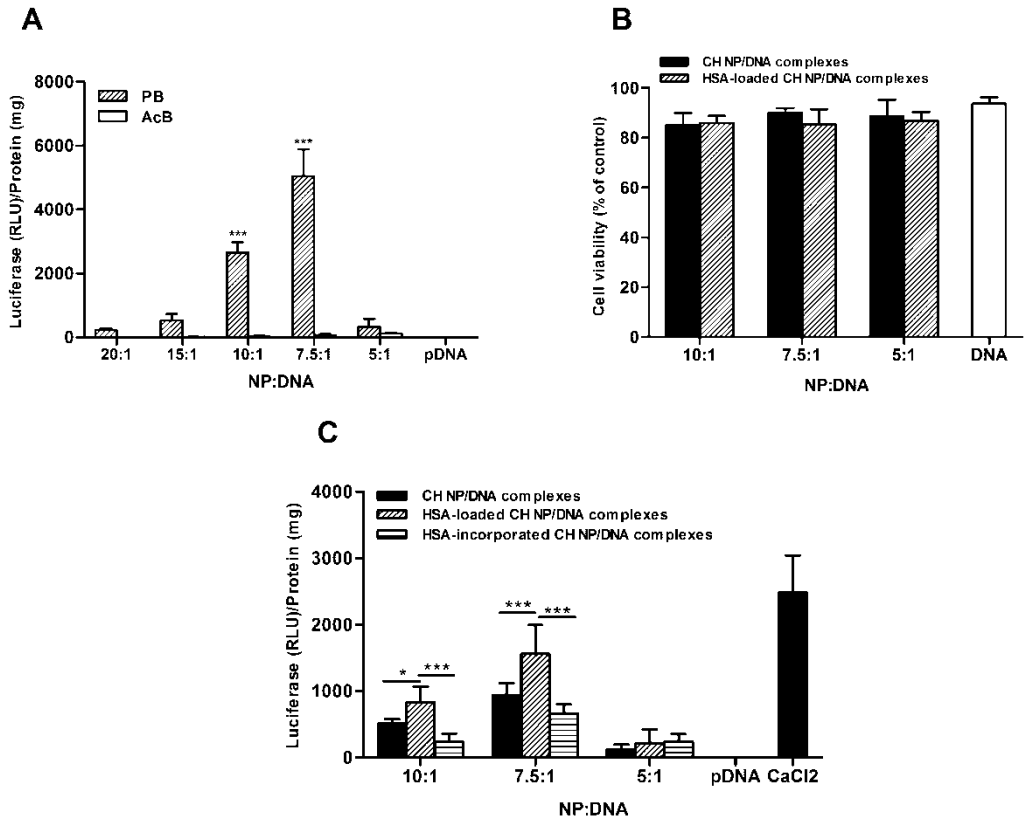

Figure 5.2 - Association of HSA to chitosan nanoparticle/DNA complexes surface efficiently improved transfection activity without affecting cell viability: Effect of buffer, CH NP:DNA ratio (A) and complex composition (C) on luciferase gene expression and viability (B) in A549 cells. The CH NPs, pre-incubated or not with HSA, and CH NPs with incorporated HSA were complexed with 1 μg of pDNA in PB (A, B and C) or AcB (A), pH 5.7, at the indicated CH NP:DNA ratios. Cells were rinsed with serum-free medium before HSA-loaded CH NP/DNA complexes were added. After incubation for 4 h, the medium was replaced with F12 Ham containing 10 % FBS and the cells were further incubated for 48 h. The level of gene expression was evaluated as described in 'Materials and methods'. The data are expressed as the percentage of the RLU of luciferase per mg of total cell protein of the control. Cell viability was measured by MTT assay as described in 'Materials and methods'. The data are expressed as the percentage of the untreated control cells (mean ± SEM obtained from triplicates). All data are representative of at least three independent experiments *$p \leq 0.05$, **$p \leq 0.01$ and ***$p \leq 0.001$ indicate values that differ significantly from other conditions.

Studies suggest that DNA unpacking is one of the major intracellular barriers to transfection. It has been recognized that a balance between DNA protection and its ability to dissociate from the nanoparticles must be achieved to obtain efficient transfection [41-43]. As observed, increasing the NP:DNA ratio above 10:1 led to severe impairment of transfection activity, suggesting that, at such high ratios, the interactions between DNA and the nanoparticles were too strong to allow DNA dissociation from the particles. Lower transfection levels at higher NP:DNA ratios may also be related to the possible competition of excess of cationic chitosan nanoparticles, present in the formulation, which also bind to the cell surface, preventing complexes from being efficiently internalized [41]. Most cationic polymers have cytotoxic effects at high concentrations because of their strong electrostatic interactions with the cell membrane proteins, which can lead to destabilization and eventually rupture of the cell membrane [44]. As demonstrated in figure 5.2 B, cell viability was not significantly affected upon exposure to CH NP/DNA complexes, both in the absence and presence of HSA and, therefore, the observed low transfection activity cannot be attributed to reduced cell metabolic activity.

To study the effect of the association of HSA with CH NP/DNA complexes on transfection efficiency, A549 cell were incubated with 3 different formulations: HSA-loaded and plain CH NP/DNA complexes and HSA-incorporated CH NP/DNA complexes. In the latter formulation, HSA was incorporated in the CH NPs rather than being adsorbed at their surface in order to test whether HSA localization in the formulation would influence transgene expression. Transfection of A549 cells with HSA-loaded CH NP/DNA complexes resulted in a significantly higher transgene expression compared to that observed with other formulations at 10:1 and 7.5:1 NP:DNA ratios (Fig. 5.2 C). Work from other groups suggested that the incorporation of an anionic compound in the formulation had a positive effect on their transfection efficiency [26, 27]. In the present study, the results obtained when HSA was incorporated in the nanoparticles, instead of being adsorbed to their surface prior to incubation with DNA, were similar to those obtained for the complexes prepared with plain nanoparticles. This suggests that HSA was able to potentiate transfection efficiency but it needed to be on the surface of the nanoparticles in order to have a positive impact on their biological activity A possible explanation is that when incorporated into the nanoparticles, HSA is no longer able to interact with the cell in the same way as when adsorbed to the surface of the nanoparticles. It is possible that when HSA is incorporated into the particle, its binding site on the cell surface is impaired So far, the mechanism by which HSA is able to enhance transgene expression is not fully understood, although HSA is believed to have

fusogenic properties under acidic conditions that could increase endosomal escape [29, 45], another important barrier to effective transfection. The fusogenic properties of HSA may contribute to explain the differences observed in the transfection efficiencies of different formulations. Additionally, HSA adsorbed onto particle surface may also decrease the electrostatic interactions between DNA and CH NPs, thus facilitating cytoplasm release of DNA.

We also examined the impact of the amount and type of HSA on transgene expression of protein-loaded CH NP/DNA complexes. As opposed to the results from previous studies performed in our laboratory with lipoplexes, transfection efficiency of CH/DNA polyplexes was independent of the amount of HSA adsorbed at the surface of the nanoparticles and of the type of albumin tested (human or bovine, data not shown).

Overall, several factors, such as NP:DNA ratio, composition of the formulation and ionic strength of the medium were found to influence transfection activity of chitosan nanoparticles, which should be taken into account towards their successful application in gene delivery.

5.4.3 Albumin-loaded chitosan nanoparticle/DNA complexes were efficiently internalized by cells

Impaired cellular uptake of DNA-loaded particles is one of the several barriers to non-viral gene delivery. Chitosan interacts with cell membranes through nonspecific attractive electrostatic forces [46], since no specific receptor to chitosan has been identified. Positive surface charge of CH NPs promotes binding with the negatively charged membrane facilitating their cellular uptake. To further explore the mechanism by which HSA enhances transfection efficiency of the CH NP/DNA complexes, formulations with or without albumin were incubated with A549 cells and the complex cell uptake was assessed. Our results show that the uptake efficiency was similar for both plain and HSA-loaded CH NP/DNA complexes (Fig. 5.3 A and B), being enhanced as the amount of the particles placed in contact with the cells was increased (Figure 5.3 B), which indicates that the presence of HSA does not affect particle uptake efficacy. Therefore, the differences observed in transfection mediated by CH NP/DNA complexes with or without albumin could not be explained by different extents in their cell internalization

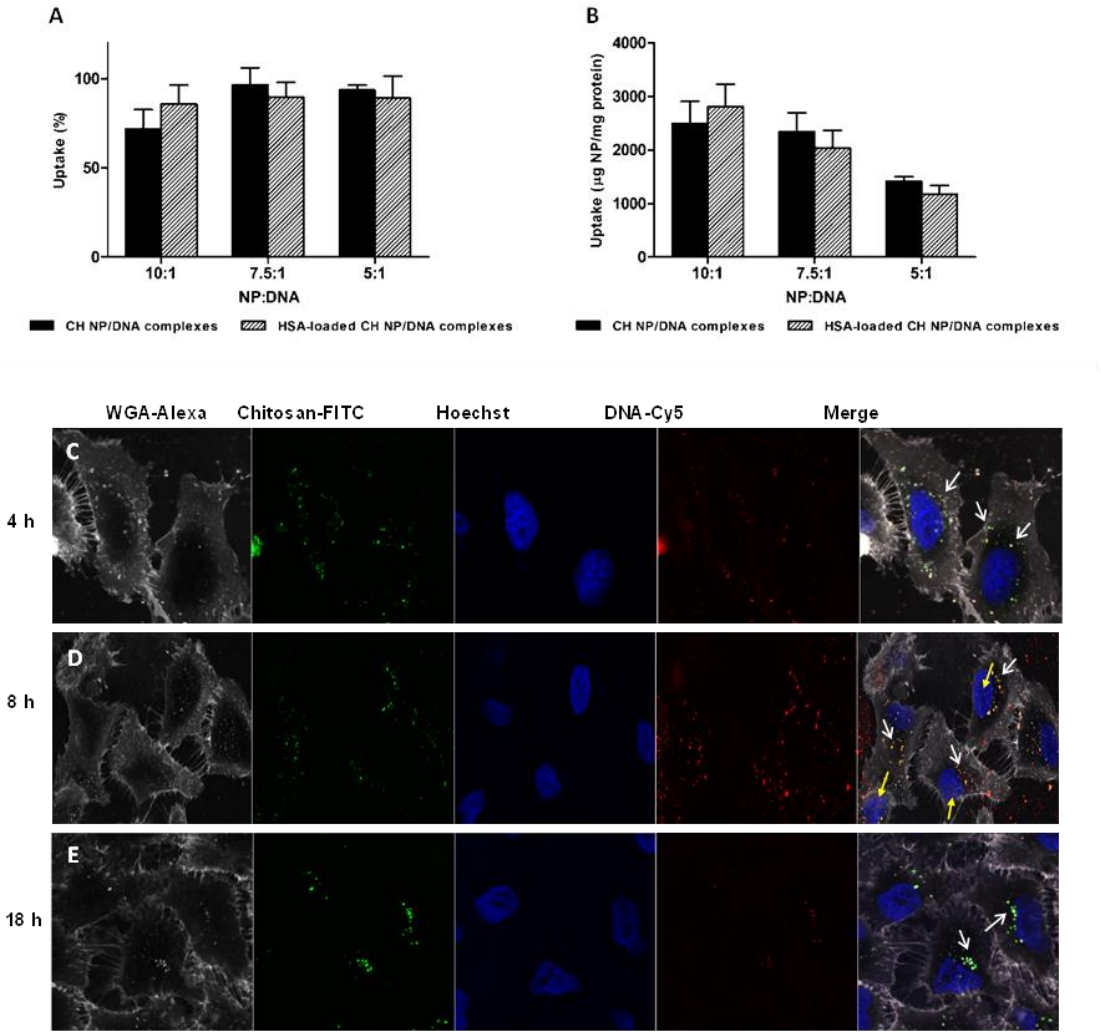

Figure 5.3 - Chitosan nanoparticles/DNA complexes were efficiently internalized by A549 cells. Cellular uptake (A, B) and intracellular distribution of FITC-CH NP/Cy5-DNA complexes (C-E). For quantitative cellular uptake studies, complexes containing FITC-labelled chitosan were added to the cells in serum-free medium followed by 4 h of incubation at 37 °C. Complex internalization was quantified by analyzing the cell lysate fluorescence. Uptake percentage correlates the amount (µg) of CH NP/DNA complexes added to the cells to the amount that was internalized. Cellular uptake was expressed as the amount (µg) of CH NP/DNA complexes normalized to cell lysate protein content (mg). Data (mean ± SEM, obtained from triplicates) were obtained from three independent experiments. Representative confocal fluorescence images for different treatment conditions and time points (4 h to 18 h post-incubation). Confocal images show single and overlaid images of the fluorescent probes, membrane staining with wheat germ agglutinin Alexa Fluor 594 conjugate (white); chitosan staining with FITC (green); nuclear staining with Hoechst 33342 (blue); pDNA staining with Cy5 (red); colocalization of CH NPs with DNA (yellow). White arrows indicate CH NPs inside the cell, yellow arrows indicate pDNA inside the nucleus.

Low transfection observed by non-viral gene delivery systems has also been attributed to poor release of the DNA from the particles and inability to escape lysosomal degradation [25].

To elucidate the intracellular fate of the developed nanoparticles, cellular uptake and distribution of complexes containing HSA-loaded FITC labelled CH NP (green)/Cy5-DNA (red) (7.5:1 ratio) were studied using confocal microscopy. As observed, fluorescent HSA-loaded CH NP/DNA complexes (yellow) appeared inside the cytoplasm at 4 h (Fig. 5.3 C), with no fluorescent pDNA in the intracellular space or in the nucleus. This data correlates with results from experiments on CH NP/DNA complex stability, where albumin-loaded NP/DNA complexes were shown to be stable in culture medium (Fig. 5.1 B), therefore being capable to be internalized by cells. After 8 h of incubation, it was still possible to observe NP/DNA complexes within the cell cytoplasm (Fig. 5.3 D), and to a significantly less extent after 18 h (Fig. 5.3 E). Although an efficient gene delivery system needs to guarantee DNA protection from cytoplasmic nuclease digestion, after endosomal-lysosomal escape [47], the nuclear translocation and gene expression is not attained unless DNA is released from the particles intracellularly. In fact, confocal images indicated that 8 h after incubation, a large amount of the DNA was released from the complexes (red), and thus, DNA release was not a limiting step for efficient gene delivery. Furthermore, at the same time-point it was possible to detect naked pDNA in the nucleus (yellow arrows), indicating that the CH NPs have the potential to successfully deliver DNA into the nucleus for transcription to occur in agreement with the results obtained in the transfection studies. Moreover, after 18 h incubation, little co-localization of HSA-loaded CH NPs and pDNA was observed. The few complexes present were located in the perinuclear region which confirms that the release of DNA from the complexes has occurred. Our findings indicated that DNA was not tightly trapped within the CH NPs, but rather adsorbed on their surface, which enhances transfection efficiency as these nanoparticles do not need to be degraded in order to release DNA.

5.4.4 Intranasally immunized mice generated significant quantities of antigen-specific IgG and IgA antibodies

Nasal immunization is a promising vaccination strategy that has been shown to induce mucosal immune responses in addition to systemic responses [5, 6]. However, vaccination with naked DNA is challenging as only a small fraction is taken up by the nasal epithelium resulting in low production of the encoded protein. One of the main reasons for this low bioavailability, besides the limited transport across the epithelium, may be the inadequate retention time in the nasal cavity due to mucociliary clearance. Although DNA is negatively charged due to the presence of phosphate groups, CH NP/DNA complexes exhibit a positive charge (Fig. 5.1 A), when suspended in any of the buffers (AcB and PB) used in the

vaccination experiments. Therefore, free amine groups are, most likely, available to bind to sialic acid residues present, not only on the cell surface, but also on mucus, thereby allowing prolonged retention time of the formulation in nasal cavity. This hypothesis is supported by previous experiments, performed in our laboratory, where we showed that chitosan nanoparticles delayed antigen clearance from the nasal cavity [48].

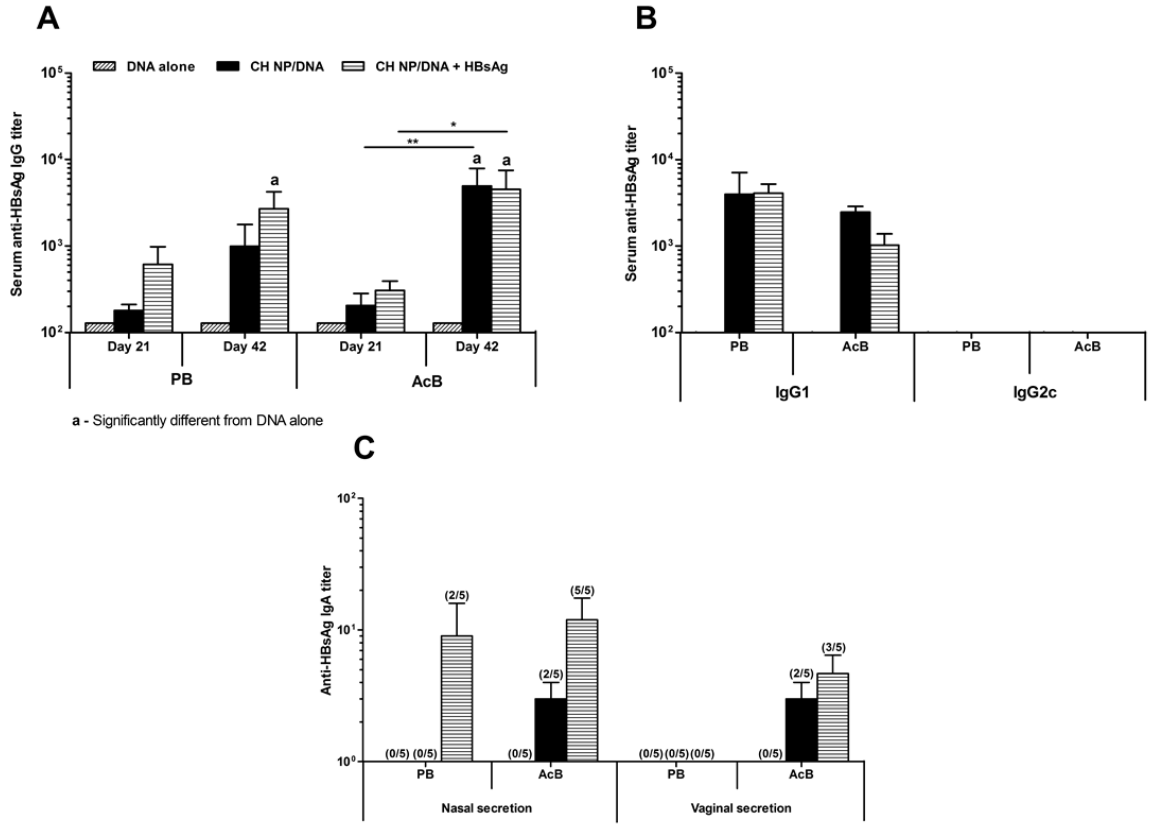

Figure 5.4 - Immune response profile. Serum anti-HBsAg IgG (A), IgG1 and IgG2c (B) and mucosal IgA (C) levels of mice immunized with HSA-loaded NP CH/DNA in the presence or absence of 10 μg of HBsAg, on days 0, 7 and 21. Control corresponds to free DNA. Blood was collected on days 21 and 42; nasal and vaginal secretions were collected on day 42. Antibody levels were determined by ELISA as described in 'Materials and methods'. The end-point titer presented in the results represents the antilog of the last log 2 dilution for which the value of OD was at least two-fold higher than that of the naive sample equally diluted. The log 2 endpoint titers were used for statistical analysis. Data (mean ± SD) corresponds to groups of 5 mice each. The numbers above the columns indicate the number of responders per group. Statistical analyses are shown only between the groups showing 5/5 responders; *$p \leq 0.05$ and **$p \leq 0.01$ indicate values that differ significantly from other conditions; a indicates values that differ significantly from DNA alone.

Naked DNA is very sensitive to nuclease digestion and requires an efficient carrier capable of protecting and transporting DNA across extra- and intracellular barriers. Our *in vitro* results

showed that albumin-loaded CH NP/DNA complexes were able to protect DNA from DNase degradation and to transfect cells. Together, these results have supported the decision to evaluate the immune response generated after nasal vaccination with the most promising formulation, the HSA-loaded NP/DNA complexes (7.5:1 ratio).

Systemic and mucosal immune responses were evaluated in mice intranasally immunized with complexes suspended either in AcB or PB, alone or in combination with HBsAg. The strategy to co-administer HBsAg with the DNA complexes was adopted in order to enhance the amount of HBsAg, immediately available to be processed by the antigen presenting cells (APCs). The pH of both buffers was adjusted to 5.5–5.7, since this value was observed to be the best for complex formation and stability and because the pH of nasal secretions is normally in the range 5.5–6.5 [49]. Naked DNA was used as a control.

On day 21 (after 1st boost), mice immunized with DNA formulations suspended in acetate buffer showed similar anti-HBsAg IgG antibody titers in all 3 groups (Fig. 5.4 A). Three weeks after the second boost (day 42), mice vaccinated with CH NP/DNA complexes (associated or not with the HBsAg) showed a strong and significant enhancement of specific IgG titers, while no significant difference in IgG titers in comparison to day 21 was observed in the group immunized with naked DNA. As expected, DNA complexed with CH NPs was capable of generating antibodies specific to HBsAg at a much higher extent than naked DNA, but the association of HBsAg to the complex formulation did not result in any additional benefit. Interestingly, similar results were obtained for phosphate buffer-based formulations (Fig. 5.4 A), which contrast with those from *in vitro* experiments that showed a weak ability of the formulation to transfect cells.

The subtype profile of anti-HBsAg IgG was investigated. The results displayed in figure 5.4 B showed that IgG1 was the predominant antibody produced in all mice groups that received complexes. Although this Th2-type immune response was in accordance with the results of cellular immune response after spleen cell restimulation with HBsAg, the cells failed to produce significant INF-γ levels (data not shown).

Mucosal immunity plays an important role in protection against pathogens that can enter the host via urogenital route like HBV [7, 8]. It is commonly accepted that mucosal immunity generated after nasal vaccination is not restricted to the upper airways, as IgA antibodies can also be detected in other mucosal secretions due to the common mucosal immune system (CMIS) [6, 7]. Mucosal immune response elicited by various formulations was assessed by measuring secretory IgA (sIgA) levels in mucosal fluids collected on day 42. As shown in figure 5.4 C, it was not possible to detect any anti-HBsAg sIgA following the administration

of the pDNA alone (not complexed with NP). Formulations containing DNA complexes were able to induce detectable sIgA (Fig. 5.4 C), although at different extents. Mucosal antibody profile was significantly better in mice immunized with antigen containing DNA complexes suspended in sodium acetate buffer as sIgA levels were detected in nasal secretions of all 5 mice and in vaginal secretions of 3 out of 5 mice. As previously stated, the appearance of the anti-HBsAg sIgA in vaginal secretions is indicative of distal mucosal immune response [7]. In this regard, the phosphate buffer-based formulation was not able to induce a good mucosal immune response. A possible explanation is that the mucoadhesive property of chitosan and particulate nature of the CHNP/DNA complexes contribute, to improve retention in the nasal cavity and uptake of DNA by APC, respectively, [50]. Differences in mucosal immune response between formulations may also stem from changes in DNA-complex stability in different buffers in a similar way as that observed in the *in vitro* transfection studies. Although our results were obtained in female mice and a direct extrapolation to male mice cannot be made, no significant sex differences are expected.

Overall, formulations containing antigen performed better at inducing higher specific antibody titers on mucosal sites. We suggest this is due to heterologous prime-boost vaccination effect as different immune mechanisms are elicited resulting in a more effective response to a single vaccine.

Our findings are encouraging and suggest that albumin-loaded chitosan nanoparticles can be used to complex DNA to form a good plasmid delivery system for nasal vaccination since it can trigger a high level of antigen-specific immune response.

5.5 Conclusion

Low immunogenicity has been the major limitation on using DNA vaccines and numerous approaches have been investigated to increase the potency of vaccine-induced immune responses. Cationic chitosan nanoparticles have shown technological potential as a non-viral vector for gene delivery, though their use is limited due to the low transfection efficiency observed *in vitro*. In this study, we have combined the bioadhesive and immunostimulating properties of chitosan nanoparticles with HSA capability to enhance transfection and to reduce DNA-chitosan interaction in order to develop and test a new approach to mucosal vaccination. Overall, our results illustrate that a proper design of the chitosan-based formulation is vital in order to generate an effective gene delivery system, as a simple change in the nanoparticle suspension buffer impacts on the *in vivo* performance. This feature showed to be particularly critical to achieve antigen-specific antibodies at the mucosa level which is of

major importance for sexually transmitted virus such as HBV. The prospect of DNA vaccines is exciting and the continual refinement of these technologies is considered to be the future of the vaccine field.

References

1. Who.int, *WHO | Hepatitis B*, Accessed 23 March 2015.
2. Sjogren, M.H., *Prevention of hepatitis B in nonresponders to initial hepatitis B virus vaccination.* Am J Med, 2005. **118 Suppl 10A**: p. 34S-39S.
3. Slutter, B., N. Hagenaars, and W. Jiskoot, *Rational design of nasal vaccines.* J Drug Target, 2008. **16**(1): p. 1-17.
4. Csaba, N., M. Garcia-Fuentes, and M.J. Alonso, *Nanoparticles for nasal vaccination.* Adv Drug Deliv Rev, 2009. **61**(2): p. 140-57.
5. Borges, O., et al., *Mucosal vaccines: recent progress in understanding the natural barriers.* Pharm Res, 2010. **27**(2): p. 211-23.
6. Neutra, M.R. and P.A. Kozlowski, *Mucosal vaccines: the promise and the challenge.* Nat Rev Immunol, 2006. **6**(2): p. 148-58.
7. Kiyono, H. and S. Fukuyama, *NALT- versus Peyer's-patch-mediated mucosal immunity.* Nat Rev Immunol, 2004. **4**(9): p. 699-710.
8. Meeusen, E.N., *Exploiting mucosal surfaces for the development of mucosal vaccines.* Vaccine, 2011. **29**(47): p. 8506-11.
9. Pasetti, M.F., et al., *Immunology of gut mucosal vaccines.* Immunol Rev, 2011. **239**(1): p. 125-48.
10. Pavot, V., et al., *New insights in mucosal vaccine development.* Vaccine, 2012. **30**(2): p. 142-54.
11. Kutzler, M.A. and D.B. Weiner, *DNA vaccines: ready for prime time?* Nat Rev Genet, 2008. **9**(10): p. 776-88.
12. Huygen, K., *Plasmid DNA vaccination.* Microbes Infect, 2005. **7**(5-6): p. 932-8.
13. Donnelly, J.J., B. Wahren, and M.A. Liu, *DNA vaccines: progress and challenges.* J Immunol, 2005. **175**(2): p. 633-9.
14. Seow, Y. and M. Wood, *Biological Gene Delivery Vehicles: Beyond Viral Vectors.* Molecular Therapy, 2009. **17**(5): p. 767-777.
15. Illum, L., *Chitosan and its use as a pharmaceutical excipient.* Pharm Res, 1998. **15**(9): p. 1326-31.
16. Baldrick, P., *The safety of chitosan as a pharmaceutical excipient.* Regul Toxicol Pharmacol, 2010. **56**(3): p. 290-9.
17. Lebre, F., et al., *Progress towards a needle-free hepatitis B vaccine.* Pharm Res, 2011. **28**(5): p. 986-1012.
18. Panos, I., N. Acosta, and A. Heras, *New drug delivery systems based on chitosan.* Curr Drug Discov Technol, 2008. **5**(4): p. 333-41.
19. van der Lubben, I.M., et al., *Chitosan for mucosal vaccination.* Adv Drug Deliv Rev, 2001. **52**(2): p. 139-44.
20. Illum, L., et al., *Chitosan as a novel nasal delivery system for vaccines.* Adv Drug Deliv Rev, 2001. **51**(1-3): p. 81-96.
21. Borges, O., et al., *Induction of lymphocytes activated marker CD69 following exposure to chitosan and alginate biopolymers.* Int J Pharm, 2007. **337**(1-2): p. 254-64.
22. Zaharoff, D.A., et al., *Chitosan solution enhances both humoral and cell-mediated immune responses to subcutaneous vaccination.* Vaccine, 2007. **25**(11): p. 2085-94.

23. Brown, M.D., A.G. Schatzlein, and I.F. Uchegbu, *Gene delivery with synthetic (non viral) carriers.* Int J Pharm, 2001. **229**(1-2): p. 1-21.
24. Vaughan, E.E., J.V. DeGiulio, and D.A. Dean, *Intracellular trafficking of plasmids for gene therapy: mechanisms of cytoplasmic movement and nuclear import.* Curr Gene Ther, 2006. **6**(6): p. 671-81.
25. Adler, A.F. and K.W. Leong, *Emerging links between surface nanotechnology and endocytosis: impact on nonviral gene delivery.* Nano Today, 2010. **5**(6): p. 553-569.
26. Douglas, K.L., C.A. Piccirillo, and M. Tabrizian, *Effects of alginate inclusion on the vector properties of chitosan-based nanoparticles.* J Control Release, 2006. **115**(3): p. 354-61.
27. Peng, S.F., et al., *Effects of incorporation of poly(gamma-glutamic acid) in chitosan/DNA complex nanoparticles on cellular uptake and transfection efficiency.* Biomaterials, 2009. **30**(9): p. 1797-808.
28. Liao, Z.X., et al., *Enhancement of efficiency of chitosan-based complexes for gene transfection with poly(gamma-glutamic acid) by augmenting their cellular uptake and intracellular unpackage.* J Control Release, 2014. **193**: p. 304-15.
29. Faneca, H., S. Simoes, and M.C. Pedroso de Lima, *Association of albumin or protamine to lipoplexes: enhancement of transfection and resistance to serum.* J Gene Med, 2004. **6**(6): p. 681-92.
30. Gan, Q. and T. Wang, *Chitosan nanoparticle as protein delivery carrier--systematic examination of fabrication conditions for efficient loading and release.* Colloids Surf B Biointerfaces, 2007. **59**(1): p. 24-34.
31. Slutter, B. and W. Jiskoot, *Dual role of CpG as immune modulator and physical crosslinker in ovalbumin loaded N-trimethyl chitosan (TMC) nanoparticles for nasal vaccination.* J Control Release, 2010. **148**(1): p. 117-21.
32. Nimesh, S., et al., *Enhanced gene delivery mediated by low molecular weight chitosan/DNA complexes: effect of pH and serum.* Mol Biotechnol, 2010. **46**(2): p. 182-96.
33. Molina-Bolivar, J.A., F. Galisteo-Gonzalez, and R. Hidalgo-Alvarez, *Specific cation adsorption on protein-covered particles and its influence on colloidal stability.* Colloids Surf B Biointerfaces, 2001. **21**(1-3): p. 125-135.
34. Mao, H.Q., et al., *Chitosan-DNA nanoparticles as gene carriers: synthesis, characterization and transfection efficiency.* J Control Release, 2001. **70**(3): p. 399-421.
35. Mumper, R.J., et al., *Novel polymeric condensing carriers for gene delivery.* Proc. Int. Symp. Controlled Rel. Bioact. Mater, 1995(22): p. 178-179.
36. Mao, S., W. Sun, and T. Kissel, *Chitosan-based formulations for delivery of DNA and siRNA.* Adv Drug Deliv Rev, 2010. **62**(1): p. 12-27.
37. Duceppe, N. and M. Tabrizian, *Advances in using chitosan-based nanoparticles for in vitro and in vivo drug and gene delivery.* Expert Opin Drug Deliv, 2010. **7**(10): p. 1191-207.
38. MacLaughlin, F.C., et al., *Chitosan and depolymerized chitosan oligomers as condensing carriers for in vivo plasmid delivery.* J Control Release, 1998. **56**(1-3): p. 259-72.
39. Gao, Y., et al., *Arginine-chitosan/DNA self-assemble nanoparticles for gene delivery: In vitro characteristics and transfection efficiency.* Int J Pharm, 2008. **359**(1-2): p. 241-6.
40. Ishii, T., Y. Okahata, and T. Sato, *Mechanism of cell transfection with plasmid/chitosan complexes.* Biochim Biophys Acta, 2001. **1514**(1): p. 51-64.
41. Strand, S.P., et al., *Molecular design of chitosan gene delivery systems with an optimized balance between polyplex stability and polyplex unpacking.* Biomaterials, 2010. **31**(5): p. 975-87.
42. Lavertu, M., et al., *High efficiency gene transfer using chitosan/DNA nanoparticles with specific combinations of molecular weight and degree of deacetylation.* Biomaterials, 2006. **27**(27): p. 4815-24.

43. Koping-Hoggard, M., et al., *Chitosan as a nonviral gene delivery system. Structure-property relationships and characteristics compared with polyethylenimine in vitro and after lung administration in vivo.* Gene Ther, 2001. **8**(14): p. 1108-21.
44. Fischer, D., et al., *In vitro cytotoxicity testing of polycations: influence of polymer structure on cell viability and hemolysis.* Biomaterials, 2003. **24**(7): p. 1121-31.
45. Simoes, S., et al., *Human serum albumin enhances DNA transfection by lipoplexes and confers resistance to inhibition by serum.* Biochim Biophys Acta, 2000. **1463**(2): p. 459-69.
46. Huang, M., et al., *Uptake of FITC-chitosan nanoparticles by A549 cells.* Pharm Res, 2002. **19**(10): p. 1488-94.
47. Borchard, G., *Chitosans for gene delivery.* Adv Drug Deliv Rev, 2001. **52**(2): p. 145-50.
48. Bento, D., et al., *Development of a novel adjuvanted nasal vaccine: C48/80 associated with chitosan nanoparticles as a path to enhance mucosal immunity.* European Journal of Pharmaceutics and Biopharmaceutics, 2015. **93**(0): p. 149-164.
49. Kim, D., *In Vitro Cellular Models for Nasal Drug Absorption Studies*, in *Drug Absorption Studies*2008, Springer US. p. 216-234.
50. Xiang, S.D., et al., *Pathogen recognition and development of particulate vaccines: does size matter?* Methods, 2006. **40**(1): p. 1-9.

CHAPTER 6

Concluding remarks and future perspectives

No other medical intervention has had a more profound global effect than vaccination. Although many vaccines have been developed using attenuated whole organisms (e.g., smallpox, polio), there now exist safer approaches such as DNA vaccines and particularly subunit vaccines. However, most purified antigens do not induce a protective T cell response and fail to elicit mucosal immune responses, when administered without adjuvants. Adjuvants can be incorporated into vaccines to enhance the magnitude and quality of the immune response to antigens. Although they have been used in vaccine formulations for a long time, a comprehensive understanding of their mode of action has only begun to emerge in recent years. For that reason the aim of this thesis was to investigate the potential of innovative chitosan-based delivery systems combined with aluminium salts and DNA to enhance mucosal and cell-mediated immunity after nasal vaccination and to explore the mechanism of adjuvanticity behind the newly developed system. This was the first time that the effects of the association of aluminium salts with chitosan nanoparticles on the induction of an immune response were investigated.

One of the initial challenges of this project was endotoxin contamination that could originate misleading results. Therefore, we developed and validated an easy and effective methodology to purify chitosan, to support the development of endotoxin-free formulations. The presence of endotoxin contamination was assessed according to the recommendations of ICH Guidelines, as well as using dendritic cells, since they are very sensitive to low levels of LPS contamination. We were able to develop endotoxin-free chitosan-based formulations which alone do not promote the secretion of proinflammatory cytokines by BMDCs, while retaining their ability to synergize with TLR-agonist, thus making them suitable for biological and medical applications.

Several studies in the literature suggest that combining different immunostimulants would be a good strategy to boost immunogenicity, as well as to direct the type of immune response generated [1]. In fact, a few combination adjuvants are already in use in licensed vaccines. GSK has been the front runner in the design of adjuvant combination strategies, developing adjuvant systems (AS) based on the association between classical adjuvants and immunopotentiators [2]. AS04 is a combination of aluminium salts and the TLR4 agonist MPL, present in the recombinant hepatitis B vaccine, Fendrix® and human papillomavirus vaccine, Cervarix®. The reported mechanism of action of AS04 relies on the ability of MPL to locally induce cytokine and chemokine secretion leading to dendritic cell and monocyte recruitment and subsequently an increase in antigen-loaded DCs and monocytes in draining lymph nodes. Aluminium salts were found to prolong the cytokine responses generated by

MPL at the injection site [3]. AS03, an adjuvant combining α-tocopherol and squalene in an oil-in-water (o/w) emulsion present in influenza vaccines, has a similar mechanism, enhancing the recruitment of granulocytes and of antigen-loaded monocytes in the draining lymph nodes [4]. Thus, we hypothesize that the association between chitosan and aluminium salts would act synergistically to further potentiate the adjuvant effect. Our protocol allowed us to produce large amounts of NPs, using a mild process suitable for antigen loading or adsorption. Optimization of chitosan and aluminium salt relative proportions resulted in CH-Al NPs with a mean size of 280.9 nm and a positive zeta potential. Remarkably, incorporation of aluminium sulfate into the particles markedly increased their thermal stability and biological stability under physiologically relevant conditions.

The valuable results obtained during the characterization of CH-Al NPs were important to support the decision to continue our work with *in vitro* assays and assess the potential of these NPs as antigen delivery systems. Particles were efficiently internalized and displayed low cytotoxicity, even at high concentrations, in two different human epithelial cell lines (A549 and Calu-3) and in splenocytes. This fact is particularly relevant for prophylactic vaccines since most of the recipients are healthy and a risk-benefit analysis of vaccination favors safety over efficacy.

Since we were interested in unveiling the potential of CH-Al NPs as an adjuvant, particularly for HBsAg, we assessed their ability to act as a delivery system using a range of model antigens (i.e. α-casein, bovine serum albumin, ovalbumin, lactalbumin, lysozyme, myoglobin, HBsAg). The characteristics of the antigens (i.e. molecular weight, isoelectric point, structures), were correlated to their loading efficacy after incubation with the nanoparticles. We show that CH-Al NPs preferentially adsorb antigens with low isoelectric point, but, other factors, such as conformational structure play a role in protein adsorption. So, looking from a technological perspective, if key physicochemical characteristics of the antigen of interest are known, it will be possible to predict antigen loading efficacy, thus reducing the amount of antigen required for formulation development.

The potential of chitosan-aluminium nanoparticles to act as adjuvant for the hepatitis B vaccine was evaluated following subcutaneous administration. We observed a significant enhancement of the anti-HBsAg IgG, compared to antigen in solution. Furthermore, contrary to antigen alone, subcutaneous immunization with HBsAg adsorbed on CH NPs elicited a more balanced Th1/Th2 immune response as indicated by IFN-γ and IL-4 cytokine production and elevated levels of anti-HBsAg IgG2c antibodies. As an adjuvant, chitosan has been described to promote skewing towards Th1 cells [5, 6], which are critical for cellular

immunity and, importantly, these observations correlated with enhanced IgG class switching to IgG2c compared to antigen alone.

The mechanism responsible for chitosan-nanoparticle adjuvanticity was elusive at the time so we decided to further investigate it. The induction of antigen-specific immune responses requires the activation of APCs, such as dendritic cells, and is characterized by the increased surface expression of antigen presenting molecules, increased surface expression of costimulatory molecules (CD80, CD86, and/or CD40) and secretion of cytokines (e.g. IL-1β, IL-12 and IL-23) necessary for the induction and activation of antigen-specific effector T cells [7]. A mechanistic study was, therefore, undertaken to evaluate the activation of murine bone marrow derived dendritic cells by incubating these cells in the presence of varying concentrations of CH-Al NPs, CH-Na NPs, chitosan in solution and aluminium sulfate solution. To this end, experiments were performed to evaluate the modulation of cytokine secretion from DCs and the expression of cell surface markers on DCs that had been incubated with the different formulations. We observed a concentration-dependent enhancement of IL-1β secretion in cells treated with chitosan-based formulations in combination with the TLR-ligand, CpG. It is important to note that DCs stimulated with any formulation alone, failed to secrete any proinflammatory cytokine. The secretion of the inflammatory cytokine IL-1β was found to be NLRP3 inflammasome and ASC-dependent. Chitosan-based formulations could activate the NLRP3 inflammasome by a combination of distinct mechanisms. All studied pathways were shown to be important for chitosan-induced inflammasome activation, particularly lysosomal destabilization, probably because the positively charged polymer can lead to charge-induced lysosomal swelling. Notably, contrary to the established vaccine adjuvant alum, chitosan-based formulations did not inhibit the production of IL-12p70 and IL-23, implicated in T cell polarization and important in cellular immunity, making them an attractive candidate for vaccine formulations. Additionally, all chitosan-based formulations tested, in general, increased the expression of the co-stimulatory molecules CD80, CD86 and CD40.

Since little was known about chitosan-based nanoparticles regarding the innate immune response they induce following vaccination, we investigated how CH NPs would affect the patterns of innate immune cell recruitment and cytokine production following injection. *In vivo* studies showed that CH NPs were able to induce cell recruitment to the site of injection. Injection of CH-Al NPs and CH-Na NPs mediated a long-lasting depletion of mast cells and macrophages while at the same time driving a transient recruitment of inflammatory immune cells (neutrophils, and eosinophils) with a similar profile to the vaccine adjuvant alum, in line

to what is described in the literature [8]. Moreover, due to differences in the relative proportions of immune cells present in the peritoneal cavity, PECs recovered from mice injected with chitosan particles secreted significantly lower amounts of the regulatory cytokine IL-10, while the concentration of the pro-inflammatory cytokine TNF-α was significantly higher compared to those in AcB injected mice. Remarkably, only mice given chitosan formulations, but not alum, were able to secrete the Th1 hallmark cytokine IFN-γ, which correlates with *in vitro* data. While alum inhibits the secretion of Th1 polarizing cytokine IL-12p70, the same is not true for DCs treated with CH NPs, leading to the polarization of naïve T cells and subsequent secretion of IFN–γ. Subcutaneous vaccination with the particulate formulations resulted in significantly higher antigen-specific IgG levels in the serum and in nasal and vaginal washes, compared to HBsAg alone, with the latter being of particular importance for the prevention of sexually transmitted HBV. Noteworthy, the chitosan-based nanoparticles were capable of inducing higher levels of antigen-specific IgG2c antibody compared with the commercially available vaccine, Engerix®.

Considering the promising results achieved with a recombinant vaccine via subcutaneous route, we investigated the potential of a pDNA vaccine using human serum albumin-loaded chitosan-aluminium nanoparticle as a delivery system and pDNA encoding for HBsAg, and assessed the immune response generated following nasal vaccination. Mucosal vaccines offer several potential advantages over parenteral vaccines, since they can induce local immune responses at the site of entry of the pathogen, and they are better suited for mass immunization in developing countries. We developed a chitosan-based system capable of efficiently complex the plasmid DNA and protecting it from DNases. Moreover, the inclusion of HSA in the system allowed a good intracellular pDNA release profile and an improved transfection activity. Vaccination studies confirmed that HSA-CH NP/DNA complexes were promising nasal adjuvant candidates. Nasal immunization of mice with DNA complexed with HSA-CH NPs elicited high levels of serum anti-HBsAg IgG antibodies and also promoted a greater mucosal immunity than DNA alone. Interestingly, the observed effects were affected by the buffer in which the complexes were tested, showing the importance of formulation development.

In summary, the aim of this thesis was achieved and supports the continued development of chitosan-based nanoparticles as a new generation mucosal vaccine adjuvant for the recombinant hepatitis B surface antigen. Our results show that although the incorporation of aluminium salts improved the stability of the formulation, chitosan was found to be an outstanding adjuvant, which presumably masked the synergism with aluminium salts *in vitro*

and *in vivo*. Chitosan holds significant potential as an adjuvant, and it is already approved by FDA for use in hemostatic gauze dressings due to its wound healing properties [9]. However, chitosan source, purity, degree of deacetylation and molecular weight can affect properties such as solubility, mucoadhesion, *in vivo* degradation rates and as a result influence immunomodulatory properties and hinder the possibility of a regulatory approval by international authorities (e.g. EMA, FDA). Regulatory guidelines need to be created to standardize chitosan manufacture in order to develop viable chitosan-based formulations.

Chitosan-aluminium nanoparticles were successfully developed and evaluated as an improved adjuvant for subcutaneous and nasal vaccines against hepatitis B virus. CH-Al NPs showed enhanced physicochemical properties over traditional chitosan particles, particularly in regards to thermostability. However, one downfall of this study was the lack of long term stability studies. In this regard, it would be interesting to perform a set of stability studies according to EMAs guidelines (ICH Q1A (R2) - Stability testing of new drug substances and drug products), in lyophilized formulations, to gain better knowledge on how factor such as temperature and humidity influences the quality of the adjuvant system overtime. This way we could demonstrate if CH-Al NPs would be better suited than traditional chitosan particles for the development of nasal vaccines against hepatitis B that do not require cold chain. Current vaccines are normally unstable and require cold storage. A stable powder formulation, could be more easily distributed and would allow for a longer shelf-life, essential in countries where it is difficult to maintain a cold chain. In addition, it would be advantageous to perform vaccination studies with other clinically relevant antigens, in order to demonstrate the adjuvant superior efficacy, as HBsAg alone was capable of inducing significant antigen-specific antibody responses in the serum. With this study we gained a better understanding of the safety profile and the mechanism of adjuvanticity crucial for formulation development in pre-clinical trials towards future applications in the clinic.

References

1. Guy, B., *The perfect mix: recent progress in adjuvant research.* Nat Rev Microbiol, 2007. **5**(7): p. 505-17.
2. Garcon, N., P. Chomez, and M. Van Mechelen, *GlaxoSmithKline Adjuvant Systems in vaccines: concepts, achievements and perspectives.* Expert Rev Vaccines, 2007. **6**(5): p. 723-39.
3. Didierlaurent, A.M., et al., *AS04, an aluminum salt- and TLR4 agonist-based adjuvant system, induces a transient localized innate immune response leading to enhanced adaptive immunity.* J Immunol, 2009. **183**(10): p. 6186-97.

4. Morel, S., et al., *Adjuvant System AS03 containing alpha-tocopherol modulates innate immune response and leads to improved adaptive immunity.* Vaccine, 2011. **29**(13): p. 2461-73.
5. Carroll, E.C., et al., *The Vaccine Adjuvant Chitosan Promotes Cellular Immunity via DNA Sensor cGAS-STING-Dependent Induction of Type I Interferons.* Immunity, 2016. **44**(3): p. 597-608.
6. Mori, A., et al., *The vaccine adjuvant alum inhibits IL-12 by promoting PI3 kinase signaling while chitosan does not inhibit IL-12 and enhances Th1 and Th17 responses.* Eur J Immunol, 2012. **42**(10): p. 2709-19.
7. Walsh, K.P. and K.H. Mills, *Dendritic cells and other innate determinants of T helper cell polarisation.* Trends Immunol, 2013. **34**(11): p. 521-30.
8. Oleszycka, E., et al., *IL-1alpha and inflammasome-independent IL-1beta promote neutrophil infiltration following alum vaccination.* FEBS J, 2016. **283**(1): p. 9-24.
9. Pusateri, A.E., et al., *Effect of a chitosan-based hemostatic dressing on blood loss and survival in a model of severe venous hemorrhage and hepatic injury in swine.* J Trauma, 2003. **54**(1): p. 177-82.